ELECTRICAL CONTACT BOUNCE AND THE CONTROL DYNAMICS OF SNAP-ACTION SWITCHES

By

JOHN WILLIAM McBRIDE (B.Sc).

A thesis submitted to the C.N.A.A for the degree of Doctor of Philosophy, and in partial fulfilment of the requirements for that degree.

Sponsoring Establishment: Plymouth Polytechnic, Plymouth, Devon.

Collaborating Establishment: Arrow-Hart (Europe) Ltd, Plymouth, Devon.

May 1986.

DECLARATION

I declare that this thesis is the result of my investigations only, and is not submitted in candidature for the award of any other degree. During the research programme I was not registered for the award of any other C.N.A.A or University Degree.

ADVANCED STUDIES

During the research programme I undertook a course of advanced studies. These included the use of the scanning electron microscope, and surface analysis techniques. I also attended several one day seminars, and presented a paper at the 31st Holm conference on electrical contacts.

ELECTRICAL CONTACT BOUNCE AND THE CONTROL DYNAMICS OF SNAP-ACTION SWITCHES

By, J.W. McBride

ABSTRACT

Experimental and theoretical studies are made of a typical snap-action rocker switch, to establish the wear mechanisms in the pivoting contact. The rocker switch, used extensively in consumer goods, operates in the medium duty current range, (1 - 30 Amps). Highspeed photographic studies have shown that the main cause of wear is arcing, occurring during separation and bounce at the pivot contacts. To reduce the bounce a computer-based mathematical model of the system dynamics is developed and optimised; this results in recommended design changes. These changes are tested under full current endurance conditions, and show significant improvements in wear.

The model of the switch dynamics relates the mathematics of motion to the bounce occuring at the pivot contact, without the influence of current. To show the effect of current and arcing, an automatic test system is developed for the controlled testing of electrical contacts. The system has the ability to evaluate arc energy, bounce times, and contact resistance. The results presented detail the influence of d.c current on contact bounce time, and identify the importance of the subsequent bounce time; which is defined for a single make operation, as the total duration of the bounces occurring after the first bounce. To compare the erosion profiles of the switch and test system, the system is operated under full load current endurance conditions, to evaluate wear. This comparison shows that the wear in the real switch contacts is greater, as result of the additional contact movement of slip and rolling.

ACKNOWLEDGEMENTS

I would like to thank all members of staff associated with this project, in the Faculty of Technology at Plymouth Polytechnic. In particular:

Professor D.J. Mapps, of the Department of Electrical and Electronic engineering, my main supervisor; for his advice and encouragement during the period of research.

Dr P.J White, of Electrical Engineering, (second supervisor); for many hours of useful discussion on associated topics.

Mr G. Roberts, of Mechanical Engineering, (joint second supervisor); for his clear and useful observations.

Mr A. Kendrick, of Mechanical Engineering, (Technician); for building the automated test apparatus to a very high standard.

The members of staff in the Department of Mathematics and Computing, for their help and advice, with the computer modelling; and technicians of the fine work shop in electrical engineering for their help with equipment.

I would also like to thank, Mr J. Allen (Engineering Manager), Mr B. Weeks, (Engineer), and all other staff associated with this project at Arrow-Hart (Europe) Ltd. I would like to thank Arrow-Hart (Europe) Ltd, and the S.E.R.C, for their financial support during this project.

Finally, I would like to thank my family for their support, and dedicate this work to my daughter Kirsty.

Nomenclature

Because this thesis spans the areas of both mechanical and electrical engineering, some of the nomenclature has had to be changed from that used normally. The following nomenclature is used unless specified otherwise.

B = Data from films, the blade displacement from the horizontal.

E = Arc energy.

E_s = Strain energy stored in contacts at impact.

F = The spring force in the rocker switch, and Contact force.

$F_{1,2,3}$ = Reaction forces used in the Static distribution.

G = Switch dimension.

H = Data from films, and radial position of the plunger c.g.

I = current, I_s = Supply current, I_m = minimum arc current, I_a = arc current.

I_p = Plunger inertia, I_b = IB = blade inertia, I_R = Rocker inertia.

K = The spring stiffness, and the bounce reduction time.

KEi = The angular kinetic enegy of the blade at main contact impact.

L = Lorenz Constant, and Inductance.

M = The Blade mass,

M = The contact mass, M_2 = The blade mass, without contacts.

N = The number of switching cycles, and plunger reaction on actuator.

R = The circuit resistance.

R(c) = constriction resistance, R(f) = the film resistance.

R(t) = The total contact resistance.

S = Data from films,

T = Bounce time, T_e = electrical bounce, T_m = mechanical bounce.

U = The contact volt drop, U_s = softening, U_m = melting voltage.

V = Volts, V_m = the minimum arc voltage, V_s = the supply voltage.

W = Youngs Modulus,

X = Main contact gap data, for the left hand contact.

Y = Main contact gap data, for the right hand contact.

Z = Pivot contact gap data, and displacement during bounce.

a = radius of contact spot, a´= radius of ´a´ spot.

b = blade thickness,

c = acceleration,

e = The coefficient of restistution, and max compression of the spring.

f = transient force,

g = Rocker dimension,

h = Rocker dimension,

i = Transient current,

l = Rocker dimension,

m = the plunger mass,

n = the number of bounces in a given make operation.

p = Rocker dimension,

q = Temperature,

r = the radius of the plunger, and radius of spherical contact.

s = Rocker dimension,

t = time variable,

u = contact velocity,

u_i = The velocity of the contact at impact.

u_o = The combined contact velocity in impact.

v = Transient voltage,

x = The extension of the spring in the rocker switch,

y = A general variable,

z = Rocker dimension,

GREEK SYMBOLS USED

α = The actuator angle in the rocker switch,

β = The Blade angle,

η = The recoverable strain energy at impact,

λ = The thermal conductivity,

μ = The coefficient of friction

ρ = The resistivity,

Ψ = A substitution term defined in appendix 5.

Table of Contents

CHAPTER 1

INTRODUCTION

The electrical contact and the act of switching an electric current are fundamental to many branches of engineering and technology. In addition, the hand operated switch constitutes the interface between electrical systems and the operator. A simplistic definition of the electrical contact is the interface between two conductors, while that of the switch is, a device used for changing the state of this contact. The range of devices covered by the two definitions is large, as is the overall number of units in operation. They range from the silver or gold contact pins of a micro-chip carrying micro-amps, to massive air blast circuit breakers used as isolators in power stations, interrupting Kilo-Amps.

The development of these devices has advanced over two hundred years and has been dependant on the use of materials with high electrical and thermal conductivity, such as coppper, silver and platinum. However in all this time the electrical contact interface has remained one of the weakest links in terms of reliability; and a failure of a contact can in some cases have catastrophic consequences. The weakness of the electrical contact stems from the extreme operating conditions implicit with the interface. Some of the major mechanisms leading to failure are, chemical corrosion due to the environment, arc erosion due to material transfer in the plasma developed between contacts at opening and closure, and mechanical wear due to sliding, rolling and fretting motions. Often the

overall degradation can be a complex interaction of these processes, the study of which has necessitated an interdisiplinary approach. To understand these phenomena a large research inititive has been required to identify the mechanisims involved and to thus reduce the wear.

The design of a particular contact system is primarily a function of the expected current loading, whereas the assembly design is dependent upon the nature of use. Table(1) presents some basic groups of electro-mechanical contact systems, suggesting the range of currents applied and some of the major areas of use.

GROUP	TYPE	CURRENT RANGE (Amps)	BASIC AREAS OF USE
1	Heavy power switching	> 300 A	H.V power supply, Industrial
2	Heavy duty switching	30 - 300 A	Industrial
3	Medium duty switching	1 - 30 A	Consumer goods, Power
4	Light duty switching	0-1 A	Keyboards, electronics
5	Permanent contacts	Any	Connectors, Terminals
6	Siiding contacts	< 300 A	Brushes, pick-ups

Table 1. Classification of electrical contacts, as a function of current loading

This thesis concentrates on investigations made into rocker switches used in the medium duty range. It is in this range that the snap-action has been used extensively to minimise the damage caused by the electric arc. The range of devices covered in this group includes hand operated switches often associated with domestic appliances and circuitry, industrial relays controlled by external circuitry, and small contactors similarly controlled.

The electrical contacts used require a combination of current carrying capacity with a reasonable resistance to oxidation. Silver and Silver alloys are widely used for this purpose as they have the advantages of high conductivity and freedom from oxidation combined with a relatively low cost. They can also be readily fabricated into a wide range of forms; typically this can be a copper base button with a layer of silver for protection.

In the medium duty range cost is of paramount importance because of the materials used and the highly competitive international market. This has lead to a major research effort to increase switch life and reduce unit costs. The range of currents and voltages associated with the medium duty switch have no special handling problems and the arcs generated can be observed by eye and recorded with suitable measuring equipment. One of the first reported observations of the electric arc was made by Sir Humphrey Davy in 1813 [1]. Towards the end of the same century Mrs Ayrton [2], contributed to the establishment of the arc characteristic curves and more recently Ragnor Holm [3] published an extensive work on a wide range of electrical contact phenomena.

1.1 Recent Developments in Consumer Switches, and Electro-Mechanical Devices

Recent developments in the field of consumer switches have focused on two primary areas. Firstly, the design of smaller devices with smaller operating forces, has lead to the need for an increased accuracy in the engineering. The second area has been in the reduction of silver content without degrading the contacts. The motivations for this are the reduction in unit cost, and the reduced susceptibility to fluctuations in the price of silver. Reductions have been achieved by replacing traditional silver alloys by alternatives with lower precious metal content, whilst maintaining the same level of performance for the component [4], and by optimising the contact size for a particular current rating; the switch ratings are therefore divided according to the quantity of silver required [5]. The areas of development have also been influenced by the increased interest in the dynamics and statics of the mechanisms. This has been achieved by in depth photographic studies [6], and to some extent by computer modelling.

In recent years the most significant developments to the electro-mechanical relay have been the reduced size, improved reliability and reduction in cost. The first two developments were initially brought about by the competition resulting from the introduction of the solid state relay (SSR), and all three have continued by the perceived threat of the SSR. The success of the relay manufacturers has resulted in the rejection of the belief that the SSR would make the relay obsolete. The improvements made to the traditional relay have in the main been made by improved mechanical engineering [7], and to some extent by improved magnetic circuits.

The new area of Hybrid switching, the combination of power electronics to switch the current, and contacts to provide isolation, has yet to make any impact in the areas of medium duty switching. This is primarily because of the added cost in producing and selling such devices. However some devices have been developed to test the market requirements. In a recent paper "Push Button Hybrid Switch" [8] it was established that there exists an inverse relationship between the mechanical and electronic designs. Making one relatively simple forces the other to become more complex.

1.2 Future Trends in the Switch Market

In a recent survey by Frost and Sullivan [9], it was estimated that the total European switch markets, (including keyboards but not relays) was worth $1531.2 million in 1984. With an average predicted growth of 6.38 per cent per annum over a six year period leads to a predicted switch market of $2218.6 million in 1990. The snap action lever/rocker switch at present accounts for 7 per cent of the market, $105.9 million. This share is expected to fall to 6 per cent by 1990, but because of the overall increase this will account for $133.16 million of the overall market in 1990, an increase of 25.7 per cent on todays market. Figure (1.1) shows a breakdown of the market prediction for lever and rocker switches in the context of the overall trends.

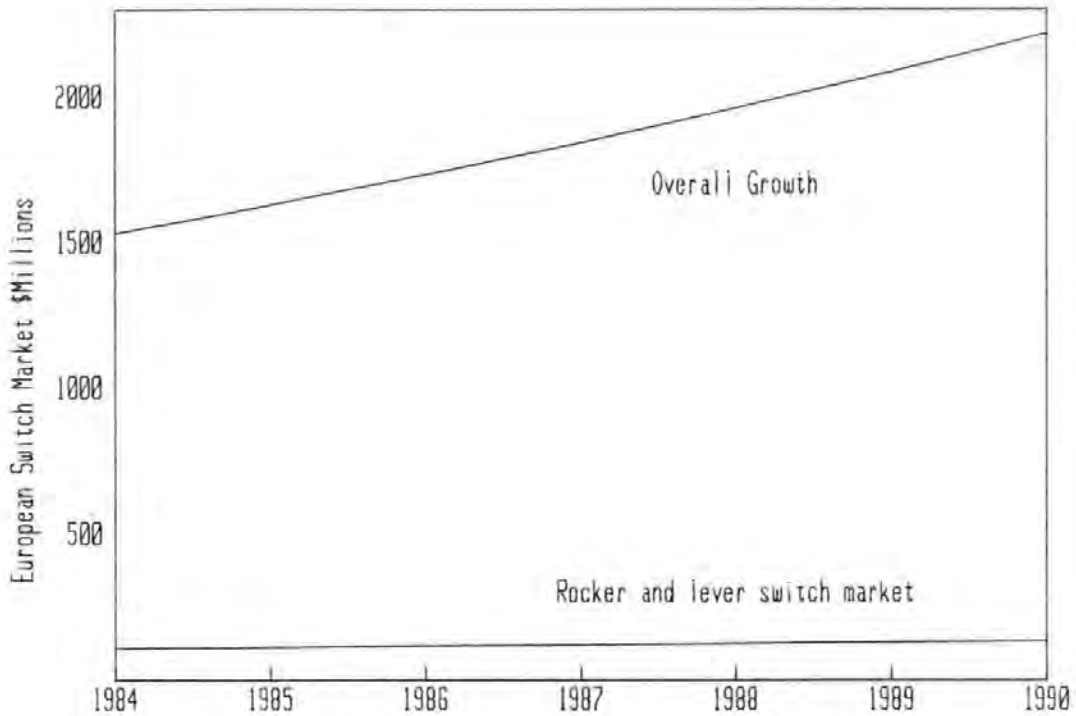

Figure 1.1 The predicted rate of growth in the European switch market to 1990

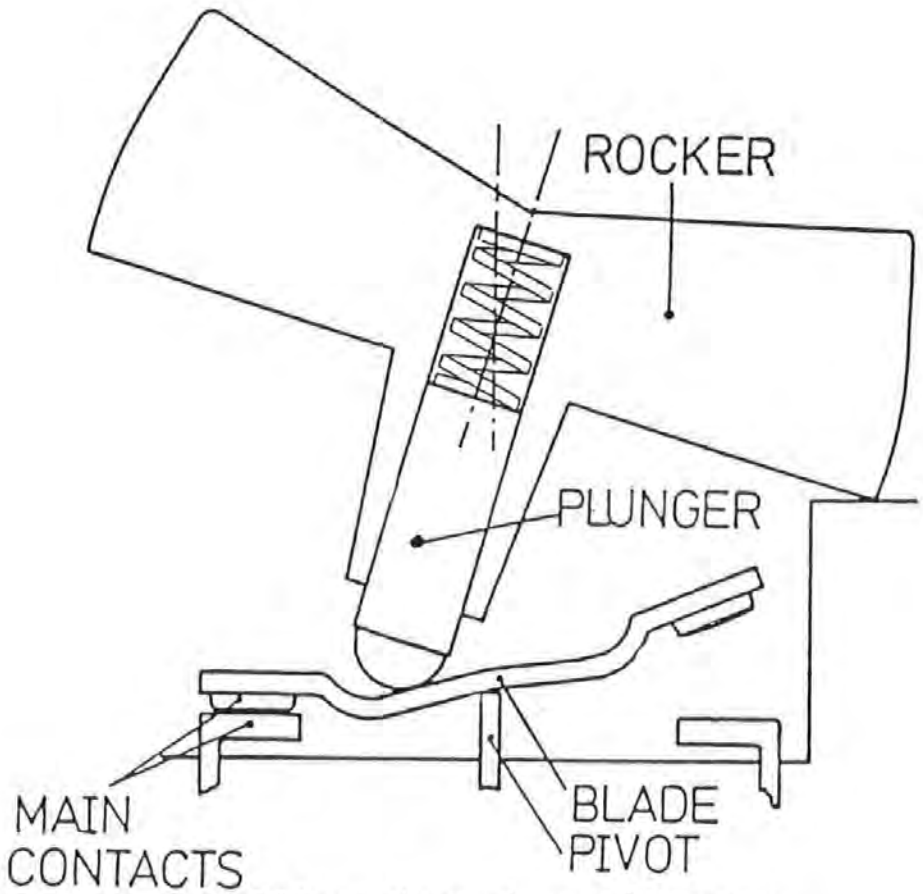

Fig1.2, A Schematic diagram of a typical change-over Rocker switch, identifying the major components

1.3 The Hand Operated Rocker Switch

The rocker switch is a hand operated switching device, utilised in the medium current range, (1-30 amps). It is commonly used in consumer type goods, and for general purpose switching. The switch mechanism is of the snap-action, see-saw type, a typical layout of which is shown in figure (1.2). The snap action is partly used to make the moving blade contact independant of the hand forces after the toggle position has been reached. The simplicity of the mechanism and the small number of parts in the assembly, eight in the case of figure(1.2), is a major factor in the economical production of these switches, and facilitates simple changes to achieve variations on the basic design.

The rocker switch has been in use for many years, though no substantial research has been applied to the device, as a consequence the basic design and that of the different variations has been left to empirical methods. The result of this design approach has been some disparity in the operating characteristics and failure modes of the switches. Two recent papers have looked at the rocker switch, the first "Pivot contact behaviour in snap-action rocker switches",[10], considered some of the benefits of the make-up device whilst the second was a result of the research undertaken for this thesis and is presented in appendix(1).

In common with most hand operated devices the rocker switch has two areas of electrical contact, the main switch contacts and the interface between the moving contact and support, called the pivot interface. It is common for rocker switches to exhibit electro-mechanical wear at both these interfaces. The main contacts are however often well protected by silver alloys which have been developed and

improved over many years; where as the pivot interface is left relatively unprotected because the contact is theoretically in contact during the switching action. The protection is typically a fine silver inlay of 0.06mm on the copper moving contact (referred to as the blade), and often the pivot is made of plain copper with no protection. In operation it is often the pivot interface that experiences the most severe wear and this can in some cases lead to premature failure. A typical example of the wear is shown in figure(1.3) for a switch blade after 10,000 cycles of 16 Amps, 200 Volts, 50 Hz, on standard test equipment. It shows how the fine Silver inlay has eroded to expose the Copper base material. It is therefore the initial aim of this thesis to investigate the mechanisms responsible for the wear occuring at the pivot interface, and to then produce an overall design approach for a typical switch.

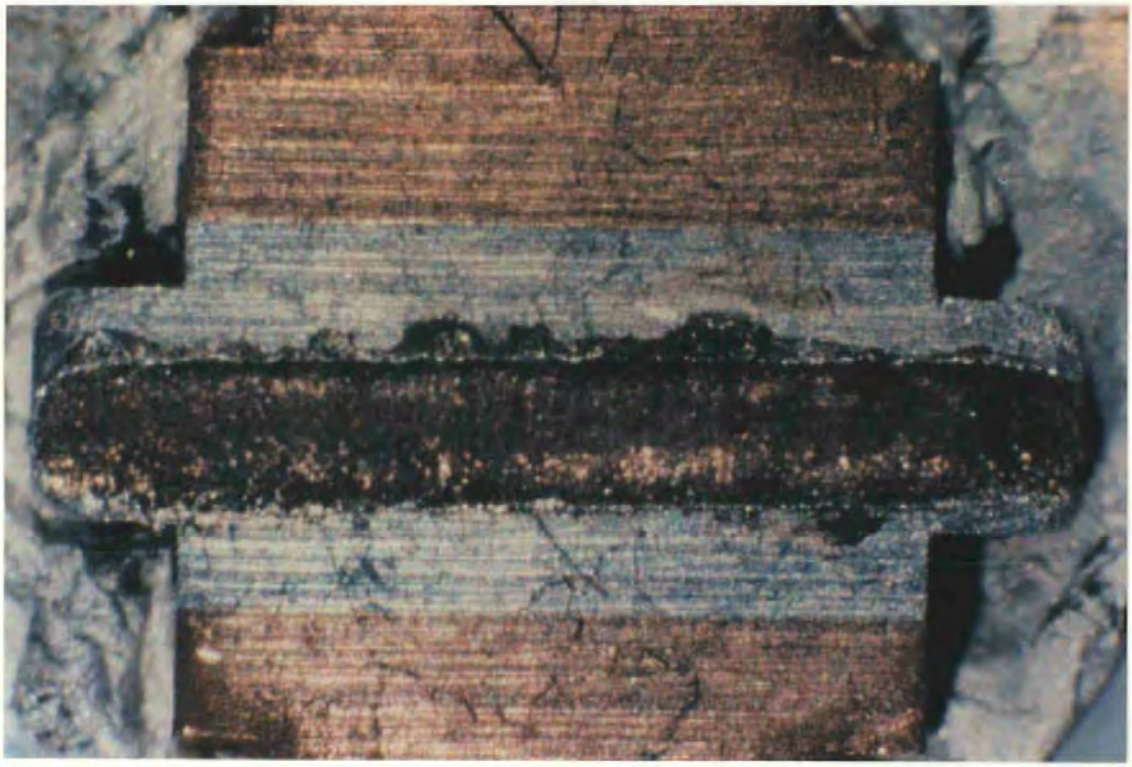

Figure 1.3 The erosion of the pivot interface, showing the removal of the silver inlay.

In operation current passes through the central pivot to a main contact selected by the rocker/actuator. The switch detailed in figure (1.2) shows a change over configuration; and in this case the current path could be through either of the main contact pairs depending on the rocker position. In figure (1.4) a range of rocker switches are shown to the same scale, demonstrating a range of possible mechanism configurations. Each switch has been sectioned to show the internal configurations of pivots and main contacts.

a

b

c

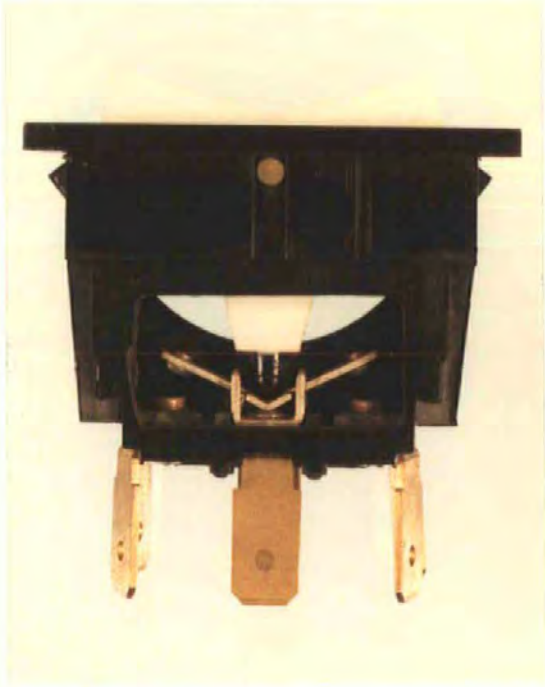

d

Figure14.

A typical range of rocker switches.

14a Change over make down.
14b On-off make up.
14c On-off make down.
14d 3 - position make down.

REFERENCES TO CHAPTER 1

[1] H. Davy Elements of Chemical Philosopy (French Trans), 1813,pp187-189.

[2] H. Ayrton The Electric Arc, The Electrician, London 1902.

[3] R. Holm, Electric Contacts, Springer-Verlag, Berlin/Heidelberg, 1967.

[4] M. Label, J.P. Debauge, "Silver savings improve profits without degrading contacts", Electrical Review, Vol 213 No 19, Nov 1983, pp 29.

[5] S. Ono, "Consumer switches Keeping Pace with Technological Developments", J.E.E, Feb 1981, pp 36-38.

[6] P.J White, "Investigation of Parameters Affecting the Operating characteristics of Toggle-Switches with Silver-Cadmium-Oxide Contacts", Ph.D Thesis, Plymouth Polytechnic, 1979.

[7] "Relays, Switches and Keyboards", Product Focus in Electronic Engineering, Aug 1985, pp 48-63.

[8] S. Krstic, P.J Theisen, "Push Button Hybrid Switch", in Proc. Holm conference on Electrical Contacts, 1985, pp 201-205.

[9] Frost and Sullivan, "The Switch Market in West Europe", E738, taken from executive Summary, March 1985.

[10] D.J Mapps, P.J White, G Roberts. "Pivot contact behaviour in Low Inertia Snap-action switches", in IEEE Trans. CHMT. Vol CHMT-7,1984.

CHAPTER 2

ELECTRICAL CONTACT AND BACKGROUND TO INVESTIGATIONS

2.1 Introduction

This chapter details the existing theory of electrical contact phenomena, and develops some of the ideas as a basis for the discussions in the following chapters. Consideration is primarily given to current loadings in the medium duty range, however many of the phenomena discussed are applicable to most applications where electrical contacts are used.

Many switch contacts remain in contact for a significant period of their duty life, thus this review starts by considering the stationary contact phenomena associated with transmitting a current across an interface between two electrodes. When the contacts open, arcs are often generated; this is refered to as the "Break" operation. The closure of the contacts is split into two sections; the impact of the contacts, and the following contact bounce; both are considered in the "Make" operation. The following sections are covered in this chapter:

2.2 Static contact Theory,

2.3 Electrical contact Phenomena during Break,

2.4 Eiectrical contact Phenomena at Make,

2.5 Contact Erosion and Contact Failure,

2.6 Switch Dynamics and the effect on Erosion,

2.7 The Nature of this Investigation.

The sections (2.5), and (2.6) are primarily concerned with the effects of arc erosion on the reliability of electrical contact.

2.2 Static Contact Theory

When the nominally smooth surfaces of two contacts are placed in contact one upon the other in apparant contact over a substantial area, it is well known that actual contact only occurs at a small number of microscopically small areas, known as asperities. This fact is fundamental to the laws of friction, as developed by Coulomb in his 1781 book "Theory of machines". It is responsible for the independance of surface area in the laws of friction, [1].

The actual size of the eventual area of contact is a function of the applied contact force, current loading in the case of electrical contact, the surface condition, materials, and other variables. In 1981 J.P.B Williamson, [2], in describing the areas of contact described the magnitudes of the asperities on a connector surface as "typically a hundred micro-inches high (2.5 μm) and perhaps a few thousandths of a inch across (50 μm). The individual areas of contact are rarely more than five hundred microinches wide (12.5 μm) ". The actual area of pure metallic contact is often only a few percent of the apparent area, because of surface oxide films produced by the chemical reaction of the metal with the atmosphere. Other molecular films can also form depending on the environmental conditions; for example the noble metal silver will react with sulphur in the atmosphere to produce silver sulphide. Silver oxide

forms only in the presence of ozone, [3]. The films produced are usually insulating or semi-conducting and are often remarkably tough, leading to the reduction in the actual area of metallic contact.

When an external force is applied to the areas of contact there will at first be elastic deformation of the contact areas in the asperities. An evaluation of this deformation was first developed in 1886 by Hertz, [4]; and lead to the classical Hertz equation relating real contact area to the applied force, for a spherical contact applied to a flat surface.

$$\text{(Eq 2.1)} \qquad a = 1.1 \times \left(\frac{F \cdot r}{2} \left(\frac{1}{W1} + \frac{1}{W2} \right) \right)^{\frac{1}{3}}$$

where, F = The applied force,

a = the radius of the contact spot,

r = the radius of the sperical contact,

W1 = Youngs modulus of the flat surface,

W2 = Youngs modulus of the sperical surface,

In a series of experiments using a nylon hemisphere and glass surface by Lincoln, [5], it was demonstrated that the areas of contact were proportional to the applied force to the power 1.5; in agreement with Hertzian theory. In recent years the analysis has been extended to include hemispherical specimens with superimposed spherical asperities, [6]. In 1967 Greenwood and Tripp, [7], considered the application of the Hertzian theories to the electrical contact, and identified that the classical Hertzian solution was the high-load limit for a rough surface, and that at low loads significant differences are found.

The elastic deformations considered in equation 2.1 are only applicable up to certain contact pressures after which the local elastic limit of the material is reached. At this stage the asperities will deform irreversibly and plastically. The transition point has been defined by Bowden and Tabor to be (1.1 x the elastic limit) of the softer metal, [8].

2.2.1 Electrical Conduction Through the Area of Contact

When a potential difference is applied, the areas in electrical contact are within the boundaries of the apparent mechanical contact. Holm identified these areas of pure metallic contact as 'a' spots, [9]. An example of this type of contact is given in figure (2.1). At the 'a' spot the electrons may transfer from one atomic lattice into that of another, in the opposite contact. In addition to the 'a' spots there are areas of quasi-metallic contact, where the surface films are sufficiently thin to be easily punctured by the electrons. This effect is known as the tunnel effect or fritting. The remainder of the apparent area of contact consists of non-conducting films.

In a recent publication J.P.B Williamson, 1981, [10]; proposed that for connector contacts the apparent area of contact was punctured by a large array of extremely small micro-spots. However in switch contacts the phenomena is likely to be simplified as a consequence of the disruption of the surface films caused by arcs and metallic softening during a "make" operation. Small tangential movements and the passage of time could however affect the interface by the ingress of oxides, [11].

2.2.2 Contact Resistance

With metallic contact occuring at only a small number of asperities the current flowing through the junction is required to flow through a constriction, this gives rise to a constriction resistance. This is not a transition resistance but caused simply by the reduction in current path. For a circular 'a' spot between similar materials the resistance can be given as:

Eq. (2.2) $$R(c) = \rho / 2a'$$

where ρ = the resistivity of the material,

a' = the radius of the 'a' spot,

Additionally there can be a film resistance R(f) at the interface, resulting from the fritting of the films, the total contact resistance R(t) is then given by,

Eq. (2.3) $$R(t) = R(c) + R(f)$$

Contact resistance is of great importance to the reliability of electrical contact, and is related to surface degradation and certain failure modes, [12], [13]. It is also a well proven method for testing surface cleanliness or measuring contamination in materials research. As a result of the importance of this, much research has been focused on the automatic and accurate measurement of contact resistance. In order to standardise measuring procedures the ASTM have recently set up a new standard, B667-80, [14].

The methods used for surface film measurements are usually based

upon the 'Dry Circuit' measurement of contact resistance, that is a contact whose electrical performance is totally dependant on mechanical and chemical phenomena. The measurement of the dry-circuit resistance has been considered in two recent papers, under the context of instrumentation, for monitoring the dry-circuit performance of electrical contacts, [15]; and automated measurement, [16].

2.2.3 The Influence of Force and Temperature on Contact Resistance

There are two important influences upon the dry circuit value of contact resistance, the external contact force applied and the current loading. Increasing the contact force deforms the material and leads to a larger radius of the 'a' spot, thus reducing the constriction resistance. The current flowing through the constriction causes heat generation at or near to the interface, depending on the materials. The heating of the contact spots can then lead to thermal softening or melting of the metals, which in-turn reduces the ability of the material to locally resist the applied force, leading to an increase in the area of contact. In the case of melting the increased area will lead to a cooling of the interface, because of the reduced contact resistance, the cooling could then lead to the freezing of the metal, resulting in the contacts welding. This case is known as the static welding of electric contacts. The static welding of contacts occurs in practice in the contacts of contactors and other switching devices in series with a protective fuse which operates on fault conditions, resulting in the passage of a pulse of high current, typically of several thousand amps for a few milliseconds, [17].

The changes in contact resistance due to the applied force have been studied extensivly, usually on crossed rods with cleaned contact surfaces. Holm made measurements of the conductance for a range of contact materials and applied forces, and clarified some of the difficulties with this type of measurement, by giving consideration to the diversified resistance measurements of various other experimenters, [18]. The experiments indicated that as the load decreases the resistance increases in a fairly reproducible manner and follows a relation of the type;

$R = k \cdot F^{-n}$, where k is a constant; [19].

For clean metal surfaces Holm showed that,

$R^{2} = k \cdot 1 / F$, for plastic deformations, and

$R^{3} = k \cdot 1 / F$, for elastic deformations, [20].

With current passing through the interface, heat is generated by Joule heating, and a potential drop (U) can be measured across the constriction. The heat dissipation results in a 'super temperature' at the contact interface for similar materials. The temperature is usually evaluated from the potential drop by manipulation of the Wiedemann-Franz relation, which relates the resistivity and thermal conductivity to temperature. Thus;

Eq. (2.4) $\rho \cdot \lambda = L \cdot q$, where L (Lorenz Constant) $= 2.4 \times 10^{-8}$, $(V/K)^{2}$.

where q = the absolute temperature,

λ = thermal conductivity,

ρ = resistivity,

For a monometallic junction, it can be shown that, [21], [22],

Eq. (2.5) $q^2 - q_o^2 = U^2 / 4 L$, where q_o = the bulk temperature.

This can be further simplified to,

Eq. (2.6) $q \simeq 3200. U$, at a room temperature of $22^{\circ}C$.

Thus as the current is increased through the junction the potential drop (U) will increase until the softening voltage of the material is reached (U_s). Further increases in current still increases (U) however to a different relation because of the simultaneous changes in contact area. As the current further increases, the potential drop will cause the metal to melt; this is known as the melting voltage (U_m). In Figure(2.2), (U_s) and (U_m) are shown as a function of the supply current as reported by Sato, [23]. This figure shows the current and voltage varying reversibly up to the point B, beyond B irreversible changes take place, as the contact area reaches the softening temperature of the material. At C the contact areas reach the melting temperature and welding occurs between the contacts. At this condition equation (2.5) can be rearranged to give;

Eq. (2.7) $U_m = [4 L (q_m^2 - q_o^2)]^{1/2}$

where q_m = the melting temperature of the material.

Sato compared experimental values of (U_m) for various materials, to the temperature function, and the results showed good agreement with the curve given by equation (2.7). In table (2.1) some of the values

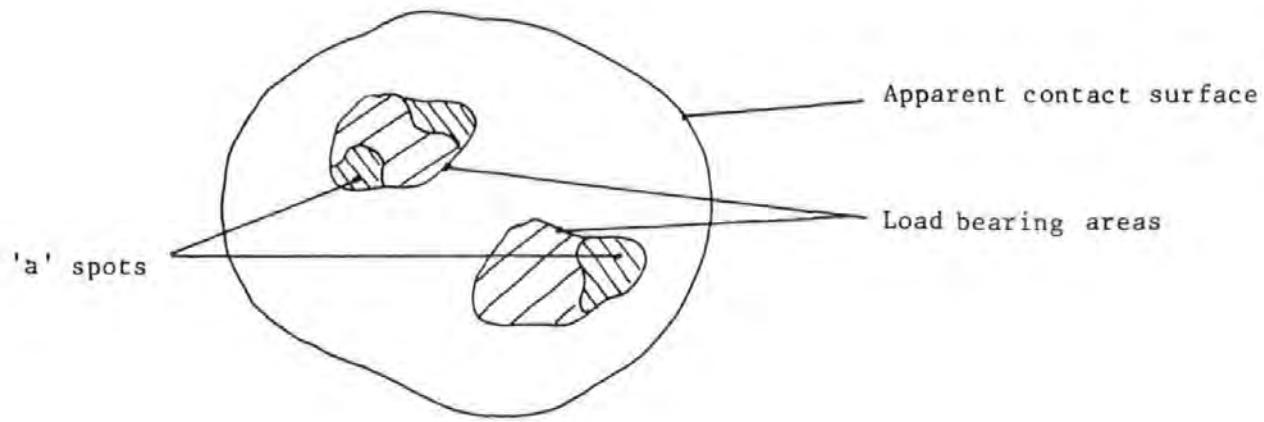

Figure 2.1 Areas of electrical contact

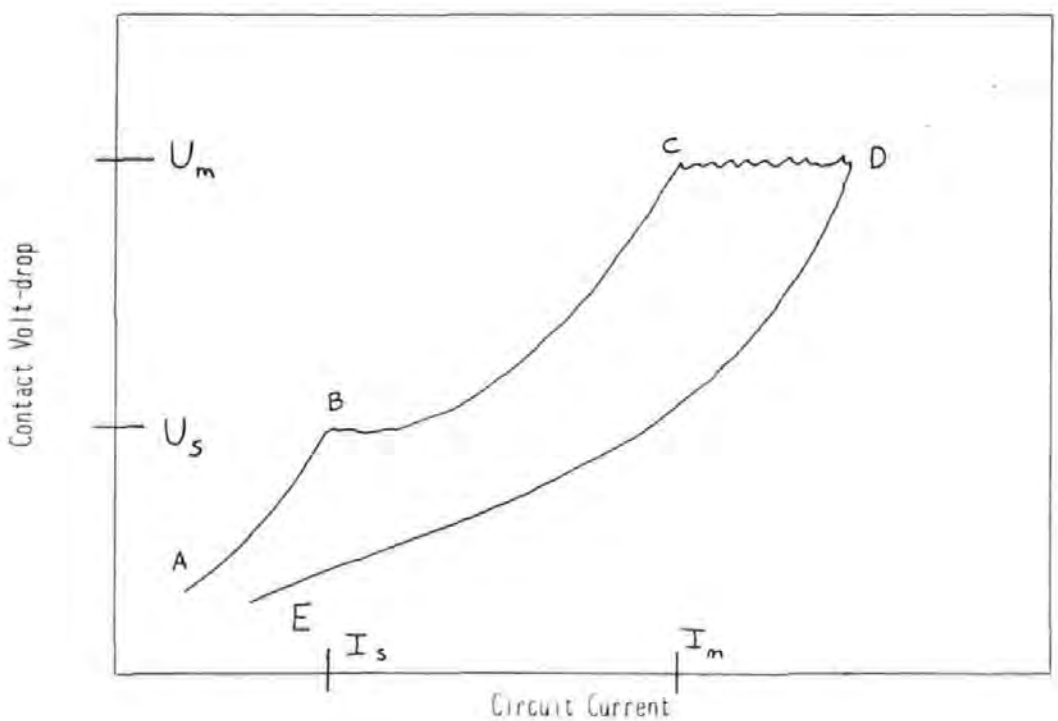

Figure 2.2 The relationship between contact voltdrop and circuit current

given by Holm, [24] and Sato are compared. Sato also identified that in most metals and alloys the softening temperature is approimately 40 percent of the melting temperature. The well establised relation given by equation (2.5), has been shown not to hold for junctions where the 'a' spots are very small, [25].

	(Sato)		(Holm)	
	U_m	U_s	U_m	U_s
Ag	0.38	0.1	0.37	0.09
AgCdO	0.16	/	/	/
Sn	0.12	/	0.13	0.07
Ni	0.54	0.21	0.65	0.22
Cu	0.38	0.13	0.43	0.12
Au	0.38	0.09	0.43	0.08
Pd	0.56	0.25	0.57	/

Table 2.1 Experimental Values of Melting and Softening Voltage

2.2.4 The Measurement of Contact Resistance

The method used to measure contact resistance, should always be defined since the resistance is a function of the current loading. In the case of monitoring surface film phenomena the dry-circuit method is often used so as not to damage the film. However for switch contacts, measurment of resistance should be taken at a reasonable current loading. The measurement of the volt-drop across the contacts, is usually achieved by positioning the probes as close to the area of contact as possible.

This is known as the "four wire" method. The resistance is then obtained from a knowledge of the supply current, by Ohms Law. The resistance obtained will include an element due to the bulk resistance, which can often be considerably larger than the actual contact resistance. In laboratory experiments the bulk resistance can be cancelled by the use of the "true four wire" or "crossed rods" method. Much of the early work on material phenomena such as the effects of contact pressure were studied using this method, [26],[27].

In the measurement of contact volt-drop in real switch contacts it is particularly important to specify the current, supply voltage and contact forces, in order that valid comparisons can be made with the data produced by other researchers. To simplify this the ASTM have set up further standards for the measuring of contact resistance in static contacts (i.e connectors), [28], and for arcing contacts, [29]. The latter standard however is concerned mainly with the configuration of the measuring instruments, to reduce errors caused by ground loops, and thermocouple potentials in d.c measurements. The former details the importance of the current loading and identifies three levels; 1) dry circuit, 2) standard test current, and 3) rated current.

Two further methods have been developed for use with real contacts, so as to isolate the bulk component inherent in the four wire method. Both depend on the different thermal behavior of the metallic contact spots and the bulk material.

The Pulse method, allows very short current pulses to pass through the contacts. The current is increased after each pulse until the softening voltage is reached. At this point using the known value of (U_s) for the material used, the true contact resistance will be given, by

Eq. (2.8) $$R(t) = U_S / I\ (crit)$$

With this method no use is made of the contact volt drop, and the accuracy only depends on the accurate measuement of the current, [30].

The second method, known as the non-linear method is based upon the voltage-current property of metallic conduction. This property is nonlinear for metals, high current causing more heating, and the resulting temperature rise increasing the resistivity. Under a.c excitation a measurable d.c voltage is generated across the test contact which is a direct function of the constriction resistance part of the overall measured resistance, [31]. It is then possible to measure the resistance accurately using the standard four wire method. Little practical work has been reported using this method, however a new device has recenty come on to the market based on the principle and is reported in "Measuring the true contact resistance", [32].

2.3 Electrical Contact Phenomena during the Break Operation

When the force holding two contacts together is decreased towards zero the areas of contact are gradually reduced causing an increase in the constriction resistance. With sufficient current passing through the interface, there will be a point at which the increased resistance produces a volt drop equal to the softening voltage and eventually the melting voltage of the contact material. The molten metal is then drawn into a molten metal bridge between the moving contacts. Extensive research has been focused on the events occuring up to this point. If in

general the voltage across the contacts is too small to result in significant arcing, a mechanism of fine transfer predominates. This fine transfer is caused by the molten metal bridge, and often results in a pip and crater formation, on the contacts. Fine transfer is commonly found on the electrical ignition systems for internal combustion engines, and in telephone relays and is often the limiting factor in their life. In 1972 Hopkins and Jones looked at the voltage and current transients associated with the bridge, [33]; and a summary of the phenomena associated with the molten metal bridge was given by Llewellyn-Jones in 1957, [34]. Recent work has focused on newer type contact materials for example, Rhodium, and Rhodium-Tin alloys, which exhibit long life time characteristics, under the fine transefer conditions and freedom of tarnish films, [35].

As the bridge is extended by the opening contacts the molten metal will approach boiling point, with sufficient circuit voltage present. High-speed photographic studies by Price and Llewellyn-Jones, [36], have shown the bridge breaking explosively and that metal vapour and droplets are present between the opening contacts.

2.3.1 The Electric Arc and Arc Initiation

The electric arc is a form of gas discharge characterised by a volt drop at the cathode of the order of the excitation potential of the elecrode vapour, (typically of the order of 10 volts), [37]; and in which the current flowing can have any value almost without limit, above a minimum which may be 30 milliamps or less at atmospheric pressure. The temperature which exists in the gas column is generally about 15,000° to 20,000°C; and at this temperature the gas atoms are substantially ionised, in a plasma state and conductive.

A vast amount of research has been undertaken in the study of arc phenomena, primarily because of the large number of applications. In two recent reviews by A.E Guile in 1971, [38], and 1984, [39], respectively 238 and 616 references were given. The latter of the two reviews attempted to cover the literature since 1970 alone.

In the context of the switch or relay the arc is of prime importance because it is the phenomena by which a significant amount of erosion, and heating occurs, having a direct affect on the stationary contact phenomena, and contact reliability.

At the moment of bridge rupture there will exist between the contacts a potential difference, across a gap comparable to the mean free path of the electrons at the surface of the contact. If the pressure of the vapour is not too high, electrons crossing the gap from the cathode to the anode will make few ionising collisions and will therefore dissipate their energy in the form of heat at the anode. This type of discharge is generally referred to as a "short arc", [40].

As the gap increases further, the electrons will make more ionising collisons with the metallic vapour resulting from the bridge rupture. The ionised material will then be attracted to the cathode, creating the cathode fall region. As the arc continues to lengthen a corresponding anode fall, and arc column develops.

2.3.2 The Full Arc, Current and Voltage Characteristics

As a conductor the arc has a strikingly different characteristic to the normal circuit constants, i.e resistance, capacitance, and inductance. With a constant length its volt drop decreases with increasing current, as a result of the increased conductivity of the arc due to its increased temperature.

The normal characteristic of a full arc is shown in figure (2.3), expressed as a function of both time and distance through the arc at a particular instant in time, for a d.c circuit. Figure (2.3a) shows how the voltage across a fully drawn arc is split into the three regions of the anode fall, cathode fall, and column voltage. It also shows that most of the volt drop occurs close to the contact surfaces. The column volt drop results in the visible glow of the arc. Figure (2.3b) shows how the voltage and current of the arc are affected by the opening contacts. As the gap increases with time the volt drop across the arc increases thus reducing the circuit current. The initial step in the voltage characteristic is known as the minimum arc voltage.

2.3.2.1 The Minimum Arc Current and Voltage

The minimum voltage and current are both functions of the cathode material and the contact shape, [41]. The minimum arc current (I_m) is found to be additionally dependant upon the relative humidity, [42]. The arc voltage can approach the minimum value (V_m) when the arc uses only negligible voltage for maintaining the plasma. The minimum voltage is then thought of as being the sum of the anode and cathode falls. Dickson and Von Engel, 1966, [43], made a study of these voltages by considering

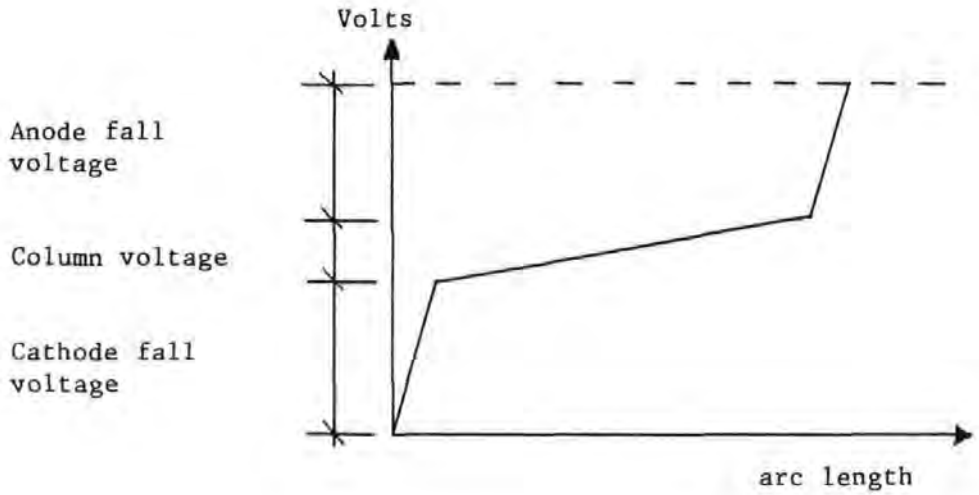

(a) The space voltage distribution for a d.c arc

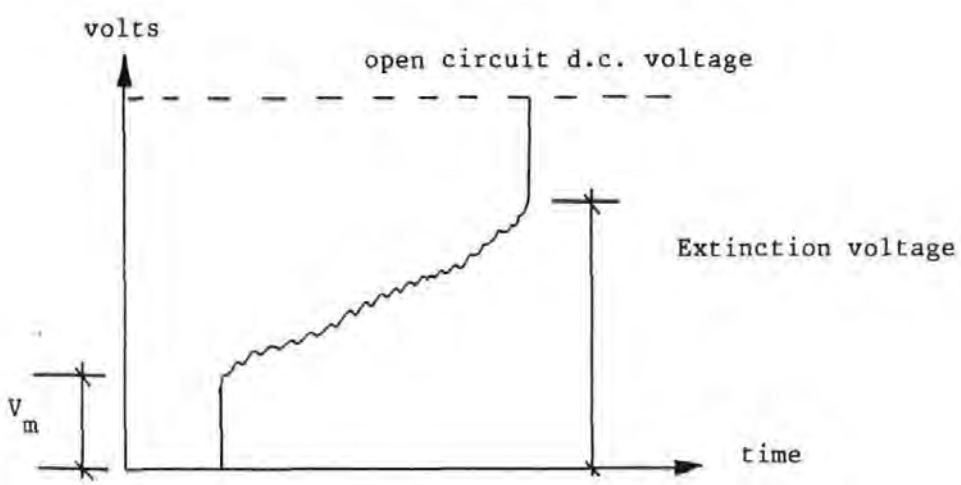

(b) The voltage time characteristic of an opening arc

Figure 2.3 Typical arc characteristics for opening switch contacts

the closure of two contacts with an arc already drawn between them. This action was found to cause a separation of the fall voltages, enabling the measurement for different materials.

2.3.2.2 The Arc Characteristics

In the case of a d.c circuit the arc can only be extinguished by lengthening until the arc requires a greater voltage than is available in the circuit. In figure (2.4) the voltage and current characteristic are shown for silver contacts. The minimum voltage and current represent asymptotes to the zero arc length line. As the arc length is increased the particular curve will change. Holm produced a set of constant arc length curves for varying current and voltage, and suggested that these curves could be used for different contact materials simply by shifting the curves with respect to the asymptotes of (V_m) and (I_m), which could be taken from standard tables, for a particular material. He published a table of values for (V_m) and (I_m), [44]. More recently, M. Sato, [45], produced equations defining the arc voltage and current in terms of d.c circuit parameters for a constant opening velocity. These equations were obtained from measurements of the oscilloscope recordings of voltage and current similar to those shown in figure (2.3b). Using silver contacts in air breaking a resistive load an equation was deduced giving the arc length (ℓ) at extinction in terms of the supply voltage (V_s) and the current immediately prior to ignition. Thus;

$$\text{Eq. (2.9)} \quad \ell = k \left(V_s - V_m - \left(V_s / I_s \right) . I_m \right)^{\frac{3}{2}} . I_s^{\frac{1}{2}}$$

where K is a constant = 1.5×10^{-3} , for an arc in mm.

ℓ = extinguishing arc length,

V_s, I_s = circuit conditions at opening.

Equation (2.9), has been rearranged by some workers to give the arc length as a function of arc voltage, [46].

2.3.2.3 The Arc Energy

The substantial heating effects of the arc along with the mass transfer associated with the ion movement, can be expressed in terms of the arc energy dissipation (E), defined as follows.

Eq. (2.10) $$E = \int_0^t v.i \; dt$$

where (v) and (i), are the voltage and current transients of the arc, over the time period of the arc, (t). With reference to figure (2.3b), the arc energy can be obtained by evaluating the areas under the curve produced by multiplying the instantaneous values of voltage and current.

The arc energy can be expressed as a function of the supply and for the general d.c conditions with some circuit inductance. Holm, [47] defines the energy in terms of the supply voltage by the equation.

Eq. (2.11) $$E = 0.5.L.I_s^2 + \int_0^t (V_s - R \cdot I_s) I_s \; dt$$

where t = the duration of the arc,

R = load resistance,

L = Inductance of circuit,

This equation is made up of the energy drawn from the supply and the energy dissipated in the arc by any stray inductance present in the circuit.

2.3.3 Circuit Conditions

The arc characteristics discussed in the previous sections apply directly to a d.c circuit, thus the arc curves can be used to determine the necessary contact gap needed to break the circuit current, [48]. With reference to figure (2.4); with a supply voltage of 40 volts (d.c) and a closed circuit current of 2.5 amps, the line drawn between A and E will give the expected arc voltages, and identify the contact gap at which the arc will be extinguished. At the onset of contact motion, B gives the minimum arc voltage of the particular contact material. As the contact gap increases the arc voltage will increase; at C with a gap of (0.05mm) the voltage drop across the arc will be approximately 15 volts. As the gap increases the arc voltage increases, until D at which point the circuit can no longer maintain the arc. For the condition shown the contact gap at rupture would be approximately 0.23mm, and the arc voltage and current, 27.5 volts and 0.8 amps respectively. This suggests that to break the given d.c supply a contact gap in excess of (0.23mm) would be required.

With large supply currents, arc extinguishing devices are used to produce a high arc voltage as quickly as possible, for example blow out coils create magnetic fields which move the arc to guide plates away from the contacts, thus extending the arc, and cooling the plasma, [49].

In the interruption of a.c currents, the a.c zero that occurs

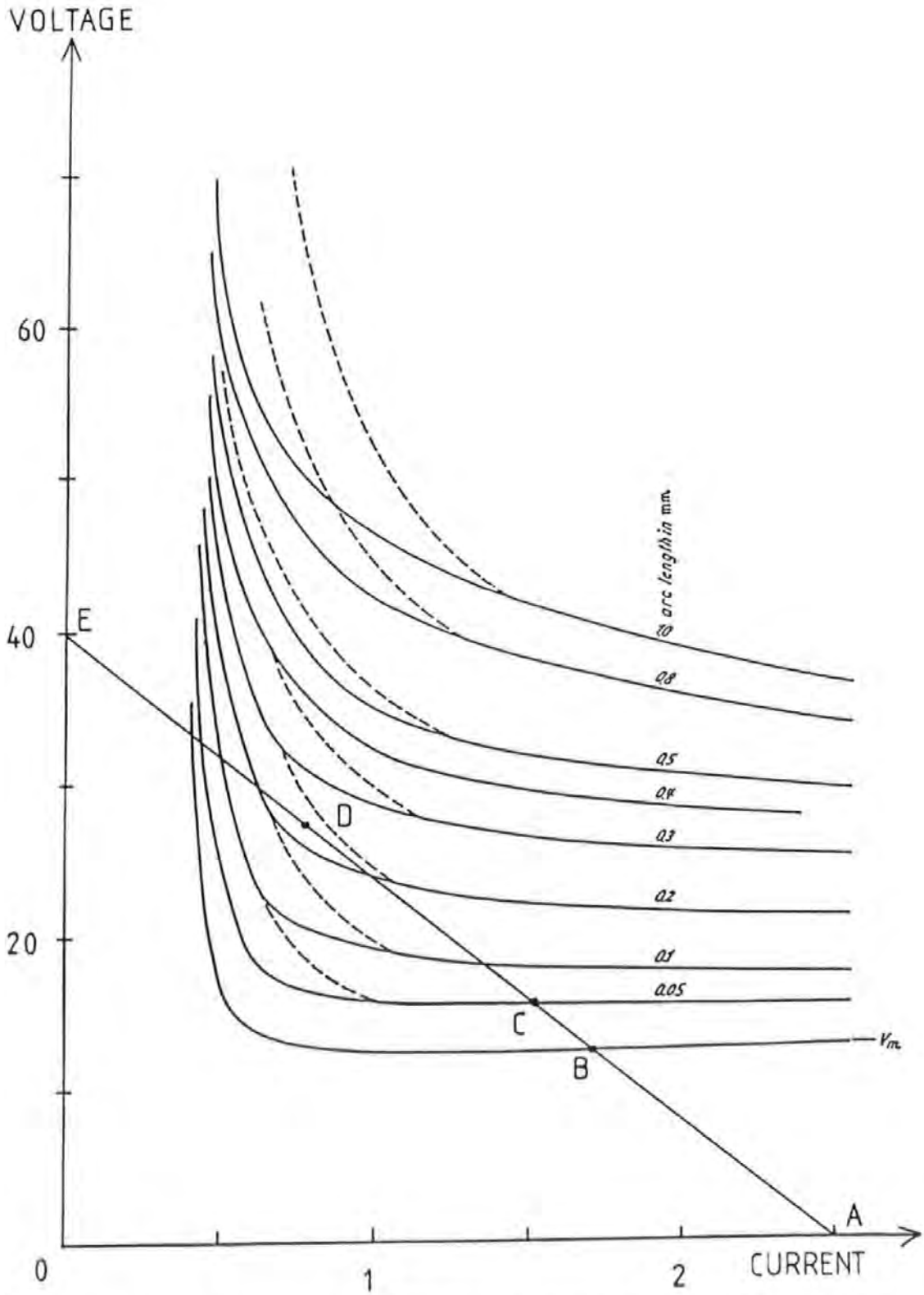

Figure 2.4 The voltage, current characteristics for Silver contacts with variation in the contact gap

twice every cycle, can be used to extinguish the arc naturally, since the zero current, or zero voltage will not sustain an arc. Under the conditions associated with the medium duty range, re-striking of the arc is usually prevented. There are two modes under which restrike can occur, the first is by the breakdown of air, which can occur at voltages as low as 300 Volts. The second mode is by thermal re-ignition. When the arcing process has ceased, there still remains between the gap a conductive plasma which consists of electrons, ions and metal atoms that require a finite length of time to dissipate. Until the plasma decays, the ability of the gap to withstand a high voltage is diminished. In a recent paper C.G Chen, [50], considered some of the mechanisms of restrike on Silver Cadmium-Oxide contacts, and demonstrated the importance of metal oxide components, and the effective ionization energy of the metal in the gap. The restriking of an extinguished arc is also effected by the surface conditions of the contacts, [51]. A practical application of the restike phenomena is in arc welding with an alternating current.

The hybrid switch or relay discussed briefly in the introduction makes full use of the a.c zero by synchronisation with the instant at which the contacts separate. In the case of the hybrid switch the synchronisation is achieved by the electronic monitoring of the zero crossing. In a recent paper by P.J White et al, [52], the magnetic circuit associated with the current path in a small snap-action switch, has been used to synchronise the opening with the a.c zero, by making use of the contact forces created by the careful design of the magnetic circuit. It was observed that a reduction of up to 40 percent in the total arc energy dissipation was possible using this method.

2.4 Electrical Contact Phenomena at Switch Closure

An essential part of this thesis is the study of the events that occur during contact bounce. The erosion observed between the pivot and the blade in a rocker switch is identified in the initial investigations in Chapter 4 to be primarily caused by small amplitude vibrations between the two contacts.

In the general case, when two solid objects collide there is inevitably a rebound, which in the case of electrical contacts, if the circuit conditions permit, results in the generation of arcs. With arcing occurring during the contact bounce, each bounce becomes a very fast break and make operation , during which the arc is not usually extinguished, unless an a.c zero occurs. The events occurring during the impact of electrical contacts thus reflect some of the events at the opening of the contacts. Often there are a number of bounces following the initial impact of the contacts which with associated arcing can lead to severe erosion of the contacts. In most circuits the current rise at impact is delayed by the effect of the circuit inductance, thus reducing the energy dissipated by the arc and thus the arc erosion. On switching a capacitive circuit however a high inrush of current can occur, which reduces as the capacitor reaches full charge. Other devices can also give a high inrush, for example metal filament lamps, and electric motors. The high in rush of current can be disastrous for the switching contacts since currents as high as ten times the normal circuit current can pass through the interface during the bounce and arcing stages, [53].

2.4.1 Arc Ignition Prior to Impact

The normal separation distance of the switch contacts will satisfactorily resist the flow of current under normal conditions, however the contact gap can breakdown without the normal initiation stage of a electric arc, as detailed in section (2.3). The electrical breakdown of a gas between electrodes is described by Paschen's Law, which expresses the breakdown potential as a function of the product of electrode gap and gas pressure. Classically this shows that the minimum voltage at which breakdown can occur to be in the region of 300 volts, [54]. However for small gaps of the order of ($1x10^{-4}$ mm), breakdown and arc ignition have been observed with voltages as small as 50 volts, [55]. Further to this at the instant of contact impact the asperities will evaporate and allow a very short period in which arcing could occur before the contacts close completely.

2.4.2 Mechanical Impact and Bounce

To understand the events occuring in the electrical contact interface during impact it is important that an understanding is given of pure mechanical impact, to which there is a long history and substantial experimental data.

Mechanical impact is a general area applicable to many areas of mechanics. The study of impact between colliding solid bodies received its first theoretical treatment in 1867, by St. Venant, who suggested that the total period of collision was determined by the time taken for an elastic compression wave to move through the solid and be reflected back. Experimental results show this theory not to be perfectly true and the

evidence suggests that for small bodies the collision process is dependant upon the deformations occuring in the area of contact. Consequently for small bodies of the order of a few centimeters in length the problem of the compressive wave can be ignored, [56]. The physical explanation of impact and rebound can then be applied to the events occuring at the points of contact.

Using these assumptions, the events occuring during impact were dealt with by Bowden and Tabor , [57], who separated the impact process into four main stages.

(1) The elastic deformation in the areas of contact, as given by the Hertz equation (2.1).

(2) The partial plastic deformation when the local pressure exceeds 1.1x the yield point of the materials.

(3) Full plasticity until the whole of the incident kinetic energy at impact is consumed by the collision.

(4) Release of the elastic stresses resulting in the rebound.

A full analysis of the four phases involved in the collision process is complicated and difficult. Early research into this area studied the quasi-static behaviour of contacts, Goldsmith [58], and Tabour [59], and concluded that extrapolation of the results to the dynamic impact process could be carried out on the basis that the difference between the dynamic and static yield stress and static and dynamic energy dissipation are often within 25-50 percent for a number of common metals. These early tests encouraged the belief that a useful if only qualitative

insight into bounce could be gained by quasi-static load tests, [60].

Experimental investigations in the field of impact have been performed for a variety of purposes. Many have been conducted with the object of assesing the validity of a proposed theory or the accuracy of an assumed model of material behaviour, for example proving the Hertz law of contact or the study of visco-elastic wave propagation. Other efforts have been directed towards the collection of empirical information in the areas of cratering and penetration, [61].

In the impact process of electrical contacts one contact would normally be stationary, and would be impacted by a moving contact. The kinetic energy of the moving contact is then absorbed at the interface, or in the support structure. During the release stage the moving contact is given back a degree of the energy, which results in a separation. With a spring acting on the moving contact the contacts will again impact until all of the incident kinetic energy of the first impact is dissipated.

The application of current to the interface during the impact and the following bounces, adds a further dimension of difficulty to the mechanical considerations.

2.4.3 Impact and Bounce Applied to Electrical Contacts

The damage caused by the erosion of the contacts during the make operation has caused a number of researchers to consider the events occuring during the impact and rebound stages of electrical contacts.

In 1965 A.Erk and H.Finke published two papers (in German) on the

events occuring at the impact of electrical contacts, [62], [63]. The first paper focused on a test apparatus designed to study the mechanical events of electrical contact bounce. With this test system they monitored the magnitude of the bounces in terms of displacement; with an aperture based optical system. Simultaneously they monitored the voltages across the contacts. The supply used was a 4.5 Volt d.c battery with a closed circuit current of 0.45 milliamps, such that no arcs would be generated between the contacts. The electrical transients thus gave a measure of the separation and impact times. Using this system they monitored how the bounce of new copper contacts was affected by their test system, for example by changing the static contact force. They identified that contrary to the expected reduction in each bounce in a particular make operation due to damping, the amplitude and duration of some of the bounces could be greater than the first bounce.

Using the same test system they went on to consider the affects on contact bounce of heavy a.c currents in the range 100-1400 Amps with a supply of 380 Volts, 50 HZ.

They considered 25 contact materials in this investigation, and concluded that with all of the materials the duration of the first bounce was independent of the magnitude of the supply current. However the total number of bounces was reduced by increasing the current. The durations of the subsequent bounces, that is those occuring after the first bounce, were reduced by the increase of current. Their data however shows no fixed relation with current, in the magnitude of the reduction of the subsequent bounces, only an overall reduction. Some of these results are reproduced in figure (2.5) for fine silver and AgCdO, contacts. The times of the second bounce are shown in the case of pure silver contacts to increase from 1.3ms at 100 amps to 1.8ms at 180 amps; after which a

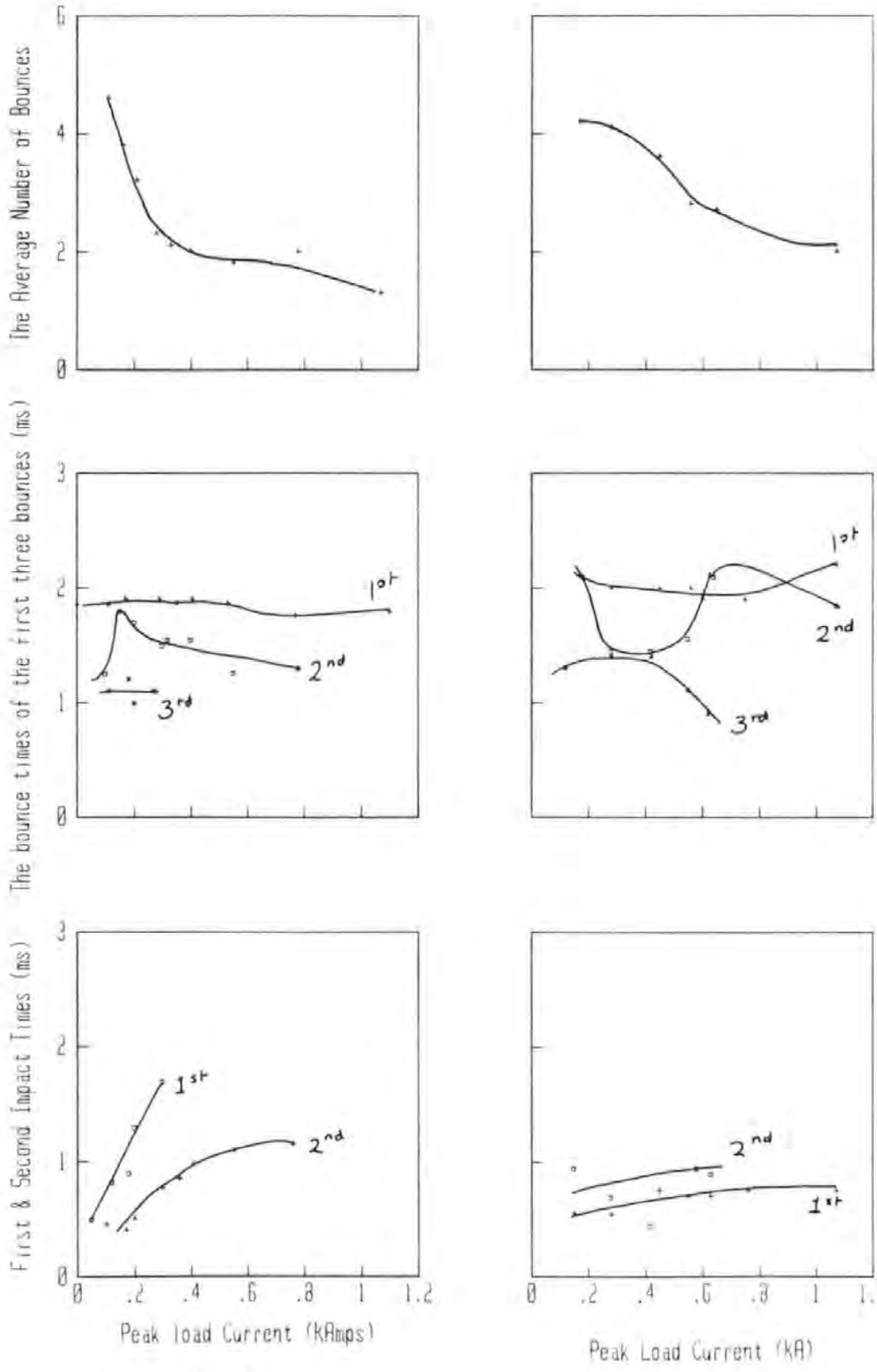

Figure 2.5 The variation in bounce times, for a.c current, by Erk and Finke

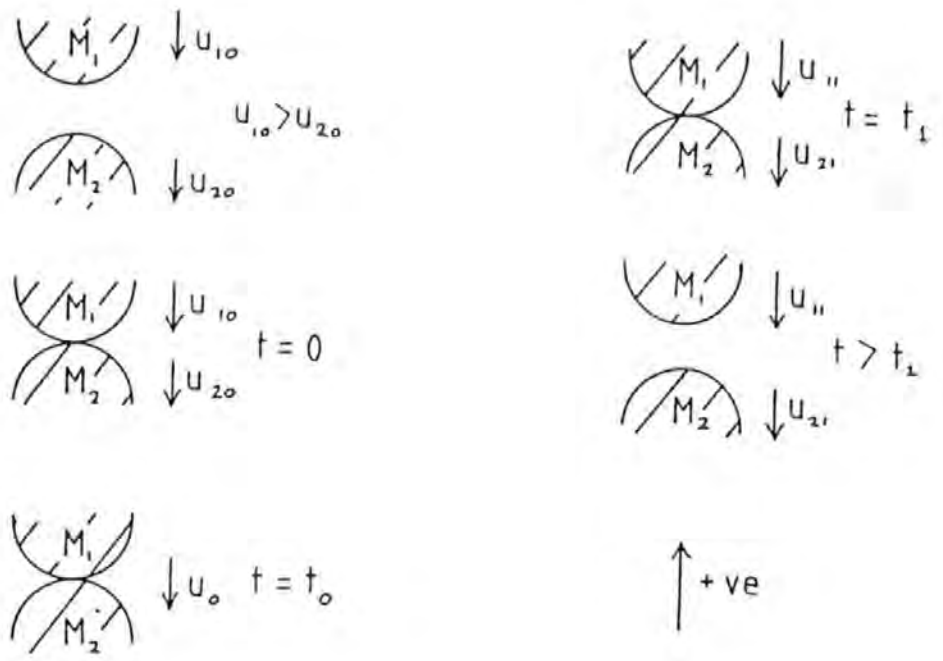

Figure 2.6 The general system of Mass and velocities at the impact of two contacts

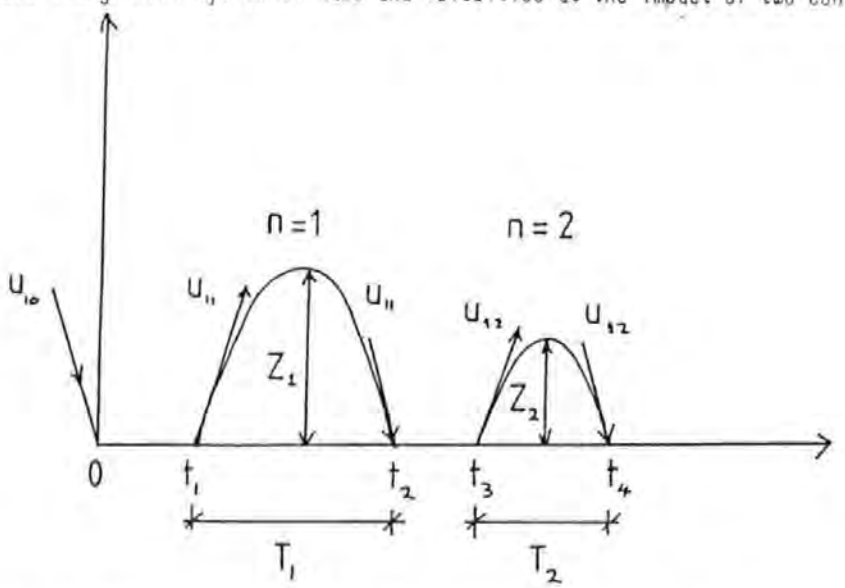

Figure 2.7 The bounce displacement characteristics with the nomenclature used

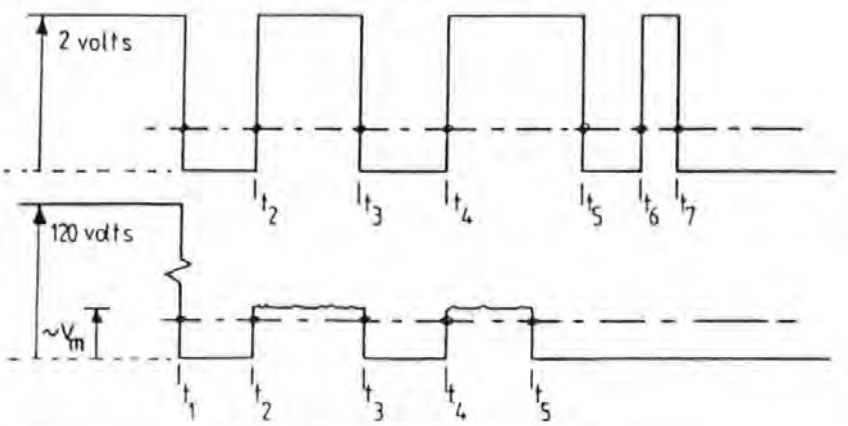

Figure 2.8 The bounce transients under signal and load d.c current

reduction is observed with increasing current. The duration of the first and second impact times were shown for the materials to increase with increasing current. No reference was given in this work to the conditions of the contacts used, however as mean values were taken from samples of 20/30 values it can be assumed that some surface degradation had occured during their tests. No full explanation was offered on these results.

As an extension of this work and to give analytical understanding to the events, a simple mathematical model was developed to represent the contact mechanics, based upon a system of masses, springs and dampers, representing the elasticity of the contact surfaces. Consideration was given to the coefficient of restitution (e) and the conservation of linear momentum. With reference to figures (2.6), (2.7), and the full definition of restitution given by Meriam, [64], and Goldsmith, [65]; the following definitions can be made.

$$e = \frac{\text{magnitude of the restoration impulse}}{\text{magnitude of the deformation impulse}} = \frac{\int_{t_o}^{t_1} F_r \, dt}{\int_{0}^{t_o} F_d \, dt}$$

where $t = 0$ is the instant of impact,

t_1 = the instant of separation,

t_o, occurs when both contact interfaces have the same velocity,

Now F_r = the rate of change of momentum during restoration, thus

$$\int_{t_o}^{t_1} F_r \, dt = (M_1 (- u_{11}) - M_1 (- u_0))$$

then $\Delta'' = M_1 (u_0 - u_{11})$

and for the deformation impulse, $\Delta = M_1 (u_{10} - u_0)$

then, Eq.(2.12) $e = (u_0 - u_{11}) / (u_{10} - u_0)$

The conservation of momentum gives, Eq. (2.13),

$$M_1 . u_{10} + M_2 . u_{20} = M_1 . u_{11} + M_2 . u_{21} = (M_1 + M_2) . u_0$$

where u_{11} = the velocity of the top contact after impact,
u_{21} = the velocity of the bottom contact after impact,
u_{10} = the velocity of the top contact before impact,
u_{20} = the velocity of the bottom contact before impact,

Or in general,

u_{1n} = the velocity of the top contact after the n'th bounce,
u_{2n} = the velocity of the bottom contact after the n'th bounce,

Then for two particles or contacts, using Eq.(2.12) and substituting for the common velocity u_o, from Eq. (2.13);

$$e = \frac{(u_{21} - u_{11})}{(u_{10} - u_{20})} = \frac{\text{relative velocity of seperation}}{\text{relative velocity of approach}}$$

or in the general case, for the n'th bounce,

$$\text{Eq.(2.14)} \qquad e = \frac{(u_{2(n+1)} - u_{1(n+1)})}{(u_{1n} - u_{2n})}$$

Often the coefficent of restitution is considered a material constant, and as such can be used to produce some useful relations for the rundown of bounce. However in reality the concept of restitution is used because of its attractive simplicity, and it would be more conceptually satisfactory to summarize results in terms of energy dissipation. The coefficient of restitution has been shown to be a function of impact velocity, and to some extent is affected by surface hardening, due to impact, [66], [67], [68].

Using the above formulations, and by simplification of the mechanical system Erk and Finke were showed that little correlation was achieved between the events measured in their test system and the expected mathematical model of the interface. The reason given for this was that after the first contact impact and rebound the contact supports vibrate at a high frequency thus complicating the subsequent bounce mechanics. This also explains the observation that some of the subsequent bounces could be larger in amplitude than the preceeding ones. Because of the complexity an analogue computer was used to study the mechanical system. Using this method good agreement was achieved with the experimental results. Erk and Finke concluded that in the mechanical system small variations in the speed of the first impact would yield considerable changes in the events after the first impact and bounce. Thus a full analytical understanding of both the first impact and the first bounce with load current would be extremely complex as a consequence of both the mechanical vibrations and the effects of arcing.

In their second paper, Erk and Finke, using an adapted version of their test apparatus, looked at some heating effects occuring during the impact process. They also considered the effects of dynamic welding and the variations in arc voltage characteristics for a range of contact materials. The supply used was 380 Volt, 50 Hz, with the current range between 100 and 2 KAmps. The current was pulsed through the contacts for only a short period of time, typically 50 ms. The contact surfaces were machined after each operation, and the force necessary to break the resulting welds were measured.

They identified that the heat generated by arcing was a function of the arc energy dissipation (E), and that during the contact bounce the arc voltage remains roughly constant for a given material, within the range 10–20 Volts. Measurements were made of the arc voltage, which correspond to the minimum arc voltage (V_m) for a range of different materials. The value of (V_m) for a particular material is therefore important at make since it will be a constant in the arc energy equation, as given by Eq. (2.10). The arc energy at make is considered in section (2.4.4). From their observations Silver Cadmium Oxide, (AgCdO), (90/10), came out with the lowest value. Some of the other results were,

AgCdO (90/10) = 10 Volts; AgNi/ZrH (60/37/3) = 15 Volts; Ag = 16.1 Volts; W (Tungsten) = 20 Volts;

It should be noted that these values are not absolute, and Holm has published different values, eg. Ag = 12 Volts, and W = 15 Volts, in air at room temperature, [69].

In conclusion to their work Erk and Finke postulated that assuming no arcs occur before the first impact, that few effects occur during the

first impact, and that no noteworthy heating effects occur before the first bounce. During the arc of the first bounce molten metal would be produced at the contact interface, thus effecting the subsequent impacts. Also during the subsequent impacts the molten metal interfaces could solidify causing dynamic welding of the contacts. It was shown that the materials with the lowest minimum voltage would take the highest current before melting occurs.

In 1967 P.Barkan, [70], considered again the events occuring in the mechanical impact of electrical contacts, he looked at some of the fundamental energy exchange processes involved, and presented the results of a range of experimental and analytical studies. He initially considered the Quasi-Static behavior of contacts, and showed that the energy absorbed in deforming virgin surfaces is irrecoverable to an extremely high degree. However it was emphasised that this would only be true until the surfaces are sufficiently deformed; after which work-hardening changes the deformation and energy dissipation characteristics. The reasons given were as follows, (1) The radius of curvature of the surface tends to grow with successive loadings reducing the peak stress for a given load, and (2) the work-hardening of the materials increases the yield stress so that a higher proportion of the energy is stored within the elastic stress range.

In the dynamic studies presented he emphasised the importance of designing a test system where the energy content of the stress waves within the contact and its support are reduced to negligible proportions compared to the strain energy stored at the interface. This required a period of impact long compared to the time required to propagate stress waves through the body. This was achieved by the use of free moving spring-loaded contacts. The contact bounce transients were monitored

between the impacting contacts, using a 6 Volt, 3 milliamp d.c circuit.

Using this system it was possible to simplify the analytical description of the impact process in terms of the dissipation of energy.

For conservation of energy, at the instant when both contact surfaces have the same velocity (u_o),

Eq. (2.15) $KE_1 + KE_2 = E_s + KE_{u_o}$

where, E_s = The strain energy stored at the suface when $u = u_o$

This equation can be simplified for the case where one contact is initially stationary to give an evaluation of the strain energy. Thus;

$$E_s = (1 + M_1 / M_2)^{-1} \cdot (M_1 \cdot u_{1o}^2) / 2$$

and,

Eq. (2.16) $\eta \cdot E_s = E_d$, the energy dissipated, and $\eta = 1 - e^2$

where η = the % of recoverable strain energy.

The value for (e) can be determined from the bounce times as shown in the following analysis. Thus Barkan was able to study the bounce characteristics in terms of strain energy and (η).

With reference to figures (2.6) and (2.7), the mechanics of bounce without the passage of current can be described as follows.

Assuming negligible gravitational effects, and a constant applied force,

$$\dot{u}_{11} = F / M$$

Where $\dot{u}_{11}$ = the deceleration of the moving contact after first rebound.

F = the applied spring force,

M = the contact mass assembly,

For a linear deceleration the duration of the first bounce is given by,

$$T_1 = t_2 - t_1 = 2 . u_{11} . M / F \qquad \text{..... Eq. (2.17)}$$

Now from Eq. (2.14), if $\ddot{u}_{20} = \ddot{u}_{21} = 0$; then

$$u_{11} = e . u_{10} \quad \text{and,} \quad u_{12} = e . u_{11}$$

therefore, $u_{12} = e^2 . u_{10}$ and, $u_{1n} = e^n . u_{10}$

where n = the number of the bounce.

then in (2.17).

$$T_1 = 2 . u_{10} . e . M / F \qquad \text{..... Eq. (2.18)}$$

and, $$T_n = 2 . u_{10} . e^n . M / F \qquad \text{..... Eq. (2.19)}$$

where T_n = the duration of the n'th bounce.

From which the total duration of bounce can be given by,

$$\sum_{1}^{n} T_n = T = 2(M / F). u_{10} . e / (1 - e) \qquad \text{.....Eq. (2.20)}$$

By the use of the relation, $\sum_{n-1}^{\infty} e^n = e /(1 - e)$

The maximum amplitude of the first bounce (Z_1) is given by,

$$Z_1 = u_{10} . T_1 . e / 2 - (F . T_1^2) / (8 M)$$

and from (2.18),

$$Z_1 = u_{10}^2 . e^2 . M / (2 . F) \qquad \text{..... Eq. (2.21)}$$

For the n'th bounce,

$$Z_n = u_{10}^2 . e^{2n} . M / (2 . F) \qquad \text{..... Eq. (2.22)}$$

Substituting for M/F from (2.19), then

$$Z_n = T_n . u_{10} . e^n / 4 \qquad \text{..... Eq. (2.23)}$$

Using these equations it is possible to relate the amplitude of a specific bounce to the duration of the bounce. For a given impact velocity and assuming "e" to be a material constant there exists a unique relation between the time of bounce and the maximum displacement. These equations do not however allow for the vibrations in the fixed contact or the presence of a current or an arc between the contacts.

In the second part of Barkan's paper, an analysis was made for the complete suppression of bounce in elementary contacts, by consideration of the stiffness of the fixed contact support, but concluded the need for an additional means of dissipating the incident kinetic energy. Some of these methods are discussed in section (2.4.5). The paper was well recieved at the time, however because of the omittance of the effects of current some discussions were added by observers; R.E Voshall of Westinghouse, picked up on the effects of load currents and suggested that Barkans results would only apply to the low voltage, low current situation, since at high currents and voltages pre-impact breakdown would occur, and during the transient stages the magnetic repulsion forces

produced by the current loops would tend to separate the contacts. He also identified that the work-hardening effects, would not apply because the presence of arcing would produce localised heating and melting of the contact surfaces which would change the metallurgical properties of the region near the surface. He concluded that the presence of current should be considered to make the analysis more general.

In his relpy Barken emphasised that if bounce is reduced without current, then on the application of current there will still be a reduction. He went on to identify three principle effects of current upon bounce behaviour. These were as follows

(1). The advent of pre-strike would increase the mechanical energy dissipation because of the associated softening of the surface, however the position of the pre-strike arc is unlikely to interfere with the actual areas of contact at the first impact. Hence the no-current consideration is still the most important.

(2). The magnetic effects at high current would tend to cause separation before expected, to monitor these effects it was suggested that a dynamic force transducer could be used.

(3). During the first bounce the presence of an arc between the slightly separated contacts could effect the bounce because of the vapour pressure of the eroding contact materials.

In 1980 B.Sandler et al, [71], considered some of the mechanics of contact bounce in the application of electromagnetic relays, with the aim of reducing erosion, welding and electrical noise. To study the contact bounce the authors considered the bounce displacement characteristics and

electrical separation times. After a review of a range of methods a laser based contact displacement system was developed based upon the same system used by Erk and Finke. Using this system the authors were able to relate displacements to the bounce transients under both signal current and load current conditions, (between 50 and 150 Amps d.c). Their measurements were however complicated by a bridge type moving contact and the associated dynamics of the relay coil system. They were able to conclude under signal current conditions that the duration of the bounces were proportinal to the corresponding displacement. In the case of the load current application they concluded in the same fashion as Erk and Finke, this time for d.c currents, that the current magnitude affects the length of the transient process. They also considered the surface changes as a result of the arcing but only identified that the contact dynamics reaches a stable characteristic after 150-200 contact "switchings", and that worn contacts behave differently when un-loaded. These later results were in general only applicable to the relay system used.

In a more recent paper, (1984) A.A Slonim, [72], produced an analytical study of the non-linear bounce implicit with the complex system dynamics of the closing relay. A good experimental and analytical relationship was obtained although only the mechanical system was considered, and as such the results of the application of current would require further modifications to the mathematical model.

In 1985 B.Miedzinski, [73], considered the importance of the surface degradation on contact bounce in reed switches used to switch a.c and d.c inductive loads of 0-3 Amps, by taking into account the bounce variations under operation. He concluded that reed switch bounce was not only a function of surface hardening but also the contact topography.

2.4.4 Summary of Electrical Contact Bounce

To summarize the observations and results of other workers, the effects of current on mechanical bounce, assuming the circuit voltage and current is sufficient to cause arcing, then:

(1) A reduction in the mechanical bounce characteristics will inevitably lead to a reduction in the electrical bounce and therefore reduce the wear due to arcing,

(2) There is a relationship between the duration of bounce and the maximum amplitude.

(3) The first bounce time is independant of current.

(4) Impact times, including the first impact time increase with current.

(5) There is an overall reduction in the number of bounces due to the passage of load current.

(6) There are complex interactions affecting the bounces after the first.

(7) To reiterate one of Barkans conclusions on this subject, "a detailed study of the interaction between high current phenomena and bounce would constitute a valuable subject for further papers". Barkan did not make this further step.

2.4.5 Arc Energy during Make and the Significance of the Contact Separation Time

This section is an extension of existing theory, and is used to justify the importance of bounce time, such that the need of measuring the bounce displacement is reduced, in the experimental work.

In addition to the evaluation of bounce time, this thesis considers the influence of current on contact bounce. To demonstrate these effects figure (2.8), shows a typical mechanical bounce with a signal current, and a load or electrical bounce characteristic, for the same conditions at impact. From this figure the bounce times can be identified, as follows,

T_e, and $T_m = \sum_{1}^{n} (t_{(2n+1)} - t_{2n})$

where n, is the time at where the contacts separate, or impact

and T_e, T_m are the total electrical and mechanical bounce times.

It was observed by Erk and Finke that during the make operation the arc voltage remains roughly constant, and equal to the minimum arc voltage. With reference to figure (2.4), with small contact gaps (< 0.1mm) the arc voltage holds close to the minimum arc voltage. Thus the statement can be made more general and related to the bounce displacement.

If (V_m) can be assumed constant, then for a d.c resistive load, the arc energy equation (2.10) can be simplified to give,

Eq. (2.24) $$E = V_m . I_a . T_e$$

where I_a = the arc current which is also constant,

and T_e = the total duration of the bounces with arcing,

Then over N cycles of make only operations,

Eq. (2.25) $$E_N = V_m \cdot I_a \sum_{1}^{N} T_e$$

where E_N = the total energy dissipated over N operations.

Hence the energy dissipated by the arc after first impact is proportional to the total duration of bounces for d.c conditions. For a.c condition the situation is complicated by the possibility of the arc extingishing due to zero current during a bounce.

Substituting for the arc current in terms of the steady state circuit current and voltage, gives

Eq. (2.26) $$E_N = V_m \cdot I_s \left(1 - V_m / V_s \right) \sum_{1}^{N} T_e$$

From which it can be concluded that if the contact separation time is measured, then this is an accurate method for monitoring the bounce phenomena in electrical contacts. Additionally by the use of equation (2.26) an evaluation of the arc energy dissipation can be achieved. The validity of the assumption of the minimum arc voltage remaining constant is considered experimentally in Chapter 5.

2.4.6 The Mechanical Suppression of Contact Bounce

The initial investigations into the support structure of fixed contacts, as undertaken by Barken, suggested that, the maximum percentage of incident kinetic energy transmitted into and retained within the

support structure could be optimised. If a means were provided for the rapid dissipation of this trapped energy, minimisation of contact bounce could be achieved. This lead L.Reiter, [74], to consider bounce with both contact members being coupled to additional light masses. This allows for a complete transmission of the initial kinetic energy into the mass absorbers.

Using a simplified model of the impact process, Reiter showed that it was possible to optimise the energy dissipation at impact, and thus increase the bounce suppression. This method proved successful and lead to a series of tests on switch contacts which showed significant reductions in wear.

The general application of these methods are however often not economically acceptable, because of the increased cost. This is particularly true in the medium duty range, where costs and the number of parts are designed to a minimum.

A further method of reducing the bounce would be to reduce the incident kinetic energy to a minimum, for a particular mechanism.

2.5 Contact Erosion and Contact Failure

In the following section the range of contact phenomena covered so far will be reconsidered in the context of contact erosion. Contact reliability is related to the wear processes at the contact surface, consideration is therefore given to ways of monitoring the wear and how the wear relates to failure.

The failure modes of electrical contacts are many and depend on the circuit and environmental conditions. Since the major problem with electrical contacts is their short and to some extent unpredictable life, a vast amount of research has been focused on this area. In this section, consideration will be given to switch contacts in the medium duty range.

2.5.1 Wear in Non-Arcing Contacts

The wear of sliding contacts is of major importance to electrical pickups of all types, for example carbon brushes in electric motors. However the interface considered in this thesis is only subjected to sliding in the sense of small amplitude slip motions. This is true of most types of switching contacts in this range, which are often subjected to a designed slip to provided clean contact surfaces after the make operation, [75].

In 1980 M.Antler, [76], detailed the erosion processes in metallic sliding contacts. In this paper a range of wear mechanisms were considered as applied to sliding contact, namely adhesion, abrasion, brittle fracture, fretting and delamination processes. The majority of these mechanisms are generally applicable to sliding contacts, however the fretting motion could be applicable to both connectors and switch contacts. In this paper fretting was defined as small amplitude oscillatory motions, which because of the limited motions, caused debris to accumulate between the contacts rather than emerging free. The wear debris from the base metals will contain products of the reaction with the environment, such as oxides and in this case the process is commonly termed fretting corrosion. It was observed that the oxide debris can cause substantial increases in contact resistance, and some experimental

results were presented to show how the increase was associated to the wearing through of noble metal plating.

2.5.2 Corrosion Mechanisms as Applied to Electrical Contacts

The mechanisms of corrosion are varied and often complex in their interactions, since more than one mechanism can be occuring at any instant.

Two different metals in contact will often react in such a way that the more base metal (i.e the metal more anodic in the electrochemical series, [77]) will corrode. In the case of the silver/ copper interface produced by plating shown in figure (5.7) any removal of the silver plate could lead to the anodic corrosion of the copper producing copper oxide.

Increases in the interface temperature as a result of Joule heating at the asperities can also increase the corrosion rate. In 1968 J.C Kosco, [78], considered the effect of the interface temperature rise due to contact resistance on the oxidation of electrical contact materials. The experimental evidence presented suggested that the temperature rise characterisics of various contact materials could be correlated to their oxidation behavior. The circuit breaker contacts considered were tested at the standard U.L (Underwriter Laboratories) endurance test, at the rated loading, with arcing present during the cycling. From the results it was concluded that the bulk electrical resistivity was of minor importance in determining the temperature rise characteristics, instead the surface resistivity which was strongly related to oxidation behavior was the dominant factor.

2.5.3 Mass Transfer in Switching Contacts due to Arc Erosion

Much work has been applied to the study of mass transfer and the associated phenomena during arcing, however some of the basic processes are not yet fully understood, because of the complex interactions of the various mechanisms. Some of the factors affecting the transfer are the materials, the environment, and circuit conditions. Holm, [79] distinguished four main types of erosion, or material transfer in switching contacts. 1) Mechanical degradation, usually small and insignificant in contacts subject to arcing. 2) Bridge material transfer or fine transfer. This type of erosion is not generally significant to contacts in the medium duty range, where full arc development usually occurs. 3) and 4) Material transfer due to arcing, with respect to the direction of transfer; the anode dominated arc, with erosion at the anode, and the cathode dominated arc with the cathode showing the most erosion. It was also identified that the transition from anode to cathode dominated arcs, appeared when the contact gap length passed a critical value. The mechanisms responsible for the arc erosion are not the subject of investigation in this thesis, however it is important to consider the influence of the erosion on the reliability of contact.

2.5.4 The Measurement of Contact Erosion

The actual measurement of contact erosion is difficult in that although the erosion can be measured and identified in terms of change of mass, the quantities of mass are often small, particularly in the medium duty range. Additionally the mass changes do not necessarily relate to the contact failure modes, since the measure gives no indication of the distribution of mass in and around the eroded areas. A solution to the

problem of mass distribution was approached in 1979 by J.Wolf, [80], and P.J White, [81], using a method of measuring the electrode erosion based on the use of a scanning surface analyser. With this method it was possible to monitor the surface degradation in terms of volume changes from a fixed datum line, usually the contact shape when unused. The method was used in 1980 by P.J White and D.J Mapps to show that there is a d.c current (8 Amps at 40 volts), where there is no net transfer between the anode and cathode contacts. It was also shown that for break arcs, the direction and the amount of material transfer was a function of the power dissipation occuring in the anode and cathode fall regions, [82]. These results support the statement of H.W. Turner and C. Turner, who suggested that the amount of material removed was not directly proportional to the arc energy dissipation but only that part of the energy close to the contact surface, [83].

2.5.4.1 Erosion as a function of Mass Change

It has been traditional in the evaluation of erosion to consider the amount of erosion as a function of mass change. To establish some relation between circiut conditions and erosion Carballeria et al, in 1982, [84], and 1984, [85], considered empirical relationships between the weight loss and the current intensity at make and break in the form,

M = f (I(make) , I(break)) : where M = the mass loss,

They showed in their test system that the erosion at break, holds a linear relation with the number of cycles,for a given contact material, and a.c current. The materials considered were Fine Silver, AgCdO (88/12 sintered), (88/12 internal oxidised), and Silver Graphite (95/5). Using

the least squares method they were able to determine empirical relations for a range of contact materials. In the case of the make only cycles the erosion rate was found to change with the number of cycles during the test. The physical meaning of this non-linear relation was suggested to be partly due to the "metallurgical evolution" of the contact surface, however some surprise was expressed at the continuous evolution after several thousand operations.

In 1982 a further paper on this subject was given by J.Muniesa, [86], who considered the correlation between this type of accelerated life test and real switch contacts. The equipment used was similar to that used by Carballeira, however arc energy was also monitored. The relationship between wear rate and the number of cycles again proved to be linear for the a.c circuit conditions considered. The relationship between the arc anergy dissipated and wear rate however showed that for a given energy dissipation the wear at closing the contacts is up to ten times greater than at opening in the field of energy considered, (0.1J - 100J). This observation, "can only be explained by totally different erosion processes during the bounce and at opening". Some suggested mechanisms were local high pressure with explosions, and the effect of molten metal being ejected during the bounce. Comparisons made with theoretical relations between arc energy and mass changes, showed that the wear rate is up to 100 times smaller than that predicted. This difference was explained by large redepositing, with metal vapourizing and redepositing away from the arc on the contact surface. It was concluded that the empirical laws of erosion could not be applied to the general case because of the dependance on the type of contact and the contact shape.

2.5.5 The Evaluation of Contact Failure

In the evaluation of failure, mass changes are often considered because most contacts are plated with expensive noble metal, usually silver based for the medium and higher current ranges. Since the change of mass represents the degradation of the surface it is often related to the eventual failure of the contacts. The redepositing discussed by Muniesa, however can cause some confusion since the mass could remain constant and just redeposit around a crater. It is therefore suggested that the volume method would lead to a more accurate assessment of contact degradation. Some further failure modes are.

1) Failure due to Welding of the contacts. This phenomena is usually associated with currents outside the medium duty range, and is commonly split into Dynamic and Static welding, [87]. It can be associated with the degradation of the contacts, defined in terms of mass or volume changes.

2) Mechanical Failure of the device. This is often ignored because of the more significant electrical problems, however sound mechanical design is important to overcome fatigue, or the dislocation of moving parts.

3) Overheating. The problem of overheating is generally not a problem of total failure, but is more often associated to the failure of switches to satisfy international standards. For example B.S 3955, [88], requires that after the endurance testing of the switch contacts the switch should be temperature rise tested at (1.1x) the rated current and the terminals should show equilibrium temperatures of less than ($50^{\circ}C$). A switch failing this test would fail to be approved, with the associated economic repercussions. Thus the contact resistance changes associated with the

arc erosion are of major importance, since the temperature rise is a function of the increase in contact resistance, [89]. Therefore the dependance of the arc erosion on the mass changes can be of significance because of the exposure of the base material usually copper, and the associated increase in contact resistance.

Additional aspects of the contact erosion phenomena have been considered by H.W Turner and C. Turner, [90], for example, concentration of burning in one area resulting in non-uniform damage, or distortion of the contact surface.

2.5.6 The Monitoring of Contact Resistance as a Function of Contact Erosion

It has been reported that the temperature rise problem associated with the failure of devices to meet standards, results from the increase in contact resistance. The monitoring of the resistance therefore constitutes a further means of monitoring the surface degradation. Such methods have been used extensively in preference to the more difficult task of monitoring mass or volume changes.

2.6 Switch Dyna mics and Contact Erosion

The study of switch dynamics is not an area of pure research, and is an area that is traditionally the realm of the manufacturing company's design engineers. The methods used in the consideration of switch dynamics are in the main based upon empirical relations, and when confronted with optimisation requirements, these often fail to be of use.

The recent developments in the availibility of computer time and software, could however have an important impact in this area.

The importance of switch dynamics to the reliability of the interface is often disregarded, however the contact motions play a significant role in the duration of arcing. The opening characteristics of electrical contacts can play an important role in the eventual erosion of the contact surface, since the arc length is controlled by the contact gap, and therefore velocity. On impact the dynamics is similarly important as identified in section 2.4.5, since the incident kinetic energy is a function of the incident velocity squared, and to some extent controls the magnitude of the bounce duration in a given system.

There have been relatively few papers in this area, however with the possibilty of complex mathematical models being solvable by the use of numerical methods and in particular finite difference methods, substantial advances could be made in optimising opening and closing velocities. As with most apparently simple devices, the rocker switch in operation exibits a complex interaction of moving parts. As a forward to the work undertaken in this thesis, D.J Mapps, et al, [91], considered the interaction of the hand operated actuator, in the switch dynamics of the moving contact, and suggested some theoretical relations between the relative motions and the switch geometry. This analysis assumed that the moving blade contact was of zero mass, and inertia.

The dynamics of relay contacts have been considered in detail by A.A Slonim, [92], who considered the theoretical analysis of bounce mechanics much in the same way as Erk and Finke, however the eighth order nonlinear differential equations used to describe the contact motion were here simplified to an approximate system of fourth order linear equations.

Using this method a good comparision was obtained with the experimental results of contact displacements.

2.7 The Nature of this Investigation

This investigation originates from the need to reduce erosion between the blade and pivot in snap action rocker switches. In the initial investigation presented in chapter 4, the study of the switch dynamics identifies that the main cause of the pivot erosion is the transient separations or bounce occurring at the interface. To reduce this separation, and simultaneously improve the overall life of the rocker switch, a model of the switch dynamics is presented in chapter 4, with the aim of reducing the kinetic energy in the system at main contact impact. The kinetic energy can then be related to the pivot bounce and pivot erosion. This relationship is by definition a mechanical relation in that the application of current to the bounce would change the bounce as identified in this chapter.

To monitor the effects of current on bounce a fully automated test system is presented in chapter 3, with the results presented in chapter 5.

REFERENCES TO CHAPTER 2

[1] F.P Bowden, D. Tabor,Friction, Heinemann London, 1974, pp 18.

[2] J.B.P Williamson, "The Microworld of the Contact Spot", in Proc. Holm Conference on Electrical Contacts, 1981, pp 1-10.

[3] R. Holm, Electric Contacts, Springer-Verlag, Berlin/Heidelberg, 1967, pp 110.

[4] K.L. Johnson, "One Hundred Years of Hertz Contact", Proc Instn Mech Engrs, Vol 196, 1982, pp 363-378.

[5] B. Lincoln, Brit. J. Applied Physics, Vol 3, 1952, pp 260.

[6] M.H. Jones, R.I.L Howells, S.P Probert, "Solids in Static Contact", Wear, vol 12, no 4, 1968, pp 225-240.

[7] J.A Greenwood, J.H Tripp, "The Elastic Contact of Rough Spheres", J. of Appl. Mechanics, ASME, March 1967, pp 153-159.

[8] F.P Bowden, D. Tabor, The Friction and Lubrication of solids, Clarendon Press, Oxford, 1964, Part 1, pp 11.

[9] Holm, pp 8.

[10] as ref [2].

[11] J.C Kosco, "The Effects of Electrical Conductivity and Oxidation Resistance on Temperature rise of Circuit Breaker Contact Material", in

Proc. Holm Conf. on Elect Contacts, 1968, pp 55-65.

[12] R. Currence, W. Rhoades, "Predicting, Modeling and Measuring Transient Resistant Changes of Degraded Electrical Contacts", in Proc. Holm Conf. on Elect Contacts, 1983, pp81-103.

[13] J.H Whitly, R.D Malucci, "Contact Resistance Failure Criteria", in Proc. Holm Conf. on Elect Contacts, 1978, pp 111-116.

[14] "Construction and the use of a Probe for Measuring Electrical Contact resistance", ASTM B 667-80, Vol 03.04, pp490-493.

[15] L. Jedynak, "Instrumentation for Measuring Dry-Circuit Contact Resistance", in Proc. Holm Conf. Elect Contacts, 1974, pp 165-169.

[16] R. Schnabl, H. Becker, "Microprocessor Controlled Contact Resistance Probe for Manufacturing Control and Development", in Proc. Holm Conf. Elect. Contacts, 1981, pp 131-138.

[17] H.W Turner, C. Turner, "Static Welding of Double-Break Contact Systems", in Proc. Int. Conf. on Elect. Contacts, 1976, pp 239-244.

[18] Holm, pp 46.

[19] as ref [8] Bowden, Tabor, pp 29.

[20] Holm, pp 43.

[21] Holm, pp 64

[22] F.Llewellyn Jones, The Physics of electrical Contacts, 1957, pp 17-18.

[23] M. Sato, "Studies in Silver Based Electrical Contact Materials", Trans. of Nat. Research Inst. for Metals, Vol 18, No 2, 1976, pp 65-83.

[24] Holm, pp 438.

[25] R.S Timsit, "On the Evaluation of Contact Temperature from Potential Drop Measurements", in Proc Holm Conf. Elect Contacts, 1982, pp 147-154.

[26] Holm, Chapter 8.

[27] W. Chow, "Crossed Rod and Practical Electrical Contact Constriction Resistance Correlation", in Proc. Holm Conf. on Elect Contacts, 1967, pp 53-65.

[28] A.S.T.M, Designation B 539-80, "Measuring Contact Resistance of Electrical Connections (Static Contacts)", ASTM 1985 Annual Book of Standards, Section 3, Volume 03.04, Metals Test Methods and Analytical Procedures, pp 424-435.

[29] A.S.T.M, Designation B 497-84, "Measuring Voltage Drop on Closed Arcing Contacts", as Ref [28], pp 418-420.

[30] M. Antler, "Measurement of Contact Resistance", Book, pub, Chapter 26, pp 334-344.

[31] as ref [30] Antler, pp

[32] R.S Gibbons, "Measuring True Contact Resistance", New Electronics, May 31st, 1983, pp 52.

[33] H.R Hopkins, R.H.Jones, "Transients, Bridges, Micro-arcs and Metal Transfer in Low Voltage Electrical Contacts", Proc. of the 6th Int Conference on Electrical Contact Phenomena, 1972, pp 399-406.

[34] as ref [22], Chapter 3.

[35] Y. Hayashi, M. Baba, T. Hara, "Study of Bridge Phenomena of Sn-Rh and Rh-Sn-Rh Contacts for Dry Reed Switch", in Proc. Holm Conf. on Elect. Contacts, 1978, pp 541-547.

[36] Price, L. Jones, Brit J. Appl. Physics 2, 1969, pp 589.

[37] A.E Guile, "Arc Electrode Phenomena", Proc. IEE Reviews, Vol 118, No 9R, Sept 1971, pp 1129-1154.

[38] as ref [37], Guile.

[39] A.E Guile, "Electric arcs: their electrode processes and engineering applications", IEE Proc., Vol 131, Pt A, No 7, sept 1984, pp 450-480.

[40] Holm, pp 280.

[41] Holm, pp 281, and 423.

[42] Holm, pp 282.

[43] D.J Dickson, A. von Engel, " Resolving the Electrode Fall spaces of Electric Arc", , pp 316-325.

[44] Holm, pp 440.

[45] Sato, as ref [23].

[46] P.J White, "Investigation of Parameters Affecting the Operating characteristics of Toggle-Switches with Silver-Cadmium-Oxide Contacts", Ph.D Thesis, Plymouth Polytechnic, 1979.

[47] Holm, pp 297.

[48] Holm, pp 283.

[49] T.Schmelcher, Low Voltage Switchgear, Heyden & Sons Ltd, London, Chapter 4.

[50] C.H Chen, "Arc reignition Phenomena of Silver Cadmium Oxide Contacts", in Proc. Holm Conf. Elect. Contacts, 1981, pp 45-50.

[51] as [49], pp 35.

[52] P.J White, D.J. Mapps, G.B Rossi, "Zero Current Synchronisation of Opening Switch Contacts", in Proc. Holm Conf. Elect. Contacts, 1985, pp 185-190.

[53] as [49], pp 16.

[54] Holm, pp 276.

[55] L.H.Germer, "Physical Processes in Contact Erosion", J. Appl. Phy, Vol 29, No 7, July 1958, pp 1067-1082.

[56] P. Barkan, "A Study of the Contact Bounce Phenomenon", IEEE Trans. on Power App. and Systems, Vol PAS 86, No 2, Feb 1967, pp 231-240.

[57] Bowden, Tabor as ref [8], pp 258-260.

[58] D. Tabor, The Hardness of Metals, Oxford Clarendon Press, 1951.

[59] W. Goldsmith, C.H. Yew, "Stress distributions in Soft Metals due to static and dynamic loading by a steel sphere", J. Appl. Mech, Vol 31, Dec 1964, pp 635-646.

[60] as ref [55].

[61] W. Goldsmith, Impact, London Arnold Press, 1960, pp 249.

[62] V.A. Erk, H. Finke, "Uber die mechanischen vorgange wahrend des Prellens einschaltender Kontaktstucke", (The Mechanical Processes of Bouncing Contacts), E.T.Z Electrotect, Vol 5, 1965, pp 129-133.

[63] V.A Erk, H. Finke, "Uber das Verhalten unterschiedlicher Kontaktwerkstoffe beim Einschalten prellender Starkstrom-Schaltglieder", (The Behavior of different Contact Materials for Bouncing Contacts), E.T.Z Electrotect, Vol 9, 1965, pp 297-306.

[64] J.L Meriam, Engineering Mechanics Vol 2, Dynamics, John Wiley & Sons, London, 1978, pp 190-191.

[65] Goldsmith, as ref [60].

[66] Barken, as ref [55].

[67] Goldsmith, as ref [60], pp 257-267.

[68] Bowden, Tabor, as ref [8], pp 265.

[69] Holm, pp 440.

[70] Barkan, as ref [55].

[71] B. Sandler, A.A. Slonim, "Experimental Investigation of Relay Contact Dynamics", IEEE Trans. CHMT, Vol CHMT-3, No 1, March 1980, pp 150-158.

[72] A.A Slonim, "Analytical and Experimental Analysis of Nonlinear Bouncing Contacts", in Proc. Holm Conf. Elect. Contacts, 1984, pp 531-537.

[73] B. Miedzinski, Z. Okraszewski, D. Hajducka, T. Zolnierczky, "The Effect Of Contact Surface Conditions on Reed Bouncing", IEEE Trans. CHMT, Vol CHMT-8, No 1, March 1985, pp 202-206.

[74] L. Reiter, "Suppression of Contact Bounce by means of Kinetic Resonance Absorption", Proc. Holm Conf. Electrical Contacts, 1978, pp 457-461.

[75] Electrical Engineering Data, Johnson Matthey Metals Limited,

Catalogue 1300, pp 503.

[76] M. Antler, "Sliding Wear of Metallic Contacts", Proc. Holm Conf Electrical Contacts, 1980, pp 3-25.

[77] Gosta, Wranglen, "An Introduction to Corrosion and Protection of metals".

[78] as ref [11]

[79] Holm, Chapter 56.

[80] J. Wolf, "Erosion and Material Transfer Measurement with the aid of a Surface Analyser", Proc. Holm Conf Electrical Contacts, 1979, pp 69-74.

[81] as ref [46]

[82] D.J Mapps, P.J. White, "Performance Characteristics of Snap-Action Switches with Silver-Cadmium-Oxide Contacts", Proc. Holm Conf Electrical Contacts, 1980, pp 177-184.

[83] H.W. Turner, C. Turner, "Contact Erosion and its Implications", Proc. Holm Conf. on Electrical Contacts, 1978, pp 1-8.

[84] A. Carballeira, J.M Clement, J. Galand, "Erosion Characteristics at Make and at Break of Contactor Contacts", Int. Conf. on Electrical Contact Phenomena, 1982, pp 175-179.

[85] B. Belhachemi, A. Carballeira, "Influence of Delay and Duration of

Bounce on Erosion Weldability and Resistance in Relay Contacts", Proc. Holm Conf. Electrical Contacts, 1984, pp 475-483.

[86] J. Muniesa, "Contact Erosion: Testing machine and Switching Devices", Proc. Holm Conf. Electrical Contacts, 1982, pp 127-133.

[87] as ref [17]

[88] "Specifications for Electrical Controls for Household and similar general purposes, Part 3, General and Specific requirements", B.S 3955, Part 3, 1979.

[89] as ref [11]

[90] as ref [83]

[91] D.J. Mapps, P.J White, G. Roberts, "Pivot Contact Behaviour in Snap-Action Rocker Switches", Proc. Holm Conf Electrical Contacts, 1982, pp 219-225.

[92] as ref [72].

CHAPTER 3

EXPRIMENTAL APPARATUS AND TEST METHODS

This chapter describes the equipment and methods used in obtaining the experimental results presented in this thesis. It also includes the design and develop ment of the experimental apparatus used and focuses on a computer based automatic test system designed to monitor a range of electrical contact phenomena in switching contacts.

3.1 High Speed Photography

High speed photography has been used for many years in the study of electrical contact phenomena. This photographic method enables the switch designer or researcher to study the details of switch dynamics and electric arc behavior, characterised by typical operation times of a few milliseconds. From the films produced, details of displacement against time can be obtained, enabling an analytical study of the events photographed [1]. The high-speed camera used in this research is a rotating prism camera, manufactured by John Hadland (U.K); it is shown in figure (3.1) with the associated test apparatus. The camera uses 16 mm double perforated film. The camera mechanism shown in figure (3.2) is based on a rotating prism, shutter assembly. The fan shutter controls the film exposure while the rotating prism directs the image on to the moving film. Using this equipment, speeds of up to 11,000 frames/second can be achieved using a full 16 mm frame, and up to 44,000 frames/second using

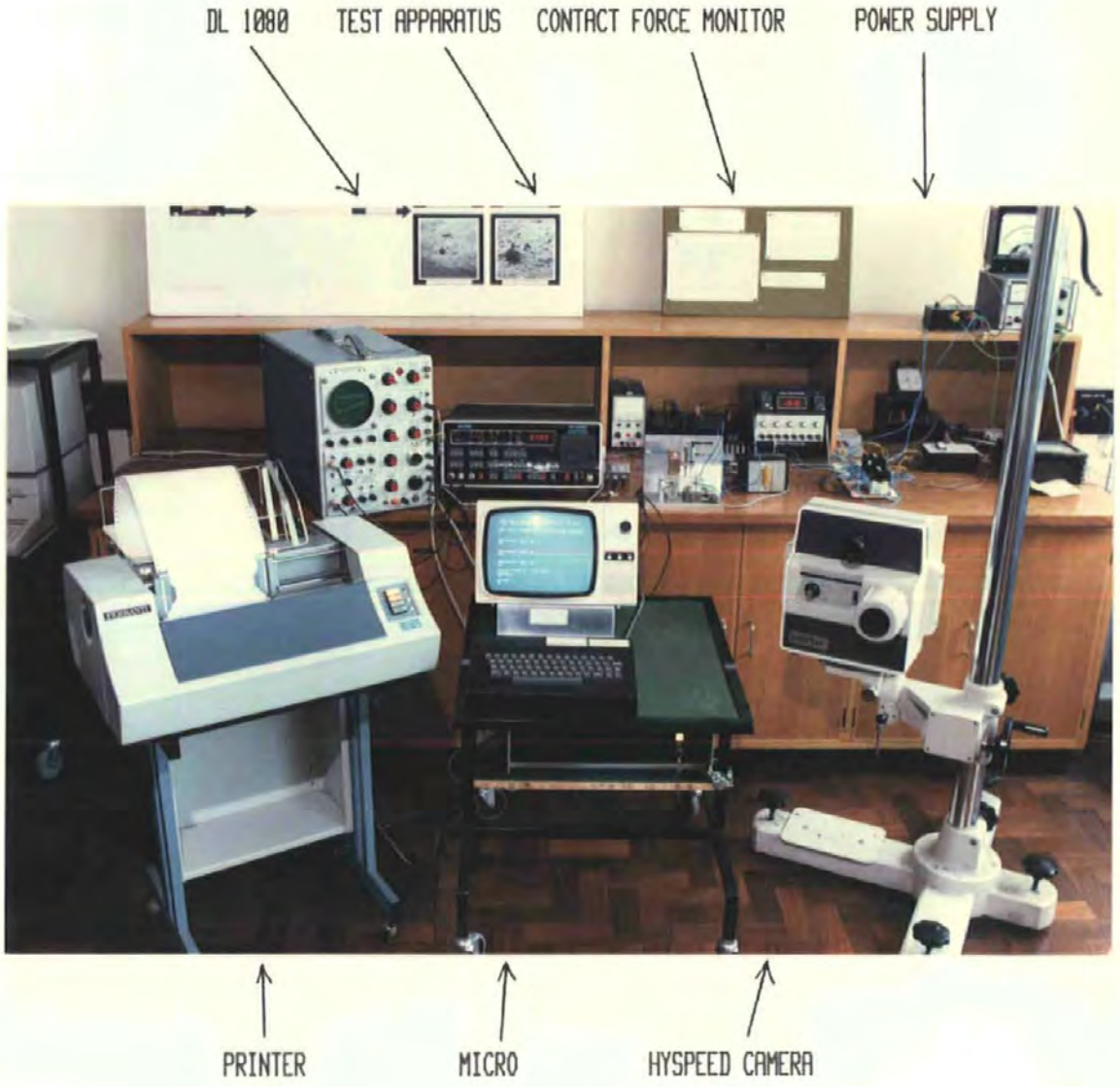

Fig 3.1 The Automatic Test System and Associated Apparatus

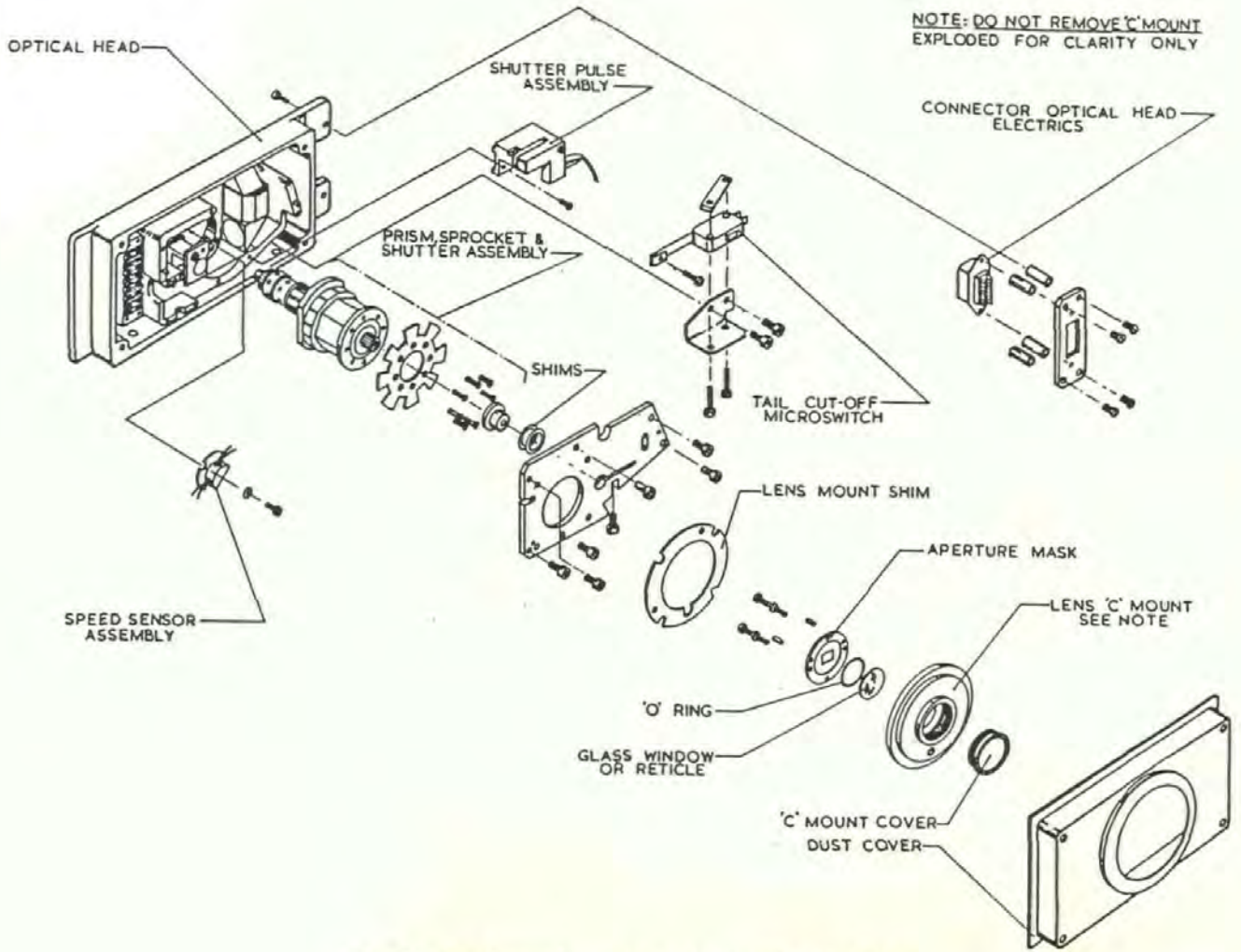

Fig 3.2 The hyspeed camera, rotating shutter and prism mechanism

quarter frame [2]. To achieve 11,000 frames/second takes approximately 1.69 seconds and 75 metres of film, and once achieved generates 11 pictures/millisecond. In this work for the sake of economy, 30 metre lengths of film have been used, enabling speeds of up to 8,000 frames/second, in 1.04 seconds, as shown in figure (3.3). For the purpose of an accurate analysis of the films the camera automatically imprints a small light pulse on the edge of the film every millisecond. These points then act as reference points when the film is studied. With film durations of approximately one second, synchronisation is required with the event being filmed. This can be achieved by setting an internal event relay to trigger at a given length of film, thus allowing a solenoid to activate the required event.

The high speed of the film, and the associated short exposure time requires that sufficient light is available to create an image. This is achieved by the use of four 250 Watt projector bulbs in series, each bulb being complete with a parabolic reflector. The bulbs are mounted so that the light could be adjusted for maximum effect.

3.1.1 The Methods used in the Study of Rocker Switch Dynamics

To study the events occuring during the switching action of a rocker switch, the switch was first sectioned, revealing the mechanism, as shown in figure (1.4). The camera picture was framed around the mechanism using a selected lens, typically a standard 50mm lens with a series of extension tubes. For the purpose of an in depth study of the switch dynamics, the camera was operated at the maximum speed for the length of film used, thus enabling only single operations of the switch to be captured on a given film. The associated solenoid and switch arrangments are shown in figures

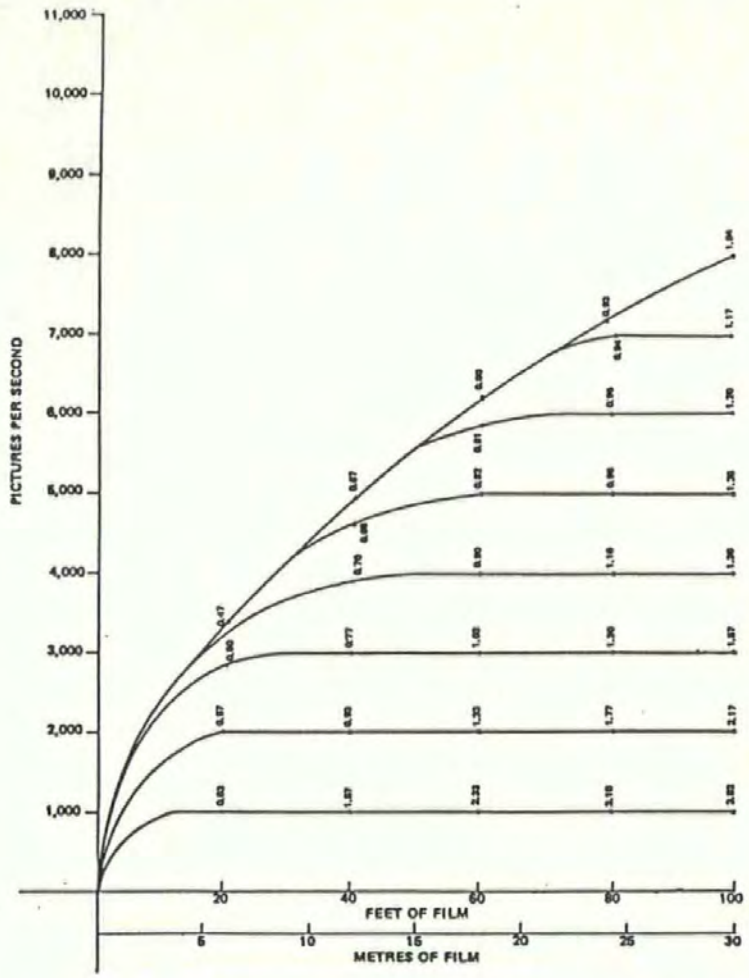

Figure 3.3 The Film Speed Curves for 100 feet of Film, Showing the Elapsed Time

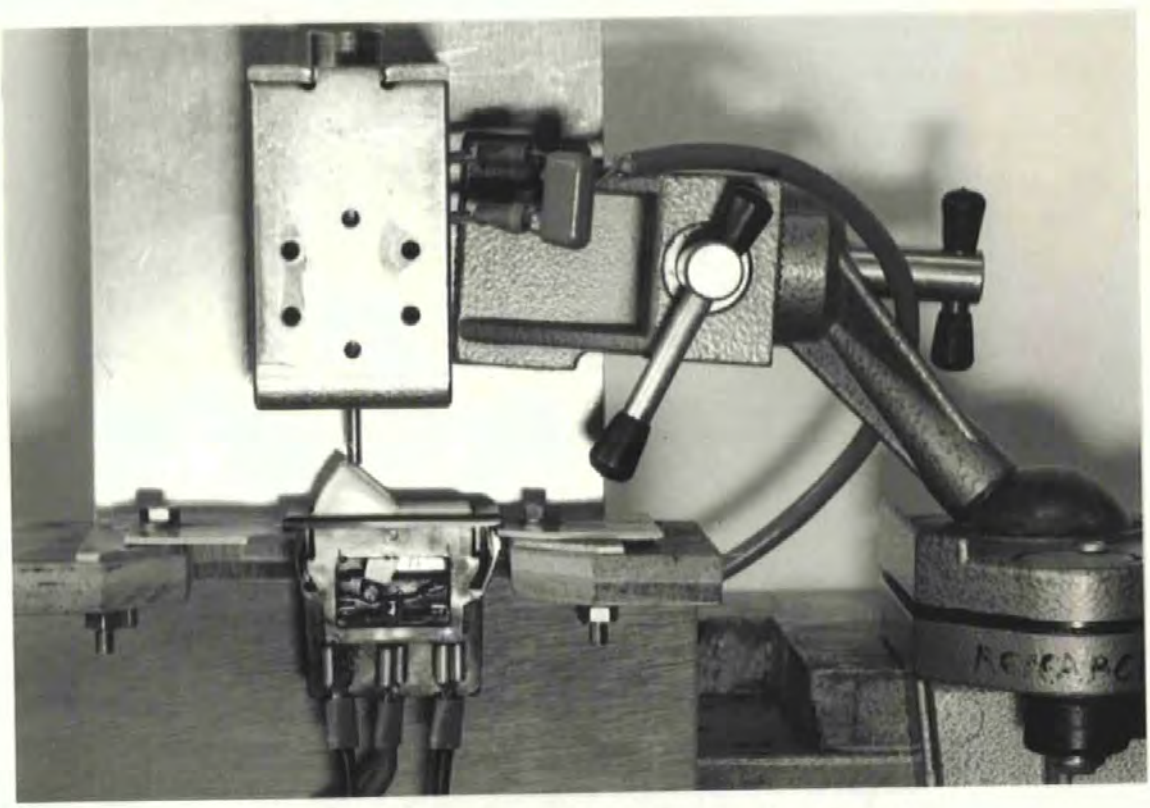

Figure 3.4 The Solenoid Operated Rocker Switch in Mounting

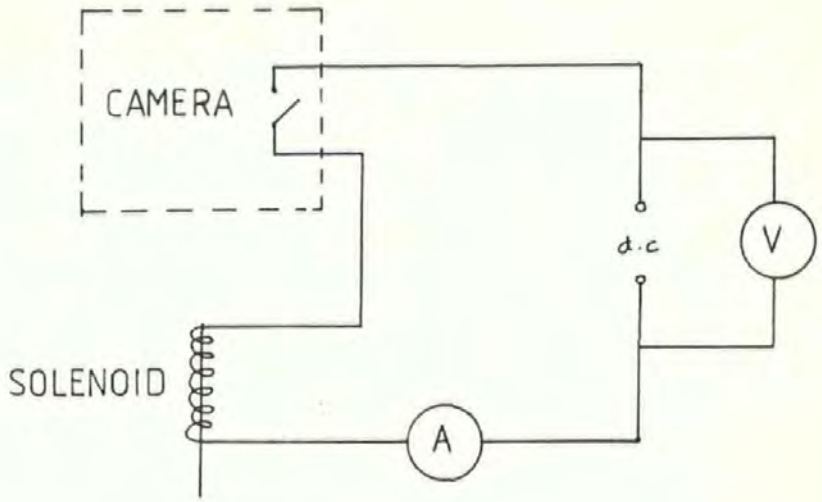

Figure 3.5 Schematic diagram of the solenoid circuit in series with the Highspeed Camera

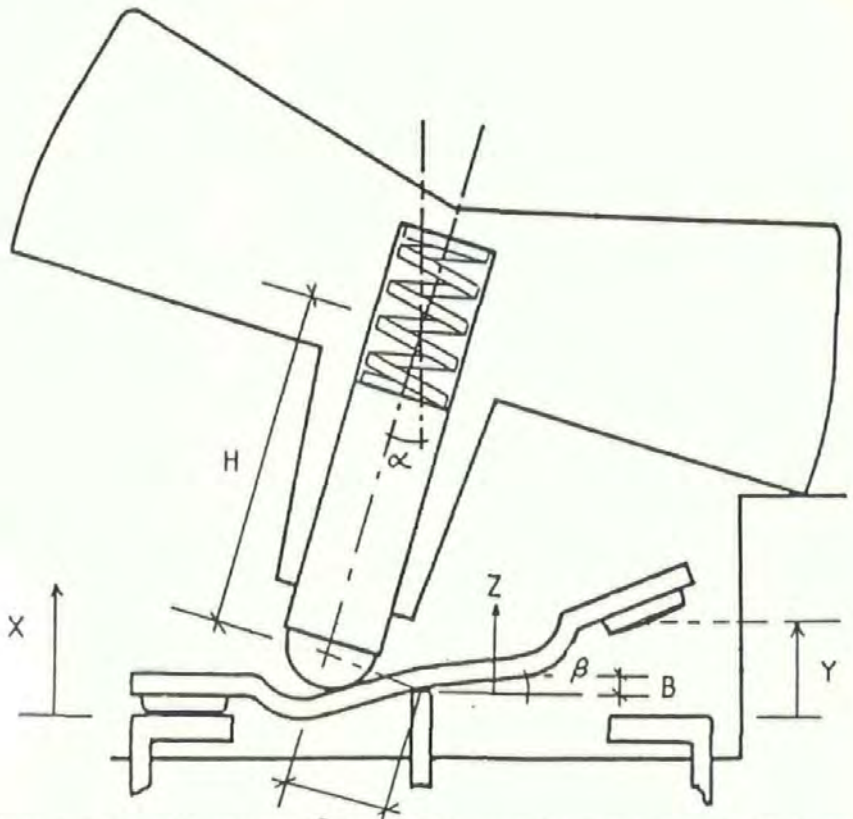

Figure 3.6 The data collection parameters used for the study of rocker switch dynamics

(3.4) and (3.5) The event synchronisation was typically set for 18 meters of elapsed film, thus closing the internal relay and activating a solenoid which in turn operates the rocker switch.

On development the films were analysed frame by frame to give data on the displacement characteristics. To facilitate the measuring of this data a small mark was used on the plunger as reference point; from this piont the displacements (H), and (S) shown in figure (3.6) could be taken. In addition the displacements (X), (Y), (Z), and (B) were taken. Using a computer programme detailed in Appendix 2, the measured dimensions are converted to give the spring extension (x), the plunger displacement angle α, and blade or moving contact displacement angle, β. The value of Z relates to any separation occuring at the pivot interface.

3.1.2 The Method for the study of the Test Apparatus Dynamics

The photographic studies of the automatic test system were based on the method above, however in this case the solenoid system is part of the apparatus. In this case the camera actuation and event synchronisation were controlled from a computer interfaced to the test system. The study of the contact bounce displacements, undertaken on the apparatus, necessitated the use of a macro lens with extension tubes. To monitor the displacements as accurately as possible, a back lighting method was used so as to silhouette the contacts against the background.

3.2 The Monitoring of Switching Transients

In addition to the visual observations and measurements made with the high speed camera, voltage, and current transients occuring during make and break operations can be used. The transients were captured on a Data Lab 1080 transient recorder (referred to in this thesis as a DL1080). The transient recorder enables the transients which occur during switching to be digitised and stored. After capture the transients are presented for continuous display by CRO; or alternatively they can be used for analogue readout to an X,Y plotter, digital storage on an internal cassette recorder or digital output to an external processor. The DL1080 is a multi-purpose dual channel recorder with a major feature that enables full remote sensing and/or control of all the instrument parameters; via a serial, parallel or General Purpose Interface Bus (GP-IB). The number of samples stored per cannel is 4096; changing the sample length thus changes both the sweep time and the maximum and minimum frequencies that may be stored. The DL1080 allows a maximum sampling rate of 20 MHz, which corresponds to a minimum sample length of 0.05 μs. The amplitude resolution is one part in 256 ,[3]. Every function of the DL1080 may be sensed and controlled by a computer via the various interfaces, this allows the assembly of powerful computer controlled instrument configurations in which fully interactive control is possible. The DL1080 also allows for full memory access, thus both storage channels may be transfered and processed externally. These advanced facilities have enabled a fast and accurate automatic test station to be developed, measuring a number of electrical contact phenomena, including arc energy and contact resistance. Figure (3.1) shows the DL1080 with the computer and associated test apparatus.

The computer used as a controller, processor and storage medium was a

Research Machines 380Z, refered to as an (R.M.L), [4]. This computer is an 8 bit processor based upon the Z80 chip. The computer has a range of input/output ports and facilitates a range of interface methods.

3.2.1 The DL1080 and GP-IB Interface

The DL1080 is used in three configurations in this work. These are as follows :

(1) - As a monitor of electrical transients in switches, in particular the rocker switch. In this configuration the DL1080 is used as a storage device, and uses a standard oscilloscope as a monitor for displaying the digitised traces.

(2) - As a monitor of electrical transients in switches, controlled by an external processor. In this mode, the processor arms the recorder and waits for the transients; these could be either manual or solenoid activated. On triggering the traces are again monitored by ocsilloscope and subsequently transferred to the processor memory for evaluation after storage.

(3)- As a monitor of electrical transients in an automatic test system. In this mode, the DL1080 has the same role as in (2), however, the whole experimental system is externally controlled by the processor and fully automated.

The interfacing of the processor and DL1080 is achieved by the use of the GP-IB interface. This bussing system allows a variety of electronic measuring and test instruments, which may well be from diverse

manufacturers, to be connected in parallel by means of standard ready made cables and connected to a controller. The GP-IB follows the standard IEEE-488 bus [5], which is based on a 16 line bus, capable of connecting up to 15 devices. The software controlling the bus is presented in appendix (3) and is based on a previous project, [6].

3.2.2 The Circuit for Monitoring Switch Transients in a Rocker Switch

The monitoring of the electrical transients in the rocker switch is made difficult by the requirement to investigate both the main contact and pivot contact behavior. In order to separate these electrical events, the circuit shown in figure (3.7) was used. This shows a circuit for monitoring the no arc condition on switching. A further circuit was used to monitor the characteristics with arcing. The connection to the moving blade contact maintains a measurable voltage across the contact gaps. On the condition where both are open circuit, a measurable voltage of (1 volt) is recorded. In this configuration both channels of the DL1080 are used to monitor the pivot and main contact switching voltages.

Using the circuit in figure (3.7) it is possible to determine switching times to support the times observed and recorded with the photographic technique. Figure (3.8) shows a typical transient response for a Rocker switch. At A, the main contacts open without an arc, to the open circuit potential. At B, the opposite main contacts close, thus defining the change-over time. There follows a period up to E in which the main contacts bounce. The bottom trace shows the corresponding pivot contact disturbance which is further discussed in chapter 4.

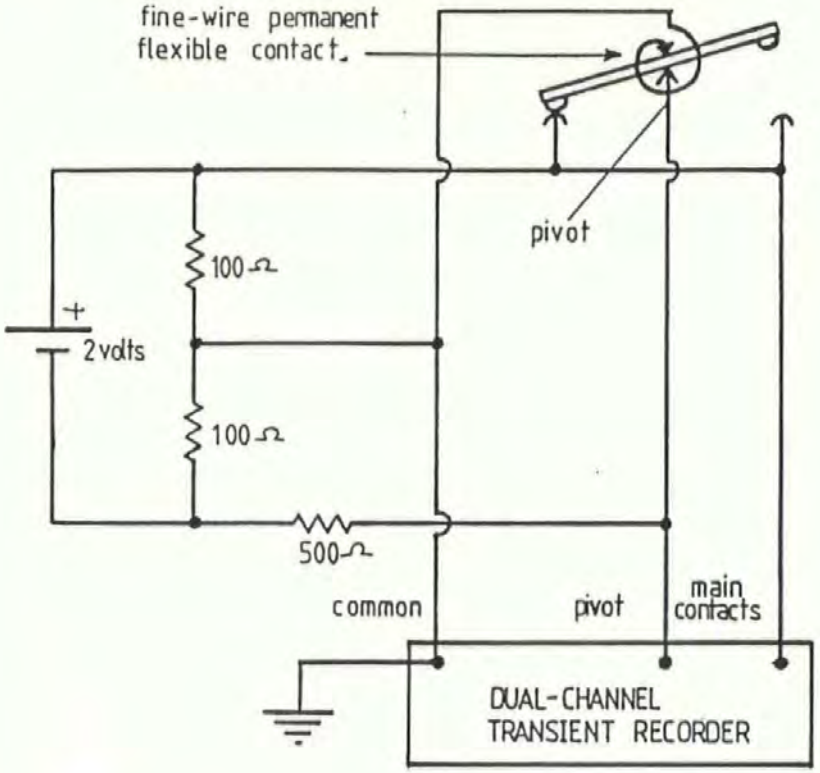

Figure 3.7 The Circuit Diagram of the Electrical Arrangement for monitoring both Pivot and Main Contact Seperation

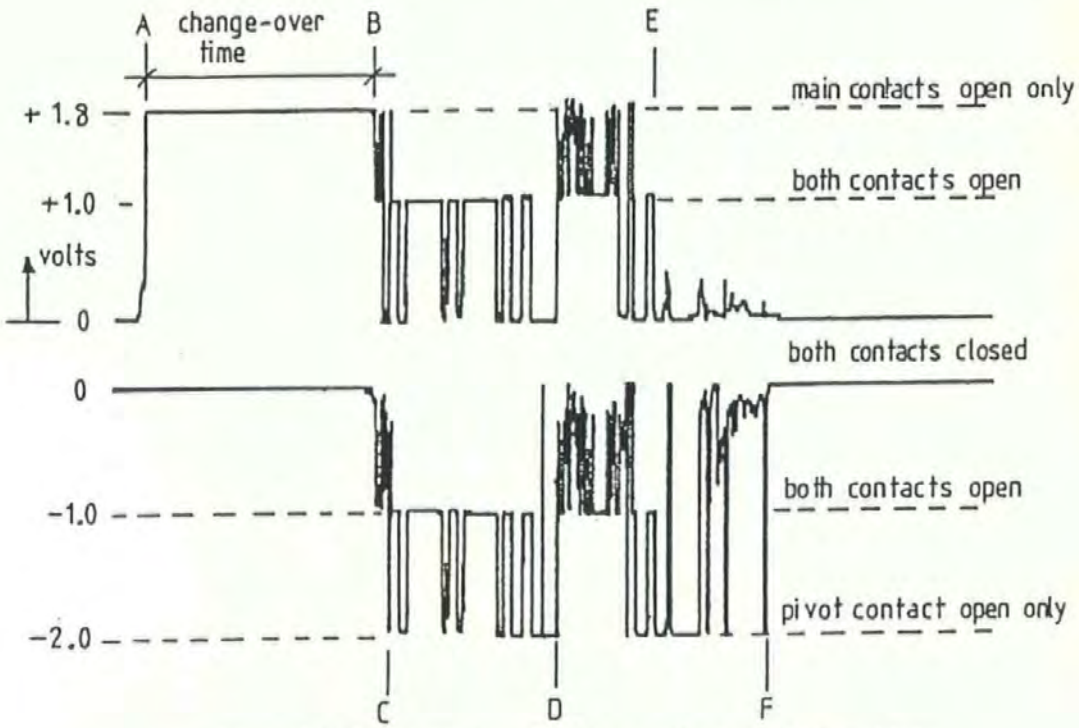

Figure 3.8 Transient Recorder Traces of a typical Switching Operation using the circuit of figure 3.7

3.3 Switch Testing Methods

Testing plays a significant role in the design and development of switch gear, and all manufactured devices must be designed and perform to the relevant standards [7]. To test the performance, prescribed test conditions are given in the relavent standard. For the rocker switch, the applicable standard in the U.K. is BS.3955: part 3. Under this specification, a switch should be tested at its maximum loading over a number of cycles, typically 10,000. Under section 17.1.4 the test conditions are given as "The speed of movement of the actuating means shall be a linear velocity of 25 +/- 2.5 mm/second",[8]. This is achieved in practice by cam operated rods which activate the rocker as shown in figure (3.9). The actuating rod is reversed by springs attached to the frame, thus maintaining contact with the cams and switching the rocker back to its original state. Initial experiments on this type of apparatus showed that the time taken for the rocker switch to complete its operation was considerably greater than the time taken when switched by hand. Table (3.1), shows some of these results for new switches of the same type by the comparison of the changeover times. The range of values given on the standard test rig are a consequence of the position of the switch with respect to the activator, [9]. To overcome this time difference and recreate accurately the manual function, two further test methods have been developed.

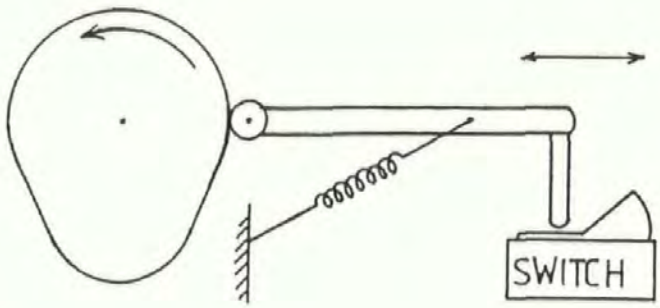

Figure 3.9 The standard cam operated test system used for endurance testing

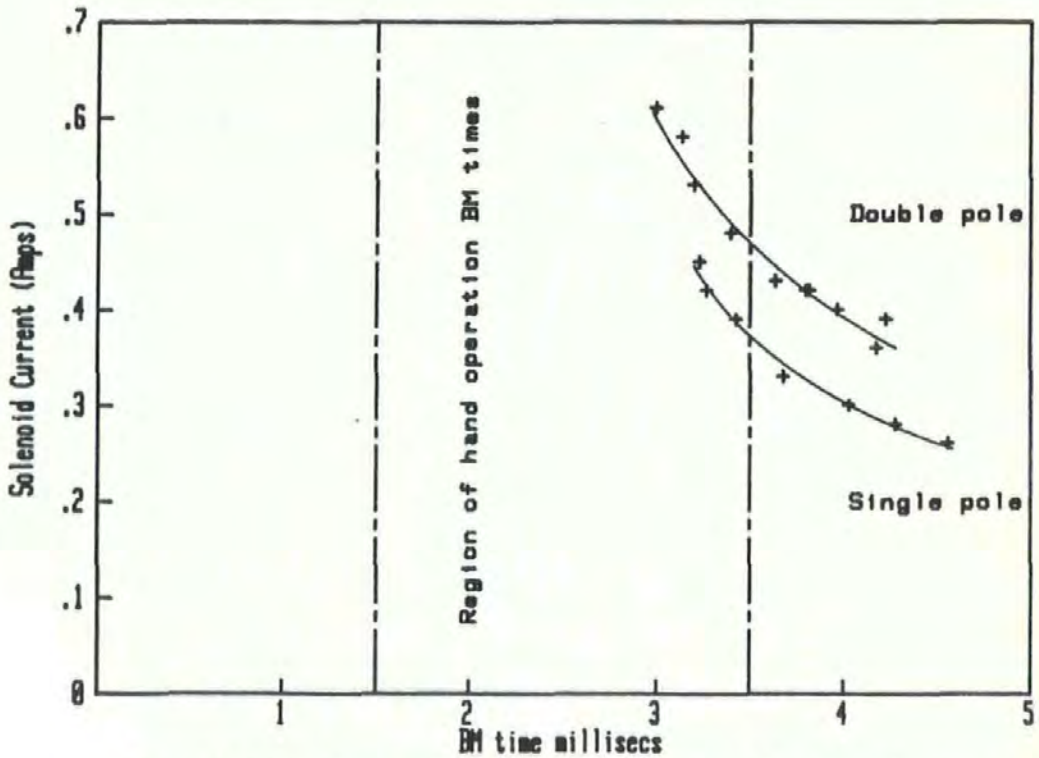

Figure 3.10 The BM time of the Rocker Switch versus the solenoid current

	c/o Time (ms)
Switch, A	14.71
Switch, B	11.48
Switch, C	11.99
Hand operation	2.5

Table (3.1), A comparison of the mean changeover times (c/o).

METHOD 1. To enable an accurate representation of hand activation for a single operation, the rocker switch was mounted in a frame and activated by a controlled solenoid, as shown in figure (3.4). This method both recreates hand activation times for a given switch, and allows for synchronisation with high-speed film recording. The force and speed of activation is controlled by the current supplied to the solenoid. Figure (3.10), shows the variation between supplied current and changeover time for a particular rocker switch and also shows the band applicable to hand activation. It clearly shows that the changeover time or BM time (the Break /Make time as it is refered to in this thesis) is directly affected by the speed at which the rocker is activated. This method is used for single operation studies of the mechanism.

Method 2. To enable an accurate recreation of hand activation for endurance testing, a system has been designed based on pneumatic control of the activating rods. This work was undertaken in a separate project [10].

3.4 An Automatic Test Station to study Electrical Contact Phenomena

The availabilty of powerful low cost micro-computers has made possible the development of dedicated automated test stations. This has lead to a number of developments in the field of electrical contacts research.

3.4.1 A Review of Automated Test Systems and the Evaluation of Arc Energy

Automated test systems for the study of electrical contacts typically facilitate studies of erosion and surface changes with respect to the numbers of cycles completed. In this way it is possible to identify the number of cycles to failure, and study the failure mechanisms.

The methods of computer controlled monitoring of electrical contacts are varied, and depend on the application. With commercial testing the interest is usually in the behaviour of a particular device. In a recent paper F.G. Sheeler, et al [11], developed a computer based test system to diagnose a "nonadjustable, low profile" relay, some of the parameters measured were coil resistance, current parameters, contact bounce times, and contact resistance. The test system achieved the initial aims of providing, flexibility, failure analysis, and reliable operation. In the study of fundamentals, Carballeira et.al, [12], [13], [14], utilised automatic test equipment to develop empirical relations between erosion (as a function of mass changes) and circuit conditions. This particular work has provided useful information on the materials used in electrical contacts.

3.4.2 The Design and Operation of an Automatic test System

To monitor electrical contact phenomena over a large number of cycles, including the evaluation of arc energy, an automatic test system has been developed based on the (RML) micro-computer, and the DL1080.

3.4.2.1 Design Philosophy

To optimise the versatility and flexibility of the test equipment it was designed to satisfy the following operating constraints.

(1) To have the capability to test any contacts under controlled conditions within the medium duty current range.

(2) To be adjustable in speed of operation (closure and opening) and reliable in maintaining that characteristic over a large number of cycles.

(3) To monitor and store current and voltage characteristic during contact operation.

(4) To enable the easy removal of contacts for a study of erosion and wear.

(5) To allow for adjustment of the static contact force.

(6) To allow for the control of a range of voltage supplies and current loadings, such that make only or break only operations can be monitored. There must also be a requirement for automated switching between two or more supplies.

In association with these requirments the monitoring system should allow for the measurement of the following parameters :

A - Arc energy (E)	Section	3.4.4
B - Time transients (T)	"	3.4.5
C - Static contact force (F)	"	3.4.6
D - Transient contact force (f)	"	3.4.7
E - Contact resistance (R)	"	3.4.8
F - The number of cycles (N)	"	3.4.9
G - Displacement characteristics.	"	3.4.10

The system developed to monitor these parameters, is shown schematically in figure (3.11).

3.4.2.2 Design of the test Apparatus

The apparatus developed to satisfy the design requirements is shown in figure (3.12). It comprises a perspex moving arm, in which is mounted the moving test contact. The arm pivots on a pair of fine ball races mounted in the vertical aluminium support. The movement of the arm is controlled by the solenoid mounted on the backing plate. The degree to which the contacts are opened is controlled by the micrometer barrel mounted in a bracket on the backing plate . The static contact force and speed of closure is controlled by the adjustable spring mounted adjacent to the micrometer. The degree of force applied by the spring is controlled by the adjustment of the barrel in which the spring is mounted. The complete assembly of the micrometer and spring may be moved laterally for a range of operating conditions, however for all of the results presented in this thesis the distance was fixed as 85 mm from the arm pivot point. The

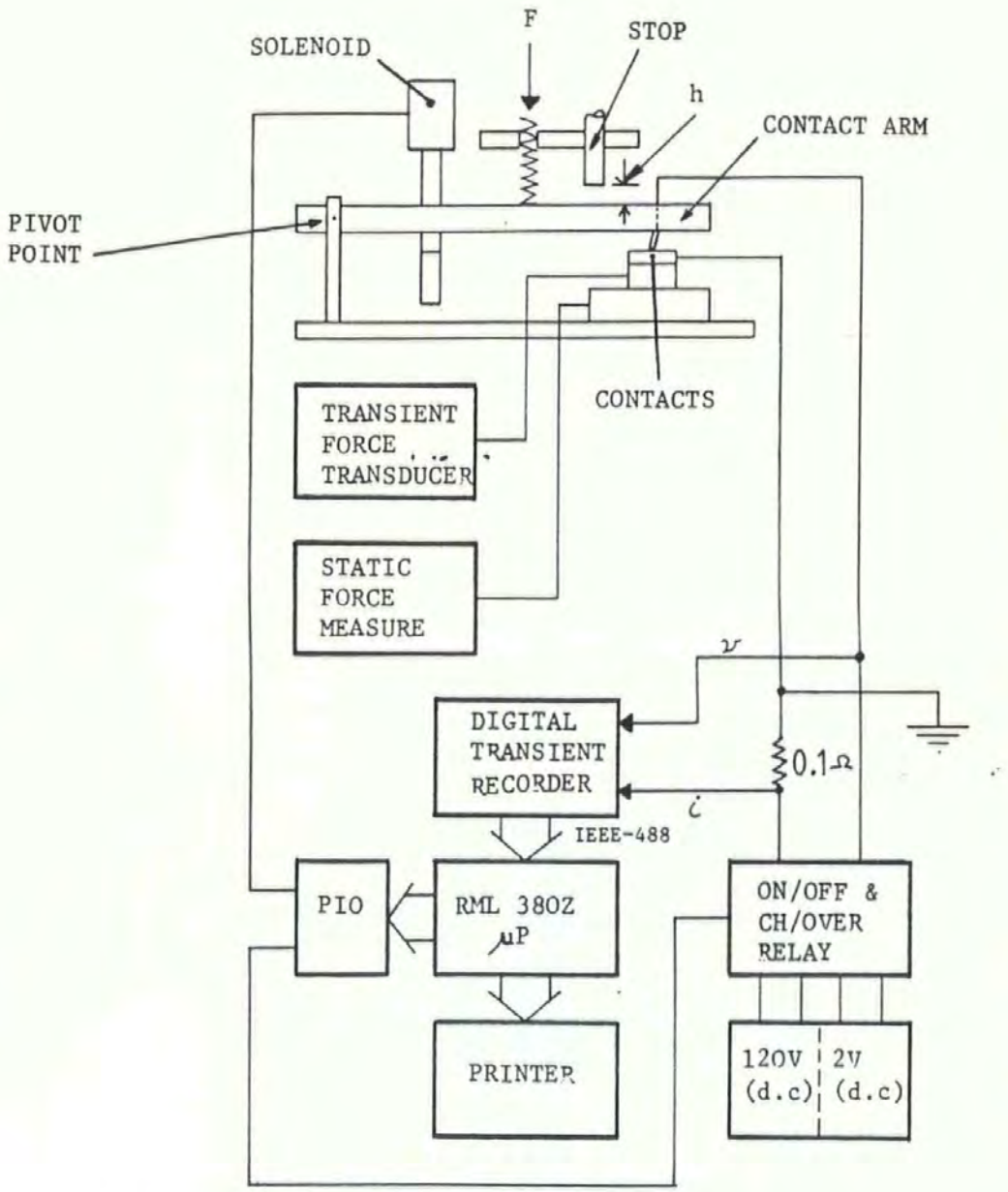

Figure 3.11 The computer controlled experimental test system, and associated apparatus

static contact is mounted in an insulated medium and supported on the load cell, used for the monitoring of the contact force. In the study of contact bouce phenomena, small amplitude vibrations could be encouraged by the use of a spring loaded weight mounted on the end of the contact arm.

3.4.2.3 Contact Support Design

For each particular contact pair a different perspex arm and fixed contact support structure is required. Both the arm and support are easily removed from the rig, the arm by the removal of the bearing spindle and the support by separation from the static load cell. In the course of this work, two supports were designed.

Rivet Contact Support: For a study of main contact behaviour, the rivet contacts tested are mounted in brass supports and held by small grub screws. The main power connections are made to the brass by means of bolted terminals shown in figures (3.12) and (3.13). The top brass support is clamped into the perspex arm and the bottom support is held secure in an insulating perspex seat. For the purpose of contact resistance monitoring a flexible wire is soldered to the base of the rivet contacts and threaded through the brass supports.

Pivot Contact Support: The particular contacts used in this suport are similar to those used in the basic switch design studied in chapter 4. They are used to study the effect of bounce on erosion. For this purpose, the pivot is mounted in the perspex arm at an angle corresponding to the angle used in the actual switch. It will be noted that this is a reversal of the arrangment used in the actual switch where the pivot is the fixed part. However because it is the relative movement which is required to be

simulated it is assumed that this difference would not affect the study. The blade (i.e the normally moving contact) is held by a brass ring to which the power connection is made. Figure (3.14) shows the pivot and blade with the associated connections, in the open circuit configuration, while figure (3.15) shows the various components used in the support. The brass ring holds down the blade on to a perspex flange, insulating the apparatus. In between the perspex and aluminium support which fits into the static load cell, lies a Kistler quartz washer for the monitoring of transient forces. To monitor the contact resistance changes, two wires are soldered to the contact materials.

3.4.2.4 The Design of the Electrical Hardware

The control of the solenoid and power supplies uses the input and output facilities of the RML computer. These (buffered P.I.O's, Periferal Input Output Ports) ports send 5 volt 'on' or 0 volt 'off' signals from the computer and are software controlled. The signals sent from the ports were used to switch transistors, thus enabling solenoid and relay control from the computer. Figure (3.16) shows the port and associated circuitry. The power requirements are controlled by 3 relays, one a change over for switching between supplies, and the other two for switching the load. The use of two relays in parallel, with parallel conections between the switching contacts, enabled currents of up to 40 amps d.c to be switched.

The monitoring of the voltage and current transients occuring during the switching action makes use of the circuit shown in figure (3.17). The DL1080 has a maximum input voltage on each channel of 20 volts. The full switch voltage was therefore reduced by the use of the voltage divider network. The calibration curve for the network is shown in figure (3.18).

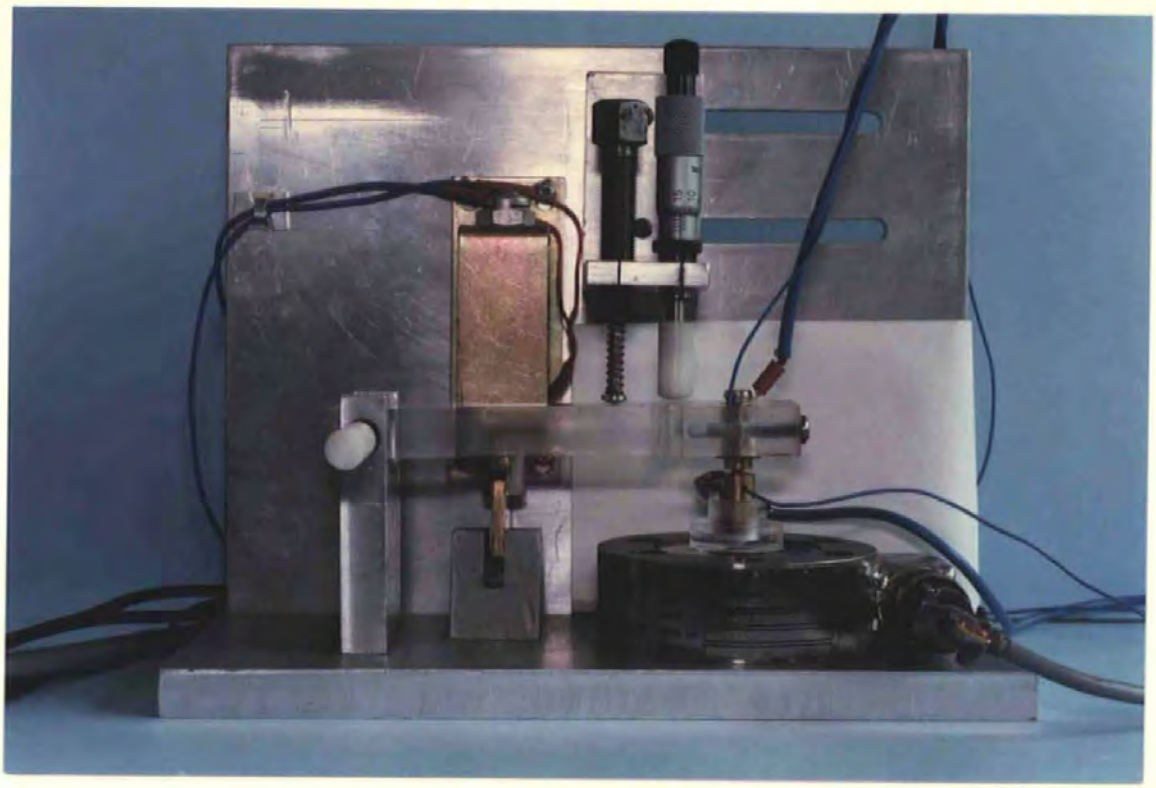

Figure 3.12 The test apparatus, with rivet contacts mounted in the moving arm and base

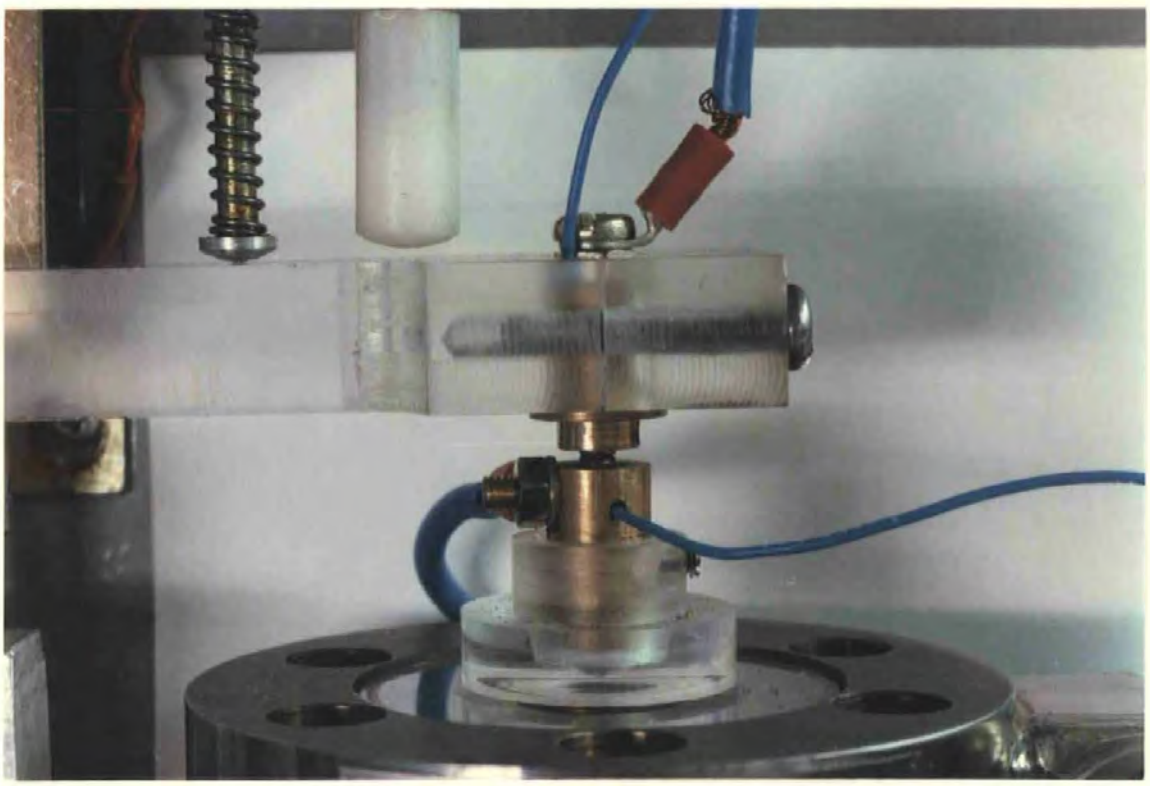

Figure 3.13 The rivet contact supports, with power and contact resistance connections

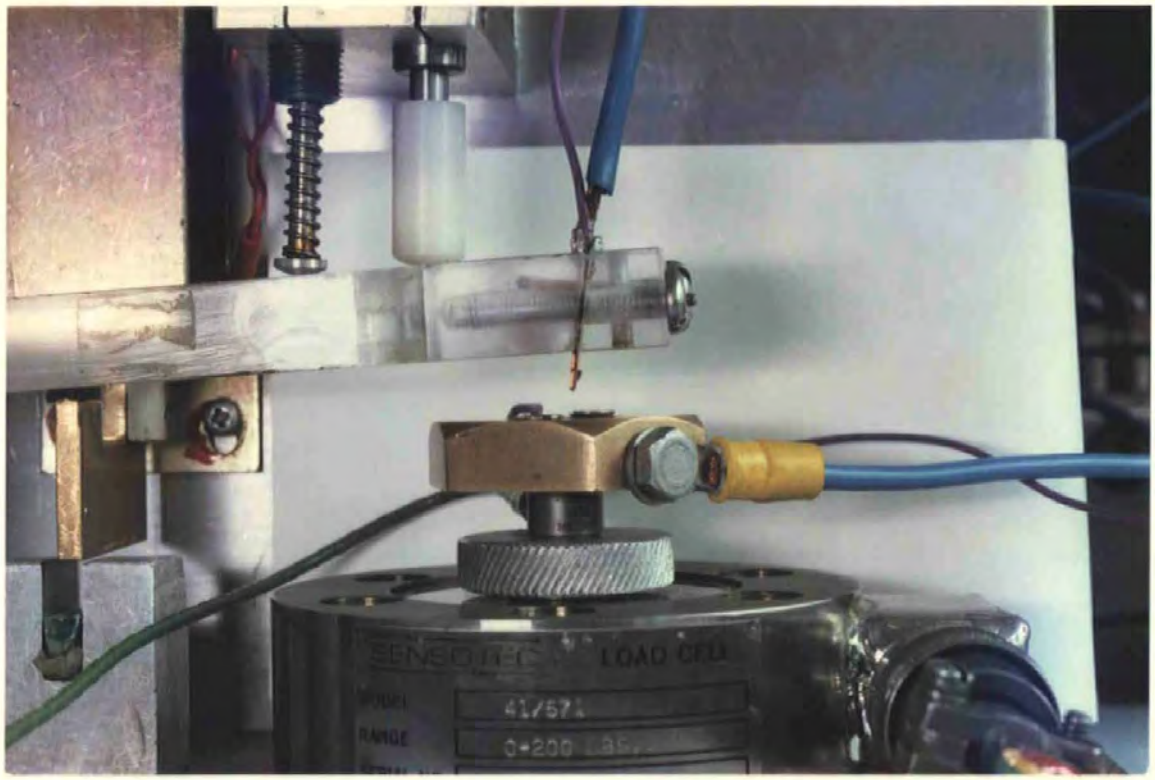

Figure 3.14 The pivot contact supports, with power and contact resistance connections

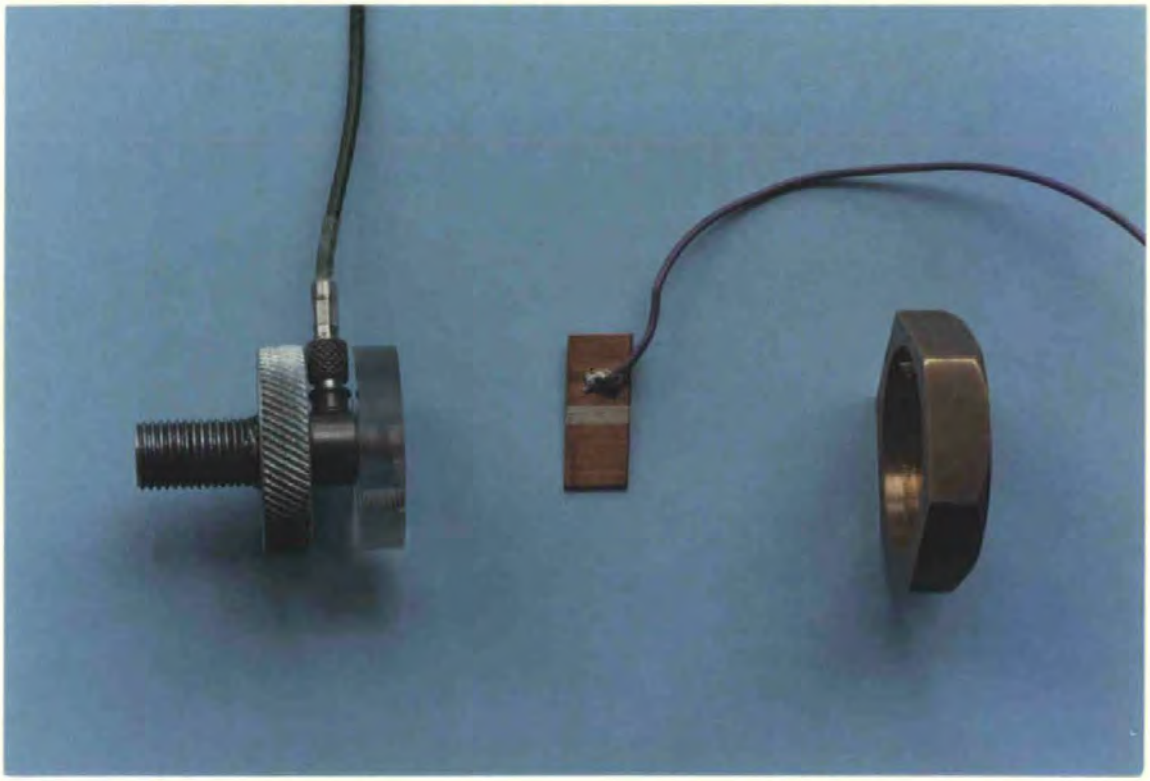

Figure 3.15 The base pivot contact support, with transient force transducer

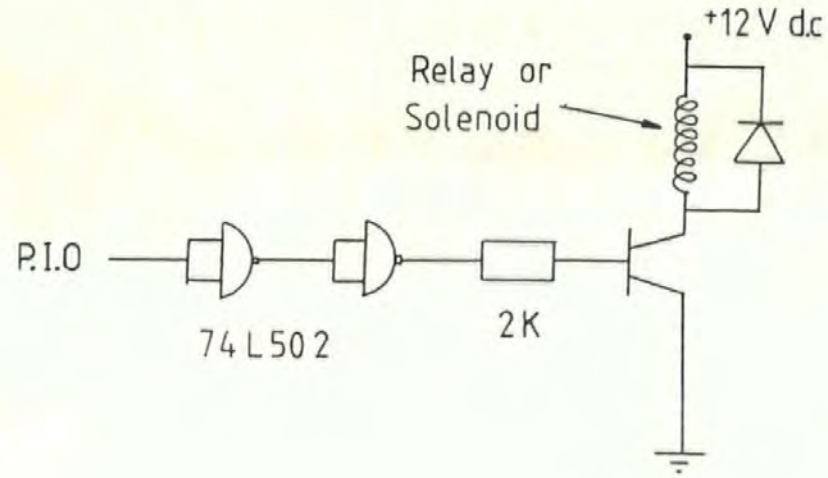

Figure 3.16 Circuit for buffering and controlling the relays from the computer.

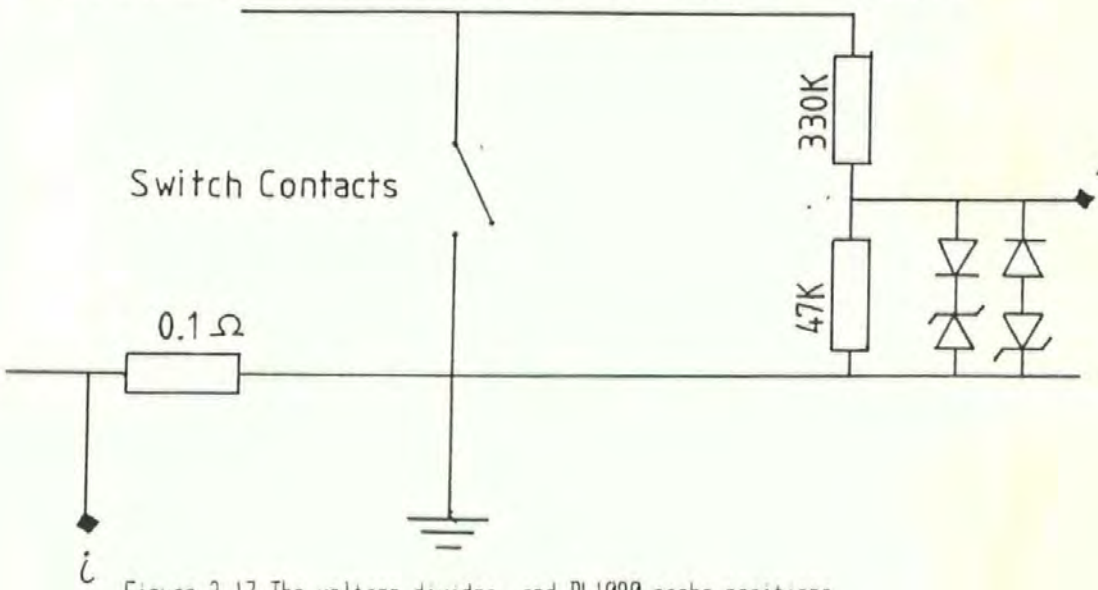

Figure 3.17 The voltage divider, and DL1080 probe positions.

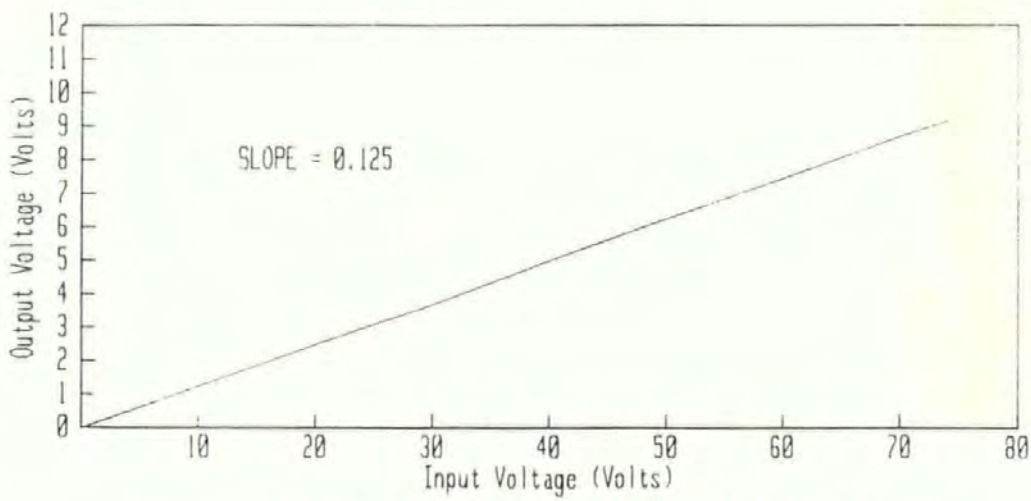

Figure 3.18 The Calibration Curve of the Voltage Divider Network

The voltage factor obtained from the slope of this line is, 0.125 (for an unclipped waveform), and is taken into consideration when determining the measured voltage values. The back to back zener diodes are used to clip high input voltages and protect the DL1080. The switch current is detected as a potential drop across a (0.1 Ω) resistor, provided with a suitable heat sink.

3.4.2.5 Description of a typical cycle

The control cycle used depends on the experiment required but the basic operation cycle of the apparatus is maintained. The solenoid mounted on the back plate, when activated lifts the arm to the nylon stop as shown in figure (3.14). The position of the stop being preset by the micrometer barrel. On closure, the solenoid releases the arm under the influence of gravity and the applied spring force. After the bounce transients are over the contacts come to rest with a static contact force supplied by the spring.

3.4.3 Data Transfer from the DL1080 to the Processor

The storage of data in the DL1080 is facilitated by the representation of the transients as a series of 4096 data values. Each value has a magnitude between 0 and 256, which is proportional to the voltage measurement. The transfer of this data along the IEEE bus has been achieved by the transfer of the numerical values as string variables. Each channel of data is then stored in an array in the processor. To speed up this operation only one value in four has been sampled thus leading to a array of 1024 data values and a transfer time of approximatly

40 seconds for both channels. To convert these values to real voltage and time samples, requires the accessing of the front pannel settings of the DL1080. The front pannel settings are software controlled from the central processor when the system is used in the automated mode. These settings are stored in a disk file and accessed by the processor.

3.4.4 The Evaluation of Arc Energy

The evaluation of arc energy is based upon the numerical integration of both the current and voltage traces of the arc characteristic. This is achieved by the transfer of both traces from the DL1080 to the computer. Once stored the arrays representing the traces are processed to give the arc energy dissipation. This calculation is based on the multiplication of the two scaled waveforms and the integration with time. Thus the energy (E) can be defined as,

$$E = \sum_{1}^{1024} i \cdot v \ \delta t$$

where i,v are the current and voltage samples, and δt is the sample length, typically (8 μs).

This method of measuring arc energy has the benifit of increased accuracy over existing methods, for example using a multiplier circuit, [15],

3.4.5 The Evaluation of Switching Times

With a given voltage or current characteristic stored in the micro computer it is possible to evaluate the times of a given event by processing the array representing the trace. This evaluation is detailed in section (3.5), as the particular method used depends on the experiment.

3.4.6 Static Contact force measurement

The measurement of the static contact force is made by a load cell. The load cell used for this purpose was a Sensotec Model 41. When a load is applied it produces a resistance change in strain gauges wired into four active arms of a Wheatstone Bridge, [16]. The transducer utilises two stabilising diaphragms, welded to the sensing member; it then senses the deflection between the outer rim bolt holes fixed to the apparatus and the threaded inner hub supporting the fixed contact. The changes are monitored on a Vishay-Ellis-20, digital strain indicator which is calibrated to read the contact force directly in Newtons [17].

3.4.7 The Transient Contact force

The transient forces occuring at impact are of a high frequency and thus are not suitable to be monitored by the load cell. These impact forces are monitored by a Kistler quartz load washer, type 9001, [18]. This type of transducer has a high rigidity and correspondingly high resonant frequency, thus allowing it to be fitted without altering the elastic behaviour significantly. The transducer produces a charge proportional to the force applied and has a rise time of about one microsecond. The

charge is applied to a Vibro-meter charge amplifier which produces a voltage signal representing the transient, [19].

The mounting of the transducer in the contact support is of critical importance. The supporting surfaces for the load washer are finely machined, level and rigid. The washer is pre-loaded by the bolt inside the aluminium housing, so that impact forces applied to the washer produce the correct stress distribution.

3.4.8 Contact resistance

The measurement of contact resistance changes, due to wear and arc erosion, is based upon the pulsed d.c current method discussed in Chapter 2. The resistance is obtained by measuring the contact volt drop across the contacts by the use of the four wire method. The probe connections are positioned as close to the contact interface as possible.

To simplify the measuring of contact resistance, and to make it applicable to automated testing, where it is not the only parameter being sensed. The method chosen was to pulse a large current through the contacts for approximately 100ms. The supply used in the measure of resistance was a 24 volt battery, thus reducing the likelyhood of ground loops. To check the accuracy of the method polarities were reversed to check for thermocouple potentials but none were monitored. The use of the DL1080 as the sensing device required that the volt drop should be significantly above the minimum voltage level of (0.309 mV) and well below the softening voltage of the materials. For the contacts tested in Chapter 5 typical measured values of 10 mV where taken using current pulses of 16 amps.

3.4.9 The Number of Cycles

The number of cycles used in the tests are defined at the start of a particular experiment. Once the required number of cycles have been completed the processor stops the experiment.

3.4.10 The Measurment of Displacement Characteristics

The monitoring of the displacement characteristics is split in two distinct requirements, to monitor impact phenomena, and to monitor contact separation characteristics. It has been argued that with small amplitude bounce, the bounce times are sufficient to describe the characteristic; however the displacements can be important. The monitoring of electrical contact displacements could be achieved by a number of possible techniques. The use of standard displacement transducers has not been made extensive in this field because most would have a direct effect on the motions monitored. This is a particular problem with switch contacts because of the low inertias involved. Capacitive and inductive type transducers could be used but these commonly exhibit non-linear characteristics and require careful application. Common methods used with electrical contacts have been the light source, aperture, and light sensitive cell, method used by Erk and Finke, [20]. This method was further advanced by K. Mano using a laser source, [21]; and B. Sandler, et al, used the same method to monitor relay contact bounce, [22].

In this thesis the high-speed photographic method has proved useful in the monitoring of real switching actions, and is used here to monitor both closure and impact/bounce characteristics. With a carfully designed test system satisfying the requirement of repeatable operations it is possible

to study a few carefully chosen operations and then correlate from these, to obtain the systems full operational characteristics. The details of this analysis are given in Chapter 5.

3.5 Experimental Procedures and the Controlling Software for the automatic test system

The investigations conducted on the test system fall into two groups:

EXPERIMENT 1 - A study of electrical contact bounce phenomena and the influence of load current on the bounce dynamics under d.c conditions.

EXPERIMENT 2 - A study of erosion and contact resistance changes of contacts at closure, under endurance conditions at 240 volts a.c, 50 HZ.

In these experiments, both rivet contacts and pivot contacts have been investigated.

3.5.1 Experiment 1

In this section, details are given of the software used to control the test system and the experimental cycle. The data processing methods are discussed in the following section.

To study the effect of load current on bounce requires that the system is used in the multi-supply mode. When test contacts are closed with no current passing between them the ensuing bounce and impact events are a

sole factor of the mechanical system, e.g the velocity of impact, surface conditions and contact supports. On the passage of a current through the same interface under the same conditions a different characteristic is observed.

The passage of the load current and the associated arcing causes major changes at the surface of the contacts, thus the following impacts will constitute a different set of initial conditions. To study the effect of current on contact bounce the test system was alternated between mechanical operations and electrical or load current operations.

To monitor the events occuring in mechanical impact and bounce a signal current supply was used; and is shown in figure (3.19), as supply (a). The corresponding load current supply is shown as supply (b). The switching between the supplies was undertaken by the change-over relay shown schematically in figure (3.11).

The sequence of events used in this experiment is shown in the flow chart in figure (3.21); and the associated software is given in appendix (4). At the initilisation stage, all of the test variables are defined, these include the number of operations, the number of additional operations (operations in which data is not transfered to the processor), and the nature of the multiple test mode. Once running, the system will continue until the requested number of cycles have been collected and processed.

In the case of contact or test system failure, safety checks have been included in the software.

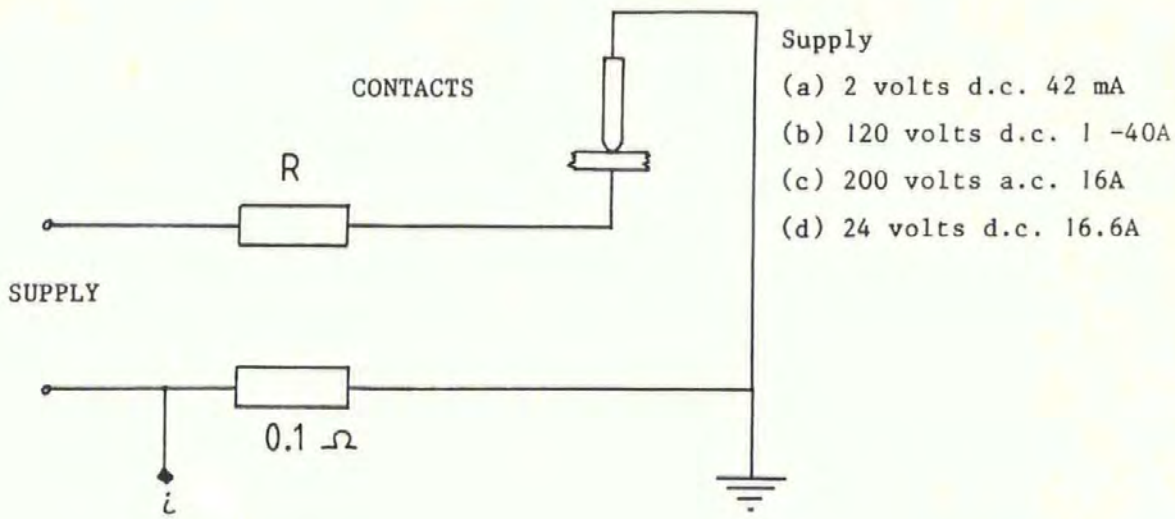

Figure 3.19 The circuits used with the automated test system

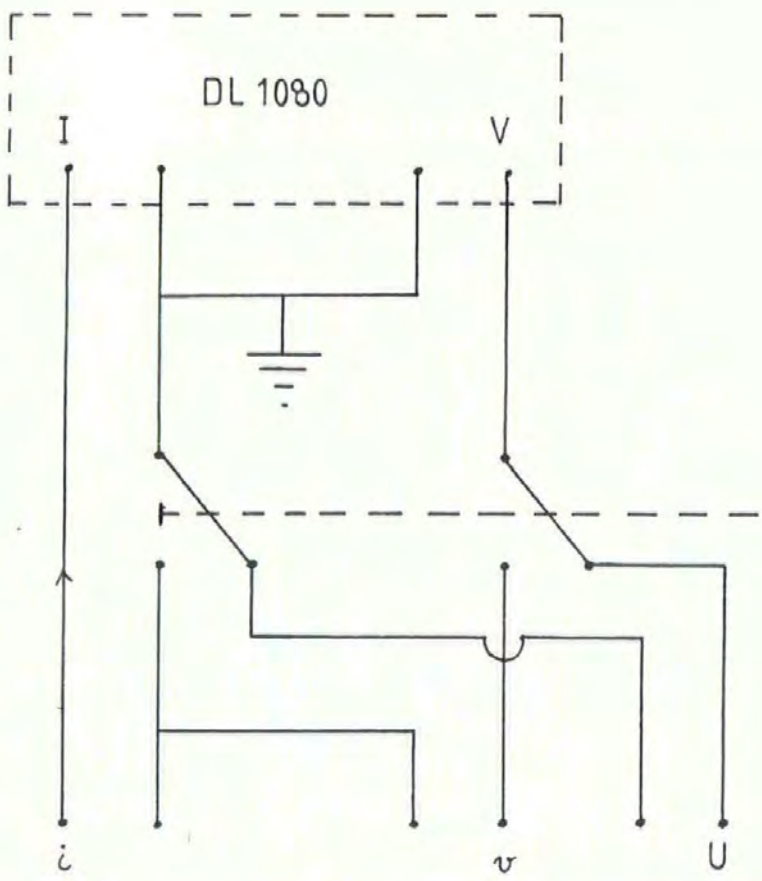

Current probe Voltage probe Contact voltage probe

Figure 3.20 The relay for changing the probe positions

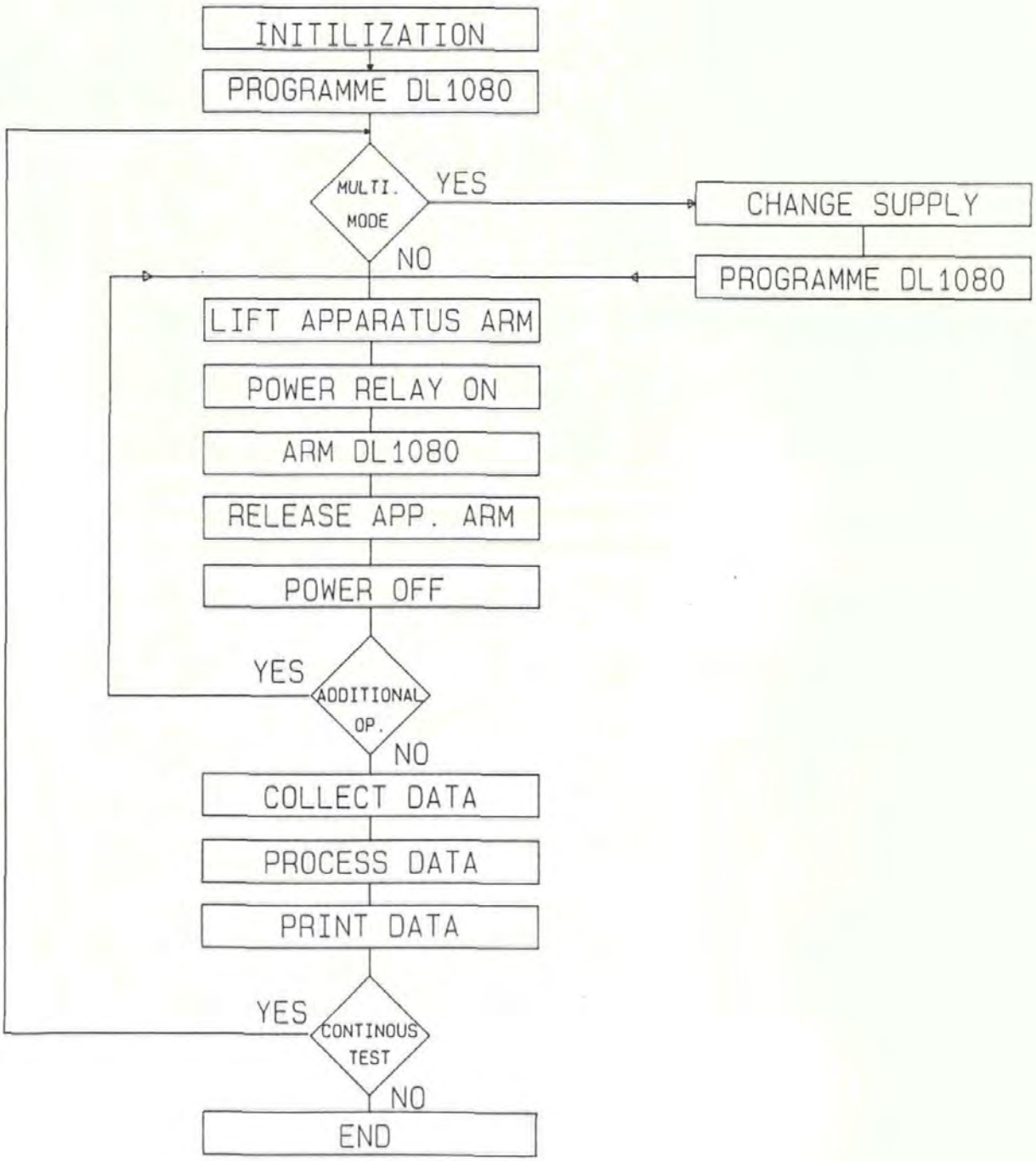

Figure 3.21 The control cycle used in experiment 1.

3.5.2 Data Processing for Experimemt 1

Examples of the transients processed in this experiment are shown in figure (2.8). For the purpose of the experiment only the voltage characteristics were of interest, however both the current and voltage traces were transfered to the computer, so that the arc energy evaluation could be maintained. The top trace in figure (2.8) is representative of a typical mechanical bounce characteristic, and shows the open circuit voltage of 2 volts. After impact the contacts remain in contact until the first separation, at which point the voltage reads open circuit. The figure shows three bounces. To determine the bounce times a fixed voltage level, or slice level is used (as shown in the figure), and the data processed to determine if the voltage levels are above or below this line. The flow diagram of the algorithm used, is shown in figure (3.22). The associated programme is given in the subroutine 13000 in appendix 4.

From the evaluation of the slice points it is a simple operation to obtain the total bounce times, as defined in section (2.4.4), as the mechanical bounce time (T_m), and the electrical bounce time (T_e).

In addition to these times individual bounce and impact times can be identified, as follows;

First bounce time = t (mbl), or t (ebl) = $t_3 - t_2$

First impact time = t (mil), or t (eil) = $t_2 - t_1$

3.5.3 Experiment 2

To study the influence of a.c current on contact resistance changes in electrical contacts at make, the test system was modified to allow for probes positioned closer to the area of contact. The a.c circuit used for this experiment is shown in figure (3.19c). In this case the load is isolated from the supply by a transformer allowing earthing in the circuit The switching between the a.c and d.c supply used for the contact resistance measurement follows the same method used in experiment 1. However in this case there is an additional requirement to move the position of the measurement probes. The changing of the probe position requires the use of a further relay, controlled from the processor, and the circuit is shown in figure (3.20).

The sequence of events controlling this experiment is detailed in figure (3.23). The additional operation mode was used in this experiment to allow for accelerated testing to 10,000 cycles. Typically one operation in fifty is transfered for processing, speeding up the cycle time considerably.

3.5.4 Data Processing of Experiment 2

The data processing to obtain the arc energy and bounce times in the a.c mode is much more complex than the method used in experiment 1, with d.c supplies. This complexity arises by the possibility of the a.c voltage going through zero during a bounce, and the subsequent reversal of the polarities. To overcome this difficulty both the current and voltage traces need to be processed and cross referenced. The algorithim used to process the data is shown in figure (3.24); and the associated software is presented in appendix 4.

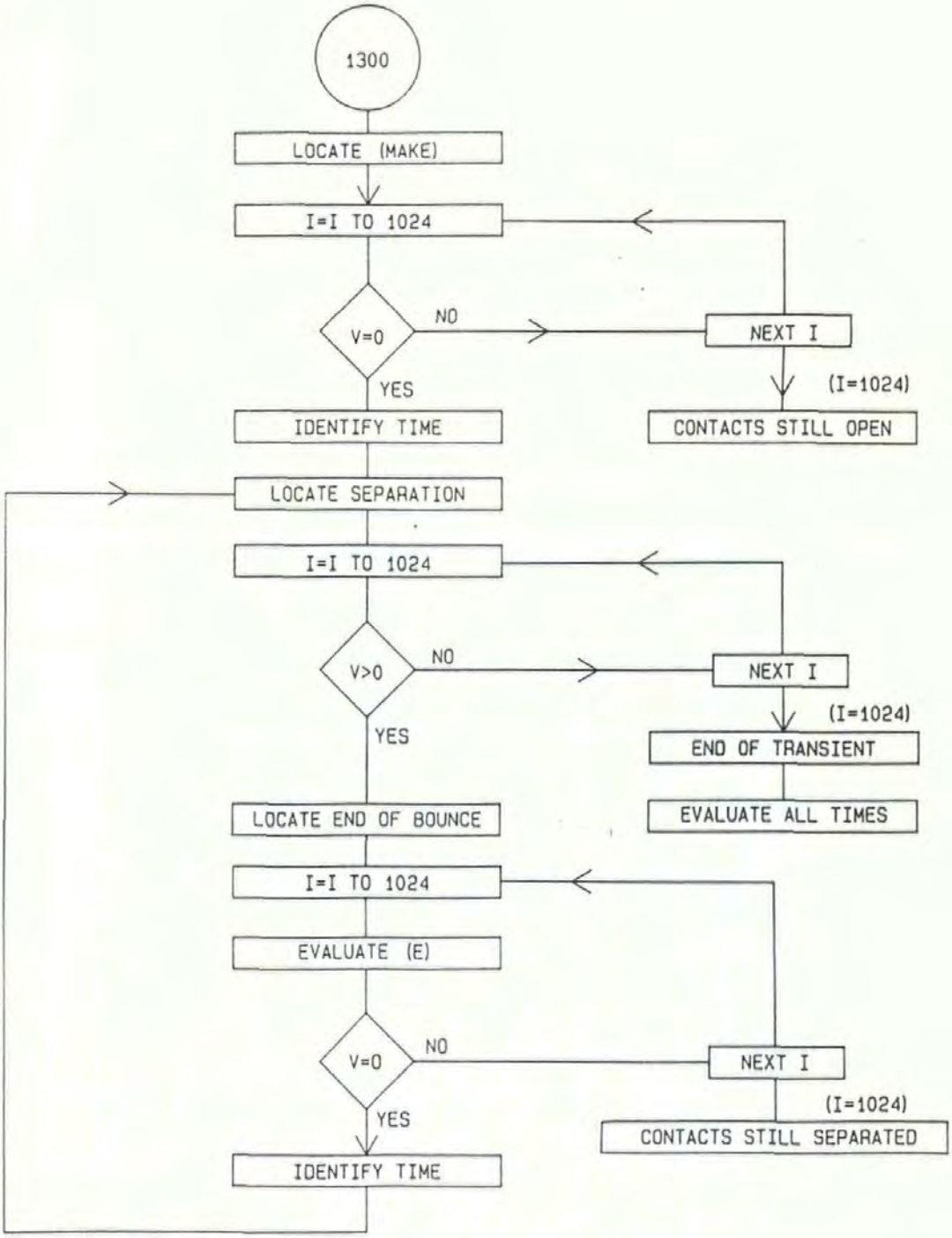

Figure 3.22 The flow chart for the evaluation of bounce times and arc energy (E), from d.c a transient.

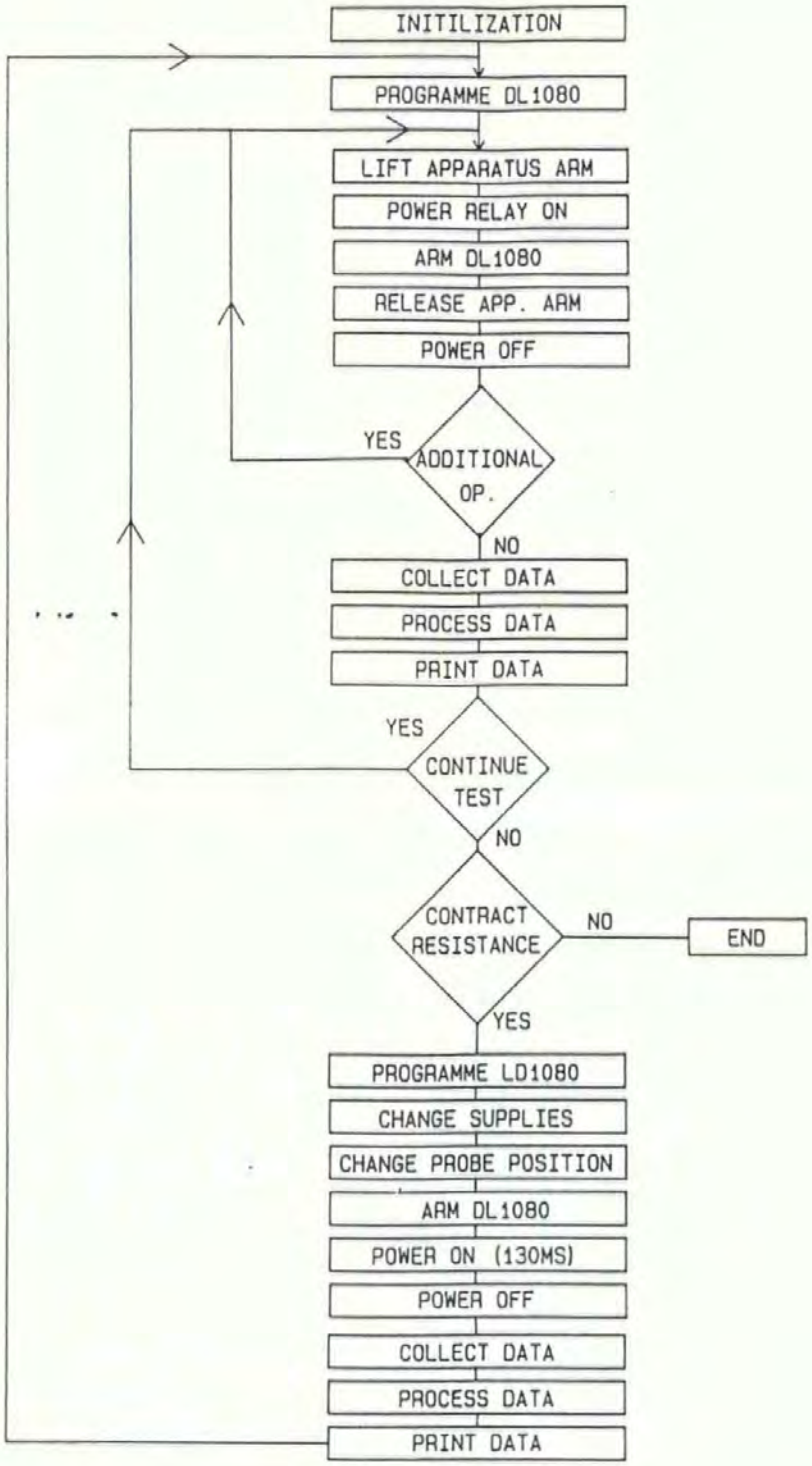

Figure 3.23 The control cycle for experiment 2.

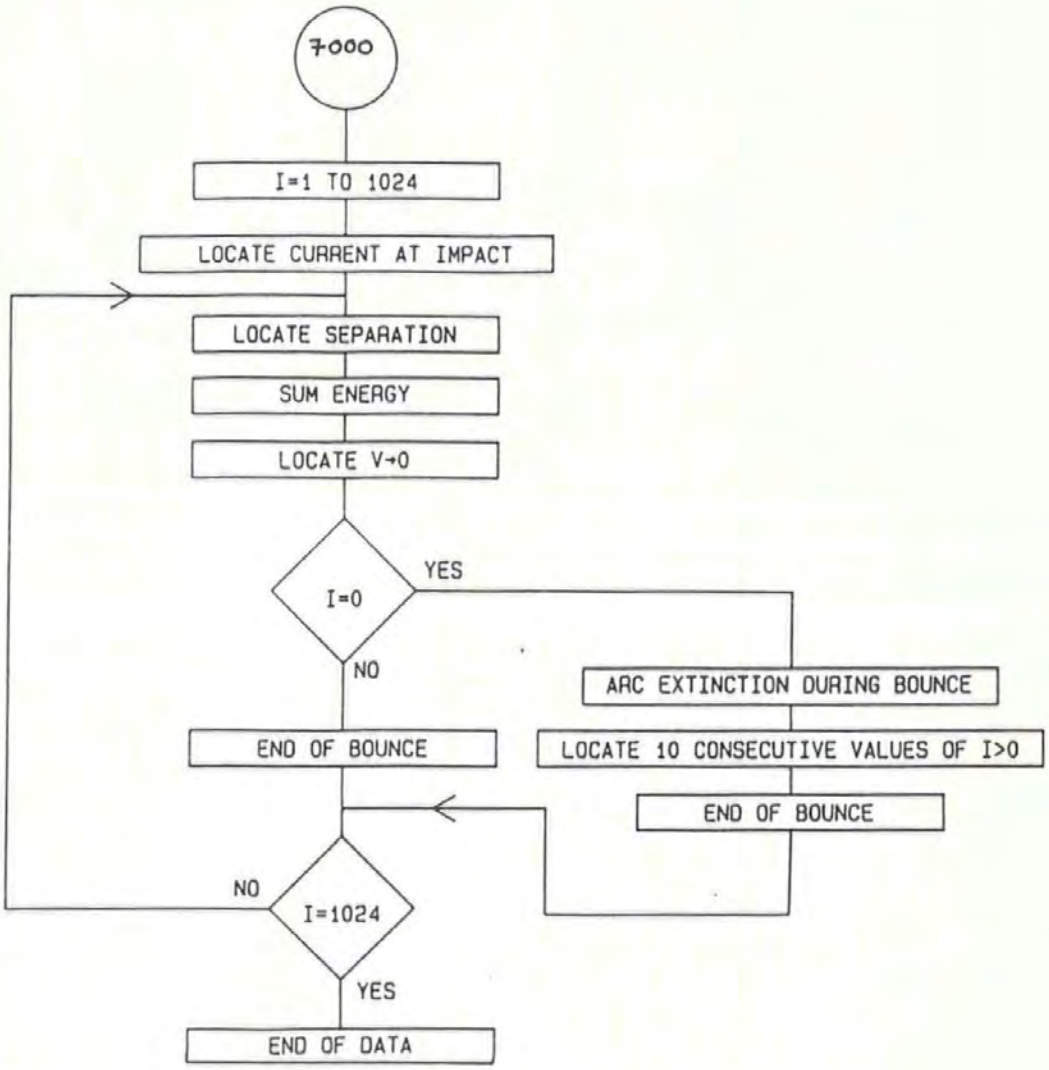

Figure 3.24 The flow chart for data processing in experiment 2

REFERENCES FOR CHAPTER 3

[1] P.J White, "Investigation of Parameters Affecting the Operating characteristics of Toggle-Switches with Silver-Cadmium-Oxide Contacts", Ph.D Thesis, Plymouth Polytechnic, 1979.

[2] High speed Camera Operators manual, John Hadland (Photographic Instrumentation) Ltd, U.K.

[3] DL1080 Programmable Transient Recorder Operating Manual, Doc No OM. 0004, Data labs Ltd, England.

[4] Operating Manual, Research Machines 380Z

[5] "An Introduction to the IEEE488 Bus Standard", Farnell

[6] O.J Youldon, "Computer Controlled Measurement of Switch Performance", Internal Degree Project Report, Plymouth Polytechnic, May 1984.

[7] G. Honey, "Appliance Switch Standards; Approvals and electrical control", Grenada, 1984.

[8] "Specifications for Electrical Controls for Household and similar general purposes", Part 3. General and Specific requirements, BS 3955: Part 3: 1979, pp 30.

[9] J.W McBride, "A design optimisation of Rocker Switch dynamics to reduce contact bounce and thus prolong contact life, using a computer based numerical method.", Internal Confidential report to Arrow-Hart Ltd, Plymouth Polytechnic, August 1984. pp 38.

[10] A Collins, "Test Rig for Electrical Rocker Switches", internal student project report, 1985.

[11] F.G Sheeler, D.W Meyer, M.P Asar, "Utilization of Computer control to Functionally Test and Diagnose Relays", Proceedings of the 29th Relay Conference, 1981, pp 3.1-9.

[12] A. Carballeria, J. Galand, "A New Equipment for Evaluating Welding and Erosion Tendencies of Electric Contacts", Proceedings of the, Japan 1976, pp 633-638.

[13] A. Carballeira, J.M Clement, J. Galand, "Erosion Characteristics at Make and at Break of Contactor Contacts", Int. Conf. on Electrical Contact Phenomena, 1982, pp 175-179.

[14] B. Belhachemi, A. Carballeira, "Influence of Delay and Duration of Bounce on Erosion Weldability and Resistance in Relay Contacts", Proc. Holm Conf. Electrical Contacts, 1984, pp 475-483.

[15] J. Muniesa, "Contact Erosion: Testing machine and Switching Devices", Proc. Holm Conf. Electrical Contacts, 1982, pp 127-133.

[16] Sensotec, Load Cells, RDP Electronics, Wolverhampton, U.K.

[17] Vishey, Ellis, Strain gauge indicator, Operating Instructions.

[18] Kistler, Quartz Load Washers, Type 9001, Operating Instructions.

[19] Vibro-Meter, Charge Amplifier, Operating Instructions.

[20] V.A. Erk, H. Finke, "Uber die mechanischen vorgange wahrend des Prellens einschaltender Kontaktstucke", (The Mechanical Processes of Bouncing Contacts), E.T.Z Electrotect, Vol 5, 1965, pp 129-133.

[21] K. Mano, A. Yonezawa, "Experimental Investigation of Contact Welding Phenomena", Int. Conf. on Electrical Contact Phenomena, Japan, 1976, pp 233-238.

[22] B. Sandler, A.A Slonim, "Experimental Investigation of Relay Contac Dynamics", IEEE Trans. CHMT, Vol CHMT-3, No 1, March 1980, pp 150-158.

CHAPTER 4

A COMPUTER BASED OPTIMISATION OF ROCKER SWITCH DYNAMICS TO REDUCE PIVOT BOUNCE

4.1 Introduction

In chapter one an introduction is given to the failure problems associated with the rocker switch. This chapter details the methods by which an understanding has been made of the rocker switch dynamics, and details a mathematical model of the system. The model comprises a series of non-linear differential equations, which describe the switch movement up to the instant of main contact impact. Some of the parameters given at the instant of impact are velocity, kinetic energy, and displacement. The equations are solved by a finite difference routine on a main frame computer. Computer modelling in this sense allows for design optimisation by the variation of parameters, and this in turn opens the way for computer-aided design.

The design optimisation studies of the rocker switch are discussed in this chapter in two contexts. The improvement of a standard manufactured switch, and the overall design of the basic mechanism. The former case involves fewer variables, and has been studied in detail. Design modifications are suggested and are tested to evaluate the improved performance under load current, and signal current conditions.

4.2 Initial Investigation of Rocker Switch Dynamics

The initial investigation was undertaken to give an understanding of the erosion processes occurring at the pivot interface of a rocker switch. The method used in this investigation, was to monitor, (i) the switch action using high-speed photography, and (ii) the switch transients using a 4 mA test current, (described in section 3.2.2). The aims of this investigation were;

1), To determine the cause of contact erosion.
2), To monitor the dynamics of a rocker switch.
3), To identify and evaluate the influence of hand operation on the device performance.

The switch considered in this investigation is shown in figure (1.4a). This switch uses a changeover configuration, which enables the monitoring of BM times (the time taken for the blade to changeover), using the circuit shown in figure (3.7).

4.2.1 The Results of the Initial Investigation

A typical example of the processed results otained using the high-speed film technique is shown in figure (4.1). It shows the closing of the right hand contact, labelled, as identified in figure (3.6), as Y. The impact of the main contacts occurs at, Y=0. After the impact there are two bounces; the first giving a displacement of (0.06mm), and the second of (0.1mm). Simultaneous with the Y contact closing, the X contact shows an increasing displacement which continues after the impact of Y. During the period of contact bounce at Y, the X contact moves beyond its

equilibrium or static positon, as indicated by the horizontal dotted line in the figure. The continuing motion of X is a result of the blade inertia, and results in a separation at the central pivot. The pivot separation is given by Z in the figure, and shows the maximum displacement to be, (0.3 mm). This was however a servere operation for the purpose of demonstrating the separation at Z, and a more typical value is less than (0.1 mm).

The high-speed photographic method used causes some inaccuracy in determining the actual times of impact. The reasons for this are two fold; firstly the film is taken of the whole mechanism, as shown by the single frame taken from the film in figure (4.2). The events at the contacts thus give a low photographic resolution, and additionally, shadows are cast by the impacting contacts which results in inaccuracy in the low magnitude displacement measurements. Secondly the frames of the films are instantaneous pictures of the event, making it difficult to identify the instant of impact. This can be overcome by the interpolation of the characteristic.

The data obtained from the film allows for a range of displacement and velocity characteristics to be obtained. For example spring extension, actuator angle, blade angle, and velocity of impact. In figure (4.3) two examples of the variation of the actuator angle, α, with time are shown. This figure also shows the period of blade motion relative to the motion of the actuator. It shows the actuator, and plunger moving from the stationary position on the left contact, (where X=0, and the actuator angle α is negative); to the central position, (where α = 0), and then accelerating to the right stop position. The films show that contact slip occurs between the blade and pivot only after the changeover and bounce period has finished. This is simultaneous with the plunger

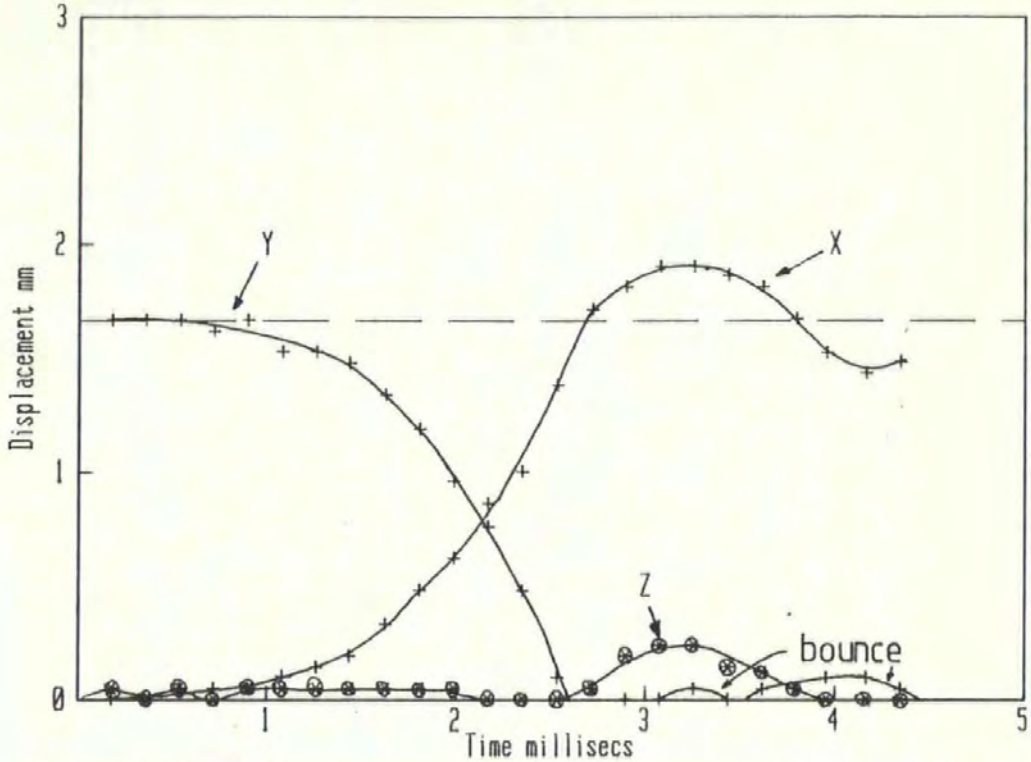

Figure 4.1 The displacement characteristics of a typical hand operated rocker switch

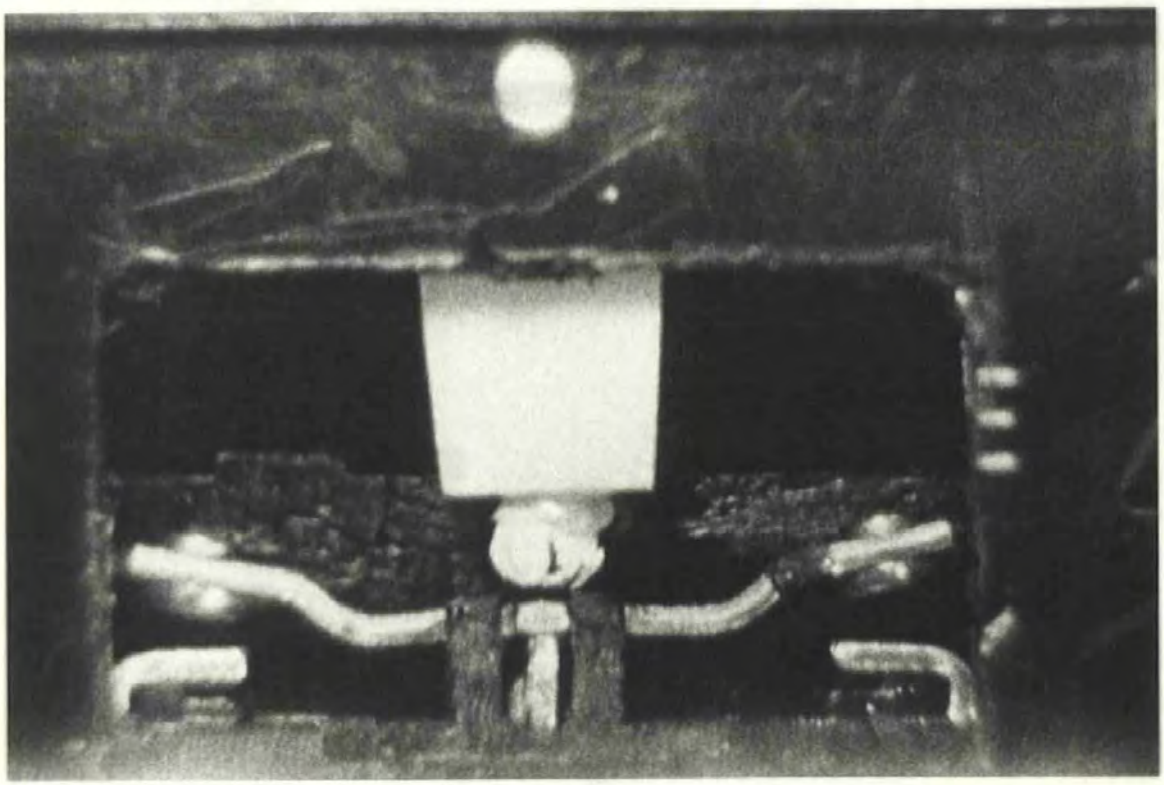

Figure 4.2 A single frame from a highspeed film

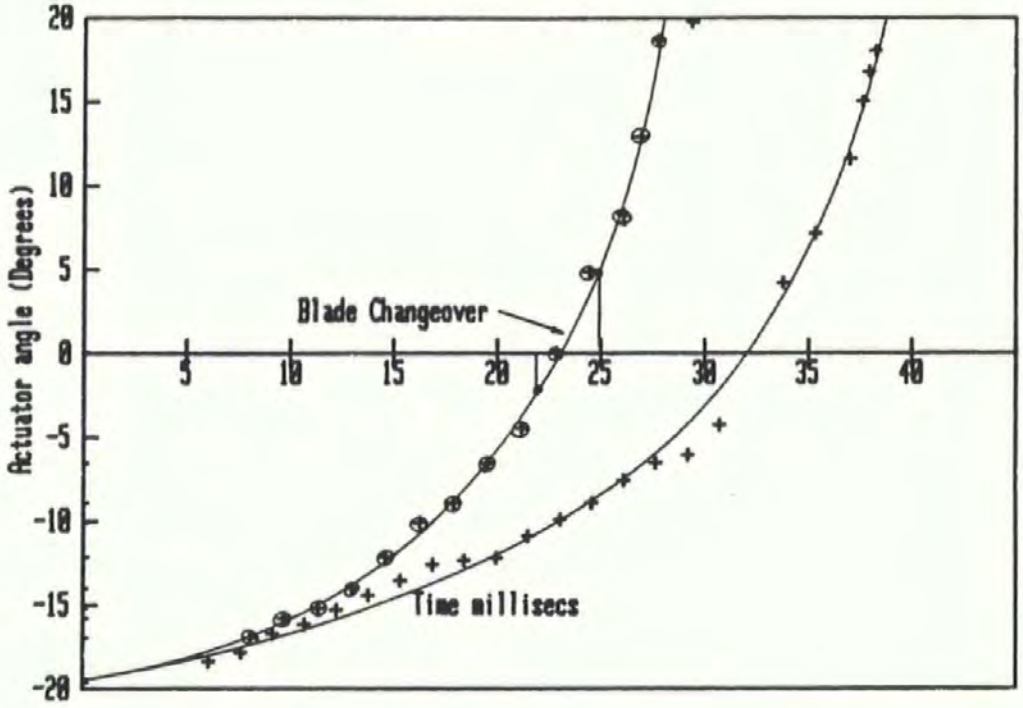

Figure 4.3 The variation of the actuator angle ($\propto$) with time, during hand operation

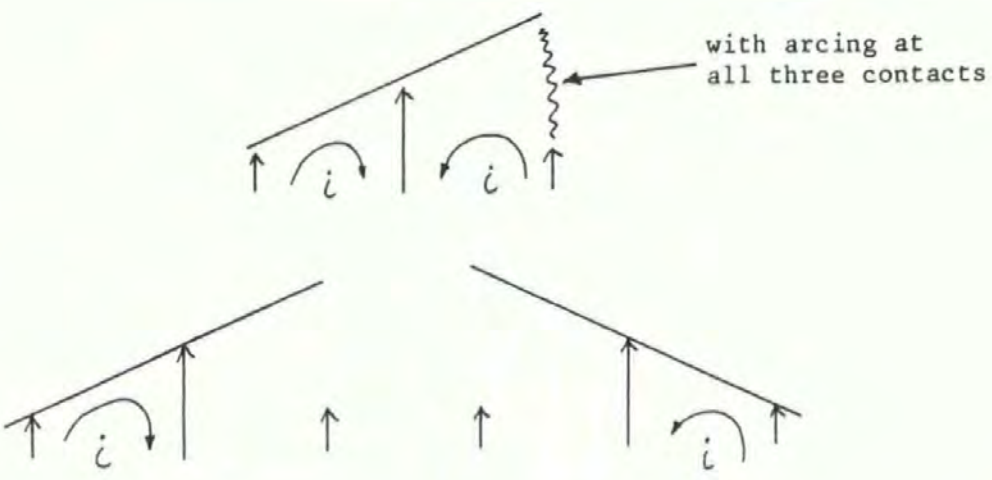

Figure 4.4 The current paths in a changeover Rocker Switch

moving down the blade, and does not affect the bounce.

To increase the accuracy of the photographic method and obtain further details of the contact bounce the signal current transients occurring during the changeover were monitored using the circuit and method detailed in section (3.2.2). Figure (3.8) shows a typical characteristic obtained. This shows that the voltage step at (A) clearly defines a separation point of the contacts. Similarly the instant of impact is given at (B). The evaluation of the times associated with these points leads to an accurate measure of the blade changeover time, defined as the (BM) time. A comparison of the changeover time can be made with the times given in the photographic method. Similarly the main contact and pivot contact bounce times can be evaluated. The figure shows that the bounces are interrelated in a complex fashion, due to the interaction between the simultaneously bouncing pivot and main contact. The pivot bounce is often described by one major separation, as identified with the photographic method, however the signal current transients of figure (3.8), show a number of additional smaller bounces. When the one volt level is monitored both contacts are temporarily open circuit.

With a load current passing through the mechanism, arcing can be observed at both the main and pivot contacts. In the changeover configuration the current is being switched between the outer contacts as shown in figure (4.4). At the opening of the main contacts arcing would be expected under normal circuit conditions (240 V, 16 A, a.c), thus if the arc is drawn out to the fully open contacts and the pivot and making main contact are separated in bounce, arcing can occur at all three interfaces. This has been observed, with a load current of 16 Amps a.c.

4.2.2 A Comparison between Film and Electrical BM times

In table (4.1), the results of the BM times for three films and simultaneous signal current transients are presented.

Film Number	23	24	25
Recorder BM time (ms)	4.49	3.99	3.5
Film BM time (ms)	3.55	3.23	2.6
Difference (ms)	0.94	0.74	0.9

Table 4.1

The difference in the BM times suggests a difference between the two measuring systems. The time given by the DL1080 (the transient recorder), must be a true reflection of the lost contact, therefore the error occurs in the photographic method.

At the onset of actuator motion the plunger will move up the blade, reducing the force at the main contacts, and causing an increase in the constriction resistance. When the plunger is over the pivot, the force will drop to zero, and the blade will start to rotate slowly. It is this initial slow separation of the blade and small contact displacement, that causes the difficulty in defining the exact moment of separation on film. In figure (4.1) the slow opening of the contact can be observed when the X contact starts moving. At impact the blade acceleration results in an increase in the blade velocity which enables a much clearer definition of the point of impact. It can therefore be concluded that

with respect to time, the signal current testing of the contacts enables a more accurate evaluation of the contact events.

4.2.3 The Variation of BM time with Applied Force

The solenoid test rig described in section (3.3) was used to establish how the applied force affects the switching time of the device, with the switching time defined by the BM time. The results of this are shown in figure (3.10), for both single and double pole switches. The double pole configuration consists of two blades in the same nylon moulding, acting simultaneously, and two plungers mounted within the same rocker. The double pole assembly requires more force to activate the mechanism, because two spings need to be overcome: this is demonstrated by the higher current applied to the device for a given BM time. The figure also shows how a reduction in BM time occurs with an increase in the applied force.

4.2.4 Observations on Rocker Switch Dynamics

Two major obsevations were made in this investigation on the switch dynamics.

(1). Previous studies made of rocker switch dynamics have generally assumed the geometry shown in figure (4.5a). In this case the radius line of the plunger is shown to continue to the pivot point, thus causing the blade to rotate as the actuator angle changes. It has been shown that this condition will hold for a blade with a small moment of inertia, [1]; however the study of the high-speed films shows the true

geometry to be that of figure (4.5b). The geometry shown in this figure implies that the blade inertia has some affect on the switch dynamics. This geometry gives added complexity to the mathematical modelling process, since both the actuator and blade displacements depend upon the interaction and friction force between the plunger and blade.

(2). The separation and bounce identified between the blade and pivot will generate arcs when switching load current. This arcing is therefore the main cause of the erosion at this interface. In addition the pivot bounce increases with increasing severity of the hand operation. This follows because the increased acceleration of the blade produces a higher impact velocity, and therefore kinetic energy.

Data supplied by the switch manufacturer supports the latter observation. A selection of standard switches tested under the standard endurance test, [2], have shown that although all switches undergo the same cycling there is some variation in the erosion of the pivot interface. In some cases the protective silver inlay remains intact. Thus assuming the same mechanical wear conditions of rolling and sliding as the blade moves about the pivot, the difference in erosion can only result from differences in arcing. A reduction in arcing as a result of reduced bounce will therefore give less wear.

4.2.5 Summary of additional Observations

To summarise the results of the initial investigation; the following conclusions were drawn on the mechanism considered.

(1) The break of the contacts is defined by the electrical break and not

the photographic. There is typically a 0.9 ms difference, for the type of switch considered.

(2) During the blade rotation the pivot interface experiences a rolling electrical contact.

(3) In normal use bounce occurs at the pivot interface just after main contact impact.

(4) Moving contact slip occurs as the plunger moves down the blade, after the changeover and bounce period.

(5) An increase in applied force increases the duration of the pivot bounce and reduces the BM time.

The observations considered in this section apply to one particular mechanism, however the general observations of the dynamics will apply to any switch using the configuration of a pivot, blade, and actuator.

4.3 The Mathematical Analysis of Rocker Switch Dynamics

To reduce the pivot bounce, a model of the dynamics is proposed which predicts impact conditions, for a given set of initial conditions. In addition it is necessary that any changes made to the system based upon this analysis, should comply with the static force conditions of good electrical contact.

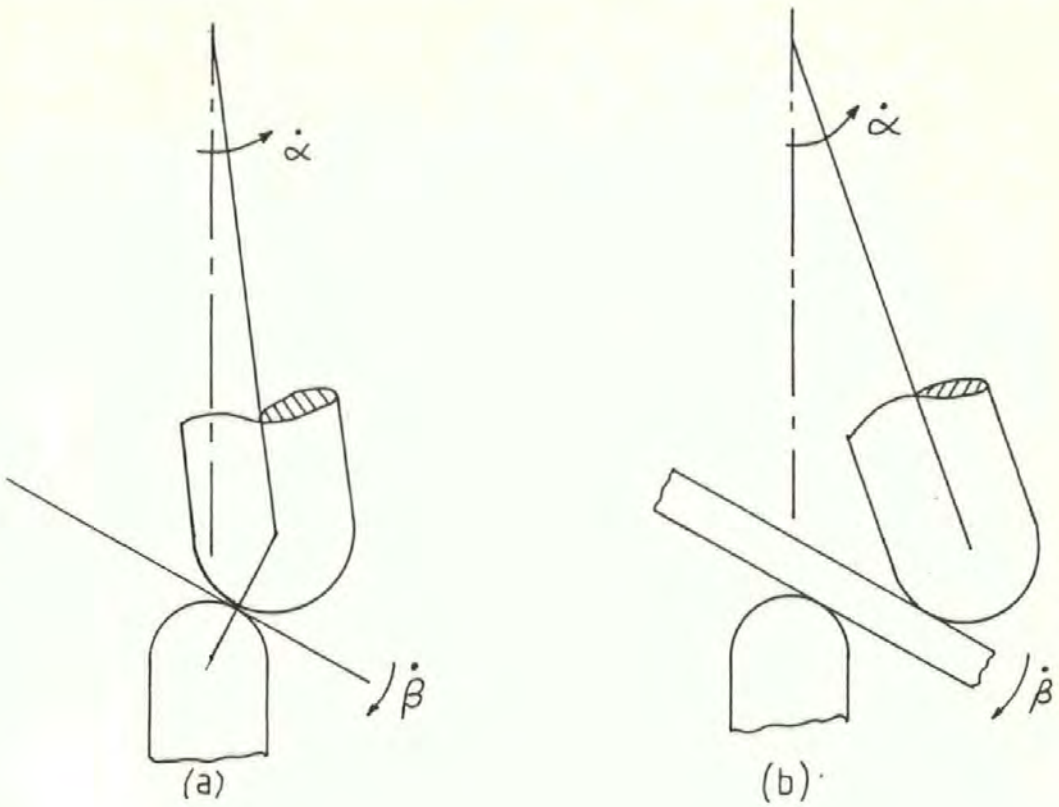

Figure 4.5 The Geometry of the Blade and Plunger during Changeover

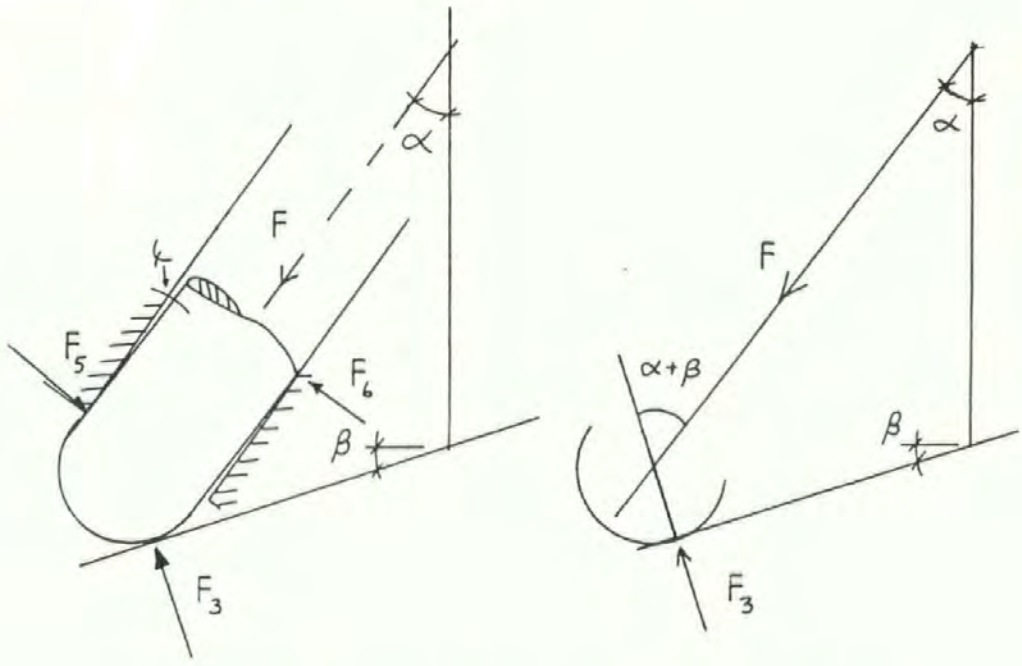

Figure 4.6 The Static Force Distribution on the Static Plunger

4.3.1 The Static Force Distribution in a Rocker Switch

The distribution of forces in the static equilibrium position are shown in figure (4.6). This shows the plunger sitting at an angle in a stationary actuator. The angle, φ, is small, and for the purpose of this analysis can be assumed zero. Thus for equilibrium along the centre line of the actuator,

Eq.(4.1), or $$F_3 = \frac{F}{\cos(\alpha + \beta)}$$

where F_3 = the force on the blade due to the stationary actuator assembly.

If the plunger sits in the well of the blade, as shown in figure (4.7), this relation is simplified, to;

$$F_3 = F$$

The distribution of the reaction force between the main contact, and pivot contact can be similarly established, with reference to figure (4.7), and assuming that the plunger sits in the well of the blade. The equilibrium conditions give;

Eq.(4.2), $$F_2 + F_1 \cos\beta = F \cos\alpha$$

$$F \sin\alpha + F_1 \sin\beta = F_4$$

and, by moments $$F_2 \cdot \ell_2 - F \cdot \ell + F_4 \cdot \ell_4 = 0$$

where, ℓ are the moment arms,

With the small value of ℓ_4, assume $F_4 \cdot \ell_4 = 0$: then, $F_2 = F \cdot \ell / \ell_2$: and

In equation (4.2), this gives the pivot force (F_1), as,

Eq. (4.3) $$F_1 = F (\cos\alpha - (\ell / \ell_2)) / \cos\beta$$

4.3.2 The Formulation of the System Dynamics

Having identified the nature of the mechanism's movement, it is clear that some relation exists between the pivot bounce and the velocity of the mechanism. In equation (2.20) the velocity of impact has been seen to be related to the total duration of bounce. In terms of energy the bounce is dependant upon the kinetic energy of impact and the dissipation at the interface. The aim of this section is therefore to mathematically evaluate the conditions at main contact impact for the mechanism considered in the initial investigation.

The formulation of the dynamics begins with a statement of the factors to be considered. Classically, only very simple models of most phenomena were considered since the solution had to be achieved by hand, however as the power of computers and numerical methods have developed, increasingly complicated models have become tractable. The basic system by which this type of problem is approached is described by the flow chart in figure (4.8). The solution to the mathematical model is compared in some validation process, for example a comparison to experimental results. If the result of the validation is unsatisfactory then some modification is required.

The initial problem is to construct the mathematical model as a compromise between the factors that have a bearing on the validity; while keeping the model sufficiently simple that it is solvable using the tools and time at hand. For example, in the problem at hand gravitational affects are neglected. It may be possible that gravity does have an affect, so a statement of the assumptions is made such that when the model is validated against experimental results the main sources of error can be identified in the case of an unsatisfactory solution.

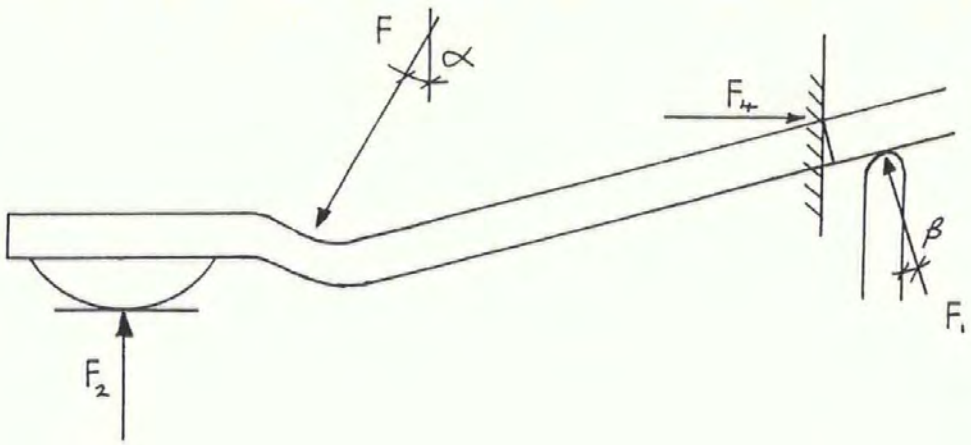

Figure 4.7 The Force Distribution on the Blade

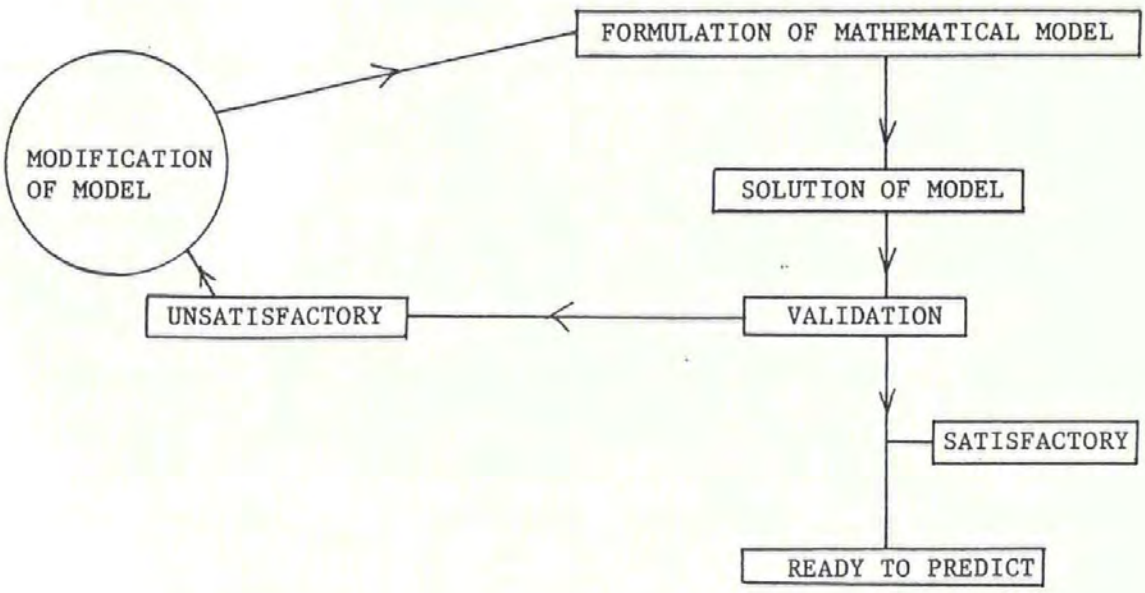

Figure 4.8 The Mathematical modeling process

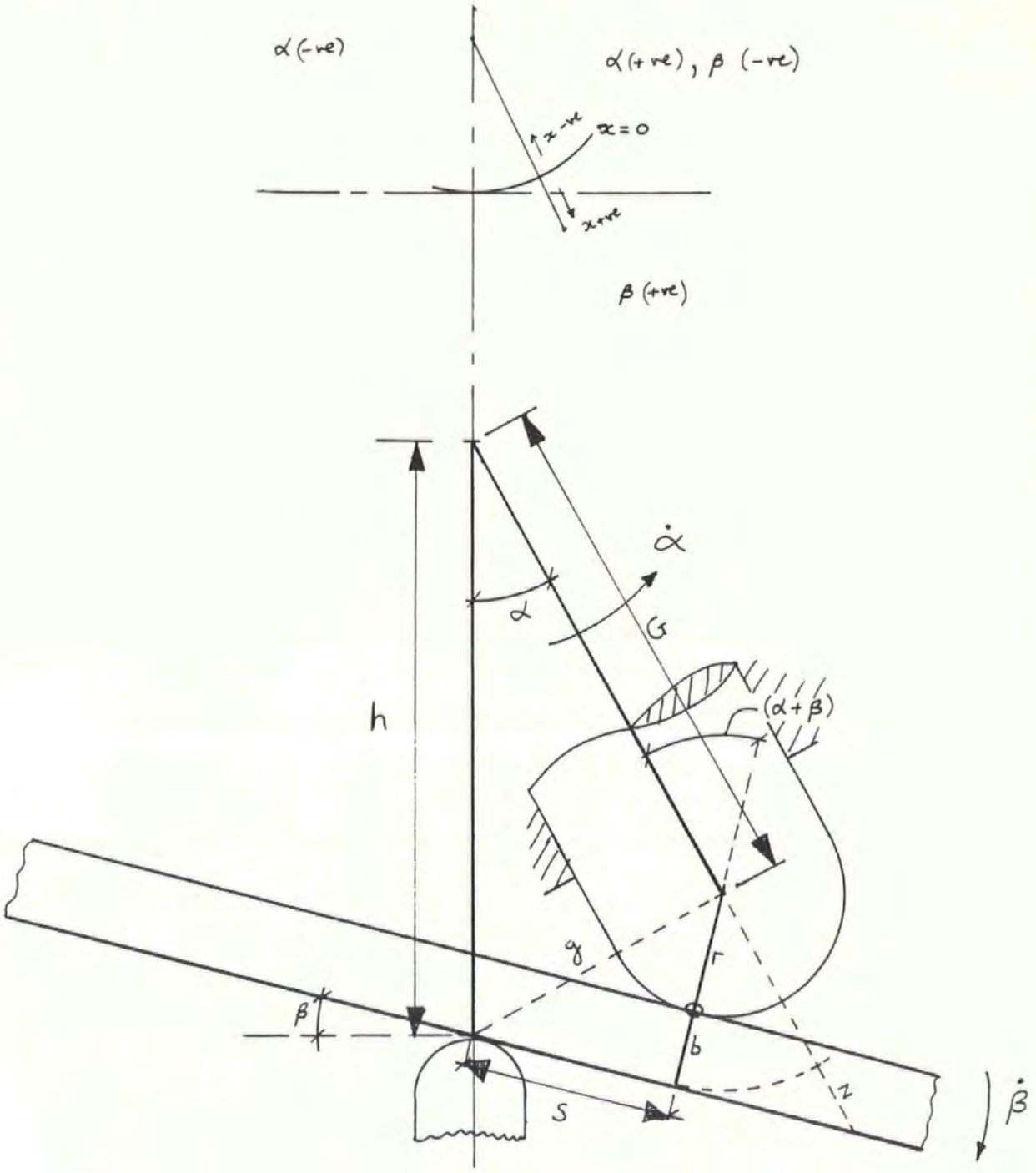

Figure 4.9 The sign conventions and notation used in the system dynamics of the Rocker Switch

4.3.2.1 Mathematics of motion

The notation and sign conventions used in this analysis is shown in figure (4.9). The various stages of motion are based on the observations made in section (4.2). The sequence of events occurring during switching are as follows, with the actuator moving from left to right.

(1). As the rocker is actuated the rotation causes the plunger to move up the blade, contracting the spring.

(2). At s = 0, α , and β , are negative (i.e. the right hand side of the blade is above the horizontal as shown in figure (1.2). At this point the contact force at the main contacts will go to zero and the blade will slowly start to rotate.

(3). As the actuator angle passes through zero to positive, the blade will accelerate causing the blade angle to pass through zero to positive. This is the situation shown schematically in figure (4.9), which also defines the angular velocity terms.

(4). At main contact impact, α , and, β , are positive.

(5). Bounce occurs at the pivot and main contacts, as the actuator assembly moves down the blade.

The mathematics of the switch motion is based upon the conditions occurring at (3). However the initial conditions of the system at the

onset of motion are important, and need defining.

The following assumptions are made with the aim of making the model tractable, so that the solution can be obtained by computation.

(i). At all times the plunger is in contact with the blade.

(ii). There is no external force applied to the system. This assumption is made since it would be too difficult to accurately evaluate the applied force as a function of time. Therefore, as an initial assumption the motion is caused by the release of potential energy from the compressed spring. This is a major assumption since the applied force clearly has an important effect.

(iii). Gravitational forces are negligible.

(iv). The blade is stiff and as such, is not subject to bending or vibration.

(v). There is no slip between the pivot and blade during blade rotation. To justify this assumption mathematically, the following assumption is also made.

(vi). The pivot is a knife edge, a frictionless bearing, and lies on the centre line of the switch.

(vii) The moment of inertia of the rocker and plunger assembly is not a function of time. In the real case because of the curvilinear motion executed by the plunger, the total moment of inertia of the actuator assembly will increase with the spring extension (x).

(viii) To satisfy assumption (vii), the mass of the plunger is taken as zero.

Using these assumptions, a series of dynamic equations are produced, defined as, equation set (1), and based upon the free body diagrams shown in figure (4.10). Equations (4.4), and (4.5) are of the form (torque = inertia x angular acceleration), [3].

Equation Set 1

Forces on the blade, in figure (4.10a).

$$R.s + \mu_1 .R.\ b = I_b .\ \ddot{\beta} \qquad (4.4)$$

Forces on the rocker assembly, in figure (4.10b).

$$R.G.\sin(\alpha+\beta) - \mu_1 .R\ (\ G.\cos(\alpha+\beta) + r\ ) = I_P .\ \ddot{\alpha} \qquad (4.5)$$

The resolution of forces in the direction of the spring force, with a simplification of the plunger friction.

$$F - \mu_2 .\ N = K\ (\ G_o - G\ ) = R\ (\ \cos\ (\alpha+\beta) + \mu_1 \sin\ (\alpha+\beta)) \qquad (4.6)$$

(a)

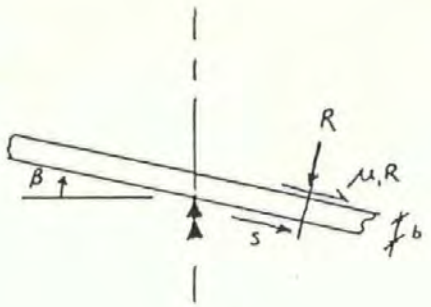

Forces acting on the blade

(b)

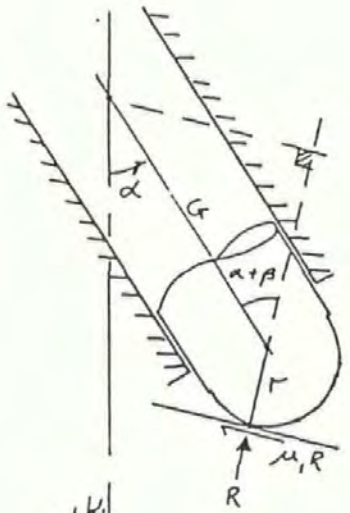

Forces acting on the actuator assembly

(c)

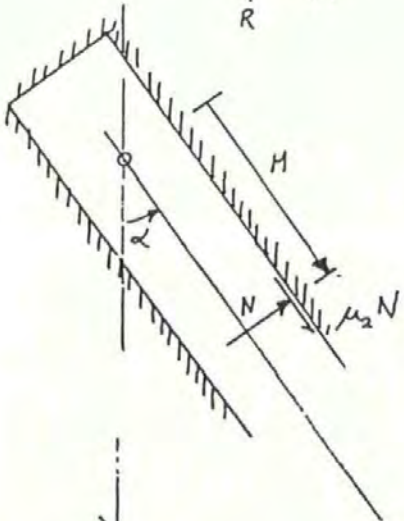

Forces acting on the rocker

(d)

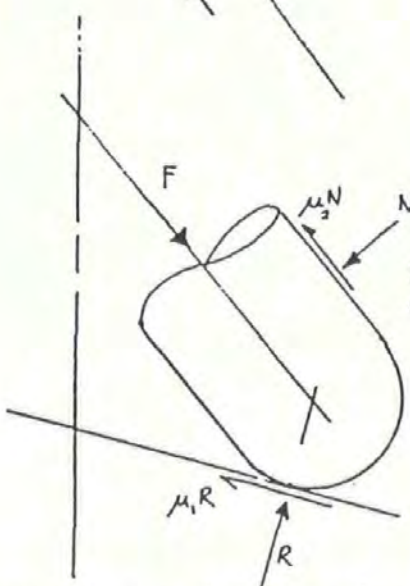

Forces acting on the plunger only

Figure 4.10 Free body diagrams of the forces during switch motion

where $G_o = (l - e - r - b + h)$

l = the free length of the spring,

e = the maximum compression of the spring at $\alpha = 0$,

I_b = The moment of inertia of the blade about the pivot.

I_P = The moment of inertia of the actuator assembly.

From (4.6), the reaction R can be obtained, and simplified with the further assumption that $\mu_2 . N$ is small compared to F.

$$(4.7) \qquad R = \frac{K (G_o - G)}{\cos(\alpha + \beta) + \mu_1 \sin(\alpha + \beta)}$$

By substituting R into (4.4) and (4.5) gives equation set 2,

$$(4.8) \qquad \ddot{\beta} = \frac{K (G_o - G).(s + \mu_1 b)}{I_b . (\cos(\alpha + \beta) + \mu_1 \sin(\alpha + \beta)}$$

$$(4.9) \qquad \ddot{\alpha} = \frac{K (G_o - G).(G\sin(\alpha + \beta) - \mu_1 G \cos(\alpha + \beta) - \mu_1 r)}{I_P . (\cos(\alpha + \beta) + \mu_1 \sin (\alpha + \beta))}$$

The geometric constraint impos ed by assumption (i), can be used to define both the dimensions G and s, thus

$$G = \frac{h \cos \beta - (r + b)}{\cos (\alpha+\beta)} \tag{4.10}$$

$$s = \frac{h \sin \alpha - (r + b). \sin (\alpha+\beta)}{\cos (\alpha+\beta)} \tag{4.11}$$

Thus both G and s, are functions of α , and β .

Therefore equations (4.10), and (4.11) can be substituted into (4.8) and (4.9), to give,

$$\ddot{\beta} = f_1(\alpha , \beta) \tag{4.12}$$

$$\ddot{\alpha} = f_2(\alpha , \beta) \tag{4.13}$$

This is defined here as equation set(2).

Thus the motion can be represented by two simultaneous second order, nonlinear ordinary differential equations in time. To solve this set to give, α, x and, β, as functions of time it is necessary to use a finite difference method in the form of a software package.

The package used is the routine D02 BBF, [4], produced by the Nottingham University Algorithm Group, (NAG). This routine integrates a system of first order ordinary differential equations over a range, with suitable initial values, using the Runge, Kutta, Merson method, [5], and returns the solution at points specified.

In order to utilise this routine the equation set must be presented in the form, of a series of first order differential equations, as shown;

$$\dot{Y}_i = F_i\ (T, Y_1, Y_2, Y_3, \ldots\ldots\ldots Y_N) \qquad i = 1,2,3,\ldots N \tag{4.14}$$

where N = the number of simultaneous equations.

F_i = A function,

$\dot{Y}_i$ = The derivatives of $\dot{\alpha}$, $\dot{\beta}$, and $\dot{x}$,

T = Time,

Y_i = The variables, α, β, and x.

4.3.2.2 Modification of Equation (Set 2), to Satisfy the Numerical Method

The first step transfers the system of second order equations to a first order system. This is achieved by introducing new variables, shown as equations (4.15) and (4.16), in equation (set 3).

EQUATION (SET 3).

$$\dot{\beta} = y_1 \tag{4.15}$$

$$\dot{\alpha} = y_2 \tag{4.16}$$

$$\dot{y}_1 = f_1(\alpha, \beta) \tag{4.17}$$

$$\dot{y}_2 = f_2(\alpha, \beta) \tag{4.18}$$

For application to the numerical method, equation set (3) is written in the form dictated, this new set can be identified in the programme, subroutine (FCN), in appendix (5). The details of notation are also given in the appendix. This set models the switch motion shown in figure (4.9).

4.4 The Numerical Solution of the Mathematical Model

The programing language used in this computer model is double precision FORTRAN 77, this compiled language is used on a PRIME main frame computer. The software routine used to solve the differental equations is stored in the main frame library and called at the compiling stage.

In order to verify the software two programmes have been produced, the first "VERT" models the simplified situation detailed in Verifcation 1. The second programme "DYNAMICS" models the conditions of a real switch operation, under the influence of an applied force external to the system. This application is important and is considered in full detail in Verification 2; this programme is given in appendix (5).

4.4.1 Computational Method and the General Programme Structure

The structure of the method is specified by the NAG routine and consists of a main programme which is used to define initial conditions and call 3 subroutines, FCN, OUT, and D02 BBF. The nature of these routines are now considered as they apply to this problem. Figure (4.11) shows the structure of the programme, and defines some of the important steps. The structure of D02 BBF is only assumed since the routine is copyright controlled.

In the following discussion, Y, is used to identify the parameters evaluated by the numerical method.

With reference to figure (4.11); after the switch parameters and initial conditions have been defined, the programme reaches the CALL statement. This opens the NAG subroutine.

The NAG routine then calls the OUT subroutine to print the initial values, the return statement in OUT, brings the routine back to NAG. However because more than just the Y terms are required at each step, OUT initially calls FCN to evaluate these. These values are then returned by use of a COMMON statement to OUT and thus printed.

The NAG routine evaluates the next values of Y, by calling FCN and evaluating the functions F(1-4). When the new values of Y, are deemed satisfactory, they are transfered to OUT to be printed, OUT then calls FCN to evaluate the additional terms, of β , $\dot{\beta}$, etc.

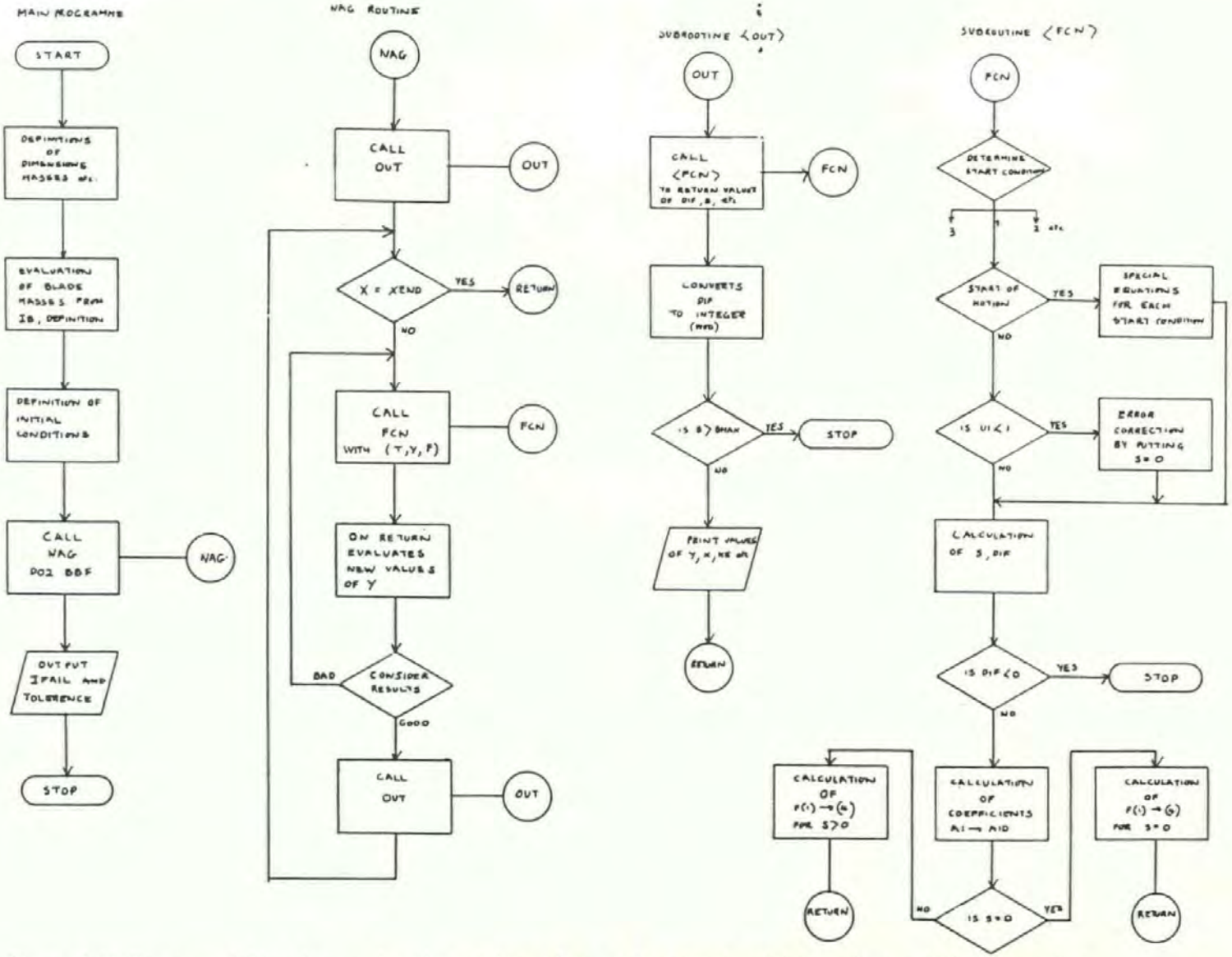

Figure 4.11 The general flow diagram for the solution of the mathematical model by a finite difference method

Subroutine FCN

The algorithim which is represented in the subroutine FCN is important to the satisfactory working of the model, since it is at this stage that all decisions must be taken regarding model errors. A discussion of some of the more typical errors follows.

(1) A problem with the numerical method was in the estimation of new values of, Y, since some of the values would lie outside the geometry defined by equation (4.16). In simple terms a value of, α and, x, can be given where, x, is too large. In this case, g, becomes less than, (r+b). In these circumstances the programme fails, thus the routine traps the error and sets, (g= r+b), which is equivalent to (s=0). With (s=0) a special block is required to stop computational problems with the zero value.

(2) A further problem occurs when, s, becomes negative. This occurs when the blade rotates faster than the actuator. In this case the spring tends to reduce the blade momentum, and causes the system of equations to fail. To monitor this problem an addition term DIF is evaluated and if DIF<0 then the routine is stopped.

4.5 Verification 1

For the purpose of this verification the initial conditions were simlpified to the following requirements.

α = a small positive angle,

β = a small negative angle,

x = a function of α, and β,

$\dot{\alpha} = 0$

$\dot{\beta} = 0$

$\dot{x} = 0$

To satisfy the verification an experiment was made to reproduce the conditions with no applied force. The switch action was filmed and the X, Y, Z, data trasfered to a, β, versus time characteristic. The dimensions of the switch used were entered into the programme VERT. A comparison could then be made for the purpose of verification.

4.5.1 Experimental Conditions

The switch used for this investigation was a standard production type, with only one plunger and blade. The switch was sectioned to reveal the contacts for filming.

To model the assumptions the moving contact was supported such that, $\beta \simeq 0$, and, α, offset in the positive direction, such that on releasing the support the spring would close the contacts. Figure (4.12) shows the configuration used.

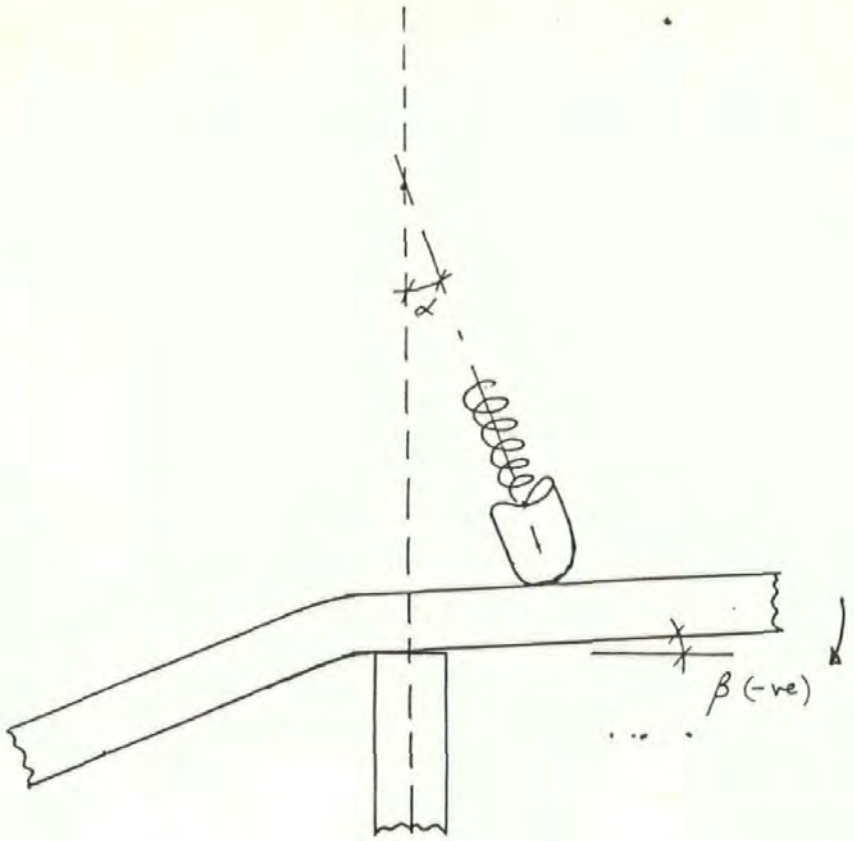

Figure 4.12 The configuration used as the initial condition in verification 1

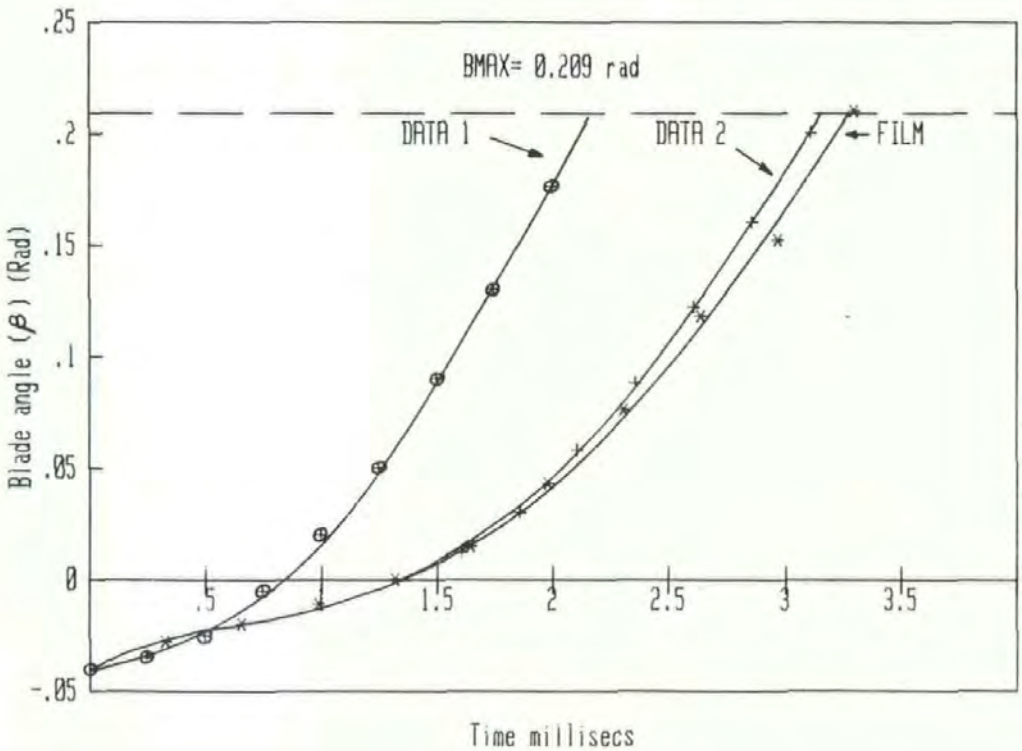

Figure 4.13 The response of the blade angle (β) with time, and a comparison with computer predicted results in Verification 1

The release of the blade support was syncronised with the high-speed camera by the use of the event relay, and the resulting film response is shown in figure (4.13).

4.5.2 Results from Verification 1

The film data shows the blade accelerating from a small negative angle and impacting the main contacts at (BMAX = 0.209 radians), where (BMAX) is the angle at impact. The values obtained in a detailed study of the switch dimensions and inertias are presented in appendix (7), and entered into the programme VERT, to produce the response shown as DATA 1. It shows the computer prediction reaching the impact angle 1.2ms before the film data. It is however important to note that the slopes at impact are similar. The delay in the film data is assumed to be caused by the release mechanism interfering with the natural blade response. To overcome this difference the initial conditions used in the computer model were adjusted to match the conditions shown on the film at, $\beta = 0$.

New Initial Conditions

At, $\beta = 0$, α = a small positive angle, t = 0, $\dot{\alpha} = 0$, and $\dot{\beta} = 39.0$ rad/sec.

Where, $\dot{\beta}$, is the slope derived from the film characteristic at $\beta = 0$.

This new set of initial conditions, assumes the actuator velocity to be the same as in the initial set. This is resonable since the actuator is slow to move under this condition. The initial value of, x, and, $\dot{x}$, can be evaluated, with reference to figure (4.14).

For the contact to be maintained between the plunger and the blade, the following conditions must be satisfied.

$$s \cdot \dot{\beta} = \dot{x} \cdot \cos \alpha$$

thus; $\dot{x} = s \cdot \dot{\beta} / \cos \alpha$

where, s, is defined from the geometry.

For the conditions specified, figure (4.13) shows the new computer predicted response labelled DATA 2. It shows how the predicted impact time is (0.15 ms) before the film impact. The slopes at impact are well matched in both cases, as shown in table (4.2), which compares the conditions at main contact impact.

	$\dot{\beta}$ (initial)	t at make (ms)	$\dot{\beta}_i$ (rad/sec)
Film Data	39.0	1.9	140
Data 3	39.0	1.75	167

Table (4.2)

where, $\dot{\beta}_i$ = the angualar velocity of the blade at impact.

4.5.3 Discussion of Parameter Changes

The number of variables and assumptions used to obtain the comparison inhibits a full error analysis, however the errors are considered by monitoring how small changes in the major parameters affect the response shown as DATA 2. For example figure (4.15) shows how changes in the blade inertia (identified here as IB), affects the computer simulated response. As the blade inertia increases the rsponse of the blade becomes slower, thus reducing the impact velocity of the contacts. This reflects the expected response of the blade in the real situation.

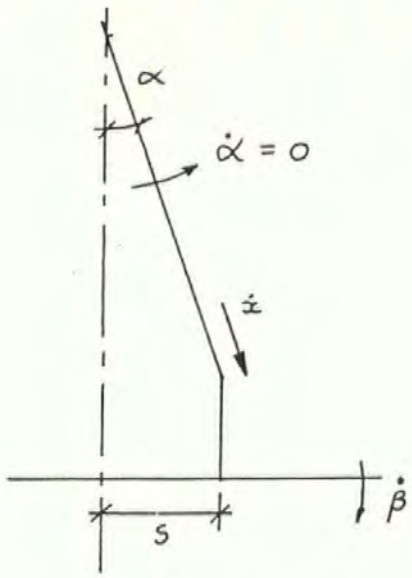

Figure 4.14 The Velocity diagram of the system for Verification 1

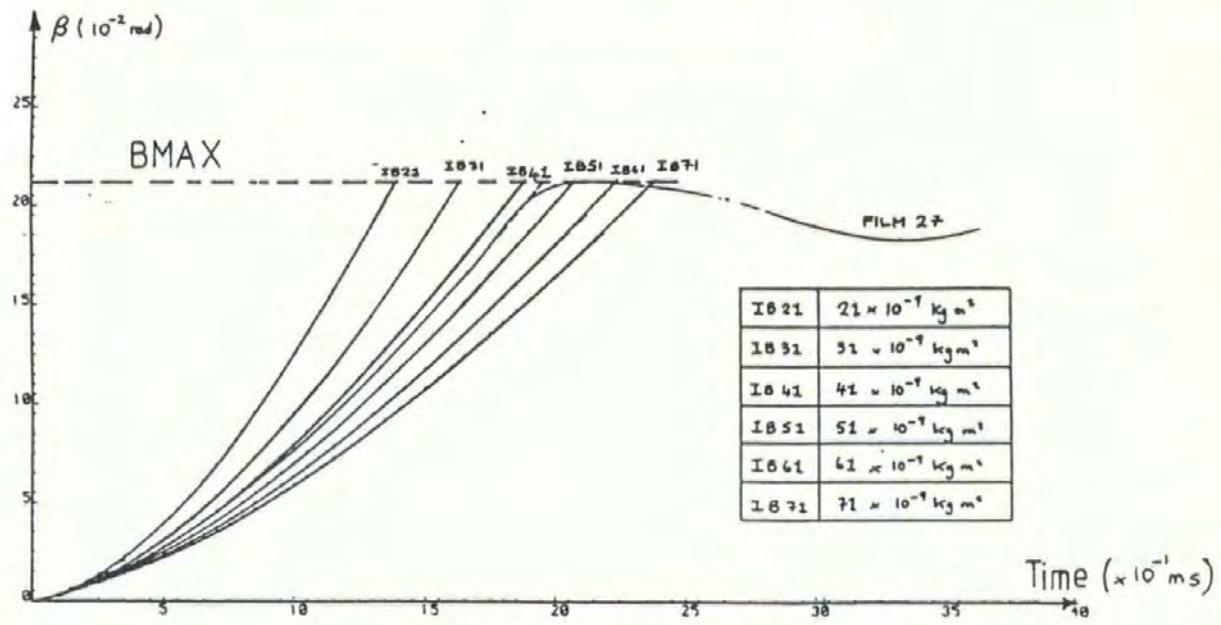

Figure 4.15 Verification 1, and the variation of the blade inertia (IB)

Hence a small increase in the blade inertia from the experimentally determined value of 41.0×10^{-9} Kgm, IB41, could bring the two characteristics together. Similarly consideration of the coefficent of friction shows that a reduction could have a similar effect. Consideration of the spring stiffness shows that an increase in K, reduces the time to impact. A full discussion of these variations are given in reference, [6].

4.5.4 Conclusion of Verification 1

With the initial conditions adjusted to match the film data, the computer prediction lies within 0.15 ms of the film data at impact. This difference can be made zero by reducing K (the spring stiffness), increasing IB, or by changing any number of parameters. This is not undertaken since the response is deemed accurate with consideration to the assumptions made. In conclusion changes in the major parameters effect the blade response in the expected manner.

The actuator response under these ideal conditions was shown on the film to move up the blade as the blade closed, and this was also demonstrated in the computer response. This condition occurs because of the slow initial acceleration of the rocker assembly from zero, relative to the high initial acceleration of the blade. In conclusion the mathematical model has been proved under these ideal conditions. In the verification 2, a real operation case is considered where the actuator moves under hand forces as the switch is operated.

4.6 Verification 2

The data presented in the initial ivestigation into rocker switch dynamics is used in this section as the basis for a further development of the computer model to represent the events occurring during a real switching action. This includes a consideration of the applied hand force and the effect of switching a double pole configuration. The initial conditions defined in the previous section must therefore be reconsidered.

4.6.1 The Real Switching Action

In theory the blade will start moving when, s = 0; and, α , is slightly negative. This can be seen to be the case in figure (4.3) where the actuator angular velocity has been shown to accelerate under the influence of the external hand force. Because the period of blade motion is small compared to the overall period of the actuator motion, it can be assumed that over the period of blade motion the angular velocity of the actuator is constant.

In the real switching action the actuator response, and blade changeover time (BM) is a function of the applied force. Thus with the switch activated quickly the actuators time for movement from static position to static position is reduced, and the slope during blade change over increased.

4.6.2 Accounting for the Applied Force

In the initial verification and model development, the applied force was neglected because of the difficulty in predicting the magnitude, direction, and time variation of the impulsive hand force. To account for this force advantage is taken of the consequence of the actuator velocity $\dot{\alpha}$, being constant. This is achieved by giving the rocker/actuator assembly a large moment of inertia such that the initial value of, $\dot{\alpha}$, is maintained. Figure (4.16) shows how the measured value of rocker inertia, 4.52×10^{-7} Kgm^2, IR-7, decelerates the actuator under the initial conditions used in the previous verification; in this case with, ($\dot{\alpha}$ = 35.76 rad/sec). The eventual backwards movement is shown by the velocity going negative at 1.4 ms. With the value of, IR, increased by a factor of ten, IR-6, the velocity response of the actuator is improved, and almost constant. A further increase by a factor of ten, IR-5, shows a constant value can be maintained. For the purpose of this verification the rocker assembly inertia was held at IR=4.52×10^{-2} Kgm^2, IR-2; a factor of, 10^5, on the real, IR. This vastly increased value of, IR, has the sole effect of maintaining a constant actuator angular velocity, during the blade changeover.

4.6.3 Initial Conditions

In the first verification the initial conditions were simplified and adjusted to match the experimental data. In this case they must be defined such that the computer programme can evaluate the problem, under the general conditions of operation where, s, and, α, must pass through zero values. The zero values can result in programme failure, thus a full series of traps have been implimented within the software, to evaluate the

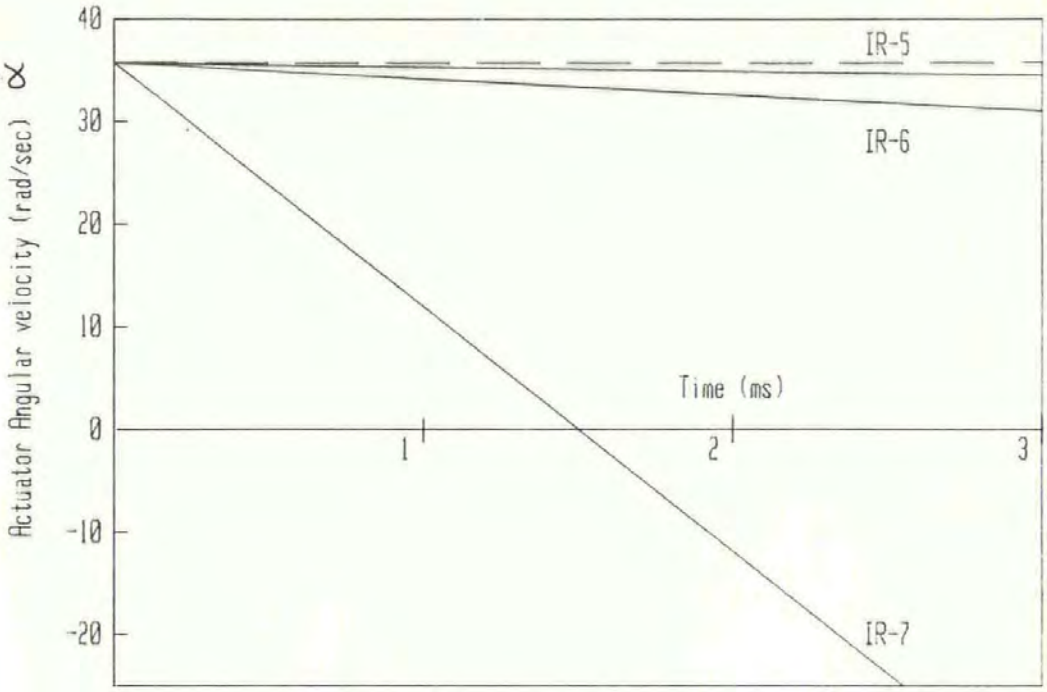

Figure 4.16, The influence of changes in the rocker inertia (IR) on the angular velocity of the actuator

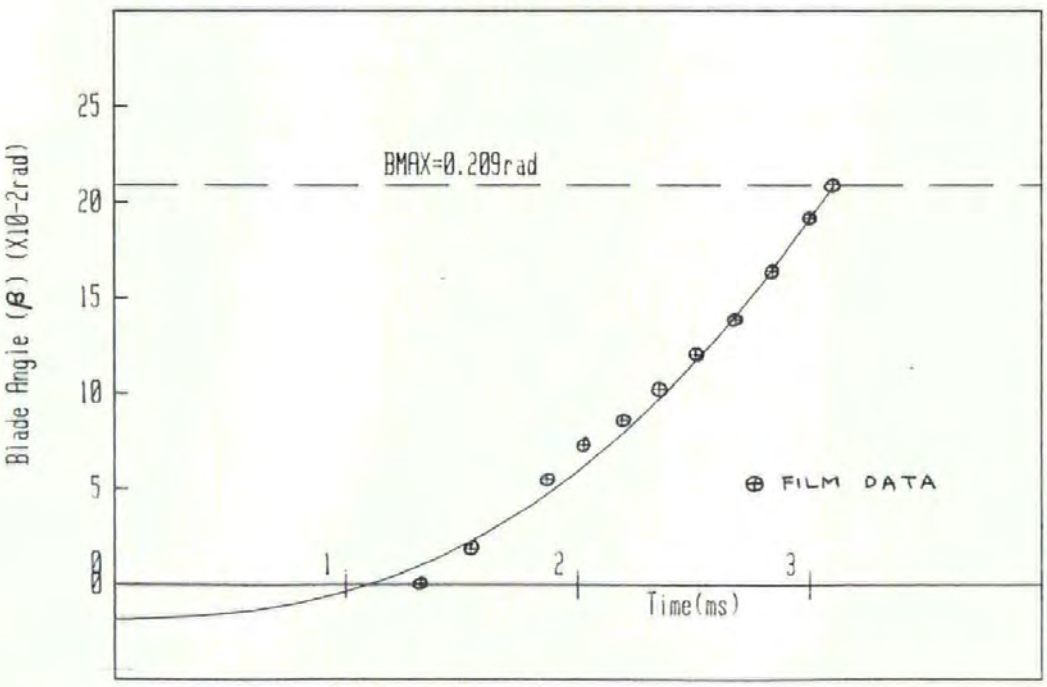

Figure 4.17, Verification 2, A comparison between experimental and computer predicted results

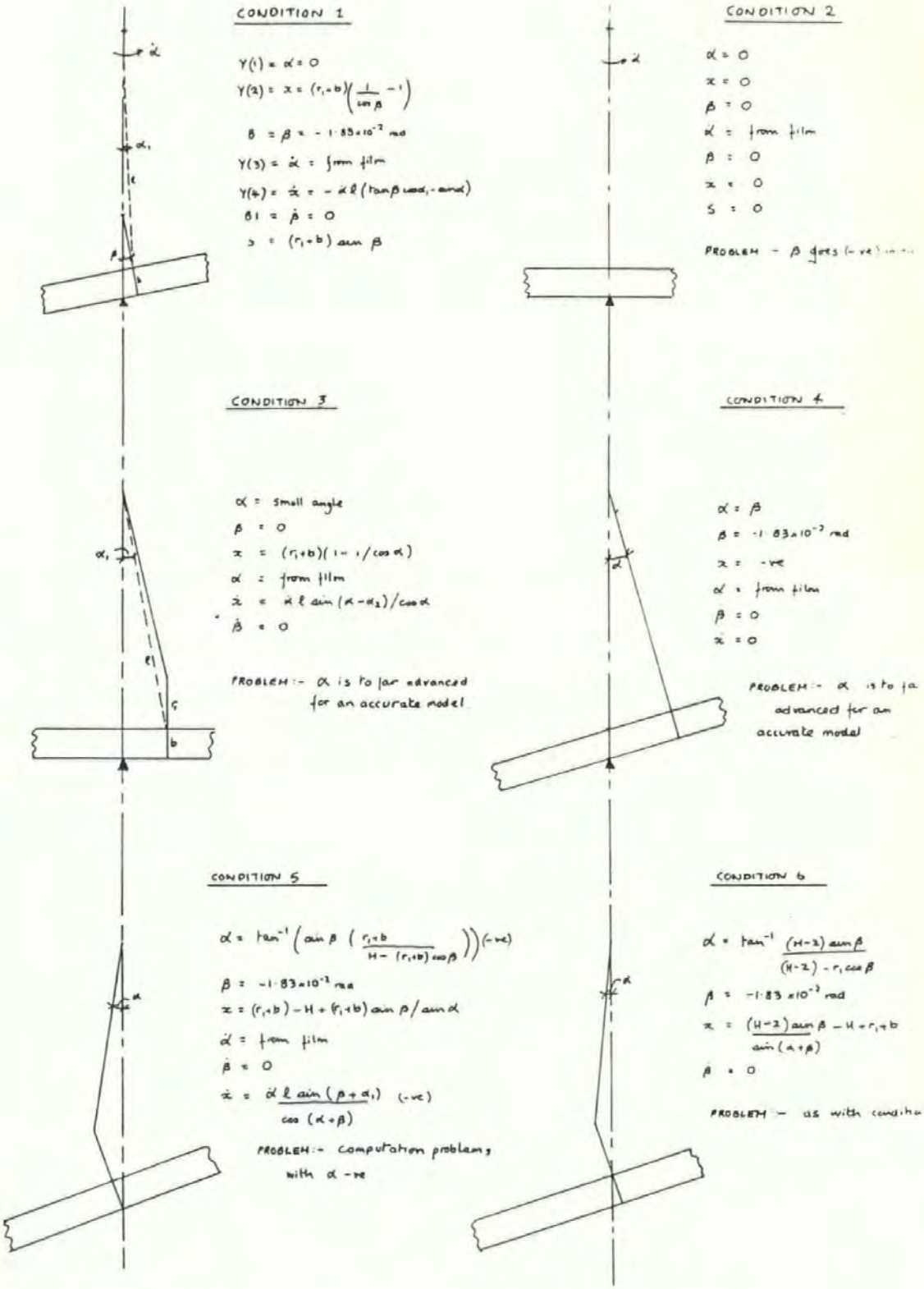

Figure 4.18 The initial conditions considered in Verification 2

equations under these conditions. A full analysis of various initial conditions gave the most computationally satisfactory to be Condition 1, in figure (4.18). The other five conditions show the range of initial conditions considered.

The other parameters used in this verification were taken in the same way as in the previous verification, and are unique to the particular switch studied. The values used are presented in appendix (5).

4.6.4 Double Pole Switching

The majority of switches manufactured are in the form of a double pole switch. To account for this condition the spring stiffness, K, and the blade inertia, IB, were doubled.

4.6.5 Results of Verification 2

The modifications discussed above are listed in the programme DYNAMICS, and the verification is based on the data in FILM 25. The resulting film and computer data are compared in figure (4.17). In this figure the times have been synchronised for the instant of main contact impact, thus cancelling the inaccuracies in the film data for the small displacement characteristic at the onset of blade motion. This inaccuracy is disscused in section (4.2.2), and for this film data a difference of 0.9 ms has been suggested. The figure shows that for the single pole switch the computer prediction of the switching action accurately models the film data, and more importantly the impact velocity of the blade is seen to be predicted.

The case of the double pole action gives the same computer response for the same switch and initial conditions.

4.6.6 Conclusions

The assumption of increasing, IR, (the rocker assembly inertia) to give the same effect as an applied force satisfies the condition of maintaining, $\dot{\alpha}$, and the initial conditions used give a response modelling the real switching action. The model is therefore considered verified and is used in the next section to consider the variation of parameters; in this way the major switch parameters are identified, and the model extended to optimise the switch dynamics.

4.7 The Variation of Parameters for Design Improvement

To enable a full design analysis this section is split into four major sub-sections. The first considers the variation of parameters on the response of the switch considered in verification 2. This data is then used to identify the major switch parameters. The second stage considers the design criterion best suited for the optimisation of the rocker switch in general. The variation of parameters is then extended to consider this criterion. The final stage is to consider the optimisation results. There are two approaches to the optimisation the first is a design improvement based upon a given manufactured switch. The second is an overall design approach for rocker switches.

4.7.1 The General Variation of Parameters and the Blade Response

The four graphs shown in figure (4.19 a-d), show how small variations in some of the parameters affect the response disscused in verification 2. The film characteristic represented by the curve FILM25, is the result of a computer generated curve fit. To enable the FILM25 curve to match the model curves from zero, a series of nine extra points with intervals of (0.1 ms), have been added, thus accounting for the (0.9 ms) delay. The mismatching of the film and model curves over the initial (0.9 ms), results as a consequence of the curve fitting method used. This is relatively unimportant since in this analysis it is the computer simulation that is important. The curve labeled CASE1 in figure (4.19a) corresponds to the verification curve in the previous section. The displacement of the film data arises because of the curve fitting exercise but the velocity at impact is still matched. In (4.19a) the assumed coefficent of friction of 0.01, is responsible for the characteristic CASE 1, by increasing this value to 0.1, as shown in CASE 2. The model shows that the time to make is reduced and the velocity at impact, increased. This is caused by the increased influence of the plunger upon the blade. A further increase to 0.2 in figure (4.19b) shows a further reduction in time to make. The influence on the blade of changing the rocker inertia IR, is demonstrated in figure (4.19c). The chosen value of, $IR=4.52\times10^{-2}$ or, IR-2, is the case identified as CASE1 in the previous two figures. This figure shows that a reduction in, IR, by a factor of (10^{-4}), IR-6, has only a small influence on reducing the time to impact. With the real rocker switch inertia, of, IR-7, the computer prediction fails. This is caused by the eventual negative velocity of the actuator, shown in figure (4.16). In figures (4.19d), the effect of changes in the initial condition, ($\dot{\alpha}$ = 35.76 rad/sec), is considered. The figure shows how small changes in, $\dot{\alpha}$, affect the blade response. Similar variations

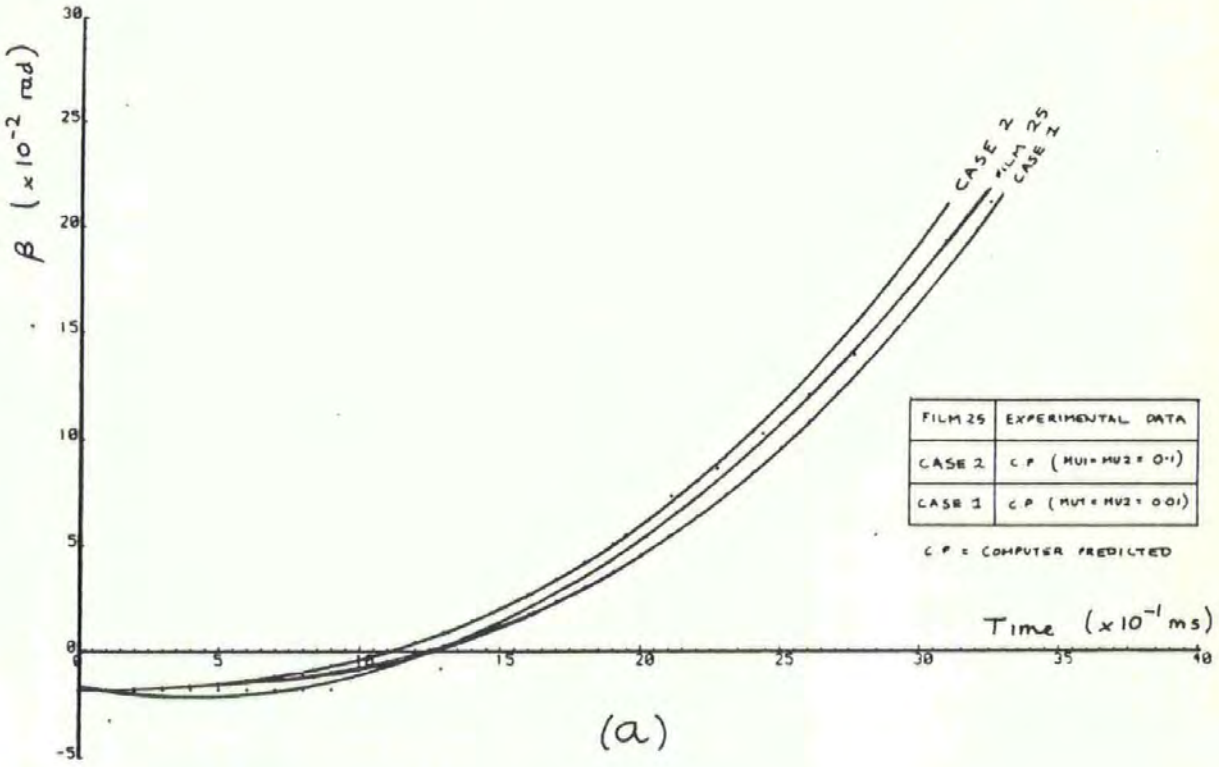

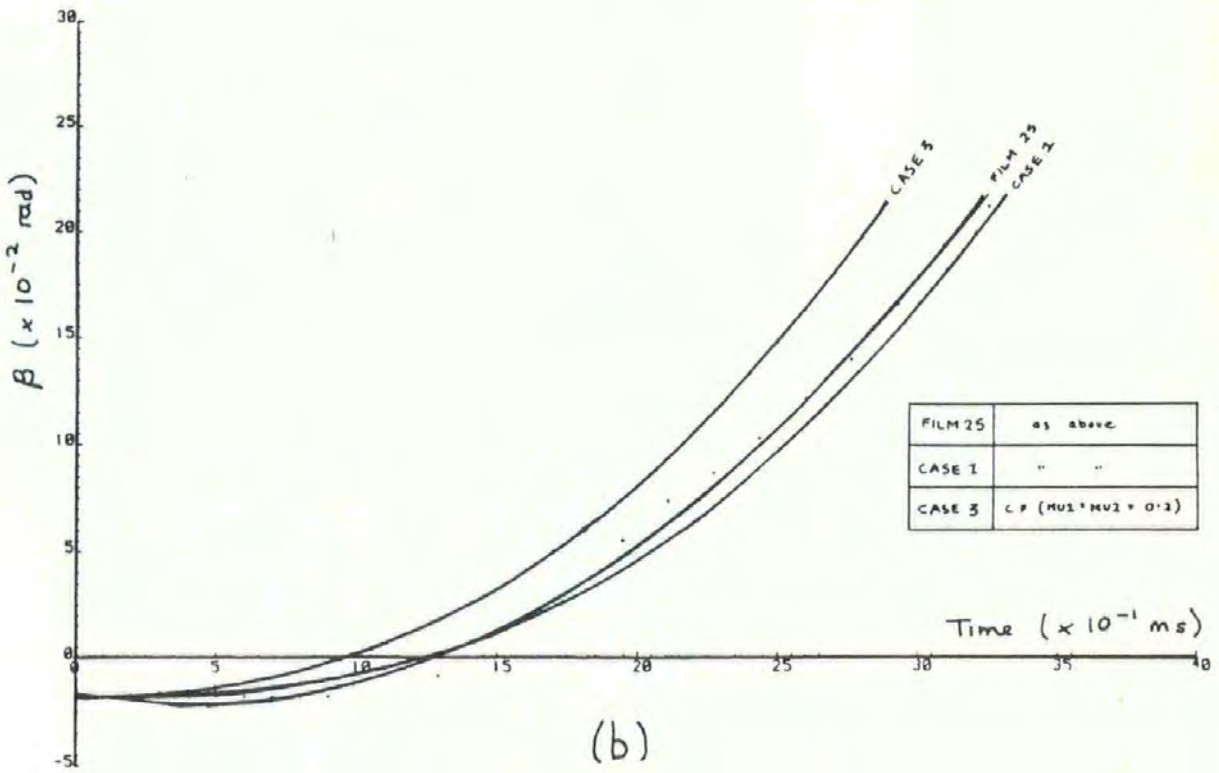

Figure 4.19 (a-b) The variation of parameters and the influence on blade response

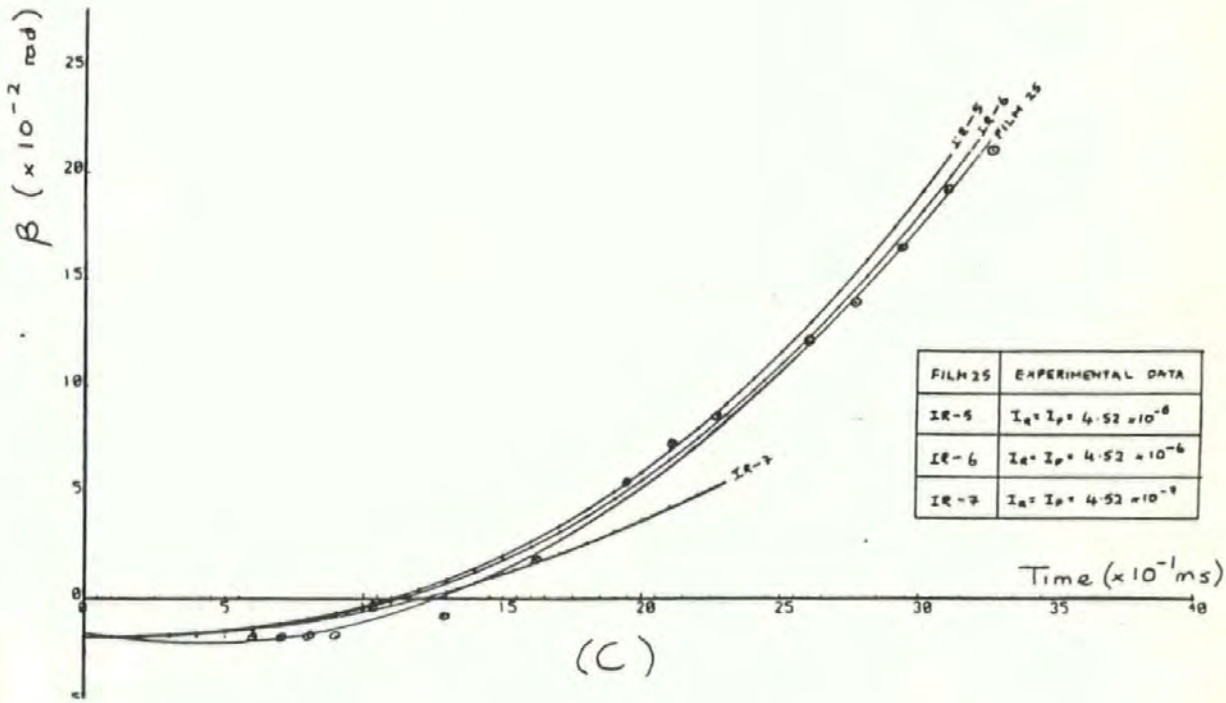

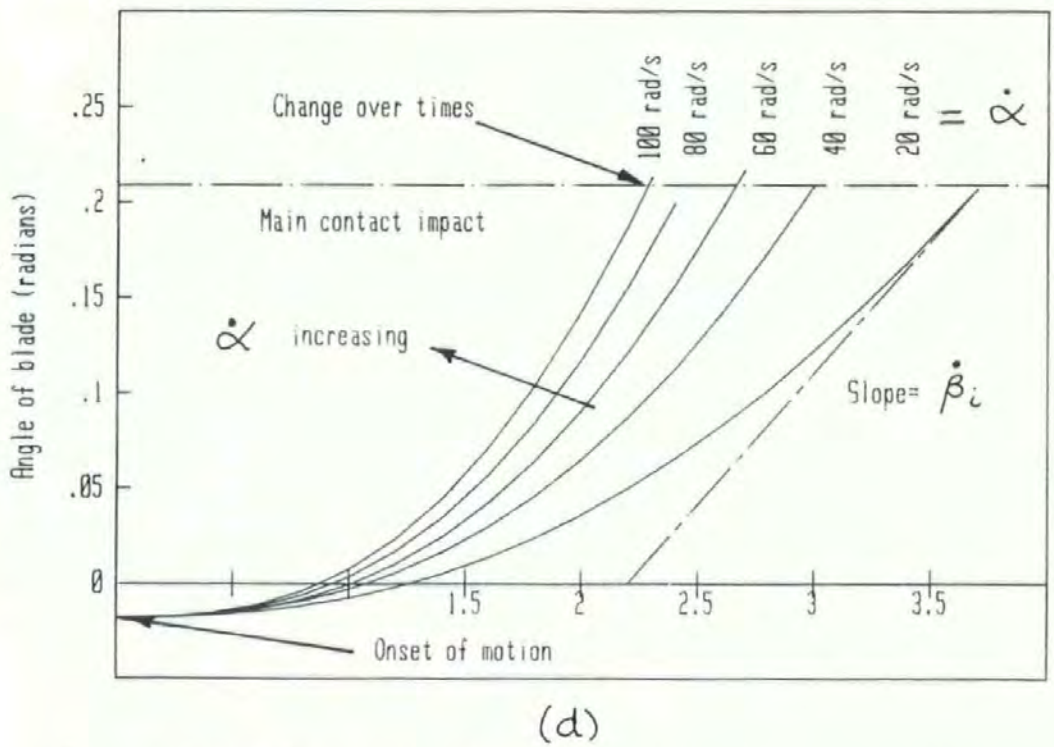

Figure 4.19 (c-d) The variation of parameters, and the influence on the blade response

considered in verification 1, show the blade inertia and spring stiffness also to be significant.

4.7.2 Design Criterion to Reduce Pivot Bounce

In section (4.2.4) the kinetic energy at impact was identified as the cause of pivot bounce, since it is the dissipation of this energy that constitutes the restitution phenomena. The computer model already predicting, $\dot{\beta}_i$, at the instant of main contact impact as shown in figure (4.19d), can thus be further modified to give the angular kinetic energy at impact. The kinetic energy at impact is given in equation (4.19), and is refered to in the text as (KEi).

Eq. (4.19), $KE_i = (IB \cdot \dot{\beta}_i^2) / 2$

where, $\dot{\beta}_i$ = the angular velocity of the blade at impact.

It is clear from this equation that the blade inertia (IB) is important in the evaluation of kinetic energy. It has been shown in figure (4.15) that increasing, IB, reduces, $\dot{\beta}_i$. Therefore, there exist a trade off in, KEi, between the increase of, IB, and the consequent reduction of $\dot{\beta}_i$.

To achieve a reduction in the impact kinetic energy the computer model is run to give the conditions at main contact impact only, while the major parameters are varied. This requires the use of Non-Local GOTO statements which are discussed and explained in appendix (6). This programme is called ENERGY, and to increase the accuracy of the evaluation of the impact energy, from the impact velocity, the number of steps used in the numerical method is increased from 40 to 160 steps. The increase

in the number of steps enables the routine to stop closer to the defined value of (BMAX).

4.7.3 Results of the Variation of Parameters on KEi

In the previous sections the importance of the angular velocity of the actuator and the kinetic energy of impact have been discussed, both are combined in this section to show how the kinetic energy is affected by changes in some of the other important parameters.

In figure (4.20) the influence of the spring stiffness is shown. For a given angular velocity, $\dot{\alpha}$, an increase in, K, will increase the value of, KEi. Similarly changes in, IB, are shown in the figure (4.21). This shows, KEi, increasing with, IB, for a given, $\dot{\alpha}$. The values of, IB, are as defined in figure (4.15).

The design approach used is to minimise the impact kinetic energy for the switch considered in verification 2; four approaches are discussed here.

(1) The variation of switch geometry.
(2) The reduction of $\dot{\alpha}$. This includes the spring stiffness.
(3) The reduction of, BMAX.
(4) The optimisation of, IB.

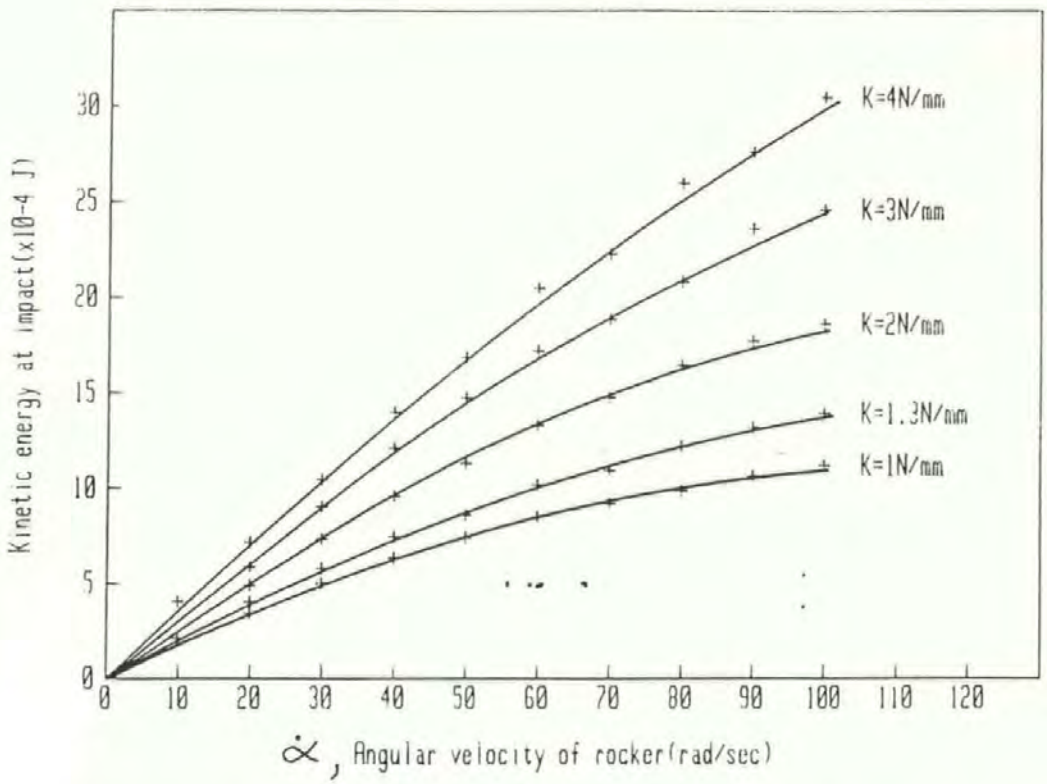

Figure 4.20, The angular velocity of the rocker, and the kinetic energy at impact

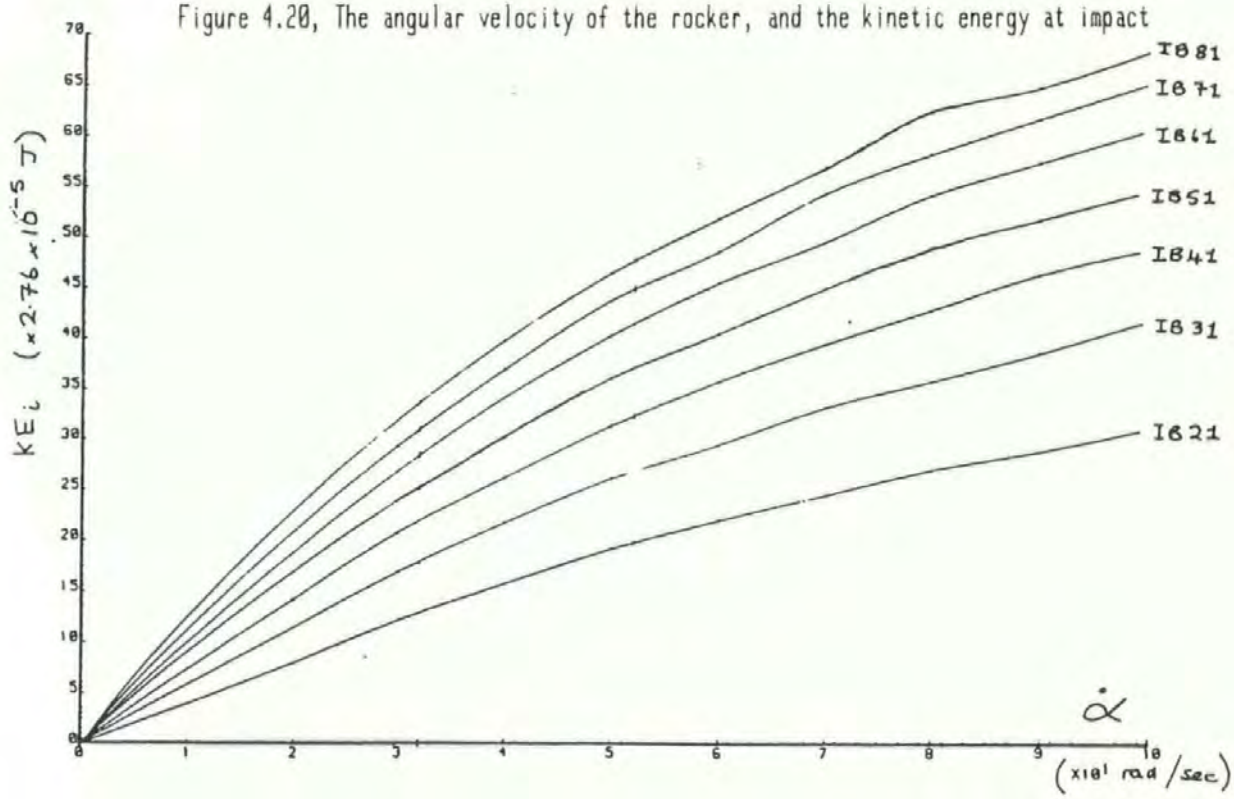

Figure 4.21 The angular velocity of the rocker and kinetic energy at impact with IB as a parameter

4.7.3.1 The Variation of Switch Geometry

The variation of geometry involves the optimisation of the following dimensions, h, and, r, as defined in figure (4.9) for a given, $\dot{\alpha}$, K, and, IB. Changes in, b, the blade thickness and, M, the blade mass, are not considered because these dimensions relate to the blade inertia.

Variation in, h, will affect the spring compression, e, at, α = 0, thus the changes in, h, are considered in two groups, e = constant, and e= f(h).

e = c (constant) = 5.76 mm, and e = v (variable)

r	h	e	KEi (10^{-5} J)
H	H	v	49.25
L	L	v	86.88
H	L	v	60.59
L	H	v	62.81
N	N	c	58.10
H	H	c	58.41
L	L	c	66.96
H	L	c	49.72
L	H	c	74.70

Table (4.3).

For the case where K=1.3 N/mm , IB = $41x10^{-9}$ Kgm^2, and $\dot{\alpha}$ = 30 rad/sec.

where h, high(H) = 15 mm r, high(H) = 2 mm

h, normal(N) = 14.35 mm r, normal(N) = 1.82 mm

h, low (L) = 13 mm r, low (L) = 0.5 mm

With reference to table (4.3) it can be seen that changes in, h, and, r, only have a small affect on the kinetic energy at impact. The

maximum reduction of 18 percent, occurs with, r, and h, high.

4.7.3.2 The Reduction of the Actuator Angular Velocity

In the switch considered the force exerted by the hand dominates the angular velocity at which the rocker operates. This means that the contribution of the spring is less than in a freely moving snap-action device. Although the value of, $\dot{\alpha}$, is mainly determined by the hand force, the hand force applied depends on the resistance of the mechanism. The resistance is the force necessary to overcome the static condition. This force is the minimum force that can be applied to the switch.

The nature of Hand Operation

The action of the rocker switch as an interface between man and machine is a very unsatisfactory from the point of identifing the actuation velocity of the device. It has been shown that with a solenoid, increasing the force, reduces the BM or changeover time. With reference to figure (4.19d), it is shown that increasing, $\dot{\alpha}$, reduces the time to make, which in this case corresponds to the BM time of the switch. In figure (4.22) the variations shown in figure (4.20) are presented in terms of BM times and variations in, $\dot{\alpha}$, for a given spring stiffness. Thus increasing the applied force increases, $\dot{\alpha}$, and reduces the BM time. This computer prediction matches the experimental relationship show in figure (3.10). In figure (4.23) the BM timesare related to the computer predicted values of, KEi, for a range of, K.

In hand operation the more se vere the handling the faster the BM time and thus KEi. For a given device there can be a range of operating

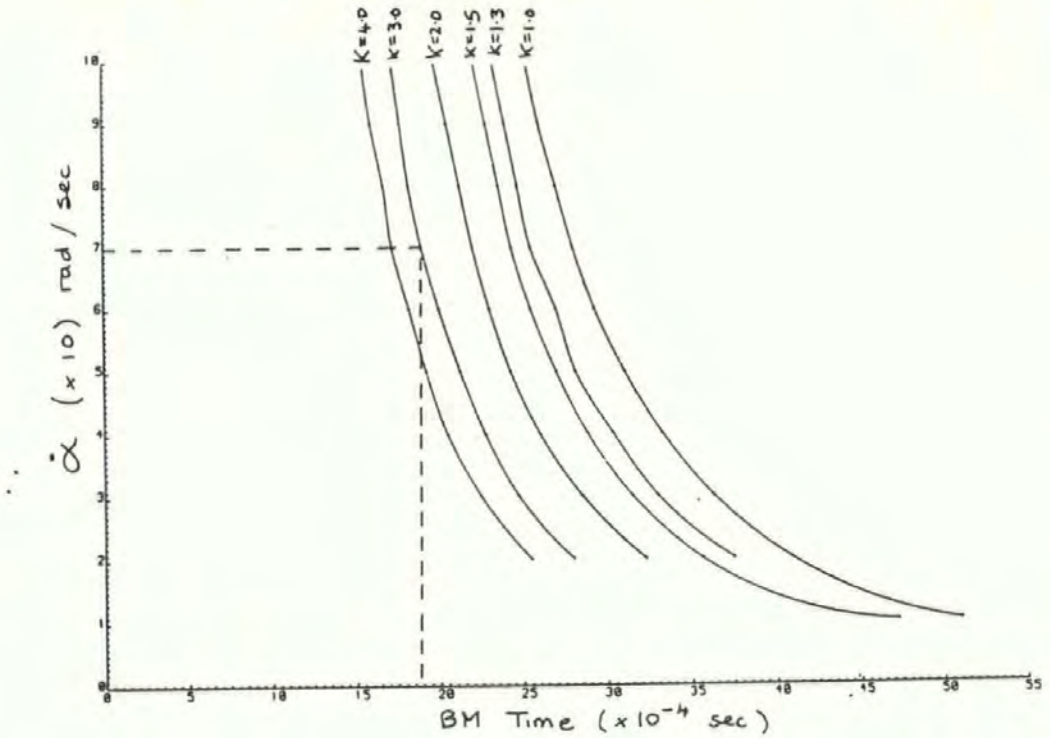

Figure 4.22 The angular velocity, and the resulting BM time, for a range of (K)

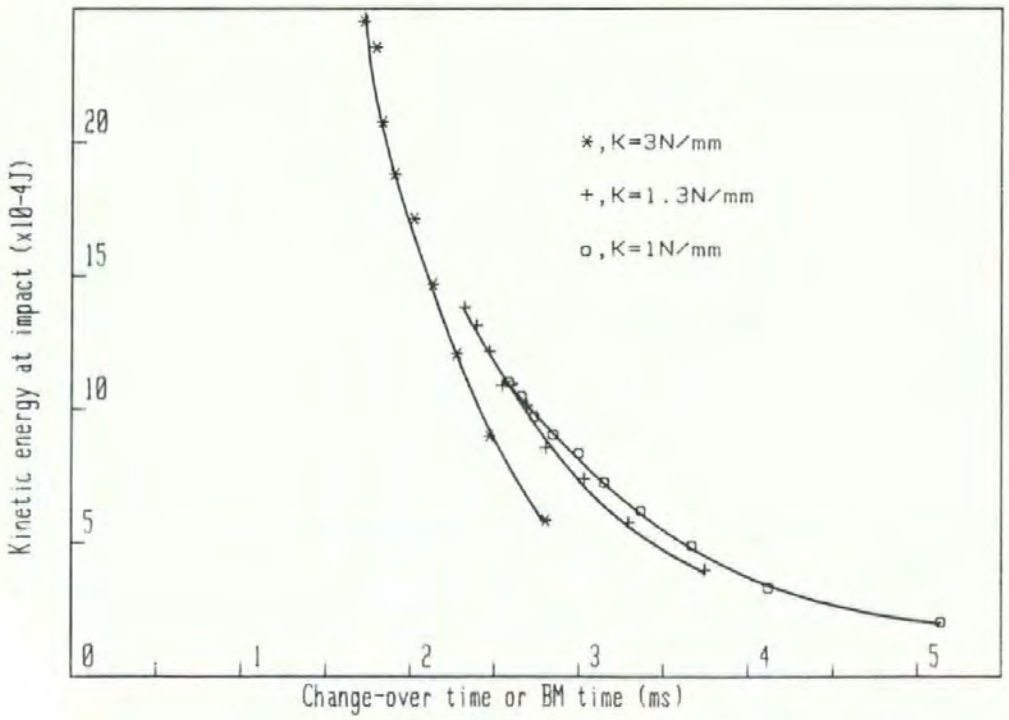

Figure 4.23 The Kinetic energy at impact for a given BM time, for a range of (K)

times depending on the method of operation. To evaluate this behaviour the switch under analysis was operated by hand in three regimes, soft, normal, and hard. In the soft operation the switch was purposfully actuated slowly. In the normal operation the switch was actuated at a medium or normal rate. In the hard operation the switch was purposefully operated fast. Using figure (4.22) the measured BM times can be converted to values of, $\dot{\alpha}$. In the case of 20 normal operations applied to the switch with two different spring stiffnesses, the mean values of, $\dot{\alpha}$, where as follows and are defined here as, $\dot{\alpha}_N$. This shows the influence of the spring on the hand operation, and the resulting, $\dot{\alpha}$.

For K = 1.3 N/mm, double pole switch, $\dot{\alpha}_N$= 50.0 rad/sec

For K = 3 N/mm, double pole switch, $\dot{\alpha}_N$= 65.5 rad/sec

The reduction of, $\dot{\alpha}_N$.

A means of reducing, $\dot{\alpha}_N$, is to reduce, K; however, this would alter the static distribution of the contact forces, and therefore change the contact resistance characteristics.

To study the influence of changes in spring stiffness, and the resulting changes in contact force, the static equations are used. The results of this analysis are shown in figures (4.24) and (4.25). The first figure shows how a reduction in the actuator static angle, α_s, increases the reaction force, F_3, for a given spring stiffness, while the second shows the percentage of, F_3, acting at the pivot for a given angle. The smaller the angle the more force at the pivot. In table (4.4) a series of values corresponding to the switch used; shows that by reducing the static angle to, 11.36° , the pivot contact force (F_1), can be maintained with a reduced spring stiffness of, K=1.3 N/mm.

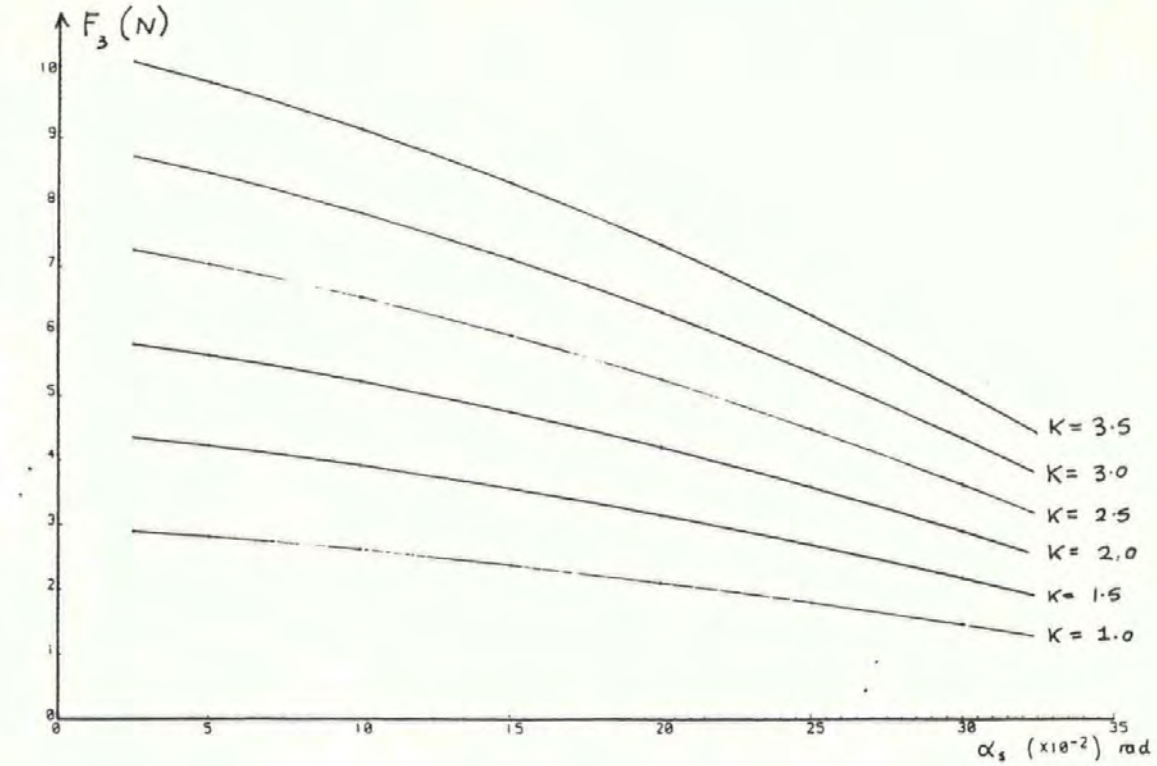

Figure 4.24 The force acting on the blade with a variation in the static angle of the plunger for a range of spring stiffnesses

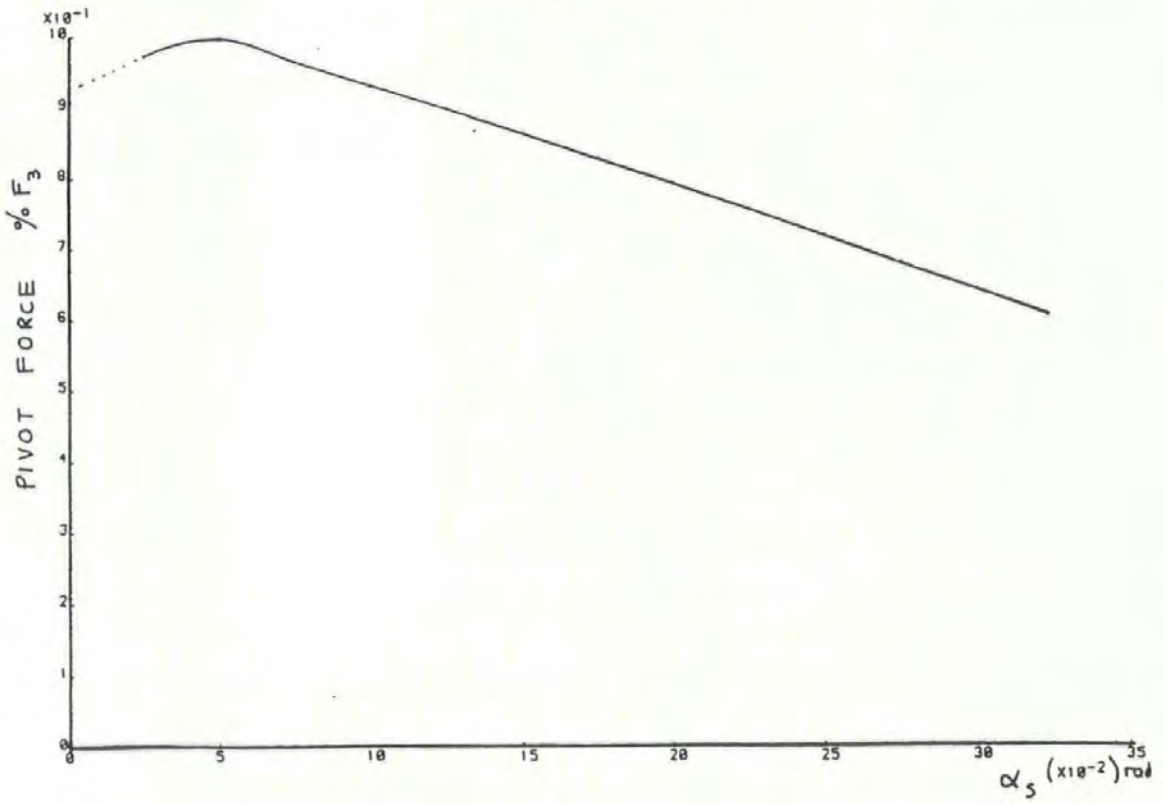

Figure 4.25 The force acting on the pivot as a % of (F_3)

The changes applied to the switch under consideration are tested in the following sections with the switch identified as SWITCH 2, SWITCH 1 being the original model, with, K=3 N/mm.

α_s	K=3 N/mm			K= 1.3 N/mm		
	F_3	F_2	F_1	F_3	F_2	F_1
18°	3.95	1.5	2.45	1.8	.36	1.44
15.01°	5.1	1.53	3.57	2.3	0.46	1.84
11.36°	6.25	1.25	5.00	2.9	0.58	2.32

Table (4.4), The contact forces in Newtons.

A further reduction in, $\dot{\alpha}_N$, is achieved by increasing the leaverage necessary to overcome the resistance of the mechanism. This is achieved by changing the rocker shape, and adding a 35 mm lever. This modification applied to the modification already discussed, is labeled SWITCH 3.

4.7.3.3 Reducing the Angle of Impact

A reduction in the impact velocity can be obtained by reducing the maximum angular displacement of the blade. Thus leading to a reduction in, KEi, for a given, IB. The effect of reducing the displacement can be seen in the figures (4.19 a-d). A smaller angle of, BMAX, leads to a reduced time to impact, reduced slope and therefore, $\dot{\beta}_i$.

The reduction of the angular displacement reduces the contact gap, therefore consideration has to be given as to how the changes would comply with the relavent standards. In the case of BS 3955, [7], two classes of device are defined in terms of the contact gaps. In the case of a class 'B' circuit disconnection the only criterion for the contact gap is that

after endurace testing the switch should pass the electrical strength test. In the case of the Class 'A' a 3mm contact gap is required. Since the contact gap requirement depends on the nature of use, the effects of reducing this demension are not considered here.

4.7.3.4 The Optimisation of IB

From the kinetic energy equation it is clear that the blade inertia, IB, plays a significant role in the value of, KEi. In this limited design approach it is only possible to consider changes in, IB, by keeping the blade length constant, since a change in this length would alter the switch significantly. Thus the blade inertia can only be changed by changing the mass. By exchanging the rivet contact for an integral blade contact a reduction in the inertia can be made.

IB, of the normal blade = 41×10^{-9} Kg m^2

IB, of the reduced blade = 28.85×10^{-9} Kg m^2

Using this reduced inertia in the computer model produced a reduction of aproximately 20 percent in the kinetic energy at impact, KEi.

4.7.4 The Overall Design for Reduced Pivot Bounce in Rocker Switches

To reduce the impact kinetic energy of the blade as expressed in equation (4.19), significant reductions can be made by reducing the blade inertia. The reduction of this inertia has been considered in previous section under the constraint of maintaining the blade length, and only

small changes in KEi were achieved. A full reduction in KEi must therefore account for reducing the blade length.

Assuming a simplified blade shape, the inertia can be given by the equation;

Eq (4.20). $IB = L1^{2} . M1 / 12 + 2.r^{2}.M2$

and $M = M1 + 2.M2$

where $r^{}$ = The position of the rivet contacts, from the centre line.

L1 = The length of the blade,

M1 = The mass of the blade without contacts,

M2 = The mass of the contacts,

M = The total blade mass.

If both the blade length and mass is reduced by a factor (1/X2), a reduction in the blade inertia can be evaluated as shown in table (4.5). It should be noted that the factor (1/X2), is arbitary and any other relation between mass and length could be used to reduce, IB. The results of this analysis are presented in figure (4.26), and show reductions in the values of, KEi, for a given actuator velocity. The practical application of this method is not considerd in this thesis.

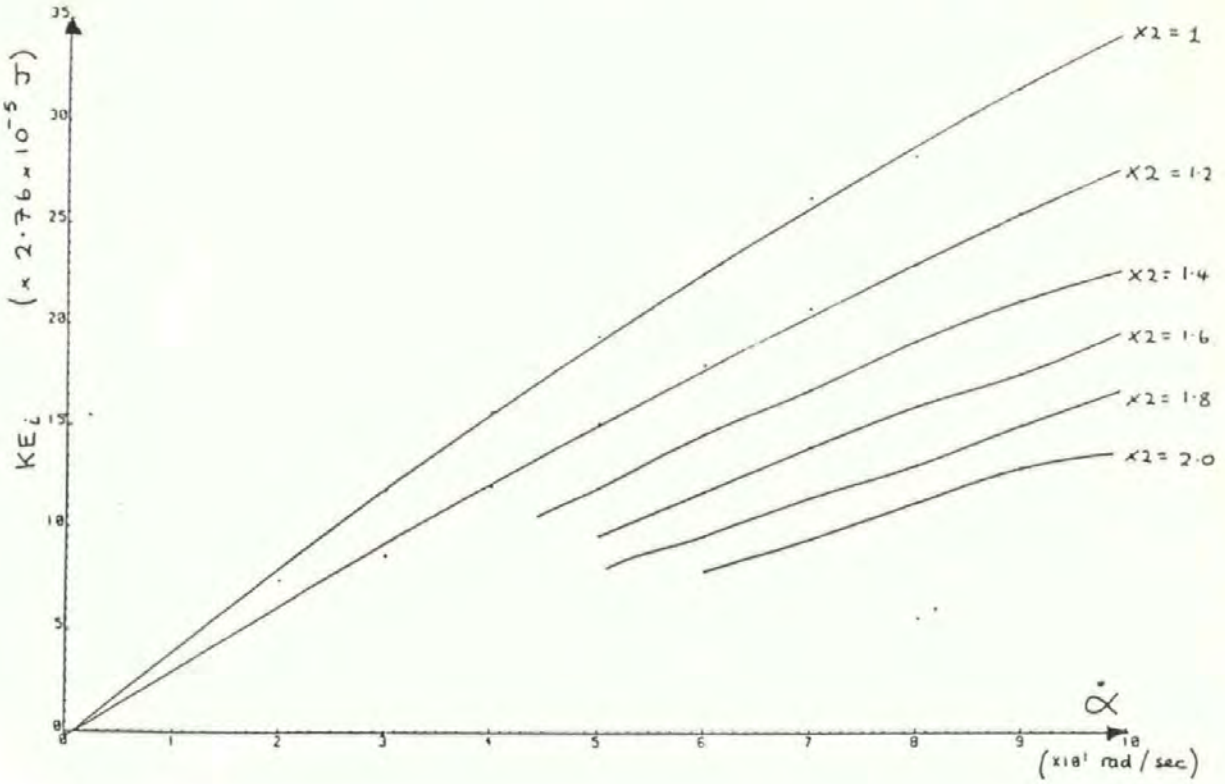

Figure 4.26 The variation of (IB) and the influence on the kinetic energy at impact

	Blade length(mm)	Total Mass (g)	IB x 10^{-8} ($kg\,m^2$)
X2 = 1	21.01	0.82	4.1
X2 = 1.2	17.50	0.78	2.37
X2 = 1.4	15.00	0.586	1.49
X2 = 1.6	13.13	0.513	1.00
X2 = 1.8	11.67	0.455	0.703
X2 = 2	10.50	0.41	0.51

Table 4.5 The changes in blade dimensions and the relation to (IB)

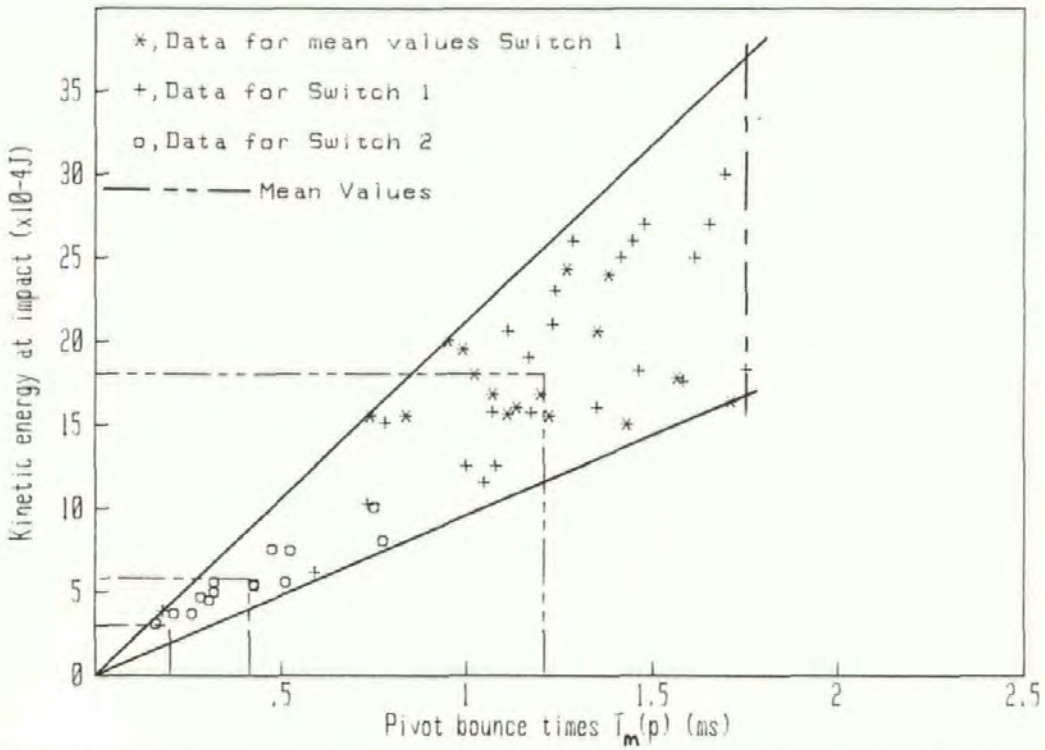

Figure 4.27 Experimental values of pivot bounce time, versus computer predicted values of (KEi)

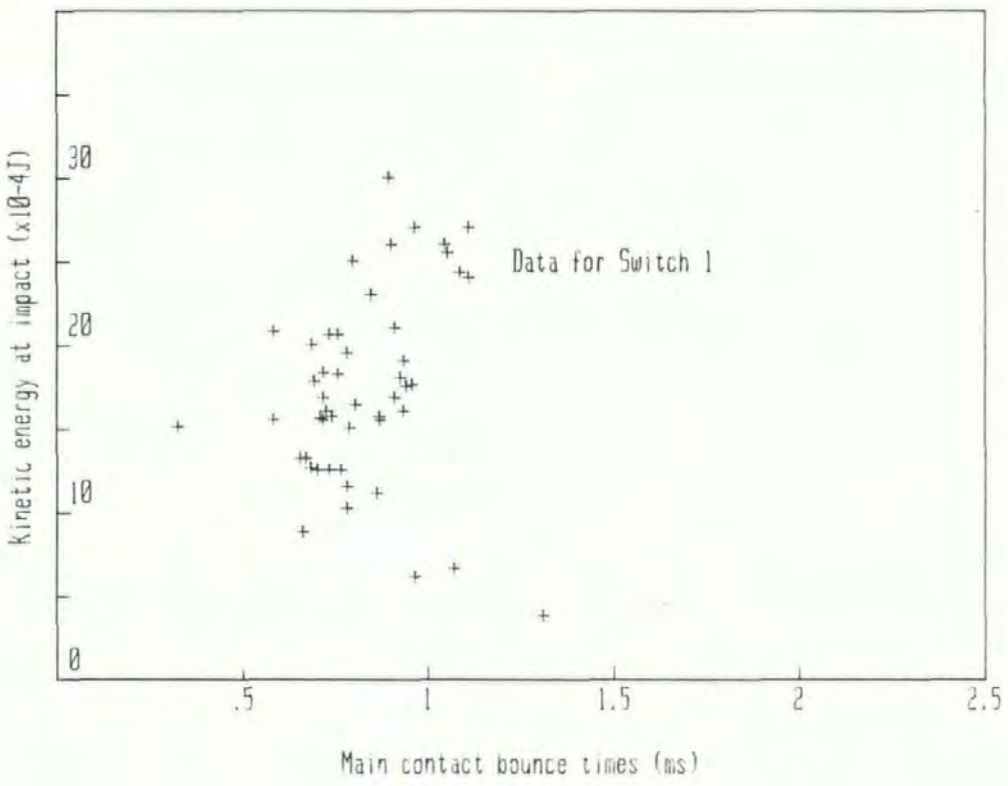

Figure 4.28 Experimental values of main contact bounce time, versus computer predicted values of (KEi)

4.8 Kinetic Energy at Impact and Pivot Bounce

The contact bounce of the pivot interface can be represented by the pivot bounce time, as established in section (2.4.4). The kinetic energy values determined in the computer model are only applicable to bounce times when negligible current is flowing. This situation has been identified as mechanical bounce, and the total time of the bounce is given by, T_m, as defined in section (2.4.5). Using the circuit shown in figure (3.7), the various switches arising from the design analysis, SWITCH 1, SWITCH 2, and SWITCH 3, were tested over a number of operations for the transient time characteristics, by the method described in section (3.2.2). From these traces the BM time, pivot bunce time, $T_m(P)$, and main contact bounce time are accurately evaluated, by the micro-computer. To arrive at a full relationship between, KEi, and pivot bounce, the BM time is transformed to a value of, KEi, using the curve for the particular spring shown in figure (4.23). With the switches purposefully operated by hand outside of the "normal" range a good span of data points was achieved, as shown in figure (4.27). In this figure the data points for SWITCH 1, and 2, can be identified. With the switches operated in the "normal" mode the range of data points were averaged to give the mean vales shown in the table (4.6), these values are also shown in the figure.

	BM (ms)	$\dot{\alpha}_N$ rad/sec	KEi (x10-4J)	$T_m(P)$ (ms)
SWITCH 1	1.95	65.5	18.8	1.208
SWITCH 2	3.2	30.2	5.82	0.415
SWITCH 3	4.0	15.0	3.0	0.2

Table (4.6)

The data points show that the kinetic energy at impact has a linear relation with the pivot bounce time, however the relation is subject to increasing deviation with increasing impact energy. The minimising of the impact kinetic energy is thus proved to be a valid criterion for reducing the pivot bounce. The mean values of, KEi, shown in table (4.6) demonstrate significant reductions, reflected in the reduced pivot bounce times.

A similar analysis applied to the main contacts is shown in figure (4.28). This shows that there is no direct relation between the main contact bounce and the reduction in, KEi. This suggests that the kinetic energy at impact is related to the bounce at the pivot, leaving the main contact bounce uneffected. This occurs because during impact at the main contacts, kinetic energy is not totally absorbed, since a significant portion is maintained in the separation occurring at the pivot.

4.9 Switch Testing Under Load Circuit Conditions

It has been identified that the hand operation of the rocker switch constitutes the most damaging operating condition. It is also the condition most difficult to recreate in the laboratory.

For the purpose of this analysis each switch was connected to a, 14 - 17 Amp, 200 V, a.c supply. The switches were then operated by hand, under the normal switching action. After cycling the switches were then dismantled to observe the pivot interface. The results of this experiment are shown in the photographs of figures (4.29 a-d). For comparison the profiles of some standard switches tested on the standard test rigs are shown in figures (4.29 e-h). Table (4.7) lists the experimental

Fig	Type of operation	Switch type	Switch Version	No's Operations	Circuit Condition	Supply Current (Amps)	Supply Volts (d.c.)	Equivalent Makes
(a)	Hand	92 c/o double pole	(1)	1,000	ON/OFF	14.8 A	200	500
(b)	"	"	(2)	1,000	"	14.8 A	200	500
(c)	"	"	(1)	2,000	"	17 A	200	1,000
(d)	"	"	(3)	2,000	"	17 A	200	1,000
(e)	Cam rig	"	Standard	5,000	C/O	16 A	200	10,000
(f)	"	"	"	20,000	C/O	16 A	200	40,000
(g)	"	"	"	10,000	C/O	16 A	200	20,000
(h)	Hand	93/ON/OFF double pole	"	2,000	ON/OFF	17 A	200	1,000

Table 4.7 The Experimental conditions relating to the eroded contacts in figure (4.29)

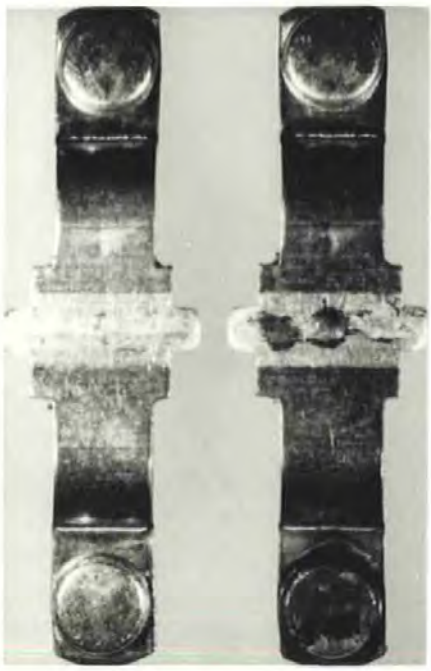

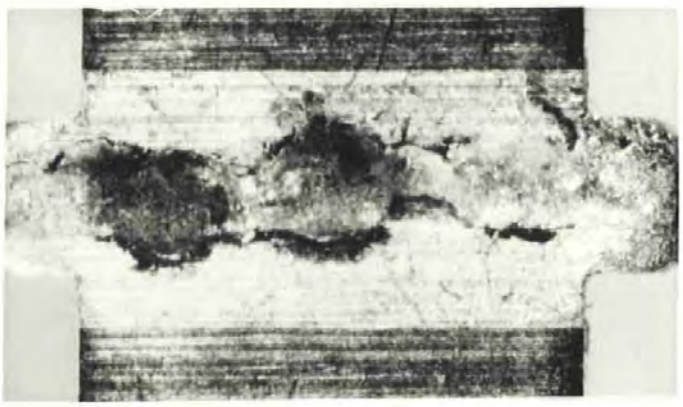

4·29 a

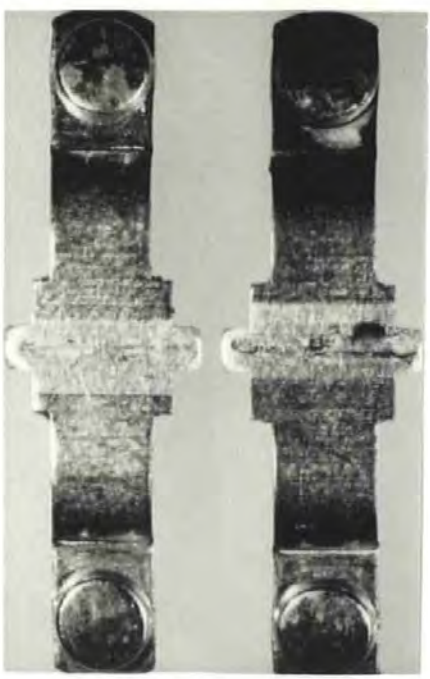

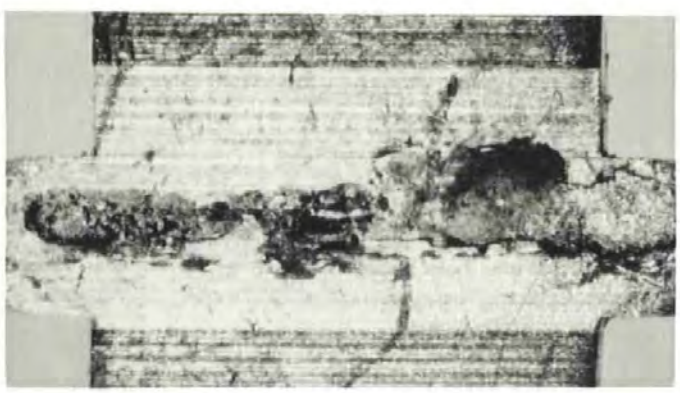

4·29 b

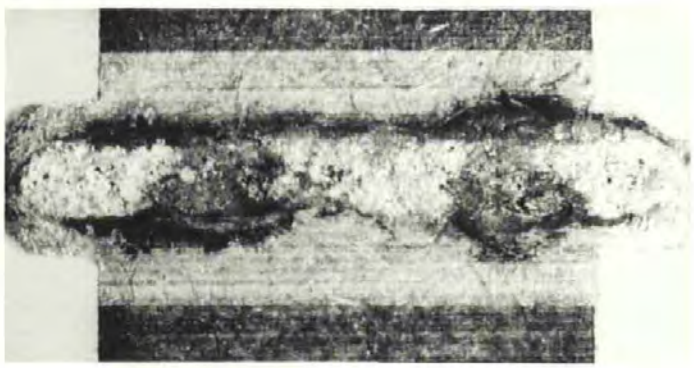

4·29 c

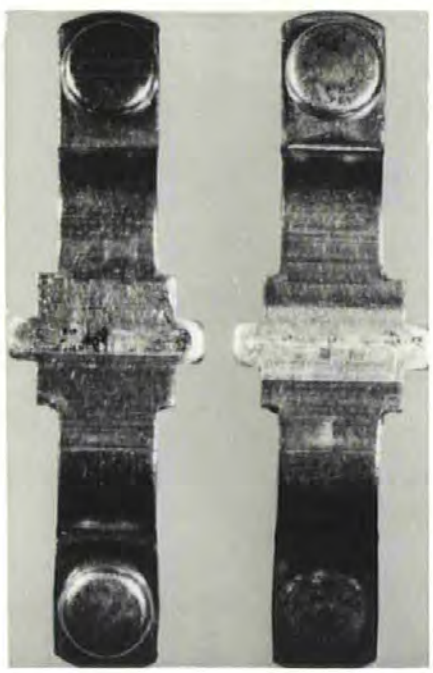

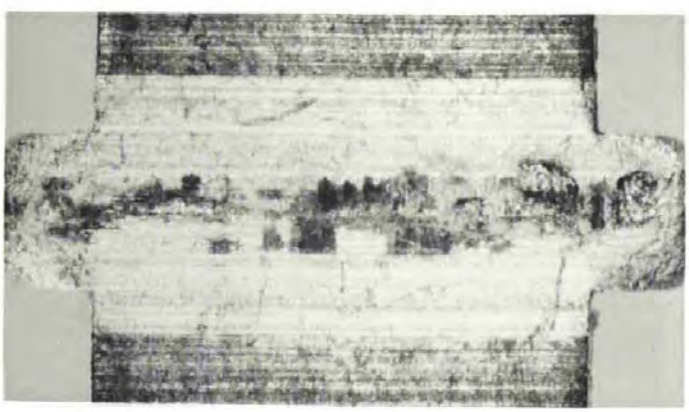

4·29 d

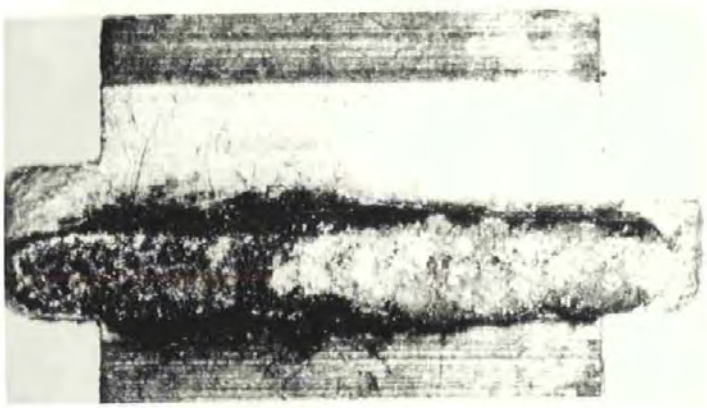

4·29 e

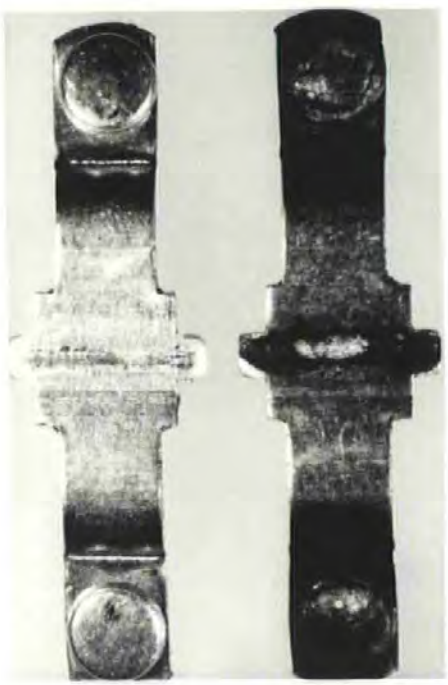

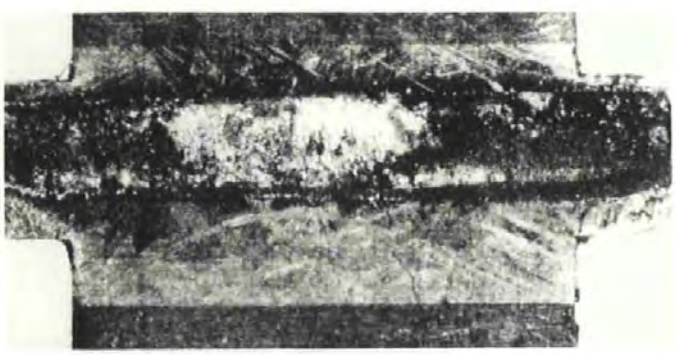

4·29 f

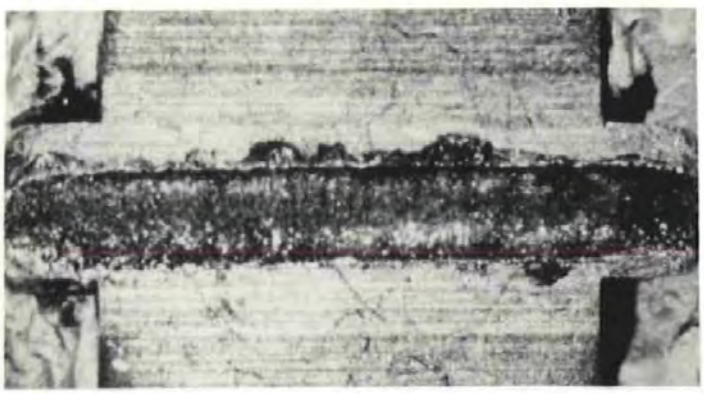

4·29 g

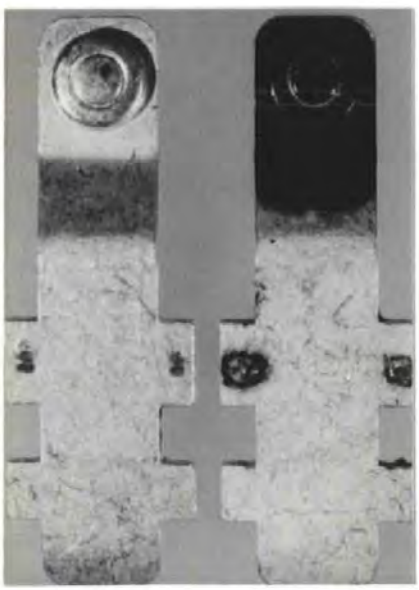

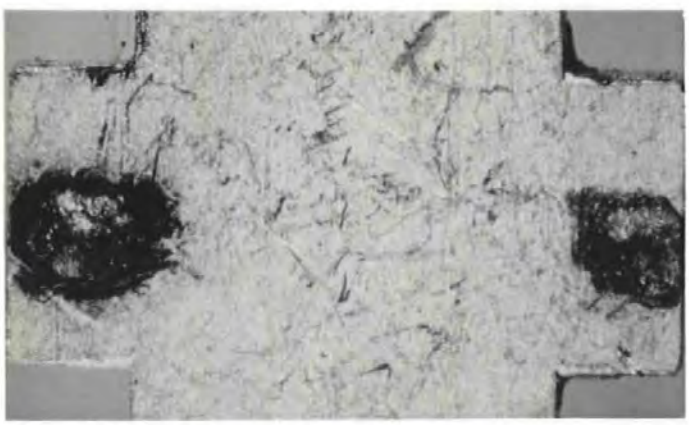

4·29h

conditions and the type of switch tested.

4.9.1 Discussion of Erosion Profiles

In all of the figures presented the right hand photograph is a close up of the underside of the blade. Because the circuit current conditions were not held constant through all the tests, comparisons must be drawn between contacts operated at the same current.

A comparison of the erosion profiles of SWITCH 1, and SWITCH 2, can be made with reference to figures (4.29a) and (4.29b). In the case of SWITCH 1, the erosion has disrupted the silver inlay along the whole length of the interface; however with SWITCH 2 the erosion is much less se vere and only significant towards the right side of the contact. Thus SWITCH 1 would be expected to wear through the silver, before SWITCH 2.

A comparison of the erosion profiles of SWITCH 1 and 3, can be made with reference to figures (4.29c) and (4.29d). In this case SWITCH 1 has undergone twice as many operations as the switch used in (4.29a), and at a higher current. This explains the increased wear obser ved. Comparing with the profile for SWITCH 3, it can be seen that a significant reduction in the erosion is achieved with the latter switch. This observation supports the reduced experimental pivot bounce times shown in section (4.8).

The following figures (e),(f), and (g), show the erosion profiles obtained with the cam test rig, over a range of cycles. In the case of figure (4.29e) the pivot interface has experienced 10,000 cycles at 16 Amps. A comparision with the profile of SWITCH 1 in (4.29c) shows that

although the test system has applied ten times as many cycles the wear profiles appear similar. This observation supports the comparisons made in section (3.3) between the BM times, with cam rig and hand operation. The hand operation is thus demonstrated to be a more se vere operation. Since the test rig design is dictated by the approval bodies, for example British Standards, some consideration could be given in making the general test method more applicable to the actual operating conditions of a switch.

The figures,(f) and (g), show the influence of increased cycling on the interface erosion. In both cases the copper blade has been significantly eroded. In figure (g) the blade has been ultrasonically cleaned. The additional figure (4.29h), shows a different switch to that studied in the optimisation procedure, and shows that under hand operation the silver can erode through to expose the base copper, after only 1,000 make, hand operations.

4.9.2 The Rocker Switch Failure Mode

In the introduction it was suggested that the main failure mode of this switch was overheating as a result of increased contact resistance. This statement can now be extended with reference to the erosion profiles produced.

(1). Oxidation of the surface materials. The blackened areas on the central pivot could be produced by two phenomena; (i) the burning of any lubricant at the contact interface, and (ii), the oxidation of the copper base metal. The former would lead to carbon deposits, and would have an unknown influence on the resistance. The latter would lead to an increase

in the contact resistance.

(2) Arcing. It is arcing during bounce that causes the burning through of the fine silver, as demonstrated in figures (4.29 f & g). The resulting surface changes could lead to an increase in contact resistance.

The interaction between the wear and contact resistance changes are unknown, and are the subject of controlled experiments presented in Chapter 5.

4.10 Conclusions to the Computer Model of Rocker Switch Dynamics

The method of modelling the dynamics of the rocker switch has produced some useful results by improving the wear characteristics of the switch. The model also allows for the estimation of pivot bounce times from a set of dimensions and conditions, via the experimental data of figure (4.27). However the bounce times evaluated are only applicable to the signal current situation and the application of current would be expected to alter the relations presented in figure (4.27). To understand the influece current on contact bounce the computer test system described in section (3.4) has been used to consider the events in the pivot contact interface, additionally the system is used to investigate the relationship between erosion and contact resistance.

REFERENCES

[1] D.J Mapps, P.J White, G Roberts. "Pivot contact behaviour in Low Inertia Snap-action switches", in IEEE Trans. CHMT. Vol CHMT-7, No 1, 1984.

[2] "Specifications for Electrical Controls for Household and similar general purposes", Part 3. General and Specific requirements, BS 3955: Part 3: 1979, pp 30.

[3] J.L Meriam, Engineering Mechanics Vol 2, Dynamics, John Wiley & Sons, London, 1978, pp 71.

[4] D02 BBF, "Integration of First order ordinary differential equations over a range", NAGFLIB 1564/ 0: Mk 7, Dec 1978.

[5] J.M Ortega, W.G Poole, "An Introduction to Numerical Methods for Differnental Equations", Pitman, London, 1981, p33.

[6] J.W McBride, "A design optimisation of Rocker Switch dynamics to reduce contact bounce and thus prolong contact life, using a computer based numerical method.", Internal Confidential report to Arrow-Hart Ltd, Plymouth Polytechnic, August 1984. pp 38.

[7] as ref [2], p 3.

CHAPTER 5

EXPERIMENTAL INVESTIGATIONS OF CONTACT BOUNCE PHENOMENA, DISCUSSIONS AND RESULTS

5.1 Introduction

This chapter details experiments undertaken using the automated test facility, described in section (3.4). The aim of these experiments are to study contact bounce, of the type occuring at the pivot interface in rocker switches under controlled conditions. The computer model developed in the previous chapter has the ability of providing useful design information on the basic rocker mechanism, however the influence of load current on the bounce times evaluated would alter the experimental relationships discussed. To evaluate the influence of current 'Experiment 1' was undertaken, the control details of which are given in section (3.5). As an extension of this work the influence of arc erosion on the contact resistance of the interface is considered, in 'Experiment 2'. The software details and data processing methods used are detailed in section (3.5.3). Both sets of experimental results are presented in this chapter; and follow the initial investigation of the test system dynamics.

5.2 The Test System Dynamics and Arc Characteristics during Make

The high-speed photographic studies presented in this section, are used to study the relevence of time as a criterion in electrical contact bounce, to support the discussion in section (2.4.4). The film characteristics also identify the nature of the bounce produced in the test system, under a range of test apparatus settings. In all of the films, simultaneous voltage and current characteristics have been monitored, processed and stored.

For reasons of photgraphic clarity the contacts used in this initial investigation were rivet contacts, with the specifications shown in figure (5.1). This type of contact mounted in the contact support, allows for the close up photography necessary for the monitoring of small amplitude bounce.

The automatic test system was used in the mode described in section (3.4.10), such that the system would pause upon the arming of the recorder. The controlling software then prompts for camera activation, and the camera event relay releases the contact arm. Thus allowing for the capture of the make operation on the high speed film. The electrical transient at impact then triggers the recorder. This method allows for the comparison of the film and experimental test data in the same fashion used in chapter 4.

5.2.1 The Velocity of Impact

To evaluate the consistency of the test system in maintaining the same impact condition and the influence of the rig settings on the impact events, a series of five films were taken. The experimental condition and results are given in table (5.1).

Film	I_s d.c (Amps)	h (mm)	h´ (mm)	F (N)	u_i (m/s)	n	Z_1 (mm)	T_1 (ms)
1	20	3	3.61	2.7	0.59	1	0.163	3.488
2	20	3	3.61	1.4	0.46	1	0.19	4.87
3	20	3	3.61	1.4	0.475	2	0.163	5.376
5	0	3.5	4.21	1.4	0.571	1	0.163	5.429
6	30	2	2.409	1.4	0.306	2	0.122	4.326

TABLE 5.1

Where I_s = The closed circuit d.c supply current in a resistive circuit,

h = The contact stop setting as defined in figure (3.11),

h´= The actual contact gap. This is a function of the position of the contact stop, and is given by (h´=1.204xh). This relation was maintained for all the data presented.

F = The static contact force, controlled by the spring, and defined in figure (3.11).

u_i = The measured impact velocity of the contacts.

n = The number of bounces observed.

Z_1 = The measured maximum contact displacement of the first bounce.

T_1 = The duration of the first bounce, evaluated from the electrical transients.

Both films, 2 and 3 were operated under the same apparatus settings, and in figure (5.2) the two impact characteristics are compared to evaluate the repeatability of the system. The figure demonsrates that with the same system settings, the velocity of impact is maintained. In addition films 5, and 6, were taken with the same static contact force, thus allowing for the evaluation of the relationship between velocity of impact and the contact arm stop position. This is shown in figure (5.3), which shows a linear relationship. The high static force used in film 1, demonstrates with reference to table (5.1), that increasing the force increases the impact velocity. As an extension of this work, a mathematical model of the test system could be evaluated to relate the impact velocity to any system settings.

5.2.2 The Bounce Characteristics of the Test System

Both films 2, and 3, taken under the same initial conditions demonstrate the influence of the surface condition on the bounce characteristics. In the case of film 2 the event monitored was preceeded by a number of 20 Amp d.c cycles, while film 3 was preceeded by 3 purely mechanical closures, i.e without any current. In the case of film 2, the initial period of impact was measured to be 0.84 ms, compared to the 0.728 ms in film 3. The larger time in the case of film 2, would suggest a larger absorbtion of the incident kinetic energy. This is reflected in the reduced bounce times. The 20 amp cycling preceeding the data for film 2 has thus generated surface roughness, which allows for more incident kinetic energy absorbtion. The condition of the surface is thus shown to influence contact bounce, under load current conditions. This is in agreement with the observations of B. Miedzinski, et al, [1].

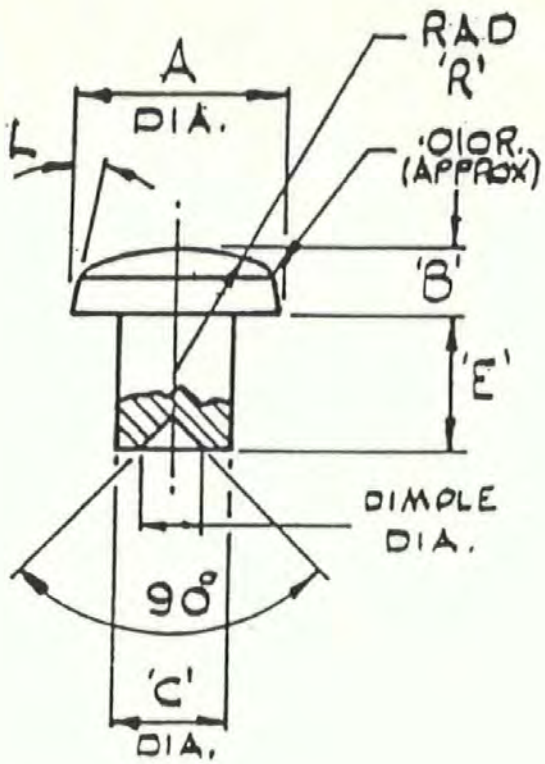

(all in inches)

A = 0.135
B = 0.032
C = 0.071
E = 0.072
R = 0.312
L = 10° Max.
DIMPLE = 0.04
DIA.
Material: 0.010 Min.
80/20 Ag/Ni
OVERLAY ON Cu

Figure 5.1 The dimensions and material specification for the Rivet contacts.

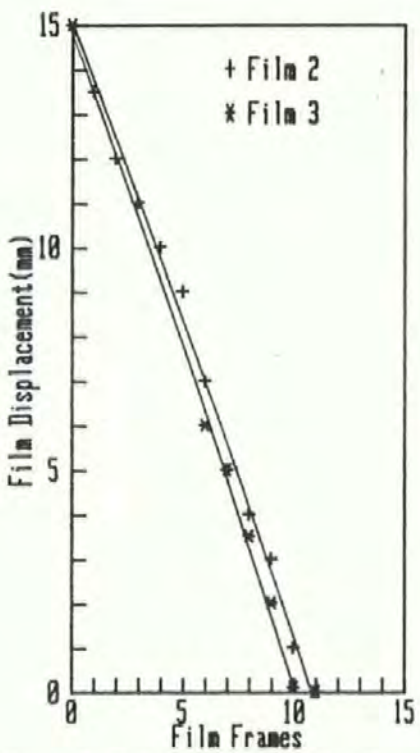

Figure 5.2 The Impact of Films 2, and 3.

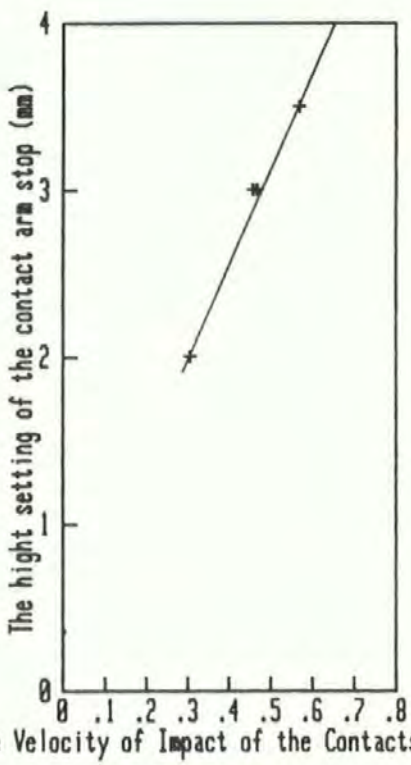

Figure 5.3 The Variation of impact velocity with (h

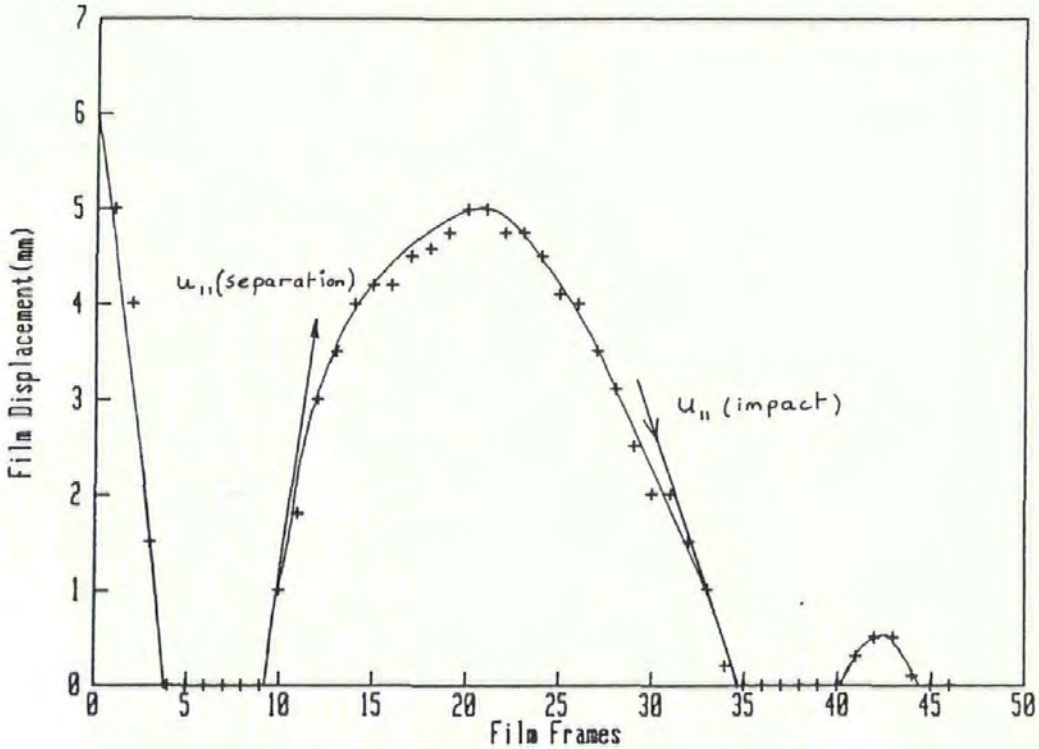

Figure 5.4 The Impact and Bounce of Film 6

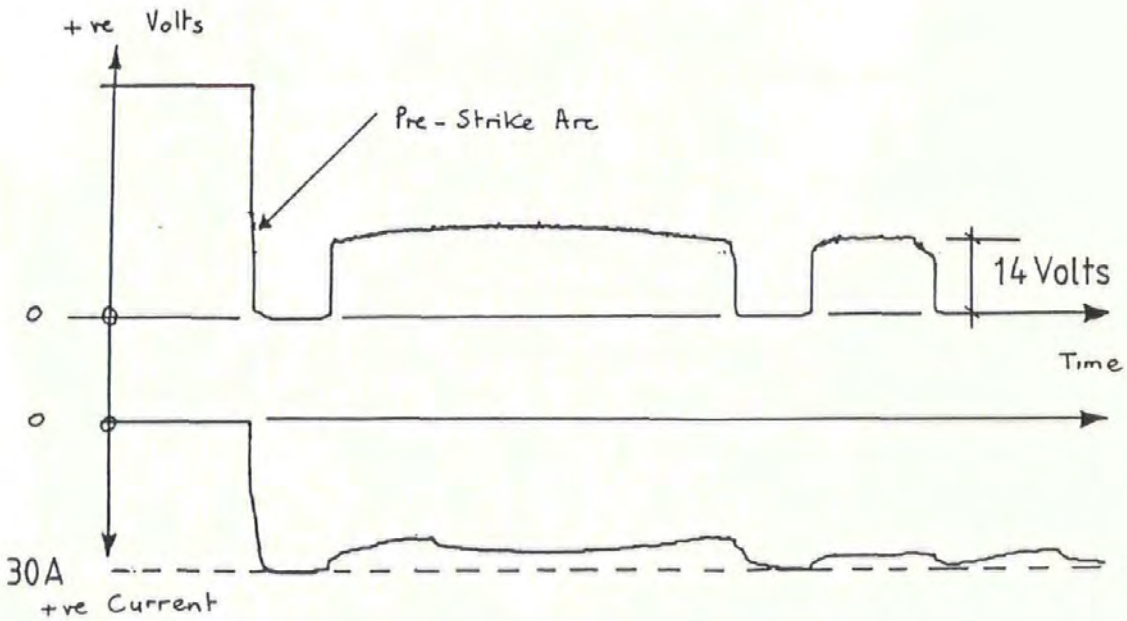

Figure 5.5 The electrical transients at impact for Film 6

5.2.3 The Arc Voltage Characteristic at Make

For the purpose of this study film 6 is used because it represents the best example of a displacement characteristic. A full analysis of the bounce is presented in table (5.2), while figures (5.4) and (5.5) show respectively the displacement and arc transients.

	t(ei1)	t(eb1)	t(ei2)	t(eb2)
Film time	0.83	4.333	0.83	1.33
Data from auto test system	0.812	4.326	0.826	1.288
Data evaluated from fig(5.5)	0.819	4.33	0.751	1.475
Z (maximum from film) (mm)	/	0.122	/	0.022
Maximum Arc Voltage	/	16.24	/	14.06

Table 5.2, with all times in milleseconds

In table 5.2, the times are defined as electrical bounce times, since 30 Amps is passing through the contacts. The times are defined using the notation given in section (3.4.2), as:

t(ei1) = the first electrical impact time period,

t(eb1) = the first electrical bounce time period,

t(ei2) = the second electrical impact time period,

t(eb2) = the second electrical bounce time period.

Correspondingly, with signal current passing through the contacts

t(mi1) = the first mechanical impact time period,

t(mb1) = the first mechanical bounce time period,

t(mi2) = the second mechanical impact time period,

t(mb2) = the second mechanical bounce time period.

In table (5.2), the film time is measured from the separation times shown in figure (5.4). The data from the auto test system is that evaluated in the processor after the transfer of the two traces shown in figure (5.5). The error in this analysis can be determined by comparison with the actual times evaluated directly from the traces, using the cursors of the DL1080, also shown in table (5.2).

Proir to the first impact some films show evidence of pre-strike arcs, due to breakdown or asperity vaporisation; and the arc voltage associated with this is shown in figure (5.5). The pre-strike arcs are however of short duration, typically less than ten microseconds. As a consequence, these arcs will have only a relatively small affect on the overall erosion, with bounce times of typically one to five milliseconds. It is however possible that the pre-strike phenomena could affect the dynamics of the system by creating local areas of molten metal at the instant of impact. This is however thought to be unlikely, since the breakdown is not necessarily at the same point as the areas of actual contact, during impact.

The arcs observed during the bounce are seen to be subject to rapid movement,and are not generally coaxial with the centre of the domed rivet contacts considered in this study. In figure (5.6), a single frame taken from the film; the arc is shown to be on one side of the contacts as the contacts impact.

The relationship between the maximum high of the bounce and the time of the bounce, as given in equation (2.23), can be considered in the context of electrical bounce, with reference to the displacement characteristic shown in figure (5.4). This shows that, contrary to the expected parabolic shape of the bounce displacement, the curve exhibits a

separation velocity higher than the following closing velocity. The value of velocity used in equation (2.23), is the average of these two. The figure presented is based on the experimental data and needs to be multiplied by conversion factors to give the actual velocities, and displacements. The conversion factors are 0.1666 ms = 1 frame, and 0.02249 mm = 1 mm on the film. Then from the data,

$u_{||}$ (separation) = 0.1617 m/s

$u_{||}$ (impact) = 0.0735 m/s

Mean, $u_{||}$ = 0.1176 m/s

Then from equation (2.14): e = 0.1176 / 0.306

In equation (2.23), this yields Z = 0.125 mm

In table 5.2, Z = 0.122 mm; thus demonstrating that although the equation is based on bounce without arcing, it can be used to give an evaluation of bounce amplitude in electrical contacts.

The non-symetric response of the bounce is thought to be a consequence of the electromechanical forces acting at contact separation, [2]; and the arc vapour pressure, at impact, [3].

The voltages occuring during arcing have been the subject of much research as discussed in section (2.3). In figure (5.5) the top trace shows that during the first bounce the arc voltage increases above the minimum arc voltage to give a maximum of (16.24 Volts). In the second bounce the arc voltage levels at (14.06 Volts), and at the end of the bounce the voltage is seen to collapse with the separation of the anode and cathode falls, [4]. The minimum arc voltage for these contacts is

taken to be the plateau value of 14 Volts. For comparison, Holm, [5] gave the value of 13 Volts for contacts with 40 percent Ni; in this case 20 percent Ni is used. The plateau value for the pivot interface is 15 Volts.

The duration of the bounces considered, are much larger that those generally found in this type of contact. A more typical value would be, 1 ms, of similar duration to the second bounce. Therefore with a duration of less than, 1 ms, the measure of contact displacement is not of importance, since the arc voltage will lie close to the minimum arc voltage. The energy equation (2.26) is therefore justified as a means of evaluating arc energy, since the importance of the bounce time in defining a bounce characteristic is justified. Additionally the arc energy evaluation used in the data processing method can be used to compare with this equation, thus also testing the minimum arc voltage assumption.

The current characteristic shown as the bottom trace in figure (5.5), shows the current increasing from zero to 30 Amps. The ripple on the d.c current is a result of the rectified supply used in this experiment. The current is seen to reduce during arcing.

5.3 The Influence of D.C Current on Electrical Contact Bounce

The automatic test system is used in this analysis to allow for the collection of data, accurately, and over a large number of cycles. The contacts used in this analysis are the pivot contacts used in the rocker switch detailed in chapter 4, and for comparison the rivet contacts used in the previous section. The details of the mounting arrangements

for these contacts are considered in section (3.4.2.3).

The method used is to compare signal current bounce, defined in this thesis as Mechanical bounce; with bounce under load current conditions, defined as Electrical bounce.

5.3.1 The Consistency of Contact Bounce in the Test System

Initial tests with pivot contacts showed that a full pivot of the type used in the switches in chapter 4, with a length along the line of contact of 9mm, produced inconsistancy of bounce under the same system settings. To overcome this problem the pivots were sectioned as shown in figure (5.7a), to give an effective line of contact of approximately 1 mm. The blade material mounted in the stationary contact support, was taken from the flat raw material, the details of which are given in figure (5.7b). The protective material is fine silver and is only applied to the blade contact. The flatness of the blade material is of importance since uneveness would cause additional restitution effects.

To evaluate the mechanical characteristics of the test apparatus, the system was operated over 1000 cycles, with new pivot contacts, h = 1 mm, and F = 2.7 N. The resulting values of bounce times are shown in figure (5.8), with the data points taken every 10 operations. The figure shows there is consistancy in the first impact and bounce times, and variation in the overall bounce time (T_m). This indicates that most of the inconsistancy occurs in the subsequent bounces. The subsequent bounces therefore have a large random factor. In the first thirty operations there is some increase in t(mbl) the first mechanical bounce time, suggesting an increased surface hardness, due to work hardening.

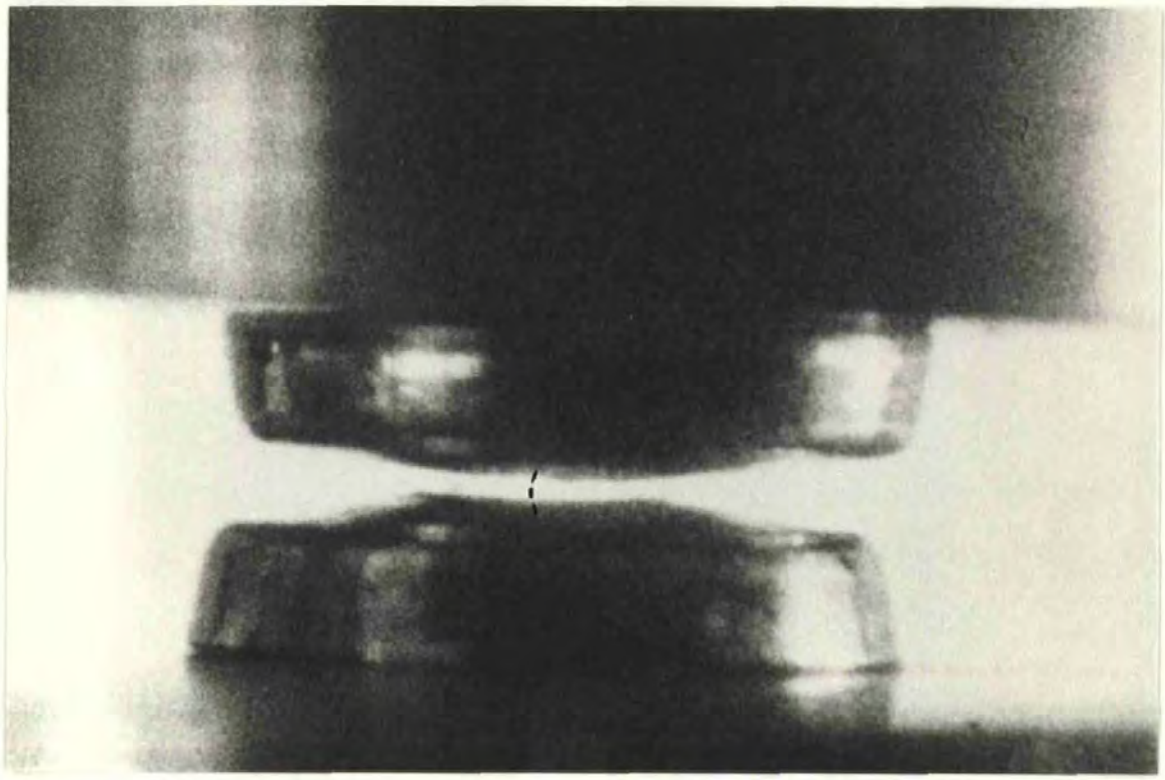

Figure 5.6 A single frame of arcing during contact bounce, with rivet contacts.

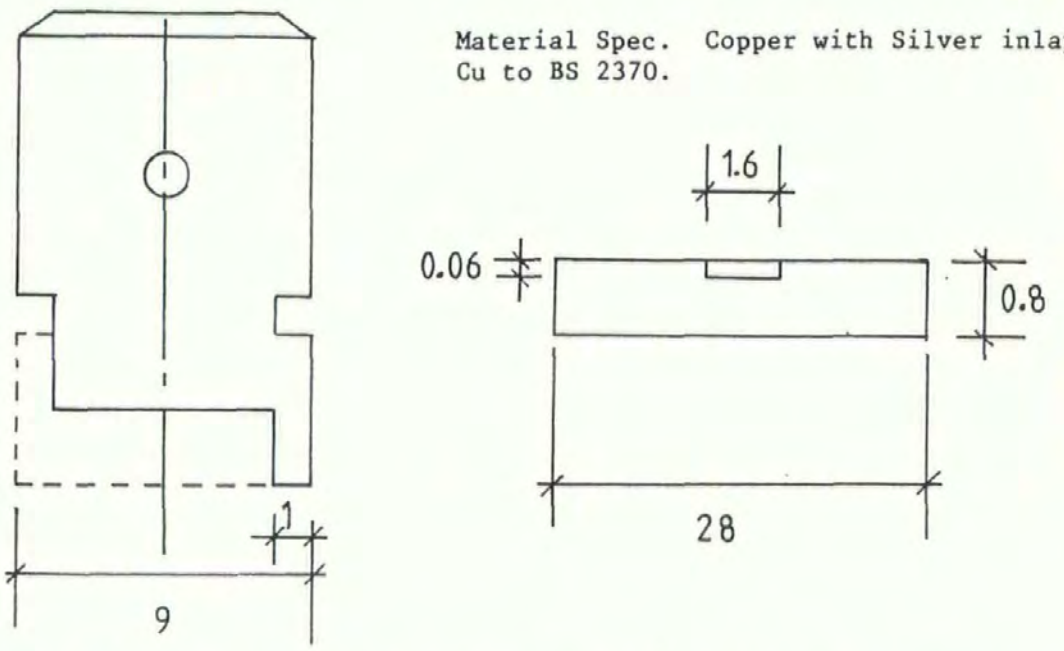

Figure 5.7 The pivot and blade contact materials, with dimensions in mm, not to scale.

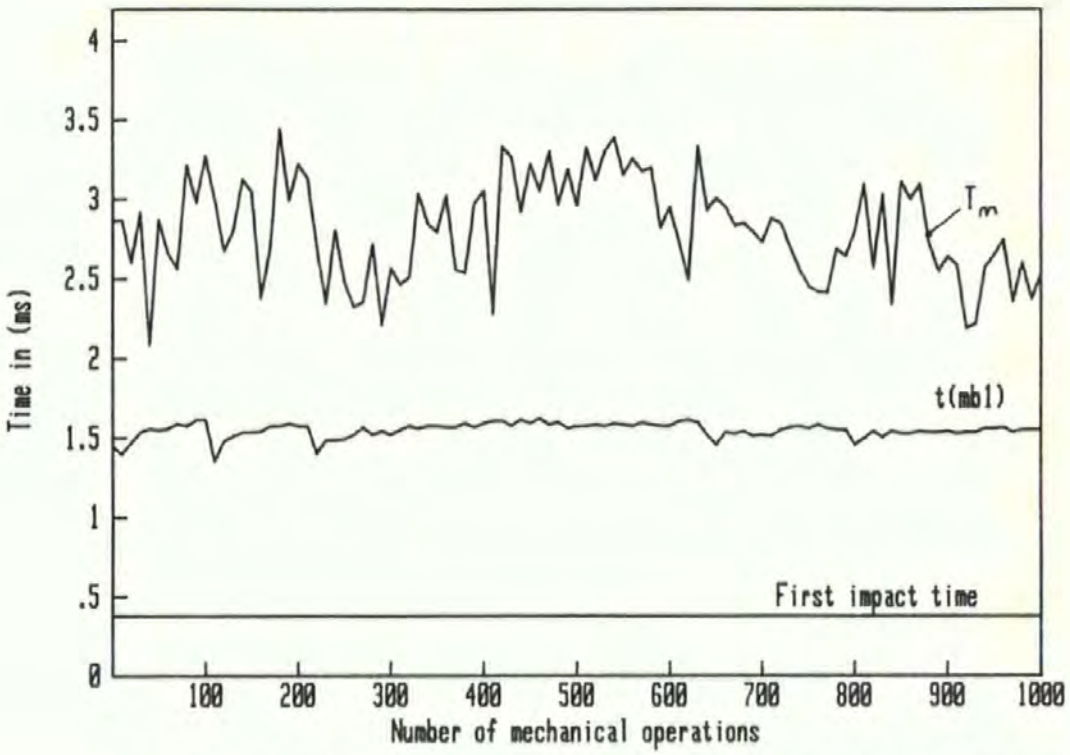

Figure 5.8 The variation of mechanical bounce times, with the number of operations

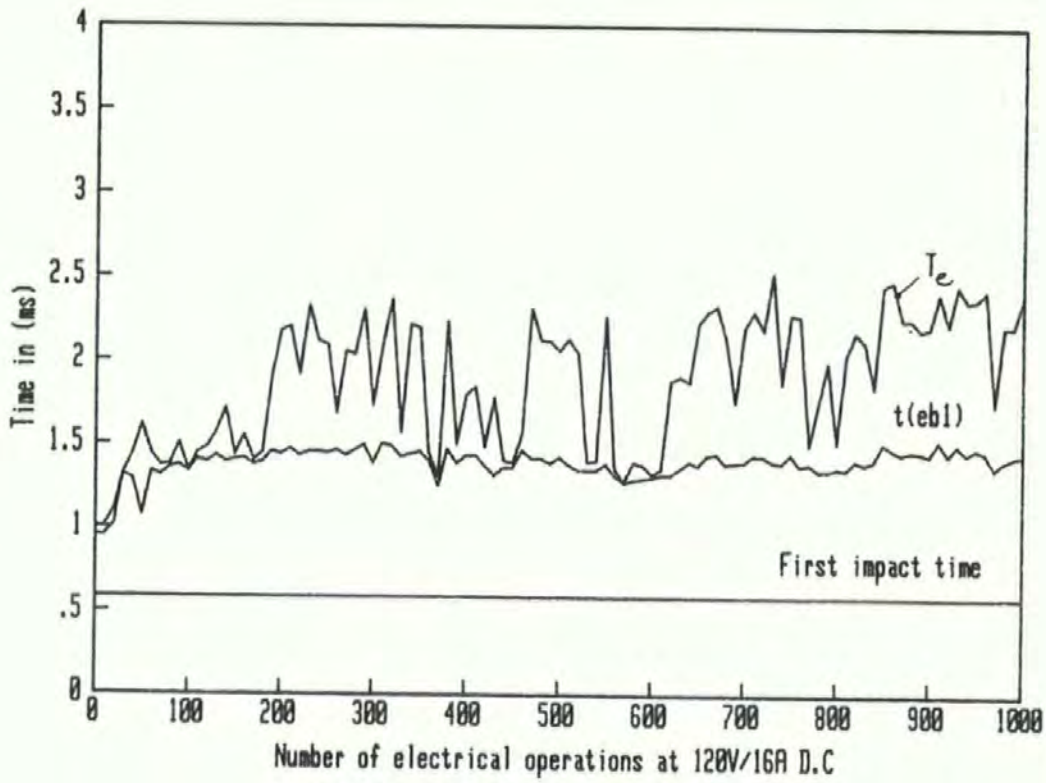

Figure 5.9 The variation of electrical bounce times, with the number of operations

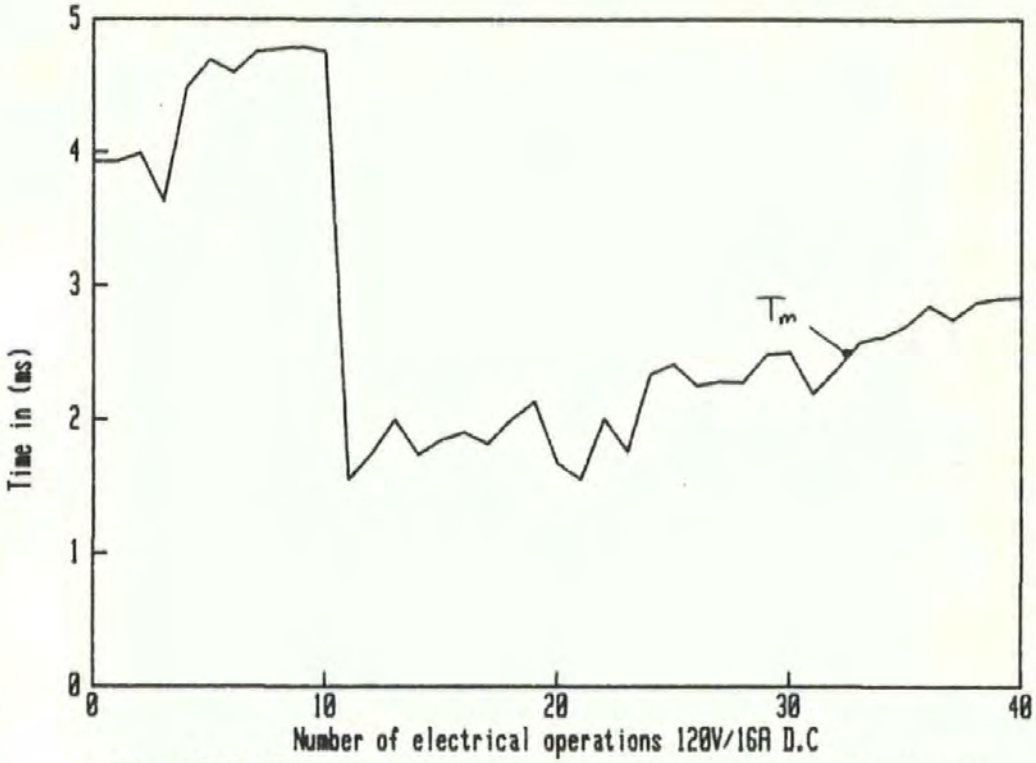

Figure 5.10, The influence of surface roughness on mechanical bounce times

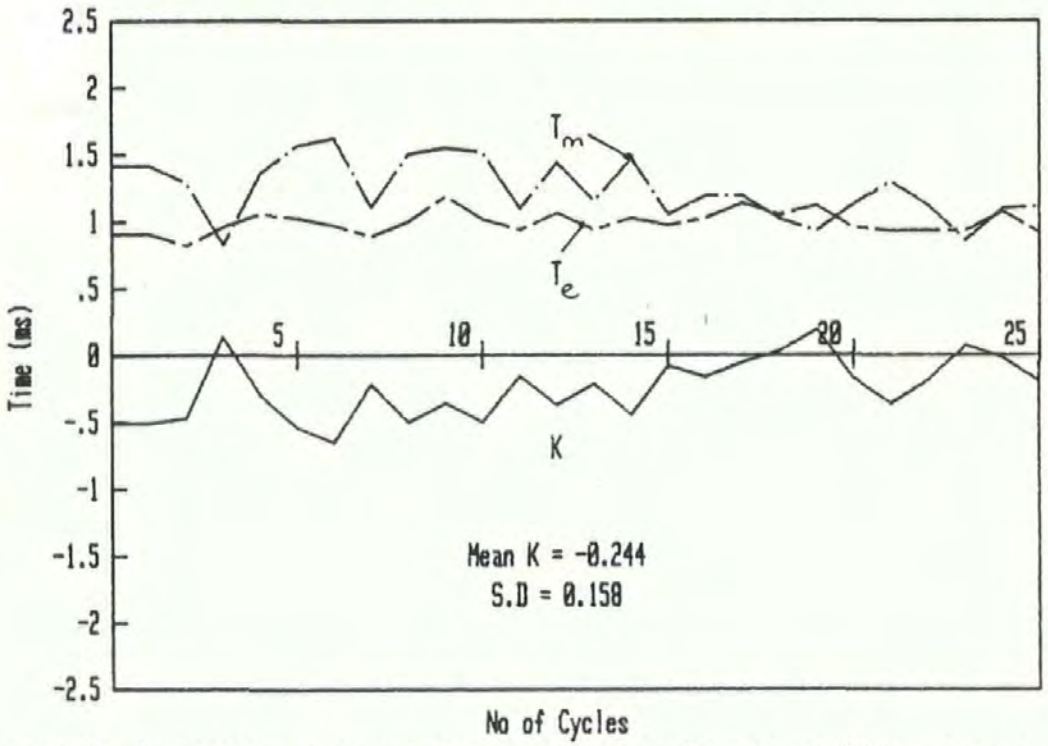

Figure 5.11, The variation of the reduction term (K), over 25 cycles at 12 Amps, for worn contacts

To evaluate the consistency of bounce under d.c load current conditions, the test system was operated over 1,000 cycles, with pivot contacts, h= 1mm, F=2.7mm, I_s=16 Amps, and V_s=120 Volts. The resulting variation in bounce times are shown in figure (5.9). As in the case of mechanical cycling, the first impact and bounce times show consistency over most of the operations, however there are some changes in the first 100 operations. This is due to the initial arcing changing the contact surface from a relatively smooth surface to an eroded surface. The low initial total bounce time indicates considerable absorbtion of kinetic energy. Similar to the mechanical case the major variations must occur in the bounces after the first; defined here as the subsequent bounce.

In figure (5.10), the influence of a single electrical operation on mechanical bounce is considered. It shows that over the first 10 operations the mechanical bounce time increases, as previously observed. Then two operations, with a suppply of 120 Volts, 20 Amps, d.c, were applied to the closing contacts. After which the mechanical cycling continued. This shows the effect of the surface disruption on the mechanical bounce times. The reduced time suggests the increased absorption of the impact kinetic energy. Identifying the influence of the surface degradation on the bounce.

5.3.2 Basic Test Method

To collect data on the reduction in bounce the contacts were initially cycled in the following fashion, defined as "cycle mode 1".

Cycle mode 1, is defined as, one mechanical make operation and data collection followed by one electrical make operation. This

constitutes one cycle. The cycle is then repeated.

The initial results obtained using this mode, identified the importance of the time period that the d.c load current supply remained on after impact. In initial testing the load current was maintained for 40 seconds, during data transfer. This had the effect of heating the contacts such that the following mechanical impact would be occuring on a thermally softened surface. To reduce this influence to negligible proportions the 'on time' was reduced to 130 ms. With approximately 1.5 minutes between operations, sufficient time was then allowed for the heat dissipation, resulting from arcing and load current flow. The bounce characteristics monitored were then functions of,

1) The supply current,

2) The test apparatus settings,

3) The contact surface condition.

5.3.3 The Results of the Bounce Reduction due to a 12 Amp D.C Current

The evaluation of the bounce reduction, K, with current is evaluated using the following relation, for one cycle.

$K = T_e - T_m$

For the reduction in the first bounce, K1, the following relation is used

$K1 = t(ebl) - t(mbl)$

A typical set of results on the evaluation of, K, for pivot contacts is shown in figure (5.11). In this figure, K, is shown to vary significantly over the 25 cycles considered. Over the period shown a mean value of, K, is determined.

The large variation in, K, is confirmed in figure (5.12), over a period of 200 cycles. In this figure the superimposed mean vales of, K, each taken over 25 samples, show, $\overline{K}$, to be consistently negative and reducing with the number of cycles. This reduction is mainly the result of a reduction in the mean mechanical bounce times, due to the surface changes.

A similar test for new contacts, under the same experimental conditions presented in the same figure, show a similar reduction, however the values of, $\overline{K}$, are seen to be different.

To establish the factors affecting the scatter, and the variations for different pivot contacts, individual bounce times were considered, in a given characteristic. In figure (5.13), taken for the same data presented in figure (5.12), the reduction term, $\overline{K1}$, is shown to be uniformly positive, indicating a larger first electrical bounce. Over the period shown in figure (5.11) the mean value of, $\overline{K1}$, is 66 μs.

5.3.4 Subsequent Bounce Phenomena under 12 Amps D.C

The positive value of, K1, implies that the overall reduction, K, must be reconsidered, since K applies to the whole bounce characteristic, and there are clearly two sectors to the bounce. The second sector, or subsequent bounce is significantly affected by the first arc, as a result of thermal effects. This causes the reduction in the subsequent electrical bounce.

The reduction over the subsequent period is defined as (K´), where,

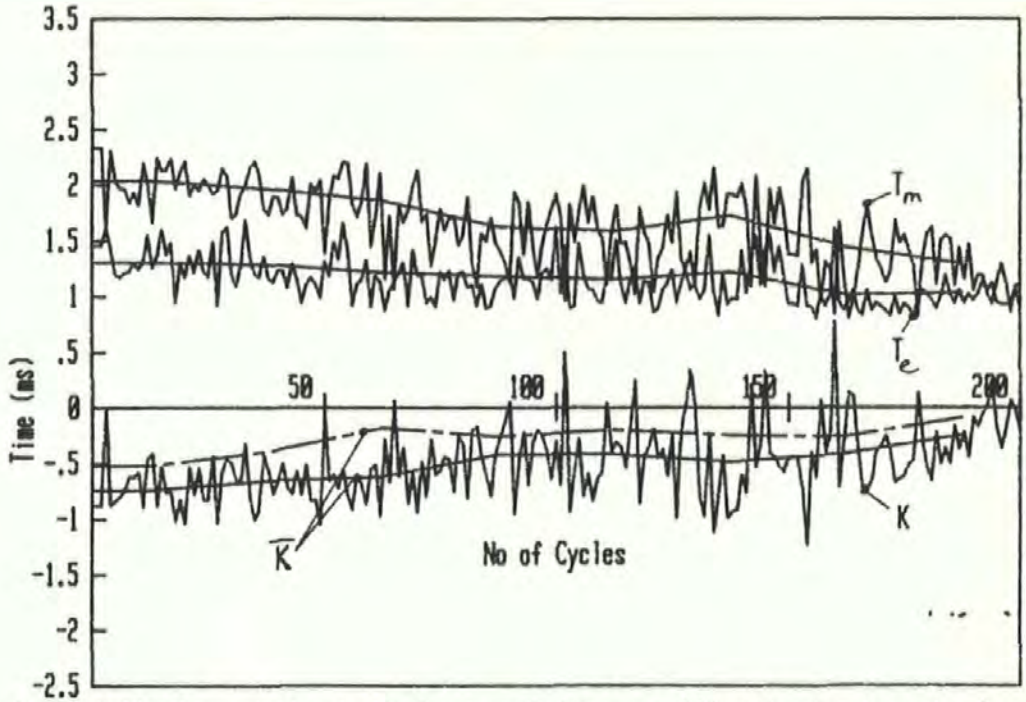

Figure 5.12, The variation in the bounce reduction over 200 cycles for two sets of contacts

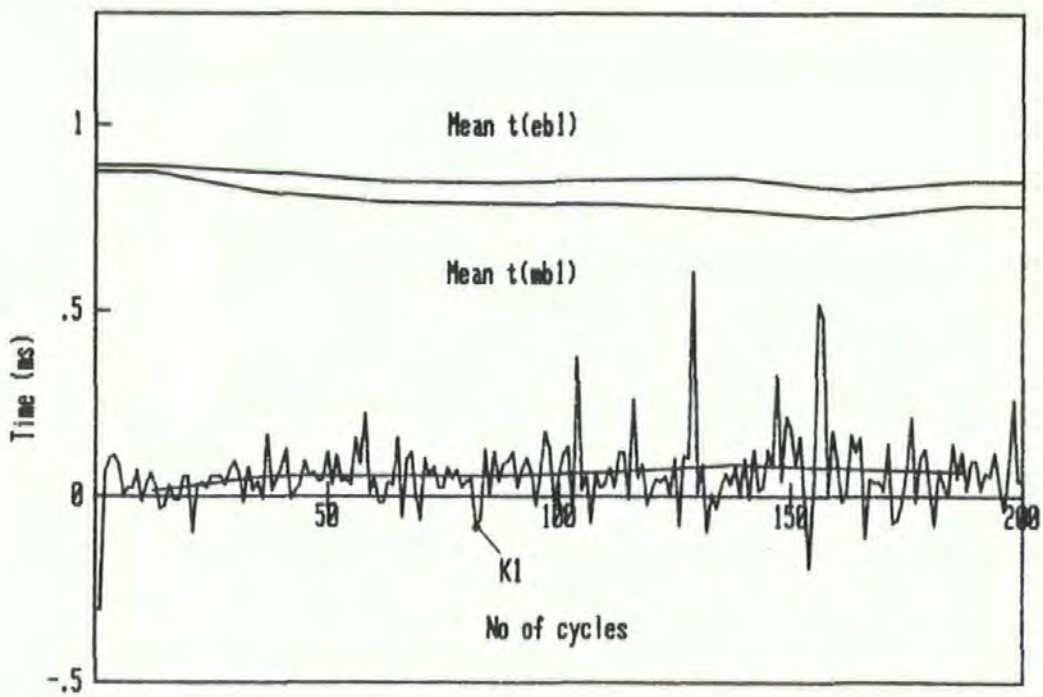

Figure 5.13, The variation of the first bounce reduction (K1), over 200 cycles at 12 Amps.

Eq.(5.1) $K' = T'_e - T'_m$

and,

Eq.(5.2) $K = K' + K1$

Where T'_e= The subsequent electrical bounce times,

and, T'_m= The subsequent mechanical bounce times.

With the small variations in, K1, the scatter in, K, must be due to the variations in, K'. By comparing the, K', data, with, T'_m, over the same period as in figure (5.11), it can be observed in figure (5.14), that most of the scatter occurs as a result of variations in, T'_m. This occurs because of the surface changes resulting from the arcing in the preceeding electrical test.

To summarise the observations, in sequence;

(1). After a single mechanical operation, the contacts close on a cold surface, with flattened asperites.

(2). At the first impact current starts to flow through the asperites, but the rebound is a consequence of the surface condition, and with no softening in the area of impact, the duration of the first rebound is constant.

(3). The arcing caused by the first separation causes significant heating of the areas of contact, such that upon the second closure, the contacts are meeting at areas of molten metal.

(4). In the second impact the kinetic energy of the contacts is more easily absorbed, because of the surface condition; leading to the supression of bounce.

(5). The following mechanical impact occurs on a cold but roughened contact surface, however the first bounce shows only small inconsistency over a large number of cycles. The majority of bounce inconsistency then occurs in the subsequent bounce time (T'_m).

To account for the inconsistency of, T'_m, the data is averaged over 25 values, and then compared to the, T'_e, over the same period. The results of this analysis for a range of times and for both pivot and rivet contact, is shown in figure (5.15). This shows that for a small subsequent mechanical time of less than (0.3 ms), there is no subsequent electrical bounce. At values above (0.3 ms) the following relation can be seen to hold.

$T'_e = T'_m - 0.3$; Where the times are in milliseconds.

Therefore with a known subsequent mechanical bounce time, the electrical bounce can be established, for both rivet and pivot type contacts, under the circuit conditions used.

5.3.5 The Subsequent Bounce Phenomena for a Range of d.c Currents

To extend the experimental relation to a range of currents required a re-consideration of the "Cycle mode 1", since significant periods of time were used in the collection of the data with the evaluation of a single point from 25 data values. For this purpose a new cycle was considered.

Cycle mode 2, In this case five mechanical operations are followed

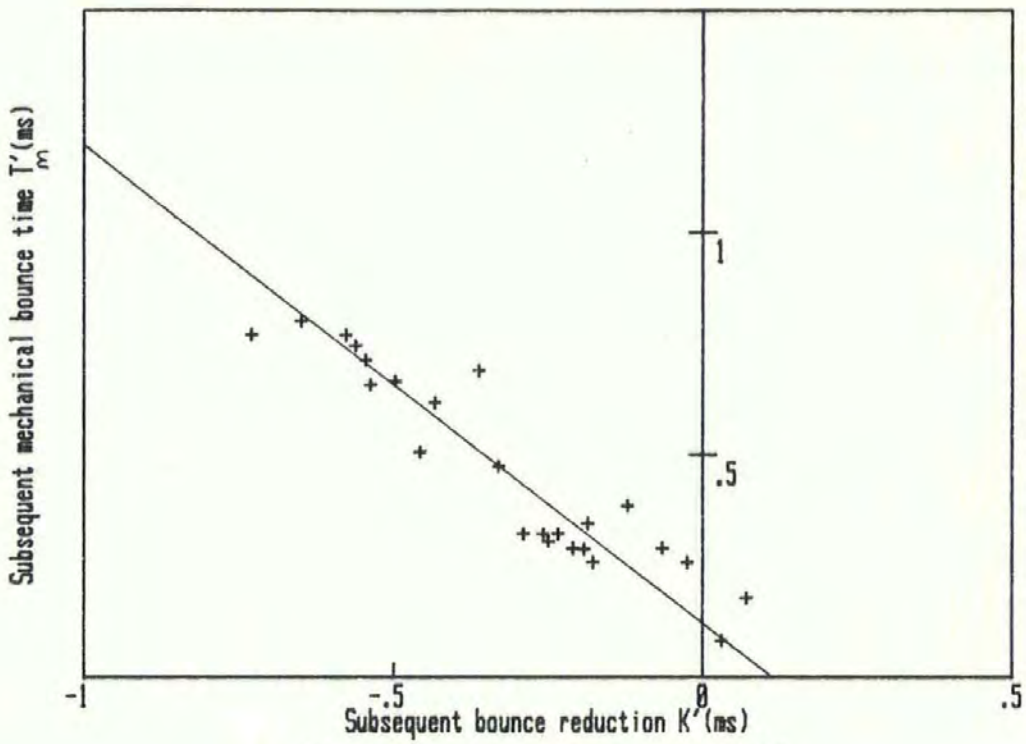

Figure 5.14, The variation of K' with T'_m

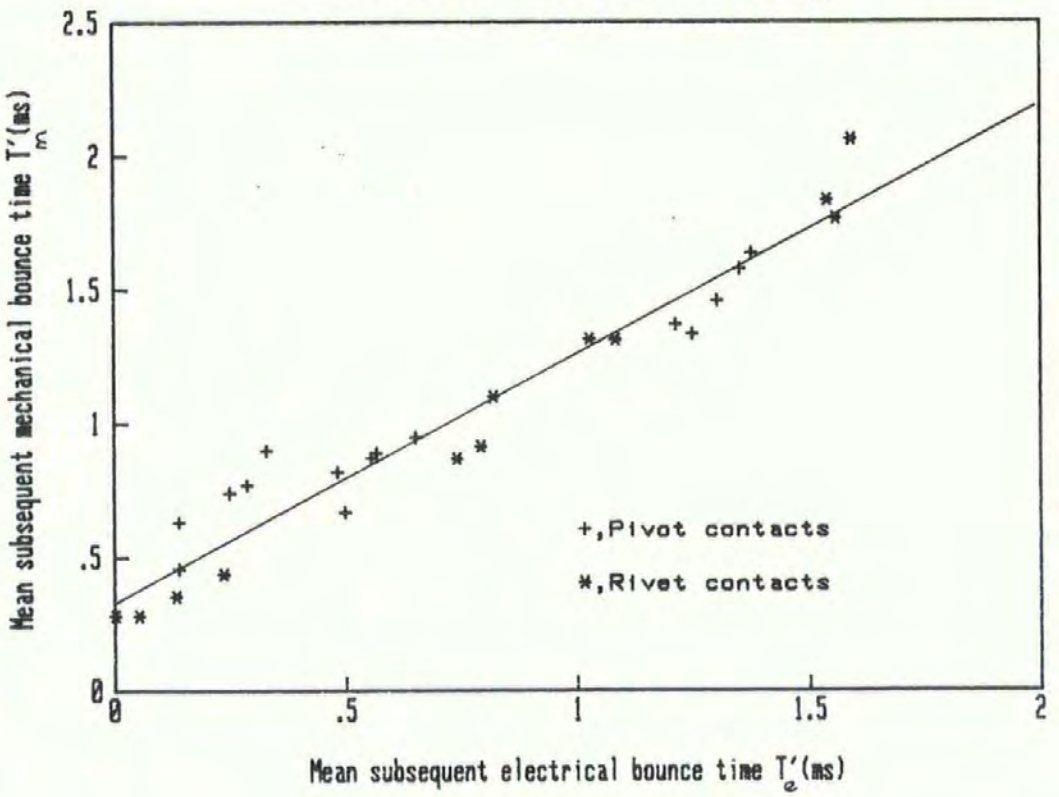

Figure 5.15, The variation of T'_e with T'_m, under 12 Amps, D.C, Test mode 1

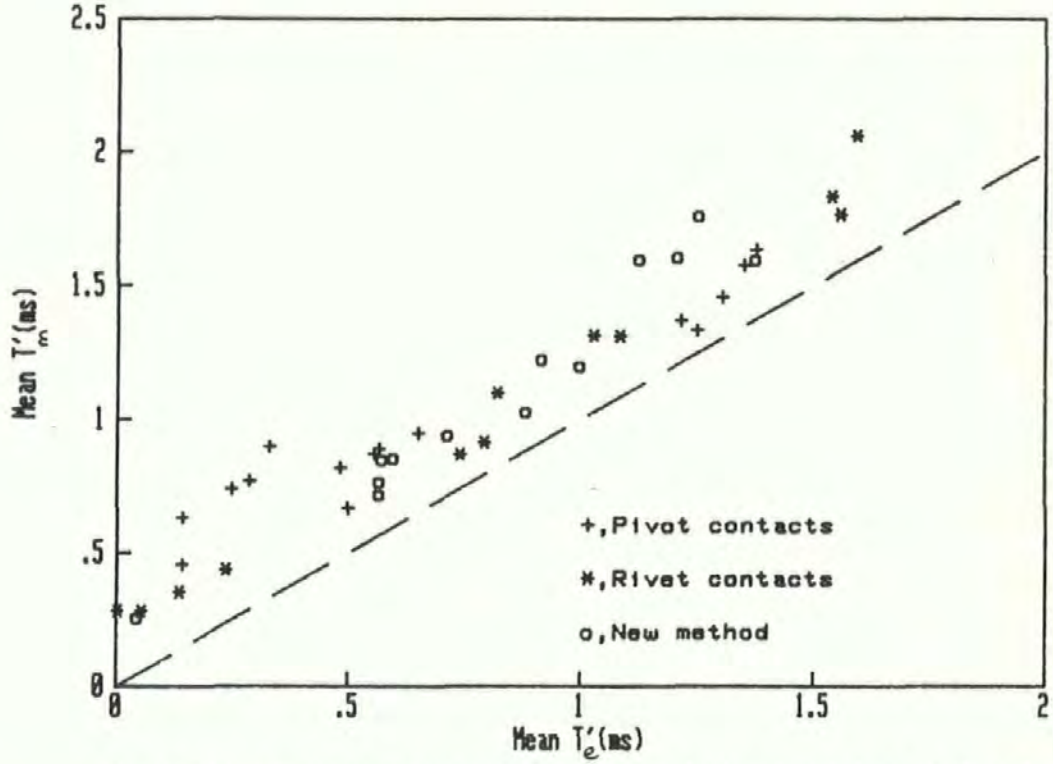

Figure 5.16, The relation between T'_e and T'_m, for both mode 1,& 2, at 12 Amps D.C

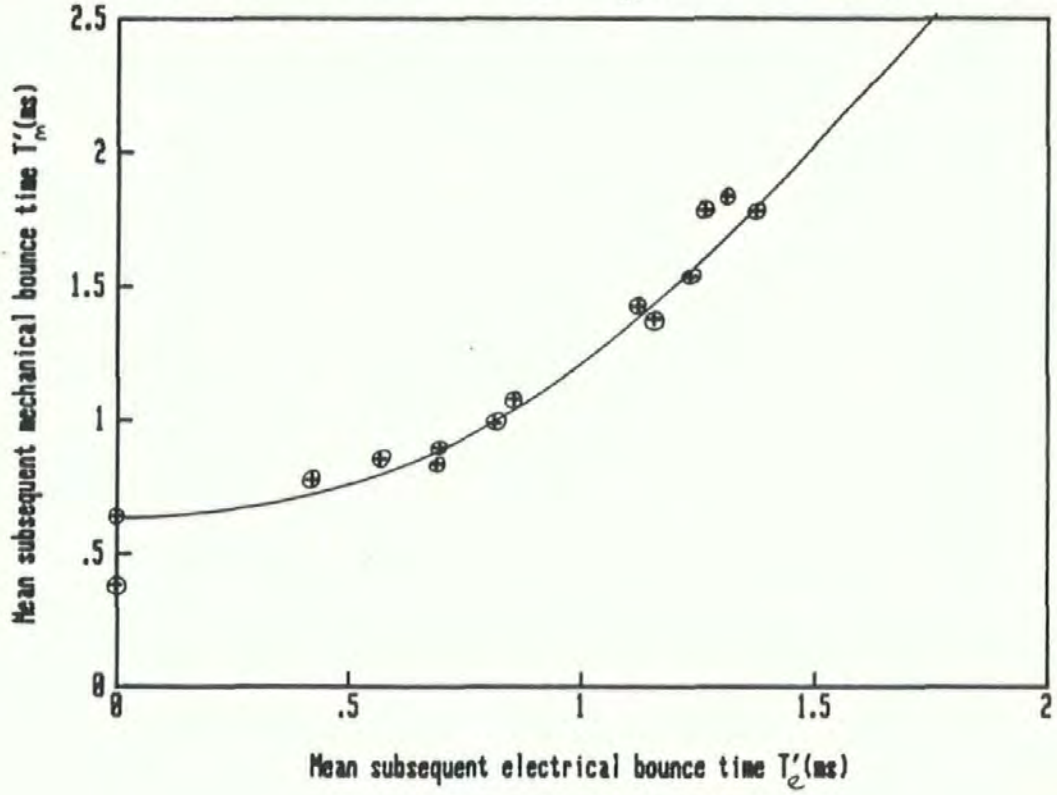

Figure 5.17 The variation of T'_m with T'_e, under 20 Amps, Test mode 2.

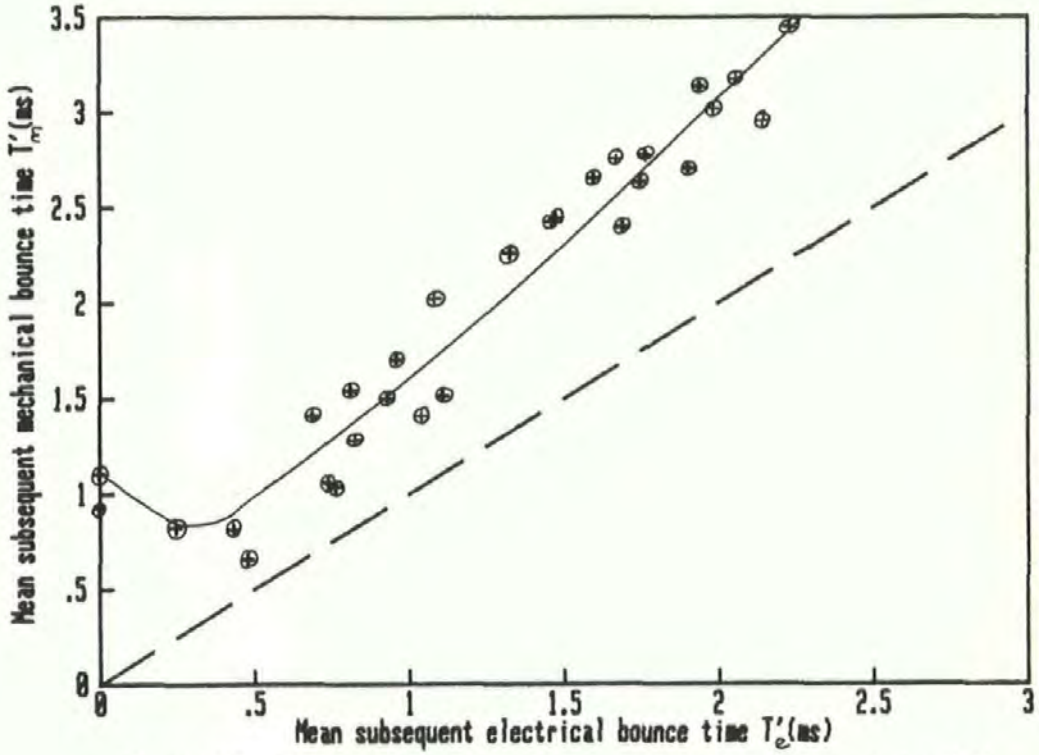

Figure 5.18, The variation of T'_m with T'_e, under 30 Amps, D.C, Test mode 2.

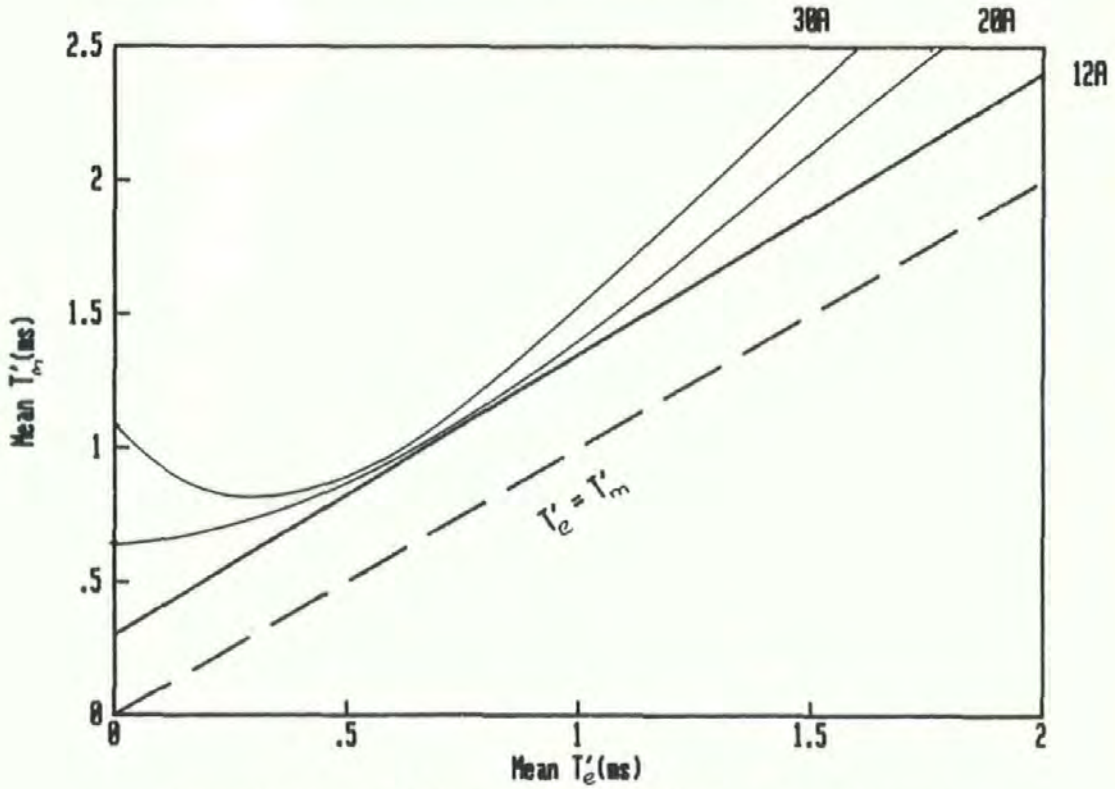

Figure 5.19, The relation between T'_e and T'_m for a range of currents.

by, five electrical operations. This is one cycle, and the system settings can be varied after each cycle to give a full range of bounce characteristics. An example of the data produced over one cycle is shown in table (5.3).

	T_m	t(mbl)	T_m'
	(all in milliseconds)		
	2.424	1.704	0.72
	2.32	1.632	0.688
	2.64	1.832	0.808
	2.696	1.872	0.824
	2.672	1.872	0.8
Mean values	2.55	1.78	0.768
	T_e	t(ebl)	T_e'
	2.112	1.648	0.464
	2.32	1.768	0.552
	2.264	1.688	0.576
	2.29	1.68	0.6
	2.24	1.68	0.568
Mean values	2.244	1.692	0.552

Table (5.3), the data for one cycle of cycle mode 2, with (h = 0.75 mm, F = 2.7 N, Rivet Contacts, 12 Amps, d.c)

The data reproduced in table (5.3), suggests a different value of K1, than that predicted by the previous method. In this case, a comparison of the first values of the first bounces gives, K1 = -0.056, indicating that the first mechanical bounce is larger than the first electrical. Similarly a comparison of the mean values gives, K1 = -0.09. This difference in the evaluation of, K1, results from the surface changes that occur using this cycle. The first mechanical bounce times, immediately follow an electrical operation thus the surface can be assumed

disturbed. The mechanical bounce times then show how the first bounce time increases over the five operations. This is caused by the flattening of the surface, and results in less absorption of the incident kinetic energy. After the mechanical operations the first electrical operation is impacting a surface more flattened that in the case of mode one.

The full extension of this method to cover a range of subsequent bounce times at 12 Amps gives the points in figure (5.16). These points clearely supplement the data obtained using mode one. It can therefore be stated that the new cycle mode allows for a accurate and fast collection of data. The method has therefore been used to consider the influence of a range of d.c currents.

5.3.5.1 Results for a 20 Amp D.C supply

Using the new data collection method, and considering the subsequent bounce times, the relation between the mean mechanical and electrical times at 20 Amps is presented in figure (5.17). This shows that the higher current has more of an effect in reducing the bounce, particularly at low and high values of subsequent mechanical bounce time. It is shown that with, T'_m = 0.6 ms, no subsequent electrical bounce would be monitored, and the amount of reduction in bounce is a function of the duration of the mechanical bounce.

5.3.5.2 Results for 30 Amp D.C supply

In the case of make operations at 30 Amps d.c the relation between T'_e , and T'_m is shown in figure (5.18). This shows a further increase of the effect of current on mechanical bounce, and shows that with T'_m = 1.1 ms, no subsequent electrical bounce would be monitored.

5.3.6 General Dicussion of Results

With a well defined mechanical bounce, split into first and subsequent bounce times, figure (5.19), allows for the evaluation of the expected subsequent bounce duration under the influence of d.c current, in the range 12, to 30 Amps. If the evaluated bounce time is then added to an unchanged first mechanical bounce time, an evaluation of the overall electrical bounce time, T_e, can be achieved.

It is therefore proposed that if the values of the mean pivot bounce times identified in table (4.6), on page 167, were split into first and subsequent bounce times a mean value of, T_e, could be obtained, and used in equation (2.26), to anticipate arc energy dissipation.

The reduction in subsequent bounce was first observed by Erk and Finke, [6], who published results of bounce time against current. Some of their results are shown in figure (2.5). The results presented here, confirm some of Erk and Fink's observations at much lower currents; and have taken the observation stage futher and present results that hold with an independance of materials and surface topography, under the conditions presented.

5.4 The Variation of Contact Resistance with Arc Erosion under Cycling

The purpose of this experiment is to give some understanding of the failure modes in the pivot, and rivet contacts. The basic details of the system modifications, the control, and processing software necessary for this are given in section (3.5.3). This is refered to as Experiment 2.

5.4.1 The Data Analysis of the a.c Transients at Impact

The data analysis of the contacts at impact under a.c cycling is more complex than the method used in the previous tests, under d.c conditions. In this case, once the waveforms have been transferred to the micro-computer the slice levels have to apply to both positive and negative values. In addition the extinguishing of an arc during the period of bounce can lead to errors in the bounce time evaluation. The software used to evaluate these waveforms is given in Appendix (4).

Figure (5.20) shows the contacts impacting, during the positive half of the A.C cycle. The current then rapidly increases during the first impact period, until the first bounce occurs. In this case both of the bounces at the contacts occur within the positive cycle, and the bounce times are taken directly from the voltage trace, since the current does not pass through zero. A comparison of the experimental and computer evaluated bounce times show only small errors.

Figure (5.21), shows the current passing through zero during the period of contact bounce, thus extinguishing the arc. In this case the software detects the current zero occuring during the bounce. A

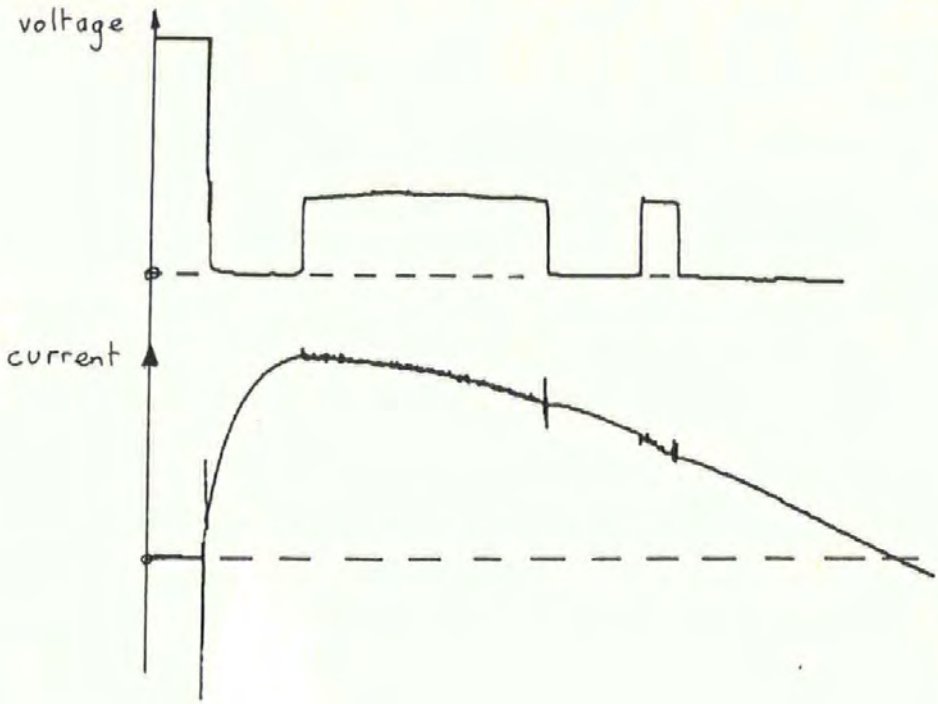

Figure 5.20 The contact transients at impact with an a.c supply

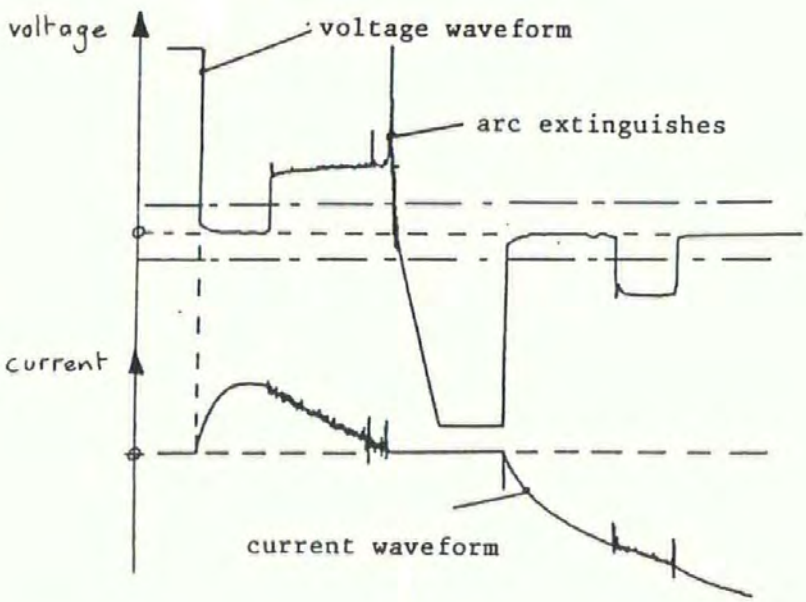

Figure 5.21 The contact transients at impact with arc extinction during bounce

comparison of the experimental and computer evaluated values of time again show only small errors.

5.4.2 The Variation of Contact Resistance with the Number of Operations

In this test rivet contacts were operated over 10,000, a.c cycles of 'make only' operations with the bounce and contact resistance monitored every 50 cycles. The experimental conditions were as follows: the supply, 200 volts, 16 amps, and the apparatus settings, h=0.5 mm, and F =1.4 N. These setting produced a mean bounce time evaluated from the 200 data points of 2.13 ms.

The evaluation of contact resistance and the methods used are discussed in section (3.4.8). To remove the likelihood of earth loops, the supply used for the monitoring of the contact resistance was a 24 Volt d.c battery, with a load current of 16.4 Amps.

The variation of the contact volt-drop with the number of operations is shown in figure (5.22). It shows that over the period of testing the contact maintains a low stable value of contact resistance, of 0.3 mΩ. The erosion profile of the contacts after the experiment is shown in figure (5.23). This shows that the protective Silver/ Nickel used on this contact has not been eroded sufficiently to expose the base metal.

The evaluation of the dissipated arc energy is not considered since the data points were only taken every 50 cycles, (to allow for the accelerated testing of the contacts). However in the light of the small contact resistance changes, this is unimportant, since there is no

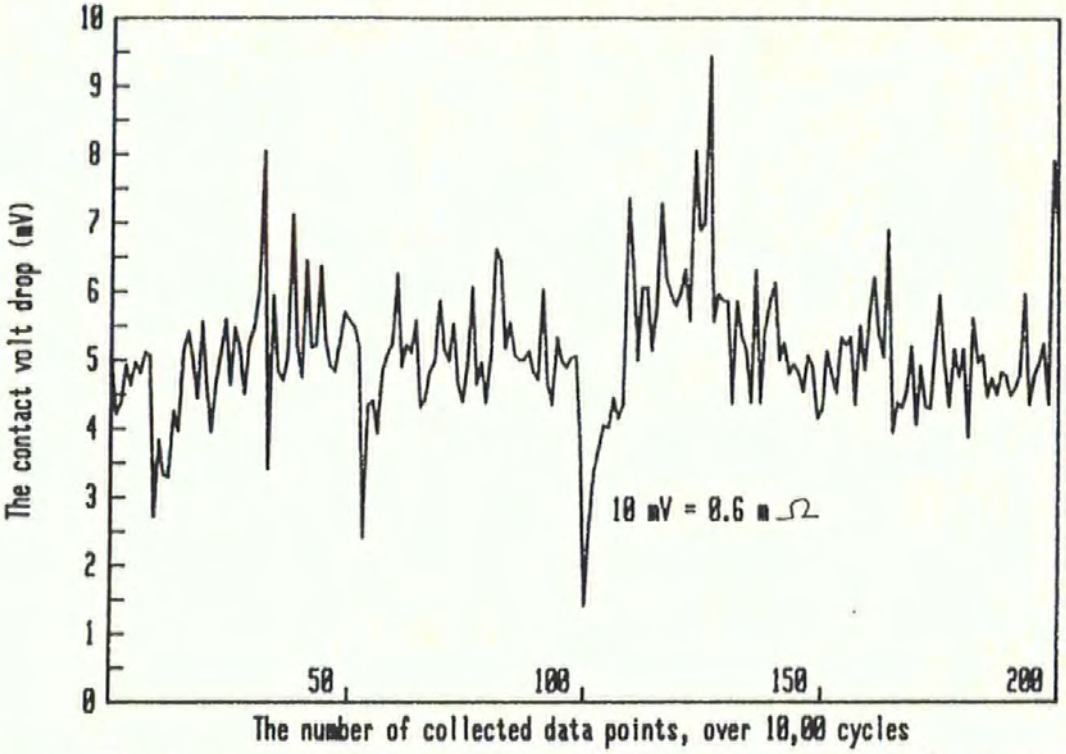

Figure 5.22, The variation of contact voltdrop with make only operations, D.C test current 16.4 A

Figure 5.23 The eroded contacts used for the data in figure 5.22, after 10,000 operations at 16 Amps a.c

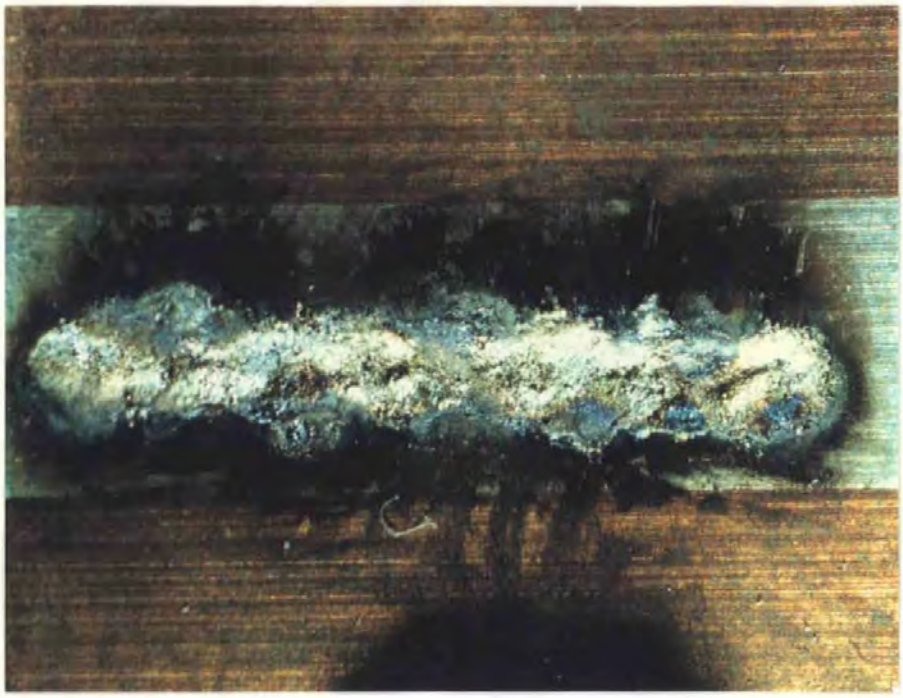

Figure 5.24 The erosion of the blade after 10,000 operations at 16 A, a.c

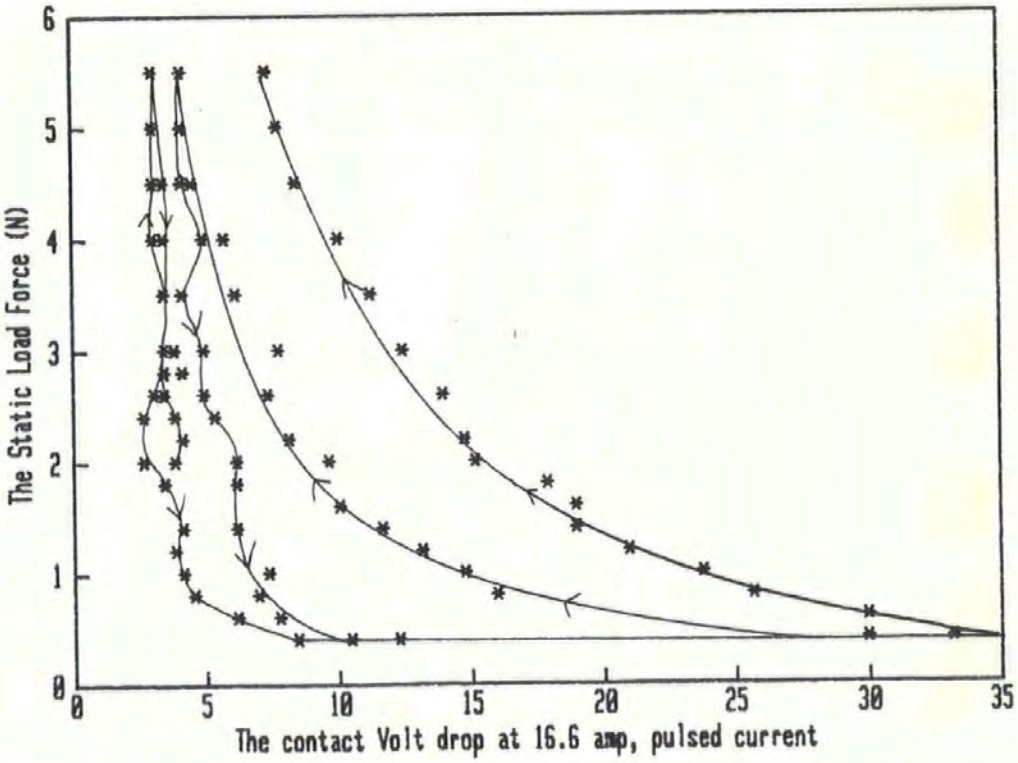

Figure 5.25 The Variation Voltdrop with contact Force

significant increase in the resistance.

The same low level of contact resistance was monitored with pivot contacts under the same experimental conditions. This again demonstrated the low resistance levels, with the resistance not increasing above 1 mΩ. In this case the mean bounce time over the period of the experiment was, 1.52 ms. This duration is of the same order of the bounce duration in the rocker switch, as shown in table (4.6). The erosion profiles associated with this magnitude of bounce is shown in figure (4.29c), for a hand operated rocker switch over 1000 make only operations. Comparing this profile with that in figure (5.24) for the same materials and bounce duration in the test system, over 10,000 operations shows that although the latter has undertaken 10x the number of operations the erosion profiles are similar in that in both cases the silver has not been penatrated.

It is therefore proposed that although the arcs occurring during bounce erode the surface, the slip and rolling motions associated with the interface in the rocker switch, must produce the added requirments for the removal the the silver. Therefore the switch erosion is a combination of arc and mechanical erosion. Where only one mechanism is in operation no significant wear is observed.

5.4.3 The Variation of Contact Resistance with Applied Force

To consider the influence of slip or the small movement of the surface after contact impact, the contact force is varied to zero, the contacts are re-seated and the resistance monitored. This test was

considered after the full 10,000 cycles.

The variation in the contact resistance with contact force is achieved by the hand variation of the spring compression on the test system, with the force monitored directly on the static load cell. The results shown in figure (5.25) apply to the rivet contacts, but could equally apply to most contacts of the type shown. A similar variation occurs with the pivot contacts after the full test. The figure shows that the contact resistance reduces with the increase in the applied force. Upon the reduction of force the resistance increases. After the first re-seating of the contacts, with the contact force increased to 2 Newtons the resistance is 0.48 m Ω, compared to the initial value of 0.24 m Ω. After a further re-seating the resistance increases to 0.9 m Ω. Thus the reseating increases the resistance by a small fraction, of 0.66 m Ω. It is proposed that in the case of the pivot contact shown in figure (5.24), a more significant increase would be monitored if the reseating were to occur at the edge of the eroded area, as would occur in the actual rocker switch with slip.

Small lateral movements of the contacts after impact do not lead to large increases in contact resistance.

5.4.4 The Evaluation of the Theoretical Arc Energy

The arc energy equation developed in section (2.4.4) can now be considered in the context of a.c, and d.c testing.

In the case of a 12 Amp tests, with an assumed constant arc voltage of 15 Volts, over 334 operations, with a mean bounce time of 2.95

ms, equation (2.26), gives the total arc energy dissipated to be (155.07J). The summation of energy evaluated in the automatic test system was (152.05J), thus showing the equation to be a useful means of evaluating arc energy dissipation.

In the case of a.c testing the assumption of constant arc energy is no longer valid. For the pivot contact endurace test, the relationship between the bounce time and arc energy during the experiment is shown in figure (5.26). In this figure the variation is considered over 191 data points. The figure shows that there is significant variation in the duration of the contact bounce. This is caused by two factors,

1) The magnitude of the current during the bounce is a variable, depending on when the contacts impact relative to the, a.c cycle. To ensure that this event is random, a time delay is utilised in the software.

2) The full pivot used in this test, has been shown to generate inconsistency in the bounce, as a result of the 9 mm line of contact.

For a comparison of the arc energy and bounce times figure (5.27) shows a magnified section of figure (5.26), and shows the independance of the two parameters. The variation in arc energy dissipation is affected by;

1) The random nature of the bounce time,

2) The randomness of the current crossover occuring during the bounce. This has the effect of producing a number of the arc energy values, close to zero, with a measured bounce time.

3) Both the supply voltage and current are sinusoidal.

To extend equation (2.26) to cover these variations the following asumptions are made.

1) A mean value of T_e can be used, and multiplied by N, the number of operations to give a summation of the bounce times.

2) The R.M.S currents and voltage can be used.

3) The minimum arc voltage for the pivot is 15 Volts.

4) In no case does the arc extinguish during bounce.

These assumtions are a significant simplification, and full statistical approach would be necessary for a full analysis.

In the case of the data in figure (5.27),

$E = 49.74$ J , and $\overline{T}_e = 1.529$ ms

Then in equation (2.26), the total E = 64.8 J.

The theoretical energy is 30 percent greater than the measured, therefore showing that although considerable assumptions are made the equation could be used, with further modifications, as a measure of arc energy in a.c circuits.

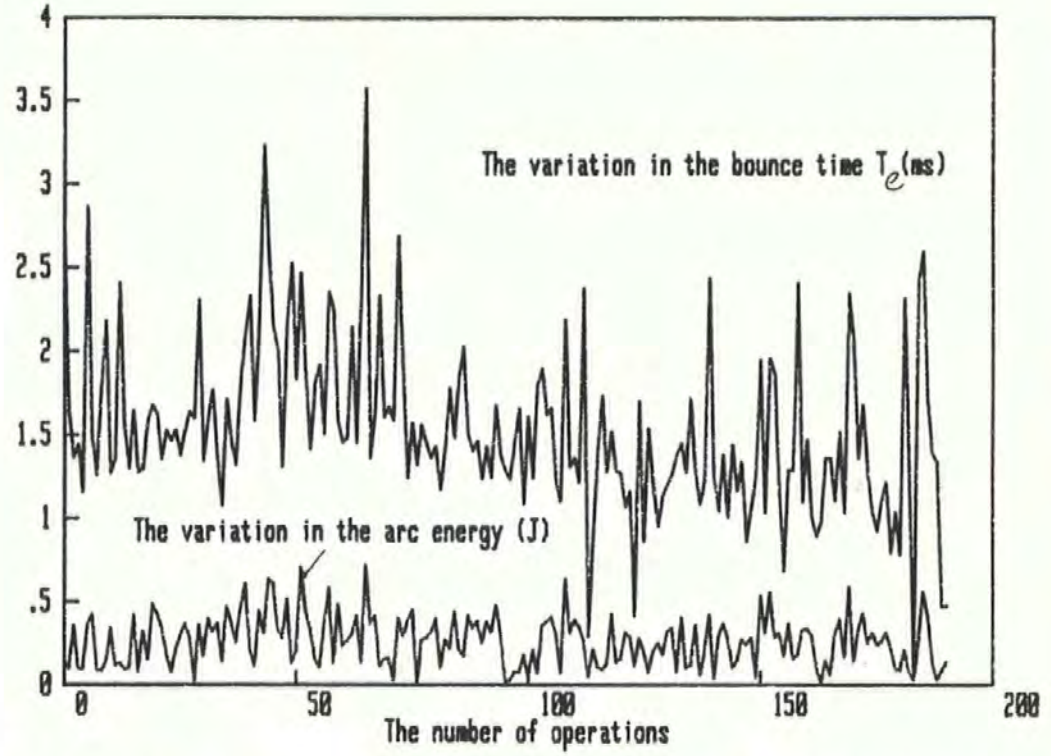

Figure 5.26, The variation of T_e and E, with the number of operations, at 200 V, 16A, A.C, make only

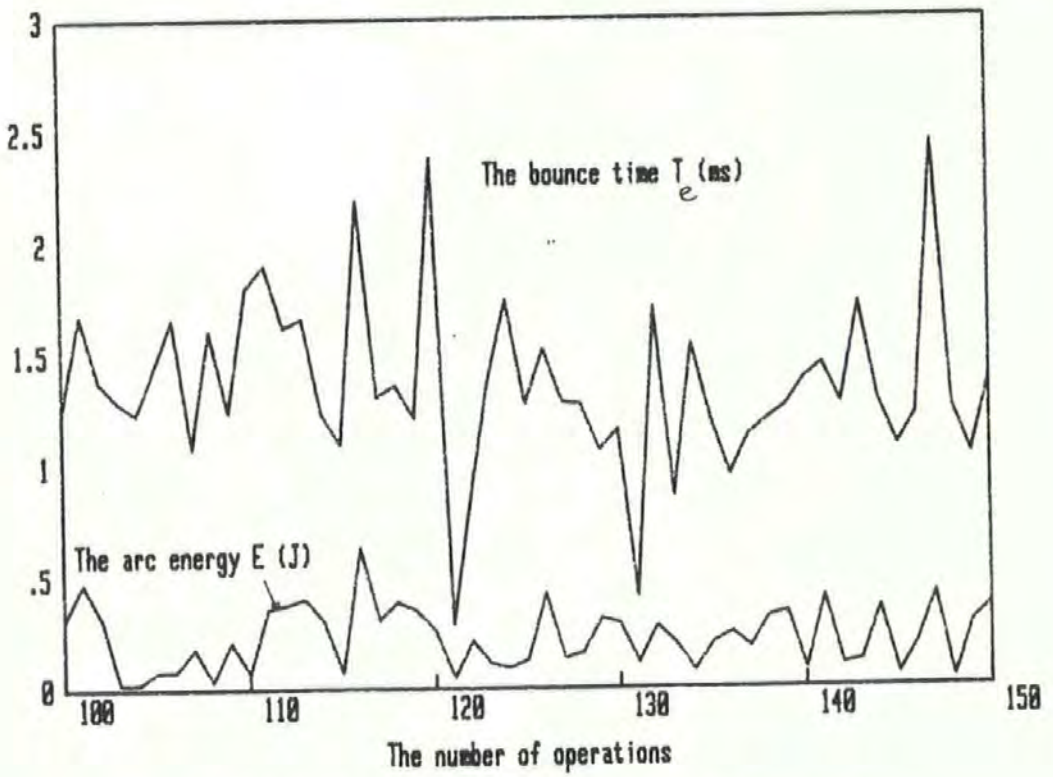

Figure 5.27, An expansion of the data given in figuer 5.26.

REFERENCES TO CHAPTER 5

[1] B. Miedzinski, Z. Okraszewski, D. Hajducka, T. Zolnierczyk, "The Effect of Contact Surface Conditions on Reed Bouncing", in IEEE Trans. CHMT- Vol 8, No 1, March 1985, pp 202-206.

[2] P.J White, D.J. Mapps, G.B Rossi, "Zero Current Synchronisation of Opening Switch Contacts", in Proc. Holm Conf. Elect. Contacts, 1985, pp 185-190.

[3] R. Holm, Electric Contacts, Springer-Verlag, Berlin/Heidelberg, 1967, pp 320-322.

[4] D.J Dickson, A. von Engel, " Resolving the Electrode Fall spaces of Electric Arc", pp 316-325.

[5] as 3 ref [3], pp 440.

[6] V.A. Erk, H. Finke, "Uber die mechanischen vorgange wahrend des Prellens einschaltender Kontaktstucke", (The Mechanical Processes of Bouncing Contacts), E.T.Z Electrotect, Vol 5, 1965, pp 129-133.

CHAPTER 6

Conclusions

6.1 Review

The research presented in this thesis has evaluated the operation and performance of the rocker switch mechanism. The results of the initial experimental work showed that the erosion at the pivot interface of 'make down' rocker switches, was caused by a separation and bounce at the interface, simultaneous with the main contact impact. This bounce and the associated arcing was therefore the major cause of the contact erosion and the rise in contact resistance, leading to an eventual over-heating failure, due to the temperature rise at the interface.

To reduce the contact bounce and thus the erosion a mathematical model of the switch mechanism was developed, with the aim of producing a computer model of the system, such that a computer-aided design exercise could be undertaken. This model accounts for the bounce in terms of the mechanical events. To extend the results to the case of bounce with the passage of current, experiments were considered on the influence of current on contact bounce. For this purpose a general automated test system was designed and developed for the study of fundamental electrical contact phenomena under controlled conditions. The apparatus was used to develop a relation between mechanical and electrical bounce in real switch contacts where the surface changes can affect the bounce, and to study the

erosion of the pivot interface under controlled conditions.

6.2 The Rocker Switch Dynamics

The high speed photogaphic study used in combination with the signal current switching transients, was used in section (4.2) to identify the pivot contact separation, bounce and system dynamics. These lead to a number of important observations.

1), During the switching motion the plunger is displaced and not acting directly over the pivot, as previous models have predicted.

2), Because of the low opening acceleration, the separation of the main contacts can only be accurately determined from the signal current transients.

3), The dynamics of the hand operated switch is affected by the way in which the switch is operated.

6.3 The Computer Model of the Switch Dynamics

The mathematical model based upon the observations made in the initial investigation, evaluates the dynamics of the system from a set of initial conditions, up to the moment of main contact impact. The model was verified experimentally in two stages, the first for an idealised initial condition, and the second for the real situation where the angular velocity of the actuator is constant during blade changeover. Both conditions were simulated, demonstrating the validity of the model. The

model was then used to study means of reducing the pivot bounce. The method used was to reduce the kinetic energy of the blade at main contact impact. For this purpose two design modes were used; the first applying to an existing mechanism, produced two suggested modifications, based on the reduction of the impact velocity. The second design method was an overall approach, based on the reduction of the blade inertia. The latter case was not tested experimentally because of the manufacturing difficulties, however the modifications made to the existing switch produced significant reductions in wear at the pivot interface. The testing of this type of switch was considered and it was shown that the standard test used by the manufacturer, is not representative of the operating characteristics in hand operated switches. The switches tested in this work were therefore all hand operated.

In an additional experiment the modified switches were compared under signal current conditions. In each case the kinetic energy at impact was related to the magnitude of bounce occuring at the pivot and main contact interfaces, over a number of operations. The former showed that for the switch considered there exists a linear relation between the kinetic energy at impact and the magnitude of pivot bounce, though with increasing energy there was increasing deviation in the data. In the case of the main contact bounce, no relation was established with increasing energy of impact. It can therefore be concluded that for the reduction of pivot bounce, a study of kinetic energy was justified.

The modifications made have proved useful in the ultimate aim of reducing the bounce occuring at the pivot and reductions of 80 percent have been achieved on the standard switch mechanisms considered.

The computer model is capable of analysing any rocker switch

design to predict operation times and the kinetic energy at impact. The extension of these values to the erosion of the contacts and the pivot bounce times under load current conditions is however less clear. It can however be concluded that a reduction in the kinetic energy at impact will reduce erosion, since with the mechanical bounce reduced the bounce under the passage of load current will also reduce.

6.4 The Influence of d.c Current on Contact Bounce

The results presented on the fundamentals of bouncing contacts, identify the importance of bounce time in defining a separation characteristic. The arc energy equation based upon this has proved to be a useful and accurate means of evaluating energy dissipation in bouncing contacts.

The test apparatus, enabling a single electrical bounce to be compared to a preceeding mechanical one, shows that with 12 Amps d.c:-

1) With the data averaged over 25 cycles, the first electrical bounce is slightly greater than the first mechanical, a typical value is 66 us.

2) The subsequent mean electrical bounce is less than the subsequent mechanical, a typical value is 0.3 ms, for worn contacts.

3) The large spread of data values of the subsequent bounce reduction, is due primarily to the variation in the subsequent mechanical bounce time. The mechanical bounces are therefore significantly affected by the surface changes, since they follow an electrical operation, whereas the electrical bounce will be acting on a surface flattened by the single mechanical

operation. Additionally the first impact in the electrical bounce will melt the surface such that the subsequent bounces are affected only by the extent of this melting, therefore with the same current and first bounce duration the subsequent bounce duration will remain, and has been shown to remain, constant.

To increase the rate of data acquisiton the experimental mode was changed such that a range of currents could be considered.

In this case each data value was averaged over 5 mechanical cycles, followed by 5 electrical. This leads to a different evaluation of the first bounce times. In this case the mean mechanical is slightly larger than the mean first electrical. The new method however produced the same results when subsequent bounce times are considered. Using the new method it was shown that for 30 Amps, with a subsequent mechanical bounce time of 1.1 ms, no subsequent electrical bounce would be expected.

It can therefore be concluded that the reduction in bounce caused by the passage of current is a function of, load current, and the subsequent mechanical bounce time.

6.5 Electrical Contact Bounce under a.c Endurance Conditions

No significant increases in contact resistance were monitored over the 10,000, cycles at 200 Volts, 16 Amps, 50 Hz, for both rivet and pivot contacts. Additionally the wear profiles of the pivot interface, for the same bounce periods experienced in the rocker switch, showed that less wear was noticable. It is therefore concluded that the wear profile at the pivot interface in the rocker switch is the combined effect of both

arcing and the rolling and sliding motion of the interface. Since with only pure bounce as in the case of the test system, and with only sliding and rolling, as in the case of SWITCH 3, where the bounce has been reduced to negligible proportions; the contacts maintain a good contact. It can therefore be concluded that if an electrical contact is to be used were small lateral motions can occur after impact and bounce is experienced, the materials should be carfully considered. It is suggested here that a suitable material might be 80/20 Ag/Cu, with a vickers harness of 85, compared to that of 26, of fine silver. The increased hardness of the material is likely to show wear improvements, during the rolling and sliding stages of the pivot interface.

If the bounce was reduced to negligible proportions, the thickness of the protective layer could be reduced, however the total removal is not recommended, since pure copper, with infrequent operation, would present oxidation problems at the interface.

APPENDIX I. Paper presented at the 31st IEEE Holm Conference on Electrical Contacts. September 1985.

DESIGN OPTIMISATION OF THE DYNAMICS OF DIRECT-ACTION ROCKER SWITCHES TO REDUCE PIVOT BOUNCE AND EROSION FOR LOW AND HIGH CURRENT CONDITIONS

Dr. D.J. Mapps
Mr. J.W. McBride
Mr. G. Roberts
Dr. P.J. White
Plymouth Polytechnic England

ABSTRACT

This paper uses a previously developed computer model of the dynamics of hand operated rocker switches with the aim of reducing pivot bounce and erosion. The method used is to study the kinetic energy at the instant of main contact impact, showing how the energy is affected by the force applied to the switch and how it relates to the switch dimensions. The study suggests some possible modifications. These are compared in experiments using a low current source. In the experiments, pivot bounce times are measured and compared to computer predicted values of kinetic energy; demonstrating the relationship between energy and pivot bounce, and showing how a reduction in energy reduces bounce. When a load current flows, a reduction in bounce time duration is observed. Results are presented of the reduction at 12 Amp d.c. for various mechanical bounce times.

1. INTRODUCTION

The rocker switch is a hand-operated switching device, utilised in the medium current range, (1-16 Amp a.c. and d.c.). It is commonly used in consumer-type electrical goods, and for general purpose switching.

The switch mechanism is of the snap-action, see-saw type (1), a typical layout of which is shown in Fig.1. The snap-action is intended to make the moving blade contact independent if hand forces after the toggle position has been reached.

In operation current passes through the central pivot to a main contact selected by movement of the rocker/actuator. During the switching process a high speed photographic study (to be published in another paper (2)), has shown that visible separations occur between the blade and pivot, after the main contacts impact. This post-impact separation or 'bounce' is then responsible for erosion at the pivot interface.

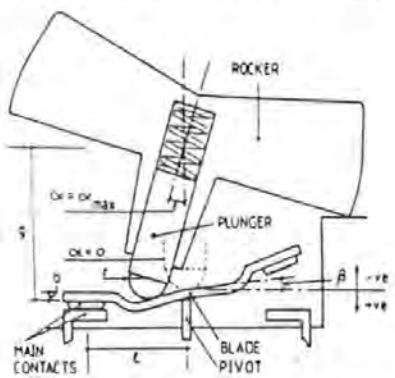

Fig.1. Schematic diagram showing the main parameters, and components of a rocker switch.

The problem of post-impact bounce has been studied by several workers. For example, Erk and Finke (3),(4), studied relationships between current and bounce for various contact materials, and identified the independence of the first bounce from current. Barkan (5) considered the mechanical characteristics of the contact surfaces and identified the importance of the stationary contacts, whilst discussing some of the effects of load current. More recent work has related bounce times to Erosion e.g. Belhachemi and Carballeira (6).

The case of bouncing at the central pivot of a rocker switch is complicated since, at main contact impact, the kinetic energy of the blade is dissipated between the pivot and main contact interfaces. In order to analyse these effects it has been necessary to derive a computer model of the mechanical system used in the switch, ref (2).

In this paper the computer model is used to investigate how the mechanical design affects the kinetic energy at impact, (KE_i) and how this is related to separation in terms of measured times of circuit interruption. Some possible switch modifications are compared.

A further investigation considers the effect of load current on mechanical bounce times and reconfirms some observation made in (3) and (5), while adding further insight into the effects of current on small amplitude bounces.

2. INITIAL STUDY OF PIVOT BOUNCE CHARACTERISTICS

A problem with the measurement of pivot bounce is that the current is interrupted not only at the pivot, but also at the main contacts. In order to separate these electrical events, the circuit shown in figure 2 was used. In this figure the 2V supply and 4 mA current maintains a no arc condition on switching. The connection to the moving blade contact maintains a measurable voltage across the contact gaps, even when both contacts are open circuit, i.e. (1V). A typical

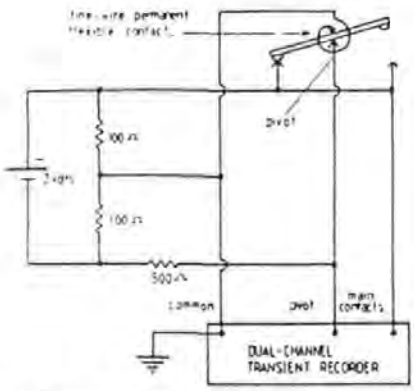

Fig.2. Circuit diagram of the electrical arrangement for monitoring both pivot and contact separation.

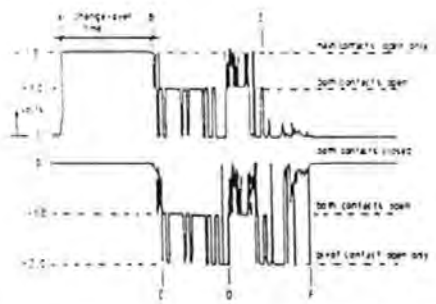

Fig.3. Transient recorder traces of a switching operation using the circuit of Figure 2.

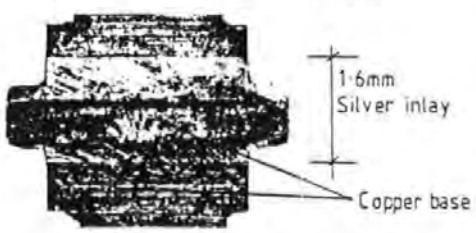

Fig.4. Erosion profile of blade after endurance test, showing the wear of the silver inlay.

characteristic is shown in figure 3, where the top trace shows the main contact disturbance. At A, the main contacts open without an arc to the open circuit potential. At B the opposite main contacts close, thus defining the change-over time. There follows a period up to E in which the main contacts bounce. The bottom trace shows the pivot contact disturbance. It shows that at C, 148us after the main contacts impact, the pivot contacts fully separate. There follows a period up to F in which the pivot contact bounces. The 1 volt level occurring simultaneously in both traces indicates that both main and pivot contacts are separated.

The pivot characteristic is dominated by one initial bounce, between C and D, in this case of 1.15 ms; followed by a number of smaller subsequent bounces. This occurs because the blade tends to continue its angular motion at main contact impact. The figure demonstrates the complexity of the post-impact dynamics.

An electrical endurance test to BS-3955, (10,000 cycles of 240 d.c. 16A) shows the effect of this separation on the centre of the blade, figure 4, where the thin (0.06 mm) Ag inlay is seen to have eroded through to the copper base.

3. THEORETICAL DEVELOPMENT AND THE USE OF THE COMPUTER MODEL

The mathematical model of the system is based upon the numerical solution of four simultaneous non-linear differential equations, representing the switch dynamics to the instant of main contact impact, (2).

3.1 Evaluation of Kinetic energy

For the purpose of this paper the model is used to evaluate the angular velocity of the blade at the moment of impact ($\dot{\beta}_i$). From this, the kinetic energy is determined,

$$KE_i = \frac{I_b}{2} (\dot{\beta}_i)^2 \qquad (1)$$

where I_b is the moment of inertia of the blade about the pivot axis.

A typical example of the data produced by the model is shown in figure 5. It shows how a constant angular velocity of the rocker assembly ($\dot{\alpha}$) affects the angular velocity of blade ($\dot{\beta}$). The impact point is defined by the line $\beta = \beta_{max}$, in this case 0.209 radians.

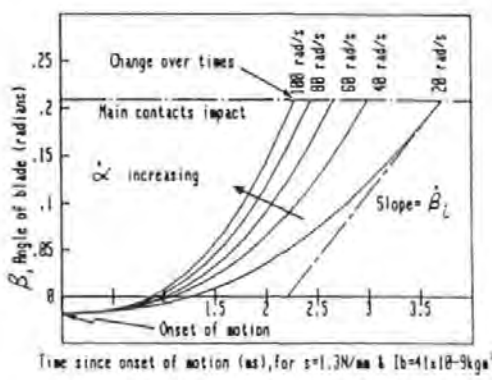

Fig.5. Theoretical curves of blade angle versus time for a range of angular velocities of the rocker ($\dot{\alpha}$).

The slope at the impact point gives $\dot{\beta}_i$, thus increasing $\dot{\alpha}$ increases $\dot{\beta}_i$ and KE_i for a given blade inertia.

In reference (2) it has been established by high speed photography that over the change over and bounce period, $\dot{\alpha}$ maintains its initial value.

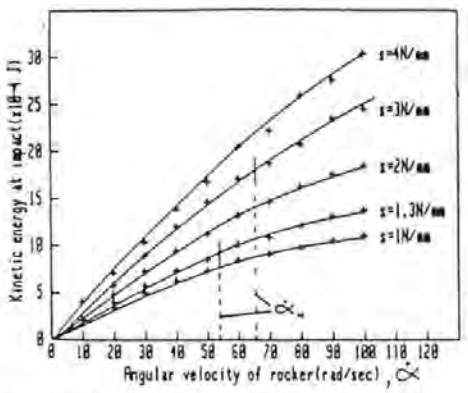

Fig.6. Graphs of angular velocity of the rocker plotted against kinetic energy at impact for a range of actuator spring stiffnesses (s).

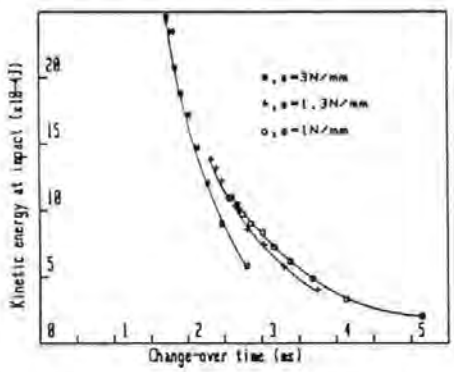

Fig.7. Kinetic energy at impact against change-over time for a range of spring stiffnesses (s).

The initial negative value of θ_i results from the blade angle at the onset of motion (see figure 1). When $\alpha = 0$, θ is negative.

The time to impact corresponds to the change over time discussed in the previous section. This proves a useful relation since from values of change over time = can be obtained.

Using the values of θ_i at impact (see fig.5), for a given I_b, curves of KE_i versus $\dot{\alpha}$ can be plotted and the computer model allows this to be done for a range of spring stiffnesses (s) as shown in figure 6. This graph shows that KE_i reduces with both $\dot{\alpha}$, and s. For the same data KE_i can be plotted against time to make, or as previously discussed changeover time, again for a range of s. Figure 7.

3.2 Use of the Computer Model

To demonstrate the use of the model in reducing KE_i the variables, have been considered in two sections, as they apply to the switch used in Figures 5,6 & 7.

(i) Changes in Geometry The computer model can be used to investigate the effects of changes in switch geometry on, for example, the switch changeover time and kinetic energy. A previous analysis (1) ignoring the effects of hand forces and inertia, showed that the dimensions r, b, g etc (see fig.1) were significant in determining switch behaviour. In this case, these parameters can be shown to be much less important, when compared to the changes possible in reducing $\dot{\alpha}$.

Changes in I_b, the blade inertia would clearly directly affect KE_i in equation (1); however within the constraints of a fixed distance between the contacts ℓ in figure 1 only small changes are possible.

(ii) Reduction of $\dot{\alpha}$ (the angular velocity of the rocker assembly). In the switch considered the force exerted by the hand dominates the angular velocity at which the rocker operates. This means that the contribution of the spring is less than in a freely moving snap-action device. Although the value of $\dot{\alpha}$ is mainly determined by the hand force, this in turn depends on the resistance of the mechanism, i.e. the minimum force necessary to operate the switch. By reducing the minimum force the $\dot{\alpha}$ generated by the user correspondingly decreases.

A typical sample of 20 normal operations on each of two switches produced $\dot{\alpha}$ values in the range shown in figure 6. The mean of these values is defined in this paper as $\dot{\alpha}_N$. Figure 6 confirms that $\dot{\alpha}_N$ is a function of spring stiffness s.

A means of reducing $\dot{\alpha}$ is to reduce s; however, this would alter the static distribution of contact forces, and change the contact resistance characteristics. To satisfy the requirement to maintain the contact forces, the static angle (α max) of the plunger is reduced, compressing the new lower stiffness spring. Reducing the static angle also reduces the force needed to actuate the mechanism, and thus $\dot{\alpha}_N$. This solution is Switch 2 and the mean values of (KE_i) which relate to $\dot{\alpha}_N$ are presented in table 1. Table 1 also indicates pivot bounce time t_m (see section 4.2) and this is seen to correlate well with the expected effect of the switch modifications.

A further reduction in $\dot{\alpha}_N$ can be achieved by increasing the leaverage necessary to overcome the resistance of the mechanism. This is achieved by changing the rocker shape; for example, by adding a 35mm lever, and is referred to as Switch 3.

These modifications are demonstrations in how computer modelling can be used in the optimisation of a given switch.

In this case $\dot{\alpha}$ has been shown to have the most significant effect on the angular kinetic energy at impact. However, to put this conclusion into perspective, it should be said that these results were produced for a single design of rocker switch. Another design variant could result in a different conclusion.

Contact Erosion: As an extension of this work the modified switches were tested at 16 Amp a.c. over 1000 operations, and a visual examination of the contact surfaces showed switch 1 to be the most eroded and switch 3 the least.

	C/O (ms)	$\dot{\alpha}_N$ (rad/sec)	$\overline{KE_i}$ ($\times 10^{-4}$ J)	$\bar{t}_m(p)$ (ms)
Switch 1 (standard)	1.95	65.5	19.8	1.208
Switch 2	3.2	30.2	5.82	0.415
Switch 3	4.0	15.0	3.0	0.2

Table 1

4. KINETIC ENERGY AND PIVOT SEPARATION

To relate the computer generated values of impact kinetic energy to the actual amount of pivot bounce, it is necessary to initially define bounce as a specific parameter.

4.1 Relevance of transient separation time

Bounce phenomena can be categorised in terms of the maximum bounce height Y and bounce time t. These are related,(5),(7) in the equation,

$$Y_n = t_n \frac{u \times e^n}{4} \qquad (2)$$

where u = velocity of first impact, e is the coefficient of resitution and n the number of bounces considered.

In this case, the first bounce, has a time t_1 typically < 2 ms, u ≈ 0.2 m/s and e ≈ 0.7. The distance Y_n from (2) is ≈ 0.07 mm and is the maximum distance of separation. This is within the limit of approximately 0.1 mm over which the arc voltage holds close to the minimum arc voltage V_m. For gaps of 0.01 mm the voltage is approximately V_m(8).

If V_m can be assumed constant, then, for d.c. resistive conditions, the arc energy dissipated over the total bounce duration is,

$$E = V_m I_a t_e \qquad \text{i.e.} \propto t_e$$

where t_e is the total time of separation. Over N cycles.

$$E_N = V_m I_a \Sigma_1^N t_e \qquad \text{i.e.} \propto \Sigma_1^N t_e \qquad (3)$$

Hence the energy dissipated by the arc after first impact $\propto t_e$ for d.c. conditions. For a.c. conditions it is suggested that a mean value of I_a might be applicable over 1000 or more operations.

Substituting for I_a in equation 3, i.e. $I_a = I_s(1 - V_m/V_s)$ gives,

$$E_N = V_m . I_s . \left(1 - \frac{V_m}{V_s}\right) \sum_1^N t_e \qquad (4)$$

where I_s and V_s are the supply values.

From the above it is clear that if contact separation time is measured then this is an accurate method for monitoring the amount of post-impact bouncing of the contacts. Additionally, using this time enables an estimate of arc energy using equation (4).

4.2 Kinetic energy at impact and pivot disturbance time

The kinetic energy values determined in the computer model are only applicable to bounce times when negligible current is flowing (mechanical bounce time t_n).

Using the circuit shown in figure 2, the various switches have been tested over a number of operations for their transient time characteristics by the methods described in section 5.1. From these times the change-over time, pivot bounce time ($\bar{t}_m(P)$), and main contact bounce time are accurately evaluated.

To arrive at the relationship between KE_i and pivot bounce time, the change-over time is transformed to a value of KE_i (using the line in figure 7), for the particular switch studied.

With the switches purposefully operated outside their "normal" range a good span of data points was achieved, as shown in figure 8a. The points for switches 1, 2 and 3 lie within the areas labelled.

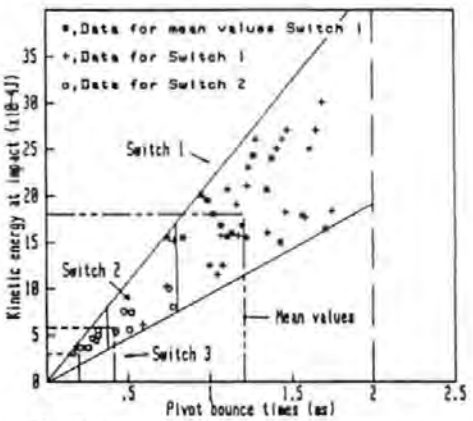

Fig.8a. Experimental values of pivot bounce time, versus computer predicted values of Kinetic energy at impact, for various switches.

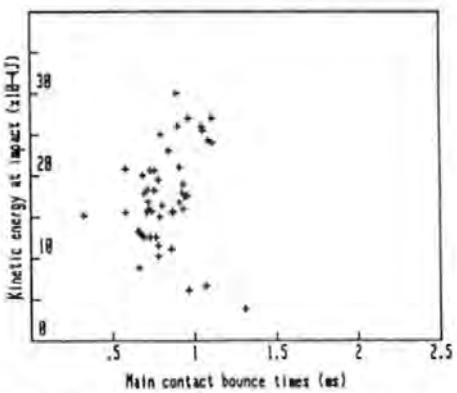

Fig.8b. Experimental values of main contact bounce time versus computer predicted values of Kinetic energy at impact, for switch 1.

The vertical line defines the extreme value of $t_m(P)$. Superimposed upon this figure are the mean values of KE_i used in Table 1, with the corresponding mean values of $t_m(P)$.

Hence it is seen that the switches suggested in the optimisation procedure (section 3.2) satisfy the requirement to reduce the pivot bounce time.

The figure also shows that if mean values are considered an approximately linear relationship exists between $\overline{KE}_i$ and $\overline{t}_m(P)$.

A similar analysis applied to the main contact bounce time, shown in figure 8b, demonstrates that this time bears no direct relation to KE_i.

5. Computer based test system

To study bounce phenomena accurately, and to evaluate the relationship between low current bounce (mechanical) and load current bounce (electrical), a computer controlled test system has been used.

The aim of this work is to define electrical bounce times (t_e) for a given current, and mechanical bounce (t_m). Thus the Kinetic energy pivot bounce relation can be extended using equation (4) to given levels of arc energy dissipation.

5.1 Experimental Apparatus

A schematic diagram of the computer-controlled test system is shown in figure 9. The test contacts are real contact pairs of reduced width set at the angle corresponding to their angles in the actual switch. The copper pivot is mounted in the arm, and sectioned to produce a 1mm line contact, instead of the 9mm of the actual switch. When the arm is released by the solenoid the copper contact drops onto the silvered contact and subsequently bounces. It will be noted that this is a reversal of the arrangement of the actual switch where the silvered contact is the moving part. However, as it is the relative movement which is being simulated it was assumed that this difference

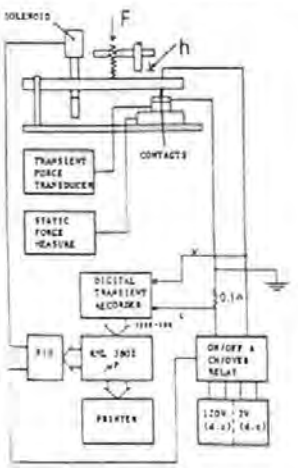

Fig.9. Computer controlled experimental test system.

would not affect this study. In all tests the positive terminal is connected to the stationary contact. For the purpose of general study and comparison the main contacts were also used. These were rivet-type Ag-Ni contacts.

The model was adjustable for static contact force (F), vertical stop height (h) to give a variety of bounce characteristics.

The system is controlled by a sequence of events defined within the RML380Z microcomputer which evaluates the transient waveforms produced.

The apparatus has the capacity to evaluate the following parameters continuously over a number of cycles defined in the controlling program:-

- i_a, the transient arc current waveform
- v_a, the transient arc voltage waveform
- F , the static contact force
- f , the transient contact force
- t , the bounce event times.

From i_a and v_a, the arc energy dissipated is accurately evaluated, by summing the product of i_a and v_a for each sample of data.

i.e. $E = \sum i_a v_a \delta t$ where $\delta t = 8us$.

The bounce times, indicated in figure 10, were measured by transfer of the digitised waveforms via an IEEE bus to the microcomputer. The slice levels were set up as indicated in figure 10, i.e. when a byte has a value > 0.5 volts the contacts are open and the time is recorded.

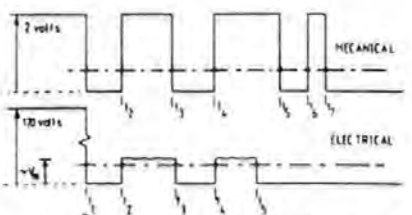

$t_e, t_m = \sum_a (t_{(2a+1)} - t_{2a})$, where a=No of bounce

First bounce time $t_{mbl}, t_{ebl} = t_3 - t_2$

First impact time $t_{mil}, t_{eil} = t_2 - t_1$

Reduction $K = t_e - t_m$

Change in first bounce $K1 = t_{ebl} - t_{mbl}$

Fig.10. Data evaluation methods for mechanical and electrical cycles.

To evaluate the effect of current on a mechanical bounce characteristic, the system is controlled such that the circuit connected to the contacts is changed after each operation. The 2V, 4mA circuit shows the actual separation times for the mechanical cycle, whilst the following 120V d.c. (1-20A) circuit in figure 9 shows the modified bounce characteristics due to load current. From the latter, electrical bounce E the arc energy, is calculated.

In this way the mechanical (negligible current) and electrical (load current) post impact bounce characteristics are established (see figure 10). It is thus possible to accumulate values of K, the

reduction over a number of cycles and to study the effects of current, arc energy and, by implication, erosion, simultaneously.

5.2 Results and Discussion

Initial experiments on pivot contacts:

To evaluate the mechanical characteristics of the apparatus, the system was operated over 1000 cycles with F = 2.7N, and h = 1 mm. The resulting values of t_a, first impact time (t_{mi}), and first bounce time (t_{mb1}), (see fig.10) are shown in figure 11. The t_m data plotted every 10 cycles shows the variation that occurs in the overall bounce duration. The corresponding values for the first bounce and impact show comparatively little variation. The subsequent micro bounces therefore have a large random factor. Interestingly no work hardening effects are noticeable.

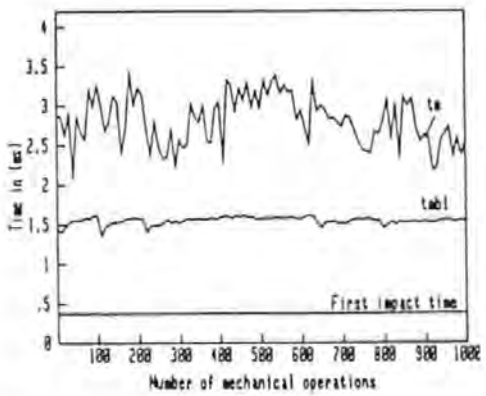

Fig.11. The variation of total mechanical bounce time first bounce, and first impact time with the number of mechanical only operations.

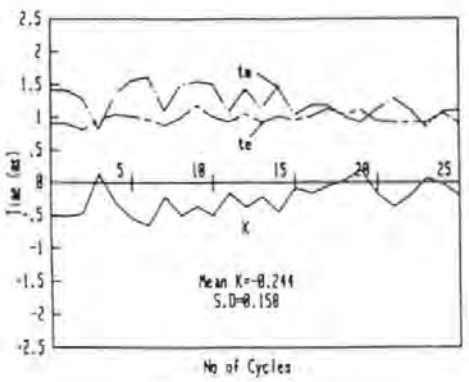

Fig.12. The variation of reduction, K over 25 cycles at 12 Amps, for worn contacts.

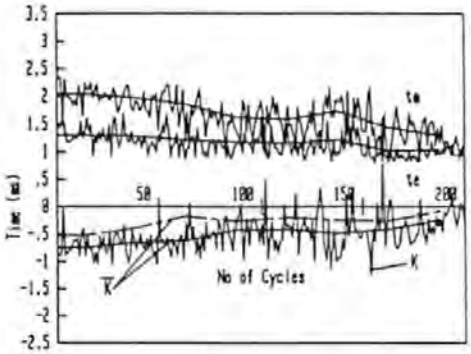

Fig.13. The variation of K and $\overline{K}$, over 200 cycles for two sets of new contacts at 12 Amps

Evaluation of the reduction term K:

A typical set of results on the evaluation of the differences in electrical and mechanical bounce (K) for pivoted contacts is shown in figure 12. K is shown to vary significantly over the 25 cycles considered. Over the period a mean value of K is calculated ($\overline{K}$).

The large scatter observed in figure 12 is confirmed in figure 13, for 200 cycles. In this figure the superimposed mean values, show $\overline{K}$ to be consistently negative and reducing with the number of cycles. This reduction seems to be principally the result in a reduction in the mean mechanical bounce time($\overline{t_m}$) presumably occurring due to surface erosion.

A similar test for new contacts at 12 Amps, shows a similar reduction, however the values of $\overline{K}$ are seen to be different in figure 13.

To establish the factors affecting the scatter, and the variation in $\overline{K}$ for different contacts, individual bounces were considered in a given characteristic. This again showed the consistency of the first bounce and showed $\overline{KT}$, the difference in time between first electrical and mechanical bounces to be unformly positive; Figure 14, indicating a larger first electrical bounce. Over the same period a figure 12, $\overline{KT}$ = 66us.

The positive value of $\overline{KT}$ may be due to the vapour pressure of the arc as reported by Holm, at much higher currents,(90 A),(9).

Subsequent bounce phenomena:

The positive value of $\overline{KT}$ implies that the overall value K must be reconsidered, since K applies to a whole bounce characteristic, and there are clearly two sectors to the bounce. The second sector, or subsequent bounce is significantly affected by the first arc, as a result of thermal effects i.e. melting of asperities. This causes the reduction in subsequent electrical bounce.

The reduction over the subsequent period K' is thus defined as

$$K' = t'_e - t'_m \quad (5)$$

also $$K = K' + K1 \ , \ (K' > K) \quad (6)$$

where t'_e, t'_m are the subsequent electrical and mechanical bounce times.

With regard to equation (6), it can be said that because of the small variation in K1, the scatter in K must be due to the scatter of K'. Plotting K' against t'_m for the same data as figure 12, shows in figure 15 that most of the scatter occurs as a result of variation in t'_m over the 25 cycles. This occurs because of the surface changes resulting from the arcing in the preceeding electrical test.

Taking mean values of t'_m,$(\bar{t}'_m)$ and t'_e,$(\bar{t}'_e)$ over 25 cycles for various worn contacts and test-rig settings produced the data showed in figure 16, for A 12 amp d.c. resistive load.

This shows that for small subsequent mechanical bounces <0.3 ms, there are no subsequent electrical bounces. At values >0.3 ms the value of $\bar{t}'_e$ is approximately $(t'_m - 0.3)$ ms.

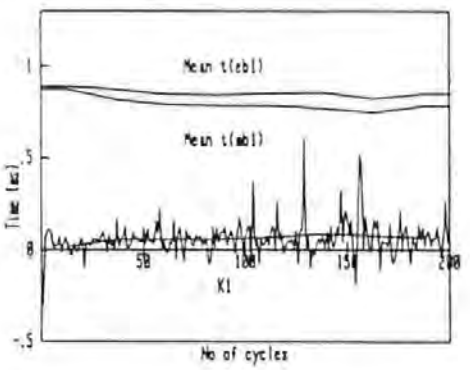

Fig.14. The variation of the first bounce difference K1 over 200 cycles at 12 Amps.

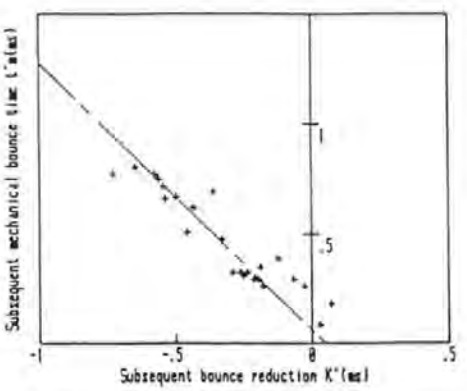

Fig.15. The variation of the subsequent bounce reduction K' with the subsequent mechanical bounce t'_m, for the same data as figure 12.

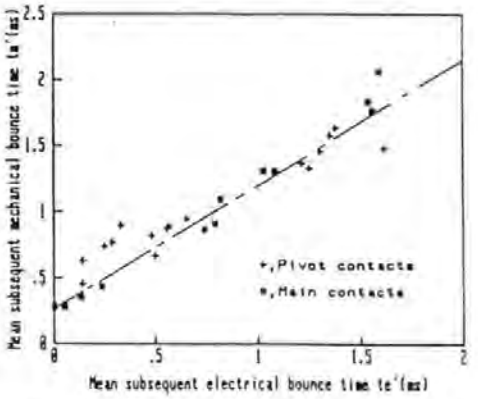

Fig.16. The relationship between the mean values of subsequent mechanical and electrical bounce times, at 12 Amps d.c. for both pivot and rivet contacts.

5.3 Application to switch contacts

With a well defined mechanical bounce, split into first and subsequent bounce times, figure 16 enables an evaluation of the expected subsequent bounce duration, under 12 Amps d.c. If this time is adapted to include the increase in first bounce an overall value for t_e is obtained.

Using the values of mean pivot bounce time identified in Table 1 with figure 16, a mean value of t_e could be obtained, and used in equation 4 to anticipate arc energy dissipation.

To compare the arc energy obtained using equation 4, to that measured in the test system, consider a 334 cycle 12 Amp test on pivot contacts. Over the test period the arc voltage was found to be constant at 15 volts, and the mean bounce duration to be 2.948 ms. Using these values in equation 4 gave, E = 155.07 J. This compares well with the computer test system value of 152.05J.

6. CONCLUSIONS

The mathematical model of the rocker switch mechanics has proved to be a useful means of identifying how a particular set of switch parameters effect the kinetic energy of the blade at impact.

The modifications made on this understanding have proved to be useful in the ultimate aim of reducing the bounce occurring at the pivot contact. Reductions of 50% in the total mechanical bounce time have been achieved.

The results presented on the fundamentals of bouncing contacts, identify the importance of bounce time in defining a separation characteristic. The arc energy equation based upon this precept has proved to be a useful and accurate means of evaluating energy dissipation in bouncing contacts.

The test apparatus developed to study the relationship between the mechanical bounce times and the electrical bounce times occurring under 12 Amp d.c. conditions, has shown that when the electrical are compared to a preceeding mechanical,

(i) the first electrical bounce is greater than the first mechanical, a typical value is K1 = 66us.

(ii) the subsequent electrical bounces are less than the subsequent mechanical, typically K' = 0.3 ms for worn contacts

(iii) the large spread in data values of K' is due to primarily the variation in the subsequent mechanical bounce time.

REFERENCES

1. D.J. Mapps, P.J. White, G. Roberts, "Pivot contact behaviour in low inertia snap-action switches" in IEEE Tran. CHMT. Vol CHMT-7, No.1, 1984 pp 125-128.

2. D.J. Mapps, J.W. McBride, P.J. White, G. Roberts, "The influence of Rocker Switch dynamics, on pivot contact erosion". (To be published).

3. A. Erk, H. Finke. "Über die Mechanischen Vorgange Wahrend des Prellens einschaltender Kontaktstucke" (The Mechanical Processes of Bouncing Contacts), Electrotech. Vol.5, 1965, pp 129-133.

4. A.Erk, H.Finke. "Über das Verhalten unterschiedlicher Kontaktwerkstoffe beim Einschalten prellender Starkstrom Schaltglieder", Electrotect. Vol.9 1965, pp 297-306. (The behaviour of different contact materials for bouncing contacts).

5. P. Barkan. "A Study of the Contact Bounce Phenomenon", IEEE Trans. Power App. Systems, Vol. PAS 86, Feb. 1976, pp 231-240.

6. B. Belhachemi, A. Carballeira, "Influence of Relay and Duration of Bounce on Erosion Weldability and resistance in relay contacts", in Proc. Holm conference on Electrical Contacts, 1984, pp475-483.

7. B. Sandler, A.A. Slonim, "Experimental Investigation of Relay Contact Dynamics", IEEE Trans. Com. Hy. and M.T., Vol. CHMT-3, No.1, March 1980, pp 150-158.

8. R. Holm, Electric Contacts, Springer-Verlag, Berlin/Heidelberg 1967, pp279-286.

9. R. Holm, Electric Contacts, Springer-Verlag, Berlin/Heidelberg, 1967, pp 320-322.

ACKNOWLEDGEMENTS

Grateful thanks are extended to Arrow Hart (Europe) Ltd., and the S.E.R.C. for financial support, and permission to publish this paper. Also to Devon County Council for use of facilities at Plymouth Polytechnic.

APPENDIX 2

The programmes for the analysis of the high-speed film data.

Programme WSX: Evaluates the X,Y,Z, data as presented in figure (4.1), from the measurement of contact gap displacements on the film. The blade angle, β , is also evaluated from this data.

Programme QAZ: Evaluates the actuator angle, α ,and the spring extension, x, as a function of time.

```
10 REM ======PROG WSX==========~======
20 REM  NOTE THIS HAS BEEN ADAPTED FOR ONLY X INPUT
30 REM
40 REM PROGRAME FOR THE NORMALISATION OFX,Y,Z,DATA & CALCULATION
50 REM OF B WHERE B NOW RELATES TO THE CHANGE IN BLADE ANGLE & ROTATION
60 PRINT"PLEASE SUPPLY THE FOLLOWING DATA"
70 PRINT"FOR THE CALCULATION OF B & X,Y,Z,FROM HYSPEED RESULTS"
80 PRINT"============================="
90 PRINT
100 PRINT"TYPE IN THE FILM & OP NUMBER"
110 INPUT Q$
120 PRINT"NUMBER OF FRAMES =?"
130 INPUT M
140 PRINT"DEFINE THE REDUCTION FACTOR FOR FILM"
150 INPUT MAG
160 PRINT"TYPE IN FILM SPEED"
170 INPUT A
180 PRINT"INPUT DISTANCE FROM PIVOT TO LEFT & RIGHT CONTACT RESPECTIVLY"
190 INPUT C,D
200 DIM F(60),G(60),H(60),I(60)
210 PRINT"TYPE IN FRAME NO & VALUES OF X,Y,Z, SEPARATED BY COMMAS"
220 FOR N=1 TO M
230 INPUT F,G,H,I
240 LET F(N)=F
250 LET G(N)=G
260 LET H(N)=H
270 LET I(N)=I
280 NEXT N
290 PRINT
300 PRINT
310 PRINT" FRAME"," X"," Y"," Z"," T"," B"
320 PRINT
330 PRINT
340 FOR N=1 TO M
350 IF G(1)>G(N) THEN GOTO 380
360 B1=G(N)/(2*C)
370 GOTO 390
380 B1=(G(1)-G(N))/(2*C)
390 B2=ATN(B1/(SQR(1-B1↑2)))
400 B3=2*B2
410 IF H(1)<H(N) THEN GOTO 440
420 B4=(H(1)-H(N))/(2*D)
430 GOTO 450
440 B4=H(N)/(2*D)
450 B5=ATN(B4/SQR(1-B4↑2))
460 B6=2*B5
470 B7=B3
480 REM   FOR X DATA ONLY
490 X=G(N)*MA
500 Y=H(N)*MAG
510 Z=I(N)*MAG
520 T=(F(N)-F(1))/A
530 T=T*1000
540 B7=B7*180/(ATN(1)*4)
550 REM   TO DETERMINE BETA
560 B7=B7-8.5
570 DEF FNZ(J)=INT((J+0.00005)*10000)/10000
580 LET X=FNZ(X)
590 LET Y=FNZ(Y)
600 LET Z=FNZ(Z)
610 LET B7=FNZ(B7)
620 LET T=FNZ(T)
630 PRINT F(N),X,Y,Z,T,B7
640 NEXT N
650 END
```

```
10 PRINT"PROGRAME FOR ANALYSING HIGH SPEED FILM DATA"
20 PRINT"============================================"
30 PRINT
40 PRINT"PROGRAME QAZ"
50 PRINT
60 PRINT
70 REM DATA IS SUPPLIED FROM THE MEASUREMENT OF 3 DIMENSIONS
80 REM THESE ARE
90 REM H,IS THE DISTANCE BETWEEN A MARK ON THE C/LINE OF THE PLUNGER & THE CENTR
E OF THE ACTUATOR
100 REM
110 PRINT
120 REM B,IS THE VERTICAL DISTANCE FROM THE BOTTOM OF THE BLADE TO THE PIVOT PIO
NT
130 REM
140 REM S,IS THE DISTANCE FROM THE PIVOT TO THE MARK ON THE PLUNGER
150 REM
160 PRINT"TYPE IN THE FILM & OP NUMBER IF>1"
170 INPUT S$
180 PRINT"NUMBER OF FRAMES M=?"
190 INPUT M
200 PRINT"DEFINE THE REDUCTION FACTOR FOR THE FILM DATA"
210 INPUT MAG
220 PRINT
230 PRINT"INPUT THE MEASURED DISTANCE BETWEEN PIVOT & CENTRE OF ACTUATOR"
240 INPUT H8
250 PRINT
260 PRINT"INPUT BLADE THICKNESS FOR THIS SWITCH"
270 INPUT K
280 PRINT
290 PRINT"INPUT PLUNGER RADIUS"
300 INPUT R1
310 PRINT
320 PRINT "MEASURED DISTANCE FROM BOTTOM OF PLUNGER TO MARK"
330 INPUT D1
340 DIM F(60),H(60),S(60),B(60)
350 PRINT"TYPE IN FRAME NUMBER & VALUES OF H,S,AND B SEPARATED BY COMMAS"
360 FOR N=1 TO M
370 INPUT F,H,S,B
380 LET H(N)=H
390 LET S(N)=S
400 LET B(N)=B
410 LET F(N)=F
420 NEXT N
430 PRINT
440 PRINT
450 PRINT"FRAME  H       S       B       BETA     BETA     ALPHA     X"
460 PRINT"NO                                       CHECK"
470 PRINT
480 FOR N1=1 TO 60
490 A1=(H(N1)↑2+H8↑2-S(N1)↑2)/(2*H8*H(N1))
500 IF A1>=1 THEN GOTO 530
510 A=ATN(SQR(1-A1↑2)/A1)
520 GOTO 540
530 LET A=0
540 B1=(B(N1)/4.69189)*MAG
550 IF B1>=1 THEN GOTO 580
560 B=ATN(B1/SQR(1-B1↑2))
570 GOTO 590
580 LET B=0
590 REM
600 REM TO DEFINE THE CENTRE OF THE PLUNGER
610 REM
620 D=(R1/MAG)-D1
630 H1=H(N1)-D
640 S1=SQR(H1↑2+H8↑2-2*H1*H8*COS(A))
650 B2=  (R1+K)/(MAG*S1)
660 IF B2>=1 THEN GOTO 690
670 B3=ATN(B2/SQR(1-B2↑2))
680 GOTO 700
690 LET B3=0
700 T1=H1*SIN(A)/S1
710 T=ATN(T1/SQR(1-T1↑2))
720 B4=T+B3-ATN(1)*2
730 X1=H1-H8+((R1+K)/MAG)
740 X=X1*MAG
750 A=A*180/(ATN(1)*4)
760 B=B*180/(ATN(1)*4)
770 B4=B4*180/(ATN(1)*4)
780 DEF FNZ(J)=INT((J+.0005)*1000)/1000
790 LET A=FNZ(A)
800 LET B=FNZ(B)
810 LET B4=FNZ(B4)
820 LET X=FNZ(X)
830 PRINT TAB(1);F(N1);TAB(8);H(N1);TAB(15);S(N1);TAB(22);B(N1);TAB(29);B;TAB(37
);B4;TAB(45);A;TAB(54);X
840 NEXT N1
850 END
```

APPENDIX 3

The software for the control of the IEEE-bus from the RML mocro-computer.

```
10 REM INIT BUS
20 PUT#7 ["INIT"]
```

This statement initilises the IEEE bus

```
30 PRINT#7 [16]. "FIRO"
```

This statement causes the command FIRO to be sent to the device at address 16. The command is device dependant.

```
40 INPUT#7 [16]. A$
```

This line causes the device 16 to input the character string A$, into the computer.

```
50 PRINT A$
```

This will print the string.

```
60 END
```

APPENDIX 4

The software for the control of the automated test system.

The additional software, subroutines 6000, and 7000, at the end of this appendix, are the adapted routines for the evaluation of bounce in a.c circuits and the control sequence for contact resistance monitoring.

```
100 REM $$$$$$$$$$$$$$$$$$$$$$$$$$$$$$$$$$$$$$$$$$$$$$
110 REM $                                     $$$$$$$$
120 REM $ TESTING OF SWITCH PERFORMANCE       $$$$$$$$
130 REM $ EVALUATION OF BOUNCE TIMES          $$$$$$$$
140 REM $        c J.W.McBRIDE                $$$$$$$$
160 REM $                                     $$$$$$$$
170 REM $$$$$$$$$$$$$$$$$$$$$$$$$$$$$$$$$$$$$$$$$$$$$$
180 REM *** CLEAR SCREEN & SET SCROLLING ***
190 PRINT "PLEASE PRESS ↑A (cntrl A)"
200 FOR I=1 TO 25:PRINT:NEXT I
210 REM %%%% INITIALIZE TL1080 %%%%
220 PUT#7["INIT"]
230 REM **** SET UP DATA VALUES ****
240 CLEAR 1000
250 GOSUB 13000
260 PUT#7[DP]
290 REM @@@@@@@@@@@@@@@@@@@@@@@@@@@@@@@@@@
300 REM @                                @
310 REM @       DISPLAY MENU             @
320 REM @                                @
330 REM @@@@@@@@@@@@@@@@@@@@@@@@@@@@@@@@@@
340 QC$="even"
350 REM ** CLEAR SCREEN **
360 PUT 31
370 RESTORE 290
380 PRINT"This program ";QC$;" gives you choice..  !"
390 PRINT:PRINT:PRINT:PRINT"I WILL ALLØW YØU TØ CHØØSE FRØM :+"
400 PRINT:PRINT"++++++++++++++++++++++++++++++++++++++++":PRINT:PRINT
410 FOR I=1 TO 7
420 READ Q$
430 IF QC$="even" AND I>5 THEN 450
440 PRINT TAB(4);I;" ] ";TAB(11);Q$;CHR$(10)
450 NEXT I
460 DATA "Run a multiple test."
470 DATA "Create and Display an arc."
480 DATA "Plot present display."
490 DATA "Re-set transient recorder."
500 DATA "Load old results from disc."
510 DATA "Re-plot distribution results."
520 DATA "Re-print results."
530 PRINT"Let me have your choice, please :";
540 Q=GET()
550 IF Q<49 OR Q>171-ASC(MID$(QC$,2,1)) THEN 540
560 PUT 31
570 REM *** DIVERT RESPONSE ***
571 QP=0 : QG=0
572 IF Q=54 THEN QG=1
574 IF Q=55 THEN QP=1
580 ON Q-48 GOSUB 1000,17000,18000,12000,19000,9000,20000
590 GOTO 230
```

```
1000 REM @@@@@@@@@@@@@@@@@@@@@@@@@@@@@@@@
1010 REM @                                  @
1020 REM @      MAIN LOOP                   @
1030 REM @                                  @
1040 REM @@@@@@@@@@@@@@@@@@@@@@@@@@@@@@@@@
1050 REM @@@@ INITIALIZE @@@@@@@@@@@@@@@@
1051 GOSUB 2000
1052 REMXXXXXXfor multi testing modeXXXXXX
1054 PRINT:PRINT"HOW MANY CYCLES":INPUT CY
1056 LET JI=1
1059 REM :loop for multi mode :SX determins odd (1),even (0)
1060 SX=JI-INT(JI/2)*2
1062 IF SX=1 THEN LET SET$="FILE6":LET XX=0:PRINT"MECH CYCLE",JI
1064 IF SX=1 THEN LPRINT"MECHANICAL CYCLE"; JI:LPRINT
1066 IF SX=0 THEN LET SET$="FILE5" :LET XX=4:PRINT"ELECT CYCLE",JI
1068 IF SX=0 THEN LPRINT"ELECTRICAL CYCLE"; JI:LPRINT
1070 OPEN#10,SET$
1072 FOR I=1 TO 8
1075 INPUT#10,A$(I)
1077 PRINT#7[CP],A$(I)
1080 NEXT I
1082 CLOSE#10
1085 LOOP=0
1087 JI=JI+1
1090 WA=0
1100 REM @@@@ WAIT FOR TRACE @@@@@@@@@@@
1110 GOSUB 4000
1112 REM @@@@@@@@FOR ADD OPS@@@@@@@@@@
1114 IF SOP=0 THEN 1120
1115 WA=WA+1
1116 IF WA=SOP THEN 1120
1117 OUT 0,XX
1119 GOTO 1100
1120 REM @@@@ COLLECT DATA @@@@@@@@@@@@@
1130 PRINT
1135 OUT 0,XX
1140 CHAN=1
1150 GOSUB 5000
1160 CHAN=2
1170 GOSUB 5000
1180 PRINT
1190 LOOP=LOOP+1
1200 REM *** RANDOM DELAY TO ENFORCE RANDOM OPENING ***
1210 FOR I=1 TO RND(0)*1000:NEXT I
1220 IF LOOP>=OPRNS GOTO 1330
1270 PRINT : PRINT"meanwhile, I am ";
1280 REM @@@@ PROCESS DATA @@@@@@@@@@@@@
1290 GOSUB 7000
1300 REM @@@@ PRINT/STORE DATA @@@@
1304 GOSUB 8000
1306 GOTO 1090
1330 REM @@@@ PROCESS FINAL TRACE @@@@@@
1340 PRINT
1350 GOSUB 7000
1440 REM @@@@ PRINT & SAVE DATA @@@@@@@@@
1450 GOSUB 8000
1460 REM *** COMPLETE PRINTING ***
1470 GOSUB 9000
1472 IF JI=CY+1 GOTO 1480
1475 GOTO 1060
1480 PRINT:PRINT "Thump any key to return to my MENU.":O$=GET$()
1490 QC$="still"
1900 RETURN
1999 REM
```

```
2010 REM @                                    @
2020 REM @     INITIALIZATION                 @
2030 REM @                                    @
2040 REM @@@@@@@@@@@@@@@@@@@@@@@@@@@@@@@@@@@@
2050 LOOP=0
2060 REM *** CLEAR SCREEN ***
2065 PRINT"IS THE SUPPLY A.C OR D.C
2066 PRINT"D.C=1"
2067 PRINT"A.C=2"
2068 INPUT ADC
2070 PUT 31
2075 PRINT"If you require a density analysis of bounce times you are limited to
150 tests"
2080 PRINT:PRINT:PRINT:INPUT"How many tests do you require :";OPRNS
2082 ON ERROR GOTO 19810
2084 PRINT:PRINT:INPUT"Do you require a density analysis of bounce times";WE$
2086 IF WE$="N" THEN 2089
2087 DIM JOULES(2,OPRNS)
2089 ON ERROR
2090 PRINT:PRINT:INPUT "What is the title of this set of tests ";TITLE$
2100 PRINT
2110 REM &&&& LOAD AND OUTPUT REQUIRED TL1000 SETTINGS &&&&
2120 GOSUB 12000
2130 QP=0
2140 REM XXXX PRINTER XXXX
2150 PRINT : PRINT "IS PRINTER CONNECTED ? ";:Q$=GET$():PRINT Q$;
2160 IF Q$=CHR$(13) OR Q$="N" THEN GOTO 2290
2170 PRINT "ES"
2180 PRINT : PRINT "WHICH PRINTER IS IT":PRINT "     1 -KODE":PRINT "     2 -PE
RANTI     ";:QP=VAL(GET$()):PRINT QP
2190 IF QP=1 OR QP=2 THEN GOTO 2220
2200 PRINT "INVALID ENTRY: re-enter ";QP=VAL(GET$())
2210 GOTO 2190
2220 PRINTER 4,5*QP-4
2230 REM XXXX PRINT HEADINGS XXXX
2240 LPRINT:LPRINT:LPRINT
2250 LPRINT TITLE$
2252 IF ADC=2 GOTO 2260
2253 LPRINT"=============================================================="
PRINT:LPRINT
2254 LPRINT"ALL TIMES IN MILLISECS":LPRINT
2255 LPRINT"NO";TAB(3);"ENERGY","IM1","IM2","IM3","DUR","TIM";TAB(80);"Z"
2257 LPRINT SPC(7),"B1","B2","B3","TBT","VMIN"
2259 GOTO 2290
2260 LPRINT "=========================================":LPRINT:LPRINT
2270 LPRINT "Test No.","ARC ENERGY(J)","ARC LENGTH (MS)"
2280 LPRINT "=========================================":LPRINT
2290 REM ** Entry pt for no printer **
2300 PUT 31
2310 PRINT:PRINT" IS THE PLOTTER CONNECTED ? ";:Q$=GET$():PRINT Q$;
2320 IF Q$=CHR$(13) OR Q$="N" THEN 2350
2330 PRINT"ES":PRINT "Don't forget to put some paper in !"
2340 QG=1
2350 PRINT:PRINT:PRINT:PRINT"Would you like the data saving onto disk ? ";:Q$=
T$():PRINT Q$;
2360 DF$=""
2370 IF Q$=CHR$(13) OR Q$="N" THEN 2450
2380 PRINT "ES"
2390 PRINT:PRINT"What would you like the file to be":INPUT"called";DF$
2400 REM *** CREATE & START DATA FILE ***
2410 CREATE#10,DF$
2420 OPEN#10,DF$
2430 PRINT#10,TITLE$
2440 PRINT#10,OPRNS
2445 LET SOP=0
2450 PRINT:PRINT:PRINT"Would you like additional switch":PRINT"operations betw
n those monitored ? ";:Q$=GET$():PRINT Q$;
2460 IF Q$=CHR$(13) OR Q$="N" THEN GOTO 2480
2470 PRINT "ES":PRINT:INPUT"How many";SOP
2480 PUT 12
2490 REM 8888 INCREASE S/M WAIT TO 55 sec 8888
2500 POKE DLY,255
2510 POKE DLY+2,215
2520 PRINT"I AM NOW STARTING THE TEST."
2530 PRINT:PRINT"You may stop me by pressing 'S' at any":PRINT"time during the
est."
2540 REM:INIT OUT PORTS ETC
2550 OUT 2,0 :OUT 2,63:OUT 2,7
2580 OUT 0,0
```

```
3000 REM @@@@@@@@@@@@@@@@@@@@@@@@@@@@@@@@
3010 REM @                                  @
3020 REM @     ARM FOR A TRACE              @
3030 REM @                                  @
3040 REM @@@@@@@@@@@@@@@@@@@@@@@@@@@@@@@@
3050 REM XXXX PREPARE FOR A TRACE XXXX
3060 REM *** ARM TL1080 ***
3070 PRINT#7[CP],"AR"
3100 PRINT : PRINT : PRINT "BEGINNING TEST No";LOOP+1
3900 RETURN
3999 REM
4000 REM @@@@@@@@@@@@@@@@@@@@@@@@@@@@@@@@@
4010 REM @                                  @
4020 REM @     WAIT FOR TRACE               @
4030 REM @                                  @
4040 REM @@@@@@@@@@@@@@@@@@@@@@@@@@@@@@@@@
4050 REM:INIT SYS
4055 FOR Z=1 TO 100:X=SIN(1):NEXT Z
4057 REM INIT SOL
4060 OUT 0,XX+2
4065 FOR Z=1 TO 200:X=SIN(1):NEXT Z
4070 REM: POWER ON
4075 OUT 0,XX+3
4080 FOR Z=1 TO 100:X=SIN(1):NEXT Z
4085 REM ARM REC
4090 GOSUB 3000
4095 FOR Z=1 TO 100:X=SIN(1):NEXT Z
4100 REM REL SOL
4105 OUT 0,XX+1
4120 REM *** CHECK SWITCH STATUS ***
4130 I=0
4140 IF (128 AND INP(0))=128 GOTO 4160 ELSE GOTO 4190
4150 REM *** SET FLAG I FOR DELAY ***
4160 IF I=0 THEN PRINT CHR$(13);"WAITING FOR SWITCH TO OPEN..";
4170 I=1
4180 GOTO 4140
4190 PRINT"OK."
4200 REM *** DELAY FOR RECORDING -IF SWITCH JUST OPENED ***
4210 IF I=0 GOTO 4900
4220 FOR I=1 TO 500:NEXTI
4900 RETURN
4999 REM
5000 REM @@@@@@@@@@@@@@@@@@@@@@@@@@@@@@@@
5010 REM @                                  @
5020 REM @     COLLECT CHANNEL DATA         @
5030 REM @                                  @
5040 REM @@@@@@@@@@@@@@@@@@@@@@@@@@@@@@@@
5050 REM *** CHANNEL NUMBER 'CHAN' ***
5060 PRINT #7[CP],"IS";CHAN-1;" FIØ "
5070 PRINT ">>> CH";CHAN;">>> COLLECTING.";
5080 FOR K=0 TO 15
5090 REM *** CHECK 'STOP' I/P ***
5100 IF GET$(1)="S" THEN GOSUB 15000
5110 FOR J=1 TO 4096/(4*16) : REM =64
5120 D(CHAN,64*K+J)=GET(#7[DP])
5130 REM *** DISCARD 3 BYTES ***
5140 I=GET(#7[DP]):I=GET(#7[DP]):I=GET(#7[DP])
5150 NEXT J
5160 PRINT "<";
5170 NEXT K
5180 REM *** GET FINAL BLANK BYTE ***
5190 I=GET(#7[DP])
5200 REM *** RETURN FROM READOUT MODE ***
5210 PUT#7[CP]
5900 RETURN
5999 REM
```

```
7020 REM @          PROCESS DATA          @
7030 REM @                                @
7040 REM @@@@@@@@@@@@@@@@@@@@@@@@@@@@@@@@
7050 PRINT "PROCESSING TEST No.";LOOP
7060 ENERGY=0
7070 REM *** DERIVE RAW OFFSETS OA,OB FROM A$ -Each to centre zero.
7080 OA=-VAL(MID$(A$(2),61,3))-128
7090 OB=-VAL(MID$(A$(3),5,3))-128
7100 REM *** DERIVE SCALE & PRD FROM A$ ***
7110 REM Scale A=VOLTS(VAL(MID$(A$(2),46,2))+1)/(255*RATIO) Volts/Unit: switch v
olts.
7120 REM Scale B=-VOLTS(VAL(MID$(A$(2),54,2))+1)/(255*RI) Amps/Unit:  -ve due to
 earth.
7130 REM SCALE = Scale A * Scale B / = VA/Unit^2
7140 SCALE=-VOLTS(VAL(MID$(A$(2),46,2))+1)*VOLTS(VAL(MID$(A$(2),54,2))+1)/(255^2
*RATIO*RI)
7150 REM PRD = PERIOD/SAMPLE (seconds)
7160 REM MA = MULTIPLIER, SA=VALUE
7170 MA=VAL(MID$(A$(3),39,1))
7180 SA=VAL(MID$(A$(3),44,4))
7190 PRD=SA*10^(2*MA-9)*(SA<>0)*(MA<>0)+4096*10^(2*MA-9)*(SA=0)*(MA<>0)-5E-8*(MA
=0)
7200 S=SCALE*PRD*4*10:REM *10 FOR PROBE(V)  : REM 1000 of 4000 used.
7202 IF ADC=1 GOTO 7590
7210 REM XXXX CALCULATE CUMULATIVE ARC ENERGY ***
7220 REM ** Find where voltage deviates from zero -beginning of arc. **
7230 FOR I=1 TO 1024
7240 IF D(1,I)>138 OR D(1,I)<118 THEN  GOTO 7270
7250 NEXTI
7260 PRINT "ERROR DUE TO LINE 7260 :ZERO VOLTAGE TRACE":OPRNS=LOOP:GOTO 1440
7270 REM ** Calculate energy until current falls to zero -end of arc. **
7280 FOR J=I TO 1024
7290 IF D(2,J+20)<138 AND D(2,J+20)>118 THEN GOTO 7340
7300 ENERGY=ENERGY+(D(1,J)+OA)*(D(2,J)+OB)*S
7310 NEXT J
7320 PRINT:PRINT"WATCH OUT! Your arc continues beyond":PRINT"the recording perio
d."
7330 GOTO 7550
7340 IF J>I THEN GOTO 7480
7350 REM ** Arc < 20 samples **
7360 REM ** Find end of arc **
7370 FOR K=J+19 TO J STEP -1
7380 IF D(2,K)>138 OR D(2,K)<118 THEN GOTO 7440
7390 NEXT K
7400 REM ** No Energy **
7410 PRINT:PRINT "No arc detected."
7420 GOTO 7530
7430 REM ** Calculate energy for K sample arc **
7440 FOR L=J TO K
7450 ENERGY=ENERGY+(D(1,L)+OA)*(D(2,L)+OB)*S
7460 NEXT L
7470 GOTO 7520
7480 FOR K=J TO J+20
7490 ENERGY=ENERGY+(D(1,K)+OA)*(D(2,K)+OB)*S
7500 NEXT K
7510 K=K-2
7520 PRINT:PRINT "Switch arced from";I;"to";K+1;"samples"
7530 JOULES(1,LOOP)=FNA(ENERGY)
7540 JOULES(2,LOOP)=FNA((K-I+1)*PRD*1000*4)
7550 REM XXXX STORE & PRINT RESULT XXXX
7560 PRINT:PRINT"ENERGY =";JOULES(1,LOOP);"JOULES IN":JOULES(2,LOOP);"ms."
7570 PRINT"!!!!!!!!!!!!!!!!!!!!!!!!!!!!!!!!!!!!!!!!!!!!!!!!!!!!!!!!!!!!!!!!"
7580 SJLS=ENERGY+SJLS
7585 RETURN
7590 REM*************D.C************
7600 REM::EVALUATION OF BOUNCE TIMES AT MAKE WITH D.C
7610 REM:SET TIME(array) TO ZERO
7615 FOR I=1 TO 30 :T(I)=0:NEXT I
7620 A=1
7630 REM::locate impact of contacts
7640 FOR I=1 TO 1024
7650 IF D(1,I)<153 AND D(1,I)>103 THEN GOTO 7680
7660 NEXT I
7670 PRINT"ERROR DUE TO LINE 7670 :SWITCH NOT CLOSED":OPRNS=LOOP:GOTO 1440
7680 T(A)=I*PRD*1000*4
7690 Z=0
7700 REM::locate beginning of bounce
7710 FOR I=I TO 1024
7720 IF D(1,I)>153 OR D(1,I)<103 THEN GOTO 7760
7730 NEXT I
7740 REM::evaluation of bounce
7750 GOTO 7980
7760 A=A+1
7770 T(A)=I*PRD*1000*4
7780 REM::energy sumation until end of bounce
7790 FOR I=I TO 1024
7800 ENERGY=ENERGY+(D(1,I)+OA)*(D(2,I)+OB)*S
7805 REM::locate end of bounce
7810 IF D(1,I)<153 AND D(1,I)>103 THEN GOTO 7840
7820 NEXT I
7830 PRINT"SWITCH IS STILL BOUNCING":OPRNS=LOOP:GOTO 1440
7840 Z=Z+1
7850 A=A+1
7860 T(A)=I*PRD*1000*4
7870 GOTO 7700
7880 REM::bounce times
7895 G=0
7900 FOR E=1 TO Z
7910 F=2*E
7920 P(E)=T(F+1)-T(F)
7924 G=P(E)+G
7926 NEXT E
7927 VM=0
7928 REM*******for the evaluation*****
7929 REM*******of Vmin*****************
7930 IF XX=0 THEN 7940
7932 LET VS=52.35:LET IS=5.235
7934 V1=4*VS*ENERGY*1000/(G*IS)
7935 V2=VS^2-V1
7936 IF V2<0 THEN 7940
7937 VM=(VS-V2^0.5)/2
7938 VM=FNA(VM)
7940 ENERGY=FNA(ENERGY)
7941 SJLS=ENERGY+SJLS
7942 IF WE$="N" THEN 7944
7943 JOULES(2,LOOP)=FNA(G)
7944 REM::duration from beginning of bounce
7946 DUR=T(A)-T(2)
7948 IM=T(A)-T(1)-G
7950 PRINT"ENERGY=";ENERGY;"JOULES"
7952 PRINT"TOTAL BOUNCE TIME=";G;"ms"
7954 PRINT"BOUNCE DURATION=";DUR;"ms"
7956 PRINT"IMPACT TIME=";IM;"ms"
7957 PRINT"NO OF BOUNCES=";Z
7960 DUR=FNA(DUR):IM=FNA(IM):G=FNA(G)
7962 I1=FNA(T(2)-T(1)):B1=FNA(T(3)-T(2))
7964 I2=FNA(T(4)-T(3)):B2=FNA(T(5)-T(4))
7966 I3=FNA(T(6)-T(5)):B3=FNA(T(7)-T(6))
7970 PRINT"IM1=";I1:PRINT"B1=";B1
7972 PRINT"IM2=";I2:PRINT"B2=";B2
7974 PRINT"IM3=";I3:PRINT"B3=";B3
7990 PRINT"Vmin=";VM;"volts"
7995 RETURN
7999 REM
```

```
8000 REM @@@@@@@@@@@@@@@@@@@@@@@@@@@@@@@@
8010 REM @                                  @
8020 REM @     PRINT & SAVE RESULTS         @
8030 REM @                                  @
8040 REM @@@@@@@@@@@@@@@@@@@@@@@@@@@@@@@@
8050 REM **** PRINT DATA ****
8060 IF QP=0 THEN 8100
8065 IF ADC=1 GOTO 8095
8070 FOR I=INT((LOOP-1)/10)*10+1 TO LOOP
8080 LPRINT I,JOULES(1,I),JOULES(2,I)
8090 NEXT I
8091 GOTO 8100
8095 LPRINT LOOP;TAB(5);ENERGY,I1,I2,I3,DUR,IM;TAB(80);Z
8096 LPRINT SPC(14);B1,B2,B3,G,VM
8097 LPRINT
8100 REM **** SAVE DATA ****
8110 IF DF$="" THEN 8900
8120 FOR I=INT((LOOP-1)/10)*10+1 TO LOOP
8130 PRINT#10,JOULES(1,I)
8135 PRINT#10,JOULES(2,I)
8140 NEXT I
8900 RETURN
8999 REM
9000 REM @@@@@@@@@@@@@@@@@@@@@@@@@@@@@@@@
9010 REM @                                  @
9020 REM @  PLOT,PRINT & SAVE RESULTS       @
9030 REM @                                  @
9040 REM @@@@@@@@@@@@@@@@@@@@@@@@@@@@@@@@
9050 IF OPRNS>10 THEN PRINT"I am now summing the density array."
9060 REM *** SUM DENSITY ARRAY X(INC) ***
9070 FOR I=1 TO INC : X(I)=0 : NEXT I
9080 K=0
9090 FOR I=0 TO 10-10/INC STEP 10/INC
9100 K=K+1
9110 FOR J=1 TO OPRNS
9120 IF JOULES(2,J)>=I AND JOULES(2,J)<I+10/INC THEN X(K)=X(K)+1
9130 NEXT J,I
9200 LPRINT : LPRINT "SUM OF ENERGY =";SJLS;"JOULES"
9210 REM @@@@ PLOT RESULTS @@@@
9220 IF QG=1 THEN GOSUB 10000
9310 REM **** CLOSE DATA FILE ****
9320 CLOSE#10
9900 RETURN
9999 REM
```

```
12000 REM $$$$$$$$$$$$$$$$$$$$$$$$$$$$$$$$
12010 REM $                                  $
12020 REM $     SET TL1080                   $
12030 REM $                                  $
12040 REM $$$$$$$$$$$$$$$$$$$$$$$$$$$$$$$$$$
12050 PRINT:PRINT "WOULD YOU LIKE STORED OR NEW":PRINT"TL1080 SETTINGS ? "::Q$=G
ET$()
12060 IF Q$="S" THEN GOTO 12300
12070 REM *** NEW SETTINGS ***
12080 PRINT "NEW"
12090 REM $$$ SET TR TO OPTIMUM LEVEL $$$
12110 PUT#7["LOCAL"]
12120 PRINT:PRINT "SET TL1080 TO NEW REQUIREMENTS, and then":INPUT "TYPE IN NEW
FILE NAME:-";SET$
12130 REM *** LOAD & STORE NEW SETTINGS FROM TL1080 ***
12140 PUT#7["INIT"]
12150 FOR I=1 TO 200
12160 NEXT I
12170 PRINT#7[CP],"FI5"
12180 FOR I=1 TO 8
12190 INPUT#7[DP],A$(I)
12200 NEXT I
12210 PRINT#7[CP],"FI1"
12220 PUT#7[CP]
12230 IF SET$="" THEN GOTO 12390
12240 CREATE#10,SET$
12250 OPEN#10,SET$
12260 FOR I=1 TO 8
12270 PRINT#10,A$(I)
12280 NEXT I
12290 GOTO 12390
12300 REM *** OLD SETTINGS FILE ***
12310 PRINT "STORED"
12320 ?:INPUT "OLD FILE NAME:-";SET$
12330 REM *** LOAD & O/P STORED SETTINGS ***
12340 OPEN#10,SET$
12350 FOR I=1 TO 8
12360 INPUT#10,A$(I)
12370 PRINT#7[CP],A$(I)
12380 NEXT I
12390 CLOSE#10
12900 RETURN
12999 REM
13000 REM $$$$$$$$$$$$$$$$$$$$$$$$$$$$$$
13010 REM $                              $
13020 REM $   SET UP ALL DATA VALUES     $
13030 REM $                              $
13040 REM $$$$$$$$$$$$$$$$$$$$$$$$$$$$$$
13050 PRINT "I am setting up data arrays."
13060 REM ***  VARIABLES USED :-  ***
13070 REM A$(8);ASub;DSub;CHan;CP;DF$;DLy;DP;D(2,1024);ENergy;I;INc;J;JOules;K;L
;LOop;MA;MX,
13080 REM OA;OB;OFf;OPrns;PC;PD;PRd;QC$;QG;QP;Q$;RAtio;RI;S;SA;SCale;SEt$;SJls;S
Op;TItle$;VOlts,
13090 REM *** ALL VARIABLES SET TO ZERO ON 'RUN' ***
13100 REM +++++ SET VARIABLES +++++
13110 DSUB=&414D:ASUB=&40A8:REM M/C SUBROUTINES
13120 DLY=&4144 : REM Sw open delay addr.
13130 CP=4:DP=11:REM TL1080 CONTROL & DATA PORTS
13140 PC=2:PD=0: REM PIO control & data ports
13150 REM ** Round off to 3 DP fn **
13160 DEF FNA(X)=INT(X*1000+0.5)/1000
13170 LOOP=0 : SJLS=0
13180 RI=0.1 : REM 'Look in' Resisitor
13190 RATIO=7.42760 : REM Voltage divider network.
13200 INC=40 : REM No. of sample intervals for profile X(INC).
13210 DIMD(2,1024),A$(8),VOLTS(57),TITLE$(40),X(INC),Q$(100)
13211 DIM T(30),P(15)
13215 RESTORE 13230
13220 FOR I=1 TO 57 : READ VOLTS(I) : NEXTI
13230 DATA 0.1,0.1067,0.1143,0.1231,0.1333,0.1455,0.16,0.1778,0.2,0.2162,0.2353,
0.2581,0.2857,0.32,0.3636,0.4211,0.5,0.5333,0.57
13240 DATA 0.6153,0.6667,0.7273,0.8,0.8889,1,1.067,1.143,1.231,1.333,1.455,1.6,1
.778,2,2.162,2.353,2.581,2.857,3.2
13250 DATA 3.636,4.211,5,5.333,5.714,6.153,6.667,7.273,8,8.889,10,10.67,11.43,12
.31,13.33,14.55,16,17.78,20
13260 PRINTER 4,1
13900 RETURN
```

```
6000 REM
6030 REM
6040 REM
6050 OPEN£10,"FILE1"
6060 FOR I=1 TO 8
6070 INPUT£10,A$(I)
6080 PRINT£7[CP],A$(I)
6090 NEXT I
6100 CLOSE£10
6130 REM MEASURE RESISTANCE DATA
6150 FOR I=1 TO 1000:NEXT I
6160 REM SWITCH TO D C &PROBE
6170 OUT 0,8
6175 PRINT£7[CP],"AR"
6180 FOR I=1 TO 1000:NEXT I
6190 OUT 0,13
6200 FOR I=1 TO 500: NEXT I
6300 OUT 0,8
6310 OUT 0,0
6320 REM COLLECT CHAN 2
6330 CHAN=2
6340 GOSUB 5000
6350 REM PROCESS
6370 SCALE=VOLTS(VAL(MID$(A$(2),54,2))+1)/255
6410 BN=0
6420 FOR I=512 TO 1024
6430 BN=D(2,I)+0A+BN
6440 NEXT I
6450 BN=BN/512
6460 BN=BN*SC
6470 PRINT SC;BN
6480 LPRINT "CONTACT VOLT DROP AT 12.25A=";BN;"VOLTS"
6500 LPRINT
6999 RETURN
```

```
7000 REM @@@@@@@@@@@@@@@@@@@@@@@@@@@@@@@@
7010 REM @                               @
7020 REM @         PROCESS DATA          @
7030 REM @                               @
7040 REM @@@@@@@@@@@@@@@@@@@@@@@@@@@@@@@@
7050 PRINT "PROCESSING TEST No.";LOOP
7060 ENERGY=0
7070 REM *** DERIVE RAW OFFSETS DA.DB FROM A$ -Each to centre zero.
7080 DA=-VAL(MID$(A$(2),61,3))-128
7090 DB=-VAL(MID$(A$(3),5,3))-128
7100 REM *** DERIVE SCALE & PRD FROM A$ ***
7110 REM Scale A=VOLTS(VAL(MID$(A$(2),46,2))+1)/(255*RATIO) Volts/Unit: switch v
olts.
7120 REM Scale B=-VOLTS(VAL(MID$(A$(2),54,2))+1)/(255*RI) Amps/Unit:  -ve due to
 earth.
7130 REM SCALE = Scale A * Scale B / = VA/Unit↑2
7140 SCALE=-VOLTS(VAL(MID$(A$(2),46,2))+1)*VOLTS(VAL(MID$(A$(2),54,2))+1)/(255↑2
*RATIO*RI)
7150 REM PRD = PERIOD/SAMPLE (seconds)
7160 REM MA = MULTIPLIER, SA=VALUE
7170 MA=VAL(MID$(A$(3),39,1))
7180 SA=VAL(MID$(A$(3),44,4))
7190 PRD=SA*10↑(2*MA-9)*(SA<>0)*(MA<>0)+4096*10↑(2*MA-9)*(SA=0)*(MA<>0)-5E-8*(MA
=0)
7200 S=SCALE*PRD*4*10:REM *10 FOR PROBE(V)   : REM 1000 of 4000 used.
7590 REM**************D.C************
7600 REM::EVALUATION OF BOUNCE TIMES AT MAKE WITH D.C
7610 REM:SET TIME(array) TO ZERO
7615 FOR I=1 TO 30 :T(I)=0:NEXT I
7620 A=1:TA(1)=0
7630 REM::locate impact of contacts
7640 FOR I=1 TO 1024
7645 REM #######START OF CURRENT########
7650 IF D(2.I)>134 OR D(2,I)<122 THEN GOTO 7680
7660 NEXT I
7670 PRINT"ERROR DUE TO LINE 7670 :SWITCH NOT CLOSED":OPRNS=LOOP:GOTO 1440
7680 T(A)=I*PRD*1000*4
7690 Z=0
7695 I=I+30:REM to clear initial trasient voltage
7700 REM::locate begining of bounce
7710 FOR I=I TO 1024
7720 IF D(1,I)>153 OR D(1,I)<103 THEN GOTO 7760
7730 NEXT I
7740 REM::evaluation of bounce
7750 GOTO 7875
7760 A=A+1
7770 T(A)=I*PRD*1000*4
7780 REM::energy sumation until end of bounce
7785 GW=0:GX=1:K1=0:K3=0:K4=0
7786 REM locate the end of bounce/arc
7790 FOR I=I TO 1024
7792 ENERGY=ENERGY+(D(1,I)+DA)*(D(2,I)+DB)*S
7794 IF K1=0 THEN 7806
7795 K2=0
7797 IF D(1,I)<153 AND D(1,I)>103 THEN K2=1
7799 K3=K3+K2
7800 K4=K4+1
7802 IF K4<10 THEN 7820
7803 IF K4=K3 THEN I=I-10:GOTO 7845 :REM contacts closed
7804 K4=0:K3=0 :REM reset
7805 GOTO 7820
7806 IF GX=1 THEN 7810
7807 IF D(2,I)<134 AND D(2,I)>122 THEN 7861
7808 IF GW=1 THEN 7820
7810 IF D(1,I)<153 AND D(1,I)>103 THEN GOTO 7835
7820 NEXT I
7830 PRINT"SWITCH IS STILL BOUNCING":OPRNS=LOOP:GOTO 1440
7835 REM CHECK FOR ARC EXTINCTION
7837 IF D(2,I+5)>134 OR D(2,I+5)<122 THEN 7845
7840 GW=1:GX=0
7841 I=I+1
7842 GOTO 7790
7845 REM END OF BOUNCE
7846 Z=Z+1
7848 A=A+1
7850 T(A)=I*PRD*1000*4
7855 GOTO 7700
7861 REM END OF THE ARC BUT STILL BOUNCEING
7862 N=1
7864 TA(N)=I*PRD*1000*4
7865 N=N+1
7866 GW=0:GX=1:K1=1
7869 GOTO 7790
7870 REM ###########################
7875 FOR I=1 TO A :PRINT T(I):NEXT I
7876 PRINT "*"
7877 FOR I=1 TO N :PRINT TA(I):NEXT 1
7880 REM::bounce times
7895 G=0
7900 FOR E=1 TO Z
7910 F=2*E
7920 P(E)=T(F+1)-T(F)
7924 G=P(E)+G
7926 NEXT E
7940 ENERGY=FNA(ENERGY)
7941 SJLS=ENERGY+SJLS
7942 IF WE$="N" THEN 7944
7943 JOULES(2.LOOP)=FNA(G)
7944 REM::duration from begining of bounce
7946 DUR=T(A)-T(2)
7948 IM=T(A)-T(1)-G
7950 PRINT"ENERGY=";ENERGY;"JOULES"
7952 PRINT"TOTAL BOUNCE TIME=";G;"ms"
7954 PRINT"BOUNCE DURATION=";DUR;"ms"
7956 PRINT"IMPACT TIME=";IM;"ms"
7957 PRINT"NO OF BOUNCES=",Z
7960 DUR=FNA(DUR):IM=FNA(IM):G=FNA(G)
7962 I1=FNA(T(2)-T(1)):B1=FNA(T(3)-T(2))
7964 I2=FNA(T(4)-T(3)):B2=FNA(T(5)-T(4))
7966 I3=FNA(T(6)-T(5)):B3=FNA(T(7)-T(6))
7970 PRINT"IM1=";I1:PRINT"B1=";B1
7972 PRINT"IM2=";I2:PRINT"B2=";B2
7974 PRINT"IM3=";I3:PRINT"D3=";D3
7980 REM ##########################
7981 REM evaluation of arc extinction
7982 IF TA(1)=0 THEN 7995
7985 FOR I=1 TO A
7986 IF TA(1)<T(I) THEN 7991
7989 NEXT I
7991 JK=T(I)-TA(1)
7993 TH=(I-1)/2
7994 PRINT "ARC EXT ";JK;"MS,BEFORE BOUNCE"; TH
7995 RETURN
7999 REM
```

APPENDIX 5

The computer software modelling the rocker switch dynamics. The programme presented is called DYNAMICS.

The following list defines the variables used in the programme and thesis text.

DYNAMICS	THESIS
H	h
BLADE	b
R1	r
K	K
L	l
E	e
BMAX	BMAX
IP	I
RI	I
IB	I
MU1	μ_1
MU2	μ_2
PE	p
Y(1) = ALPHA	α
Y(2)	x
Y(3) =	$\dot{\alpha}$
Y(4) =	$\dot{x}$
B =	β
B1 =	$\dot{\beta}$
S =	s

Measurement of values

The major switch dimensions were measured from the film data, and compared to the manufactures raw dimensions. The moments of inertia were measured experimentally using the compound pendulum method. The coefficients of friction were estimated, with reference to; "Lubrication: A practical guide, by A.R Lonsdown"; where it has been stated that, "Nylons form smooth transfer films on metal countersurfaces, and when used unlubricated their friction is fairly low, typically 0.1, 0.2 at low speeds depending on load and temperature". In this case the switch is normally lubricated.

In the case of verification 1, in the programme VERT, the following dimensions were used.

IP = 0.452D-06	RI = 0.41D-06	IB = 0.41D-07
MU1= 0.1D+0	MU2= 0.1D+0	
K = 0.16D+04	BLADE=0.81D-03	H = 0.1468D-01
L = 0.87D-02	E = 0.607D-02	PE = 0.396D-02

In the case of verification 2, the following changes were made to the dimensions.

K = 0.13D+04	H = 0.1435D-01	E = 0.576D-02

```
C PROGRAME DYNAMICS
C ==================
C  FOR THE ANALYSIS OF THE ROCKER SWITCH DYNAMICS USING NAG ROUTINE
      DOUBLE PRECISION Y(4),W(4,7),F(4)
      DOUBLE PRECISION TOL, X, XEND, B, B1, S, DIF, KE, M, R2, M1, M2, L1, L2
      REAL*8 LAB, ALPHA
      INTEGER I, IFAIL, J, N, NOUT, A, X2, IDINT
      INTEGER IR, S5, S6
      DOUBLE PRECISION Z, DCOS, DASIN, DSIN, DSQRT, G, GE, T, BMAX, G1
      DOUBLE PRECISION H, BLADE, R1, K, L, E, MU1, MU2, IP, IB, RI, MASS, PE, X1
      EXTERNAL FCN, OUT
      COMMON /DAT/H, BLADE, R1, K, L, E, MU1, MU2, MASS, IP, RI, IB, PE, X1, M, R2
      COMMON /WHY/B, B1, S, DIF, KE, S5, S6
      COMMON /UHU/XEND, Z, I
      COMMON /ZEN/BMAX
      COMMON /LAB/ LAB
C -----------------------------------------------------------------------
      CALL MKLB$F ($20, LAB)
C THE FOLLOWING ARE SWITCH CONSTANTS
      H=14.35D-3
      BLADE=.81D-3
      R1=1.82D-3
      K=1.308D3
      L=8.73D-3
      E=H-BLADE-7.78D-3
      BMAX=0.22D0
      MU1=.1D0
      MU2=.10D0
      IP=4.52D-2
      R2=9.4D-3
      IB=41.0D-9
C AFTER DEF OF IB THE CALCULATION OF MASS DISTRIBUTION TO MATCH IB
      M1=.61D-3
      L2=22.44D-9
      M2=(IB-L2)/(2.D0*R2**2)
      M=M1+2.D0*M2
      RI=IP
      MASS=.2196D-3
      PE=3.96D-3
      X1=4.D-3
      WRITE (NOUT,99995) IP,RI,IB
      WRITE (NOUT,*)
      WRITE (NOUT,99994) MU1,MU2,R2
      WRITE (NOUT,*)
      WRITE (NOUT,99993) M1,M2,M
      WRITE (NOUT,*)
      WRITE (NOUT,99992) K,BLADE,H
      WRITE (NOUT,*)
      WRITE (NOUT,99991) L,E,PE
      WRITE (NOUT,*)
      WRITE (NOUT,99996)
      DATA NOUT/6/
      N=4
      IR=0
      J=4
      X=0.D0
      XEND=X1
C INITIAL B,C'S FOR EQ'N SET
```

```
 C       Y(1)=ALPHA
 C       Y(2)=SPRING EXTENSION (X)
 C       Y(3)=ANGULAR VELOCITY OF ACTUATOR
 C       Y(4)=SPRING EXTENSION VELOCITY
 C       B=BLADE ANGLE FROM HORIZONTAL DATUM
 C       B1=BLADE ANGULAR VELOCITY
 C       S=DISTANCE OF SLIDING BETWEEN ACTUATOR & BLADE
 C DIF=ANGLE WHITCH IF -VE INDICATES -VE S
       B=-1.83D-2
       Y(1)=0.D0
       S5=0
       Y(2)=-(R1+BLADE)*((1.D0/DCOS(B))-1.D0)
       Y(3)=35.76D0
       GE=H+Y(2)-R1-BLADE
       Q=DSQRT(GE**2+R1**2+2.D0*GE*R1*DCOS(-B))
       Q1=DASIN(R1*DSIN(-B)/Q)
       Y(4)=-Y(3)*Q*DSIN((-B)-Q1)/DCOS(-B)
       B1=0.D0
       KE=0.D0
 C NAG DETAILS---------------------------------------------
        IFAIL=0
        Z=(XEND-X)/40.D0
        I=39
         TOL=10.D0**(-J)
           WRITE (NOUT,99999) TOL
              CALL D02BBF(X,XEND,N,Y,TOL,IR,FCN,OUT,W,IFAIL)
20            PRINT*,'NON LOCAL RETURN'
              WRITE (NOUT,99998) IFAIL
               IF (TOL.LT.0.D0) WRITE (NOUT,99997)
30              CONTINUE
      STOP
C FORMAT STATEMENTS---------------------------------------
99999 FORMAT (23HOCALCULATION WITH TOL= ,D8.1)
99998 FORMAT (8H  IFAIL=,I1)
99997 FORMAT (10HTOL IS NEG)
99996 FORMAT (T7,'T',T19,'ALPHA',T33,'BETA',T47,'X',T62,'ALPHA! ',T75,
     1'BETA',T90,'X! ',T103,'S',T117,'KE(2)',T125,'DIF')
99995 FORMAT (T5,'IP=',D11.5,3X,'RI=',D11.5,5X,'IB=',D11.5)
99994 FORMAT (T5,'MU1=',D11.5,2X,'MU2=',D11.5,4X,'R2=',D11.5)
99993 FORMAT (T5,'M1=',D11.5,3X,'M2=',D11.5,5X,'M=',D11.5)
99992 FORMAT (T5,'K=',D11.5,4X,'BLADE=',D11.5,2X,'H=',D11.5)
99991 FORMAT (T5,'L=',D11.5,4X,'E=',D11.5,6X,'PE=',D11.5)
         END
CCCCCCCCCCCCCCCCCCCCCCCCCCCCCCCCCCCCCCCCCCCCCCCCCCCCCCCCCCCCCCCCCCCCCCCC
               SUBROUTINE FCN(T,Y,F)
           COMMON /DAT/H,BLADE,R1,K,L,E,MU1,MU2,MASS,IP,RI,IB,PE,X1,M,R2
           COMMON /WHY/B,B1,S,DIF,KE,S5,S6
           COMMON /ZEN/BMAX
           DOUBLE PRECISION A(10),F(4),Y(4)
           DOUBLE PRECISION S,S1,S2,S3,LAM,GE,H,R1,BLADE,DIF,THETA
           DOUBLE PRECISION X1,U,U1,U2,U3,U4,U5,U6,U7,U8,U9,U10
           DOUBLE PRECISION U11,U12,U13,U14,G1,G2,G3,B,B1,U15
           DOUBLE PRECISION MASS,IP,IB,PE,RI,MU1,MU2,T,K,L,E,DG,G
           DOUBLE PRECISION DCOS,DTAN,DSIN,DATAN,DSQRT,DASIN
           DOUBLE PRECISION JOY,DACOS,BMAX,KE,M,R2,DABS
           INTEGER S4,S5,S6
           REAL*8 LAB
           COMMON /LAB/ LAB
```

```
C DETERMINATION OF START CONDITION----------------------------
C *********CONDITION 1***********************
C ****************************************
            IF (B.LT.0.DO.AND.DABS(Y(1)).LT.0.5D-8) THEN
                PRINT*,'B IS NEG AND ALPHA=0'
                GE=H+Y(2)-R1-BLADE
                G=H-GE
                S=-(R1+BLADE)*DSIN(B)
                IF (S5.EQ.0) THEN
                S5=1
                RETURN
                END IF
                S5=2
C *********CONDITION 2***************************
C ******************************************
            ELSE IF (S5.EQ.0.AND.DABS(Y(1)).LT.0.5D-8) THEN
                PRINT*,'ALPHA=0 AND X=0'
                GE=H+Y(2)-R1-BLADE
                G=R1+BLADE
                S4=0
C *********CONDITION 3*******************************
C ************************************************
            ELSE IF (S5.EQ.3) THEN
                B1=0.DO
                B=0.DO
                GE=H-R1-BLADE+Y(2)
                G=DSQRT(GE**2+H**2-2.DO*H*GE*DCOS(Y(1)))
                S=DSQRT(G**2-(R1+BLADE)**2)
                IF (S6.EQ.2) THEN
                    S5=0
                    PRINT*,'S5=0'
                END IF
                S6=2
                PRINT*,'S6=2'
            ELSE IF (B.LT.0.DO.AND.Y(1).LT.0.DO.AND.S5.EQ.5) THEN
                S4=0
                IF (S6.EQ.1) THEN
                    S6=2
                    PRINT*,'FIRST'
                    RETURN
                END IF
                S5=0
                PRINT*,'SECOND'
                GE=H+Y(2)-R1-BLADE
                G=R1+BLADE
            ELSE
C ************************************************
C EQUATIONS FOR NORMAL MOVEMENTS-----------------------------
C ************************************************
                GE=H+Y(2)-R1-BLADE
                G=DSQRT(GE**2+H**2-2.DO*H*GE*DCOS(Y(1)))
                U1=(R1+BLADE)/G
                S5=1
                IF (U1.GE.1.0DO) THEN
                    U1=1.0DO
                    S=0.DO
                    S4=0
                    PRINT*,'"IF BLOCK IN USE"'
```

```
                B=DASIN(H*DSIN(Y(1))/(R1+BLADE))-Y(1)
                GE=DSIN(B)*(R1+BLADE)/DSIN(Y(1))
                Y(2)=GE-H+R1+BLADE
                G=R1+BLADE
            ELSE
                U=(H-GE*DCOS(Y(1)))/(GE*DSIN(Y(1)))
                B=DASIN(U1)-DATAN(U)
                JOY=GE**2+H**2-2.D0*H*GE*DCOS(Y(1))-(R1+BLADE)**2
                S=DSQRT(JOY)
                S4=1
            END IF
        END IF
        S1=S+MU1*BLADE
        S2=GE-PE-MU2*R1
        S3=DSQRT(MU1**2+1.D0)
C DESIGNATION OF S ZERO, +VE, -VE--------------------------
C BY DIF=0, 1, 2
        THETA=DASIN(GE*DSIN(Y(1))/G)
        DIF=THETA-B
        IF (DABS(DIF).LT.0.5D-7) THEN
            PRINT*, 'FIRST DIF=0'
        ELSE IF (S4.EQ.0)  THEN
            DIF=0.D0
            PRINT*, 'DIF=0'
        ELSE IF (DIF.LT.0.D0) THEN
            DIF=2.D0
            WRITE(6,*) 'DIF HAS GONE NEGATIVE'
            CALL PL1$NL(LAB)
        ELSE
            DIF=1.D0
        END IF
        LAM=DATAN(MU1)
        A(1)=IB*(GE*S3*DSIN(Y(1)+B-LAM)-R1)
        A(2)=IP*S1
        A(3)=S1*RI*MU2
        A(4)=IB*S2*S3*DCOS(B+Y(1)-LAM)
        A(5)=MASS*S1*S2
        A(6)=MASS*Y(3)**2*(GE-PE)*S1*S2
        A(7)=K*(L-E-Y(2))*S1*S2
        A(8)=IB*S3*S2*DSIN(B+Y(1)-LAM)
        A(9)=S1*(RI+MASS*(GE-PE)*S2)
        A(10)=2.D0*Y(4)*Y(3)*MASS*S2*S1
C EQUATIONS FOR THE CASE WHERE S=0
        IF (S4.EQ.0) THEN
            PRINT*, 'S=0 IN FUNCTION BLOCK'
            U2=(R1+BLADE)**2-H**2*(DSIN(Y(1)))**2
            U3=(H*DCOS(Y(1))/DSQRT(U2))-1.D0
            U5=H**3*(DCOS(Y(1)))**2*DSIN(Y(1))/(U2*DSQRT(U2))
            U4=Y(3)**2*(U5-(H*DSIN(Y(1))/DSQRT(U2)))
            U6=(A(3)+U3*A(4))*(U4*A(1)/(U3*A(1)-A(2)))
            KE=0.D0
            F(1)=Y(3)
            F(2)=Y(4)
            F(3)=-U4*A(1)/(U3*A(1)-A(2))
            F(4)=(A(6)+A(7)-U4*A(4)+U6)/A(5)
            RETURN
            END IF
C EQUATIONS FOR THE NORMAL CONDITION
```

```
      G=DSQRT(GE**2+H**2-2.DO*H*GE*DCOS(Y(1)))
      U2=G**2*DSQRT(G**2-(R1+BLADE)**2)
      U3=Y(3)*GE**2-H*Y(4)*DSIN(Y(1))-Y(3)*GE*H*DCOS(Y(1))
      G1=G**2*(R1+BLADE)*GE/(U2)
      U4=(GE**2-GE*H*DCOS(Y(1))+G1*H*DSIN(Y(1)))/G**2
      U5=(H*DSIN(Y(1))-G1+(G1*H*DCOS(Y(1)))/GE)/G**2
      G3=2.DO*GE*Y(4)
      DG=G3+Y(3)*GE*2.DO*H*DSIN(Y(1))-2.DO*H*Y(4)*DCOS(Y(1))
      U6=2.DO*Y(3)*Y(4)*(GE-H*DCOS(Y(1)))/G**2
      U7=H*GE*Y(3)**2*DSIN(Y(1))/G**2
      U8=U3*DG/G**4
      U9=(R1+BLADE)*(Y(4)**2+Y(3)**2*GE*H*DCOS(Y(1)))/U2
      G2=(R1+BLADE)/(4.DO*U2**3)
      U10=DG**2*G2*G**2*(3.DO*G**2-2.DO*(R1+BLADE)**2)
      U15=2.DO*Y(3)*Y(4)*(R1+BLADE)*H*DSIN(Y(1))/U2
      U11=A(1)*U5/(A(2)+U4*A(1))
      U12=A(1)*(U6+U7-U8+U9+U15-U10)/(A(2)+U4*A(1))
      U13=U11*A(3)+A(4)*U5+A(5)-U4*A(4)*U11
      U14=A(6)+A(7)+A(4)*(U6+U7-U8+U9+U15-U10)+U12*(A(3)-A(4)*U4)
      B1=-(U3/G**2)-(R1+BLADE)*DG/(2.DO*(U2))
      KE=0.5DO*(IB**2/(IB+M*R2**2))*B1**2
C-------------------FCN STATEMENTS-------------------------------
      F(1)=Y(3)
      F(2)=Y(4)
      F(3)=(U14*U11/U13)-U12
      F(4)=U14/U13
      RETURN
      END
CCCCCCCCCCCCCCCCCCCCCCCCCCCCCCCCCCCCCCCCCCCCCCCCCCCCCCCCCCCCCCCCCCCCCCCCC
       SUBROUTINE OUT(X,Y)
       DOUBLE PRECISION X,B,B1,S,LAB
       DOUBLE PRECISION Y(4),F(4)
       DOUBLE PRECISION Z,XEND,T,KE,DIF
       INTEGER J,S5,S6,NOUT,I,WOO,X2,IDINT
       DOUBLE PRECISION DFLOAT,DATAN,BMAX
       COMMON /UHU/XEND,Z,I
       COMMON /LAB/ LAB
       COMMON /WHY/B,B1,S,DIF,KE,S5,S6
       COMMON /ZEN/BMAX
       CALL FCN(T,Y,F)
C DIF IS INTERGERISED
       WOO=IDINT(DIF)
       DATA NOUT /6/
C STOP ROUTINE IF B>BMAX
       IF (B.GT.BMAX) CALL PL1$NL(LAB)
       WRITE(NOUT,99991) X,Y(1),B,Y(2),Y(3),B1,Y(4),S,KE,WOO
       X=XEND-DFLOAT(I)*Z
       I=I-1
       RETURN
99991 FORMAT (2H  ,D10.4,8(3X,D11.5),1X,I1)
       END
```

APPENDIX 6

The use of non-local GOTO statements.

To allow the programme to loop, in order that variables can be incremented, it is necessary to use a PRIME dependant function called a non-local transfer; for the following reason. If it is required to transfer from the NAG routine back to the main programme when the condition B=BMAX is achieved, then because B is determined in a subroutine called from NAG, it is only possibe to return to NAG. A non-local return is used so that on the condition B=BMAX, the programme returns to the main programme, as shown in the flow chart below.